Extraction and purification of C-phycocyanin and genome analysis of an indigenous hypersaline cyanobacterium

Submitted in fulfilment of the requirements of the degree of Doctor of Philosophy: Biotechnology in the Faculty of Applied Sciences at the Durban University of Technology

Trisha Mogany

(M.Tech: Biotechnology)

2020

Supervisor: Prof Faizal Bux

Co-supervisor: Prof Feroz Mahomed Swalaha

Dr Sheena Kumari Kuttan Pillai

DECLARATION

Extraction and purification of C-phycocyanin and genome analysis of an indigenous hypersaline cyanobacterium

Trisha Mogany

I hereby declare that the dissertation represents my own work. It has not been submitted before for any diploma/degree or examination at any other Technikon/University.

Trisha Mogany **Date**

2020

Reference Declaration in Respect of a PhD Dissertation

I, Trisha Mogany, Faizal Bux, Feroz Mahomed Swalaha and Sheena Kumari Kuttan Pillai, do hereby declare that in respect of the following dissertation:

Extraction and purification of C-phycocyanin and genome analysis of an indigenous hypersaline cyanobacterium

- as far as we know and can ascertain:
- no other similar dissertation exists;
- the only similar dissertation(s) that exist(s) is/are referenced in my dissertation as follows:

_____

_____

_____

- All references as detailed in the dissertation are complete in terms of all personal communications engaged in and published works consulted.

Signature of Student **Date**

Signature of Supervisor **Date**

Signature of Co-supervisor **Date**

Signature of Co-supervisor **Date**

APPROVAL

I hereby approve the final submission of the following dissertation.

Prof. Faizal Bux

Supervisor
Doctors Degree in Technology: Biotechnology
Durban University of Technology (DUT)

Prof. Feroz Mahomed Swalaha

Co-supervisor
Doctors Degree in Technology: Biotechnology
Durban University of Technology (DUT)

Dr Sheena Kumari Kuttan Pillai

Co-supervisor
Doctor of Philosophy: Bioscience

This 22 day of April 2020, at the Durban University of Technology.

*** SUBMISSION APPROVED FOR EXAMINATION**

SUPERVISOR **DATE**

Prof. Faizal Bux

Doctors Degree in Technology: Biotechnology
Durban University of Technology

CO-SUPERVISOR **DATE**

Prof. Feroz Mahomed Swalaha

Doctors Degree in Technology: Biotechnology
Durban University of Technology

CO-SUPERVISOR **DATE**

Dr Sheena Kumari Kuttan Pillai

Doctor of Philosophy: Bioscience

* Only when your supervisor agrees that the dissertation is ready for examining will he/she then sign the above endorsement.

* Please ensure that your supervisor's abbreviated academic qualifications are inserted after his/her name.

ABSTRACT

Cyanobacteria are photosynthetic microorganisms that inhabit diverse ecological habitats and are capable of producing wide range of natural products and bioactive metabolities including peptides, vitamins, enzymes and pigments such as phycobiliproteins. Amongst the group of phycobiliproteins, C-Phycocyanin (C-PC) is a light-harvesting accessory pigment known to possess excellent biotechnological applications due to their intense colour, fluorescent properties and health benefits. This study has focused on the characterisation and full genome analysis of a unique indigenous halophilic cyanobacterium capable of overproducing the pigment phycocyanin (C-PC). Further, development of a cost-effective extraction method for high purity C-PC and characterisation of the purified C-PC was accomplished.

The strain was isolated from a hypersaline environment in KwaZulu-Natal, South Africa and was found to possess several unique traits such as its ability to accumulate high amount of phycocyanin, tolerance to high salinity (up to 180 g/L), ability to grow under varying growth conditions and high growth rate. The taxonomic identity of the isolate was revealed using a polyphasic approach including cell morphology, growth conditions, pigment composition, 16S rRNA analysis. The cells were oval to rod-shaped, 14-18 μm in size, and contained majority of C-PC, as well as some allophycocyanin and chlorophyll. The strain was moderately thermotolerant (35°C), alkalitolerant (pH 8.5) and was halophilic with an optimum NaCl of 120 g/L. Based on the 16S rRNA gene sequence phylogeny, the strain was found to be related to members of the '*Euhalothece*' subcluster (99%). Further, the whole genome sequence was also determined, and the annotated genes have shown sequence similarity (90%) to the gas-vacuolate, spindle-shaped *Dactylococcopsis salina* PCC 8305. Based on the above results, the strain is considered to represent a novel species of *Euhalothece*. The size of the genome was determined to be 5,113,178 bp and contained 4332 protein-coding genes and 69 RNA genes with a GC content of 46.7%. The full genome sequence analysis also provided important information about the strain which facilitated the identification of key genes and proteins necessary for C-PC synthesis and salt acclimation. Genes encoding osmoregulation, oxidative stress, heat shock, persister cells, and UV-absorbing secondary metabolites, among others, were also identified.

Further, single factor experiments were performed to optimise the factors (extraction buffers, freezing time, biomass:buffer ratio and lysozyme concentration) essential for C-PC extraction from cyanobacteria. A range of buffers viz., acetate, potassium phosphate (PPB), sodium

phosphate (SPB), phosphate buffered saline (PPBS), Tris-chloride and double distilled water (control) with different pH and concentrations were investigated. Cell lysis was carried out by freezing the cells at different temperatures *viz*., at -196, and -80, and -20°C, and by thawing at 4 and 25°C. The freezing and thawing time varied from 0.5-24 h. Based on the results obtained, thawing temperature, enzyme concentration and biomass-buffer ratio were further selected for optimisation for maximum C-PC yield and purity using response surface methodology (RSM). Under optimised conditions, the yield of crude C-PC was increased to 78 mg/g (>90% percentage increase) with a purity index of 2.5 compared to extraction prior to optimisation. The crude C-PC was further purified using 6% w/v of activated charcoal combined with a two-step ammonium sulphate (NH_4SO_4) precipitation and ultrafiltration which resulted in high yield analytical grade C-PC with a purity index of 5.

The purified C-PC showed a single absorption peak at 620 nm and emission at 640 nm. Based on the amino acid analysis the calculated molecular weight of α- and β-subunits were found to be 17.7 and 18.4 kDa respectively, which corresponded to the two bands seen on the SDS-PAGE. Additionally, the primary, secondary and tertiary structures of the C-PC was also evaluated based on the amino acid sequence obtained from the genome sequence. The C-PC physiochemical properties such as the molecular weight, isoelectric point, extinction coefficient, half-life, aliphatic index, amino acid property, instability index and Grand Average of Hydropathicity was predicted based on the *in-silico* analysis of the amino acid sequences. The physicochemical properties revealed that these proteins are non-polar and stable. Multiple sequence alignment analyses of the α- and β-subunits displayed significant differences amongst the amino acid residues of hypersaline/marine and freshwater cyanobacteria. These amino acids play a vital role in the stability of the C-PC. The secondary structure prediction of the α- and β -subunits consisted of > 50% of amino acid residues in α-helices, with 9-13% of amino acid residues in the extended strand.

The stability of the purified C-PC under different conditions were investigated. The optimum pH range for purified C-PC was found to be 5.0–7.0 and was found to be stable up to 45°C. However, the relative concentration C-PC (C_R%) and thermostability of the purified C-PC was observed to be pH dependent, a lower pH improved the stability at higher temperatures and vice-versa. An IC_{50} value of 0.540 ± 0.02 mg/mL was also observed using the DPPH assay indicating a higher antioxidant potential of the C-PC. C-phycocyanin exhibited a maximum absorbance of 1.37 ± 0.05 by ferric ion reducing assay. The presence of a high level of non-

polar and aromatic residues such as Ala, Gly Glu, Leu, Arg, Ser, and Val could be regarded as an indication of higher antioxidant activity levels of the C-PC. Addition of preservatives sodium azide and sodium citrate (at 4°C) proved to be suitable for preservation of C-PC for up to 42 weeks.

This research contributed to our understanding of molecular, cellular and biochemical mechanisms of the C-PC biosynthesis as well as newly identified metabolites in cyanobacteria. The study has also demonstrated an efficient extraction method for analytical grade C-PC from cyanobacterial strains for potential applications in biotechnological biomedical industries.

PREFACE

Papers Published

Trisha Mogany, Sheena Kumari, Feroz M. Swalaha, Faizal Bux. (2019). Extraction and characterisation of analytical grade C-phycocyanin from *Euhalothece* sp. Journal of Applied Phycology. 31,1661-1674

Trisha Mogany, Feroz M. Swalaha, Mushal Allam, Phillip Senzo Mtshali, Arshad Ismail, Sheena Kumari, Faizal Bux (2018). Phenotypic and genotypic characterisation of an unique indigenous hypersaline unicellular cyanobacterium, *Euhalothece* sp.nov. Microbiology Research, 211, 47-56.

Trisha Mogany, Feroz M. Swalaha, Sheena Kumari, Faizal Bux. (2018). Elucidating the role of nutrients in C-phycocyanin production by the halophilic cyanobacterium *Euhalothece* sp. Journal of Applied Phycology, 30, 2259-2271.

Papers Submitted

Trisha Mogany, Sheena Kumari, Feroz M. Swalaha, Faizal Bux. (2020). An *in silico* structural and physiochemical analysis of C-Phycocyanin of halophile *Euhalothece* sp. Algal Research.

Papers In-Preparation

Trisha Mogany, Sheena Kumari, Feroz M. Swalaha, Faizal Bux. Strategies to improve phycobiliprotein production in cyanobacteria and red algae.

Conferences

Trisha Mogany, Sheena Kumari, Feroz M. Swalaha, Faizal Bux. (2016). Media and physiochemical optimisation for enhanced phycocyanin production in *Cyanothece* sp. Oral presentation of the 19th South African Society of Microbiology (SASM) biennial congress, Coastlands, Umhlanga, Durban, South Africa, 17-20 January 2016.

Trisha Mogany, Sheena Kumari, Feroz M. Swalaha, Faizal Bux. (2016). Enhanced phycocyanin production in hallophilic/halotorelant *Cyanothece* sp. Poster Presentation at the Algae Biomass Organisation (ABO) Summit at the Renaissance Phoenix Glendale Hotel & Spa, Phoenix, Arizona, USA 24 October 2016.

ACKNOWLEDMENTS

This thesis is the culmination of my PhD journey which was like climbing a mountain accompanied with hardship, frustration and encouragement. Finally reaching the top, feeling satisfied, I am happy to have an opportunity to acknowledge and thank all the people who have made this journey possible as well as enjoyable.

No research is possible without infrastructure and resources. For this I extend thanks to the Institute for Water and Wastewater Technology. And Prof. Faizal Bux for allowing me to work under his guidance. He made me realise the importance of research, gave me every possible chance to learn, and myself better to excel in my career.

I am grateful to Prof. Feroz Mahomed Swalaha for his unfailing support and enthusiasm for science and learning. He provided a steady source of ideas and optimism and his zeal for perfection has always inspired me to do more.

I would like to thank Dr Sheena Kumari for her invaluable scientific perspective and advice that she has provided me. Under her guidance, I successfully overcame many difficulties.

Special thanks go to my colleagues at IWWT, I am delighted to have been part of an evolving mix of cultures, opinions, and personalities. I am indebted to so many of these people for their help with technical difficulties (from big to small crises), and for their friendship especially Mr Rawat, Mr Pillay, Ms Deepnarain, Ms Bhola, Mr Aaron, Mr Ramanna and Mr Gokal for the encouragement during tough times and inspiration during the long writing process.

I acknowledge the people who mean a lot to me, my parents, for giving me the liberty to choose what I desired and for always providing me with all the support and love I could ever want on this journey.

One of the things I have learned is that one of the most difficult parts is emotionally dealing with experiments that do not work. For that emotional resilience, I must primarily thank the never-ending support of my husband, Kirshlin Mogany. I am profoundly grateful for his love, patience, understanding and never-ending faith in me - these have been the keystones to my success and happiness.

DEDICATION

This work is dedicated to my beloved family and valuable treasures in my life

My late father, Dan Govender

who taught me resilience and hard works always pays off

My dearest mother, Sharon Govender

for her advice, faith, strength and love

My husband, best friend and soulmate Kirshlin Mogany,

for his unconditional love, patience, support and encouragement,

My loving son, Drelin Cahil Mogany

and

My sweet daughter, Milaya Sara Mogany

for serving as my motivation and inspiration.

CONTENTS

LIST OF FIGURES

LIST OF TABLES

LIST OF EQUATIONS

LIST OF ABBREVIATIONS

ANI	Average Nucleotide Identity
BLAST	Basic Local Alignment Search Tool
C-PC	Cyanobacterial-Phycocyanin
C-APC	Cyanobacterial -Allophycocanin
C-PE	Cyanobacterial -Phycoerythrin
CCD	Central Composite Design
C_R	Concentration of C-PC in %
Chl	Chlorophyll
DNA	Deoxyribonucleic acid
DDH	DNA–DNA hybridisation
DOE	Design of Experiments
EPS	Extracellular Polysaccharides
HGT	Horizontal Gene Transfer
HK	Histidine Kinases
IAMS	International Association of Microbiological Societies
ICNB	International Code of Nomenclature of Bacteria
ICNP	International Code of Nomenclature of Prokaryotes
ICSB	International Committee on Systematic Bacteriology
ITS	Internal transcribed spacer
LRC	Rod Linker Core
LR	Rod Linkers
LC	Core Linkers
LCM	Core-Membrane Linker
LSU	Large Subunit
MAAs	Mycosporine-Like Amino Acids
MLSA	Multilocus Sequence Analysis
PAR	Photosynthetically Active Region

LIST OF ABBREVIATIONS

PBS	Phycobilisomes
PBPs	Phycobiliproteins
PSI	Photosystem 1
PS 11	Photosystem 2
rRNA	Ribosomal Ribonucleic Acid
Rre	Response Regulators
ROS	Reactive Oxygen Species
RSM	Response Surface Methodology
SSU	Small Subunit
SPB	Sodium Phosphate Buffer
TCS	Two-Component Regulatory Systems
WGS	Whole Genome Sequencing

CHAPTER 1 : INTRODUCTION

1.1 BACKGROUND

Cyanobacteria, also known as 'blue-green algae', are a fascinating and versatile group of microorganisms with enormous biotechnological importance (Hamilton *et al*., 2016). Believed to be amongst the first organisms to colonise the Earth, with the ability to perform oxygenic photosynthesis and nitrogen fixation; they can thrive in very extreme environments previously believed to be unhabitable such as high temperatures, extreme pH, limited water availability and high salinity (Aleksandra *et al*., 2007). Hence owing to the of loss-and-gain of genes transferred by phages, plasmids, and/or insertion sequences the genomes of cyanobacteria are widely diverse in guanine-cytosine (GC) content ranging from 30 to 60% and size ranging from about 1.4 Mbp to about 9.0 Mbp (Bandyopadhyay *et al*., 2013; Cassier-Chauvat & Chauvat, 2015). Additionally, cyanobacteria exhibit different forms (unicellular or multi-cellular filaments) and cell morphologies including spheres and cylinders. Hence, they are attractive models to investigate the effect of the environmental conditions on the morphology, physiology, and metabolism (Beck *et al*., 2012).

Some strains with extreme halotolerance, such as *Halothece*, *Aphanothece halophytica* and *Halospirulina tapeticola* are able to grow in salinities close to 12-17% w/v (Garcia-Pichel *et al*., 1998; Oren, 2012). These organisms are reported to form a large part of the biota of hypersaline environments that includes solar salterns, salt lakes, hypersaline sulphur springs and hypersaline lagoons (Oren, 2012; Oren *et al*., 2009). Marine cyanobacteria are known to produce a diverse range of secondary metabolites, which have potent biological activities, some of which could be used to produce novel anticancer drugs, antimicrobial agents and UV protectants *etc.* (Rajneesh *et al*., 2017). Although various novel structures have often been reported, the knowledge of the chemical diversity present in these organisms is still quite limited (Leão *et al*., 2013). The discovery of novel and unique genes in these organisms has fueled even more interest in hypersaline environments. The amazing versatility and combination of properties exhibited by marine cyanobacteria have attracted huge interest from many researchers.

The genus *Cyanothece* can fix atmospheric nitrogen by temporally segregating the photosynthesis and nitrogenase activities (Stockel *et al*., 2011; Welsh *et al*., 2008). Some aspects of ecology, physiology, photosynthetic ability, and nitrogen metabolism of the genus *Cyanothece* have been previously studied (Bandyopadhyay *et al*., 2011). However, limited

literature is available on hypersaline tolerant *Cyanothece* species (cluster *Halothece*) and their adaption processes during hypersaline conditions. Owing to the intensive use of genetic tools, there has been a rapid increase in our understanding of the cyanobacterial diversity in hypersaline systems (Ducat *et al*., 2011). Nevertheless, regardless of their ecological and biotechnological importance, many aspects of cyanobacterial diversity are still not fully understood. Hence, the increasing availability of fully sequenced cyanobacterial genomes provides researchers with the opportunity to further understand cyanobacterial diversity and the physiological adaptations from a genomic perspective. One of the most important reasons for full genome sequencing of cyanobacteria that inhabit hypersaline environments is to better understand how they are adapted to the variability of environmental conditions. Furthermore, the mechanisms that these cyanobacteria possess are of great interest. Thus, genome sequencing provides insight into genome organisation and evolution, and the mechanisms involved during stress adaptations that can be explored for biotechnological applications (Tanizawa *et al*., 2015). Even though extensive research has been conducted on cyanobacterial secondary metabolites there is still a large selection of species, which have yet to be sequenced and investigated with many potentially important secondary metabolites yet to be discovered.

Stress adaptations of halophiles include modifications to the cell membrane and cell wall. This results in the increased production of chaperones, active uptake and release of ions and the production of secondary metabolites to help negate the stress (Agrawal *et al*., 2015; Hagemann, 2011; Pade & Hagemann, 2015). In addition, certain genes and metabolites are produced and enzymes and pathways activated in response to salt (Pade & Hagemann, 2015). Furthermore, environmental stress influences the cyanobacteria to suppress or enhance the functioning and production of some physiologically important proteins including phycobiliproteins (PBPs). The crucial function these light-harvesting antenna complexes in cyanobacteria is to efficiently absorb light in wavelengths ranging from 480-660 nm and transiently transfer to the main reaction centre of chlorophyll a (Chl a) (Sun *et al*., 2003). These PBPs can be classified into three main groups which include C-phycocyanin (C-PC), C-allophycocyanin (C-APC) and C-phycoerythrin (C-PE) and having absorption maxima between 610-620, 650-655 and 540-570 nm respectively (Bermejo *et al*., 2007; Santiago-Santos *et al*., 2004; Soni *et al*., 2006).

There has been increasing interest in the potential uses of cyanobacterial C-PC in the commercial sector (Sekar & Chandramohan, 2008). Due to the ease of application, stability,

and cost-effectiveness synthetic colourants are still commercially used in the food, cosmetic and pharmaceutical industries. However, from a health and safety viewpoint, they are not accepted by consumers, thus, there has been a growing interest in natural food colourants. C-phycocyanin is viewed as a possible natural, eco-friendly, non-toxic, cost-effective and easily degradable alternate source of blue colourant in food, cosmetic and pharmaceutical industries (Dragana Stanic-Vucinic, 2018). Blue is one of the three primary colours and so far there are few sources of natural blue food colour from fruits and plants. Dainippon Ink & Chemicals corporation and Earthrise Nutritionals LLC has developed a product called "Lina" blue which is used in chewing gum, candies, ice sherbets, soft drinks, popsicles and dairy products (Klein & Buchholz, 2013). Lineblue® complies with regulatory criteria for colouring food in many countries including the EU, USA, Japan, Korea and other Asian countries. Following the approval by the Food and Drug Administration (FDA) as a food colourant in 2013, in the last six years, the use of C-PC as a natural blue food colourant has grown exponentially. The C-PC demand is predicted to grow tremendously during 2015-2020, expanding to 7-10 times as demand for natural colours continues to increase. Besides the food industry, C-PC can be used as a dye in the textile, cosmetic and pharmaceutical industries. In addition, they can be used in skin cream to stimulate collagen synthesis (Manirafasha *et al*., 2016).

C-phycocyanin is already used as an antioxidant, due to their chemical structures and chelating properties they neutralise the reactive oxygen species (ROS), thereby reducing the oxidative stress (Bermejo *et al*., 2008; Romay *et al*., 2003). Several studies have also demonstrated the health-promoting properties of C-CP *i.e*. anti-inflammatory, antiplatelet, anticancer, nephroprotective and hepatoprotective (Cherng *et al*., 2007; Eriksen, 2008; Fernández-Rojas *et al*., 2014; Jiang *et al*., 2017; Prasanna *et al*., 2010; Yu *et al*., 2017). Spectroscopic and structural properties of PBPs show a number unique qualitative and quantitative features *viz*., (i) high fluorescence quantum yield in a broad range of pH values; (ii) broad absorption spectrum with high molar extinction coefficient; (iii) minimal fluorescence quenching; (v) high Stokes shift and (vi) active surface functional groups such as NH_2 or -COOH group for hetero-bifunctional coupling (Hermanson, 2013; Holmes & Lantz, 2001; Sun *et al*., 2003). Owing to their powerful and highly sensitive fluorescent properties, they are widely used in clinical and immunological research laboratories as labels and fluorescent tags for antibodies, receptors and other biological molecules in a fluorescence-activated cell sorter, immune-labelling experiments and fluorescence microscopy (Sun *et al*., 2003). Studies have also reported the possibility of

staining red blood cells, white blood cells, platelets, lymphocytes, nucleated cells, and genomic DNA with C-PC (Singh *et al*., 2011). To obtain analytical grade C-PC, most of the purification strategies involves multiple steps including various forms of chromatography. Hence, extraction and purification of C-PCs have become a challenging endeavour for both researchers and entrepreneurs.

1.2 MOTIVATION FOR STUDY

The isolated cyanobacterium used in this study belonged to the genus *Cyanothece* (cluster: *Halothece*). Since the cyanobacterium was isolated during drought conditions from St Lucia Estuary in KwaZulu-Natal, South Africa, this organism was exposed to extremely high nutrients and salinity concentrations, which have resulted in an upregulation of photosynthetic pigments mainly C-PC. Based on previous research the strain was moderate thermotolerant/alkalitolerant halophile with the optimum conditions for growth at 35°C, pH 8.5 and 120 g/L of NaCl. The isolate produced 43.97 mg/g of C-PC under optimised BG 11 media (*i.e.* 120g/L of NaCl, 0.10 g/L of $MgSO_4$, 1.67 g /L of $NaNO_3$ and 10 mL of minor nutrients; citric acid, EDTA-iron citrate, $CaCl_2$ and Na_2CO_3). Thus, the ability of this cyanobacteria to produce a high quantity of C-PC coupled with its high nutrient and salt tolerance made it a perfect candidate for whole-genome sequencing. The genome structure, function and evolution of this organism was studied through its complete genome. Sequencing the genome was an important step in attempting to understand how this cyanobacterium adapted to this environment and provided evidence on some of the existing pathways, including C-PC biosynthesis in comparison to reference strains. Although several studies have been conducted on the structure, biochemistry and molecular biology of PBPs, there still exist several gaps in our knowledge regarding the biochemical and molecular biology of PBPs with respect to amino acid composition, stability and functional properties in hypersaline cyanobacteria. Hence it is essential to analysis and explore the genome from a gene to an amino acid to codon level from the isolate cyanobacteria strain. In the future, the information from this study may be useful for the production of various other novel metabolites through genetic modifications.

C-Phycocyanin is a blue, water-soluble pigment-bound protein that displays antioxidant, anti-inflammatory, neuroprotective and hepatoprotective properties. In addition to these health benefits, C-PC has been used in nutritional supplements and as a natural colourant in the food,

nutraceuticals and cosmetics. Moreover, C-PC has also been used as a fluorophore in biomedical research, diagnostics and therapeutics. The great economic potential of this valuable pigment has increased the market value. However, the widespread use of the C-PC has been restricted due to the high cost of extraction and purification. Downstreaming process requires a method that extracts maximum high-quality C-PC whilst preserving the protein purity and structure. Often, conventional purification methods cannot be scaled up and require numerous steps to reach high purity. This has motivated the first part of the research, which involved evaluating and optimising simple cost-effective C-PC extraction and purification methods.

1.3 AIM AND OBJECTIVES

1.3.1 Aim

The aim of this study was to analyse the unique genetic structure of a hypersaline cyanobacteria with high C- phycocyanin content and to develop an efficient method for the extraction of high purity C- phycocyanin for potential industrial applications.

1.3.2 Objectives

1.3.2.1 To characterise and identify the indigenous euryhaline cyanobacterium using morphological and molecular methods.

1.3.2.2 To sequence and assemble the genome of the indigenous euryhaline *Euhalothece* sp. using the Illumina Miseq Genome Sequencer system and assign gene functionality.

1.3.2.3 To identify and compare the key genes encoding for C-phycocyanin biosynthesis as well as those involved in stress adaptation.

1.3.2.4 To optimise the freeze-thaw extraction process parameters in order to maximise the C-phycocyanin yield from *Euhalothece* sp. using response surface methodology

1.3.2.5 To purify the C-phycocyanin using simple and easy precipitation, adsorption and filtration methods.

1.3.2.6 To characterise and investigate the stability and antioxidant activity of the purified C-phycocyanin.

1.4 Thesis Outline

This thesis is divided into two major topics covering the sequencing of the genome of the indigenous cyanobacteria and the extraction of C-PC. An outline of the thesis structure is summarised below:

Chapter 1 provides an introduction to the research conducted in this thesis, as well as the motivation for the study. A general introduction to cyanobacteria, specifically halophilic cyanobacteria, importance of extraction and purification methods, and applications of C-PC. It also describes the aim of the research study and states the specific objectives which needed to be in complete in order to achieve the aim. Finally, a summary of the contents of each chapter is presented.

Chapter 2 presents the background to cyanobacteria, more especially cyanobacteria from hypersaline environments. It also focuses on genome sequencing, background information about different types of extraction and purification techniques which is essential for the development and improvement of these processes is given. The application of C-PC and factors affecting the stability of this protein are reviewed.

Chapter 3 presents the polyphasic approach *i.e.* ecological, morphological, ultrastructure, and phylogeny used to characterise the unicellular euryhaline cyanobacterium isolated from marine Estuary in St Lucia. This chapter also compares the 16 S rRNA gene sequences and full genome sequence of the isolate and other related marine cyanobacteria.

Chapter 4 directly addresses the first two objectives of the thesis focusing on an in-depth analysis of the genome, which provided an indication of how the cyanobacteria adapt to saline environments, as well as the biosynthesis of C-PC.

Chapter 5 focuses on the optimisation of the extraction of C-PC using response surface methodology. Thereafter common adsorption, precipitation and filtration techniques for purification are investigated.

Chapter 6 focuses on *in silico* amino acid analysis, structural characterisation, stability and antioxidant activity of the purified C-PC

Chapter 7 summarises the findings and conclusions of the thesis, tying together all the studies conducted along with recommendations for future research.

CHAPTER 2 : LITERATURE REVIEW

2.1 CYANOBACTERIA

Cyanobacteria (also known as Blue-Green Algae, Cyanophyta, Cyanophyceae and Cyanoprokaryota) represent the most abundant and significant phylum of photosynthetic prokaryotes on Earth (Broady & Merican, 2012; Walter *et al*., 2017). Since they are autotrophs containing plant-like photo-pigments such as PBPs, Chl 'a' and carotenoids, botanists (phycologists) classified them as microalgae. Conversely, microbiologist considered them as bacteria since many of the protoplasmic structures found in cyanobacteria are also known to be present in bacteria (Palinska & Surosz, 2014; Palinska *et al*., 2006). Cyanobacteria are morphologically, physiologically, and genetically a diverse group of microorganisms with remarkable ecological plasticity and long evolutionary history (Castenholz, 2001; Sciuto & Moro, 2015). They are believed to be the pioneer organisms of the early Earth with fossil records dating back 3.3- 3.5 Ga years (Whitton & Potts, 2000). Cyanobacteria are responsible in the origins of Earth's oxygen-rich atmosphere during the "Great Oxidation Event" in which oxygenic photosynthesis has evolved (Hamilton *et al*., 2016; Schirrmeister *et al*., 2015). In addition to performing photosynthesis, cyanobacteria also can actively fix atmospheric nitrogen and play a key role in carbon and nitrogen cycles. Specifically, marine cyanobacteria play a role in global importance, accounting for ~25% of the total carbon fixation in oceans (Hernandez-Prieto *et al*., 2014; Walter *et al*., 2017).

They have successfully inhabited a wide range of ecological environments including terrestrial, aquatic and prominent limnic and marine environments (Schirrmeister *et al*., 2015). Cyanobacteria have evolved to cope with abiotic stress factors and adapted to flourish under harsh conditions including high light irradiance, salinities, UV and extreme temperatures. They have been found to survive in some of the most extreme of conditions such as deserts, hot springs, hypersaline conditions, freezing environments and arid land (Kehr *et al*., 2011; Sciuto & Moro, 2015). They often live in association with other organisms forming biofilms, microbial mats and benthic communities. These associations are often the only life forms found in extreme habitats (Pikuta *et al*., 2007). Hence, this widespread distribution of cyanobacteria reflects its tolerance to wide environmental stress and a broad spectrum of physiological properties (Shalaby

& Dubey, 2018). The investigation of halotolerant and halophilic cyanobacteria surviving in hypersaline environments provide fundamental insight into the understanding of life. Furthermore, they produce a number of stable and unique biomolecules which is highly useful for practical applications and can be used commercially (Oren *et al*., 2009). The growing biotechnological applications in food, cosmetic and fuel industries has led to an increasing interest in cyanobacterial research (Abed *et al*., 2009; Al-Haj *et al*., 2016; Singh *et al*., 2017).

While cyanobacteria are classified as Gram-negative prokaryotes, they also have characteristics of Gram-positive organisms. With a thickness of about 10 nm, the peptidoglycan layer between the cytoplasmic and outer membrane of some species is thicker than typical for Gram-negative bacteria (*i.e*., 2-6 nm) while having a cross-linking structure resembling that of Gram-positive bacteria (Hoiczyk & Baumeister, 1995; Sciuto & Moro, 2015). Many cyanobacteria have an additional mucilaginous layer that surrounds the cell wall is the glucan fibril which consists mainly of polysaccharides. Depending on their amount and compactness, the EPS surrounding cyanobacterial cells are distinguished in capsules, sheaths, and slim (Sciuto & Moro, 2015). This layer protects the cyanobacteria from extreme conditions such as desiccation and has the function of a diffusion barrier of dissolved substances in aqueous environments. Thus, it plays an important role in the assimilation of nutrients (Hoiczyk & Hansel, 2000). The EPS also contain photoprotective compounds like mycosporine-like amino acids (MAAs), which can effectively absorb UV light; scytonemin, a cyanobacterial sunscreen for UV A and carotenoids, accessory pigments (Garcia-Pichel & Castenholz, 2004).

Within the cell, another membrane system, the thylakoid membranous network partially connected to the cytoplasmic membrane harbour the photosynthetic machinery of the cell. The light-harvesting structures *i.e*. PBS are located in the cytoplasm on the stromal side of the thylakoid membranes where they are attached to photosystem II (PS II) (Hu *et al*., 1999). They absorb visible light in the range of 450–660 nm where Chl has low absorptivity (Singh *et al*., 2015). Apart from the various transport systems the cytoplasm membrane also contains a fully functional respiratory electron transport chain with components such as the cytochrome oxidase and ATP synthase. Major metabolic reactions such as nitrogen and glucose metabolism occur in the cytoplasm. Cyanobacterial cells also contain several different intercellular bodies which include carboxysomes, hexagonal structures that are part of the CO_2-concentrating mechanism and

facilitates efficient carbon fixation; gas vacuoles, used in some strain's regulation of buoyancy in water; cyanophycin and polyphosphate bodies for storage of nitrogen and phosphorous respectively; glycogen granules and poly-*β*-hydroxybutyrate for energy and fixed carbon (Rajneesh *et al*., 2017).

Previous studies have demonstrated that cyanobacteria also are emerging as a prolific source of ribosomal natural products (Kehr *et al*., 2011; Micallef *et al*., 2015; Wang *et al*., 2011). Natural products also known as secondary metabolites such as peptides, polyketides, alkaloids, terpenoids are often produced by cyanobacteria in response to environmental stress (Jones *et al*., 2009; Kehr *et al*., 2011). Accordingly, they play various roles in protecting the cells including defence against predators and grazers, chemosensory, photoprotection and antioxidant (Rastogi *et al*., 2016; Żyszka-Haberecht *et al*., 2019).

Some cyanobacterial strains naturally produce large amounts of polyhydroxyalkanoates (PHA) which can be used as a thermoplastic biodegradable polyether that displays comparable properties to polypropylene (Abed *et al*., 2009). Cyanobacteria are found to have halogenated compounds such as acetogenins, phenols, terpenes, indoles and fatty acids (Derikvand *et al*., 2017; Gao & Garcia-Pichel, 2011; Singh *et al*., 2017). Furthermore, they are the rich sources of several other metabolites including alkaloids, carbohydrates, flavanoids, phytohormones, proteins, saponins, steroids, tannins, and vitamins which can be used various biotechnological applications (Abed *et al*., 2009; Guihéneuf *et al*., 2016). Accordingly, these secondary metabolites have several biological activities including anticancer, antibacterial, and antiviral hence, their potential use is as pharmaceuticals and nutraceuticals (Lau *et al*., 2015; Singh *et al*., 2017).

2.2 TAXONOMY OF CYANOBACTERIA

2.2.1 Botanical and Bacteriological Approach to Classification

Traditional blue-green algae have been placed in the phylum Cyanophyta which comprised the class Cyanophyceae. The morphological features such as (i) type of growth *i.e.* unicellular, colonial, filamentous; (ii) shape and compactness of colonies; (iii) shape of filaments; (iv) presence or absence of a sheath; (v) cell differentiation- presence or absence of heterocysts and akinetes; (vi)

size and shape of vegetative cells, heterocysts and akinetes; (vii) branching- presence or absence, false or true, when false "y" shaped; and (viii) nature of true branches: uniseriate or multiseriate are the main criteria used for traditional classification (Anagnostidis & Komárek, 1985; Rippka, 1988; Roger, 1982). International Code of Botanical Nomenclature (ICBN) is the classification system developed by phycologists, this system is based on morphological, ecological, genetic and ultrastructural information of both cultivated and uncultivated cyanobacteria (Pinevich, 2015; Wilmotte & Herdman, 2001). Rippka *et al.* (1979) divided cyanobacteria into five sections corresponding to the four orders subdivided into families, subfamilies, genera and species. Rippka *et al.* (1979) & Stanier *et al.* (1978) highlighted cyanobacterial evolutionary relations to bacteria and proposed that their nomenclature should be governed by the provisions of the International Code of Nomenclature of Bacteria (ICNB) *i.e.* the Bacteriological Code, now: International Code of Nomenclature of Prokaryotes (ICNP). The subcommittee on Phototrophic Bacteria of the International Committee on Systematic Bacteriology (ICSB) of the International Association of Microbiological Societies (IAMS) recommended that cyanobacteria be included under Division I in the eighth edition of Bergey's Manual of Systematic Bacteriology (Castenholz, 2001).

Valid publication under the ICNP comprises of a formal act of indexing and registration, centralised in a single journal *i.e.* the International Journal of Systematic and Evolutionary Microbiology (IJSEM). This concept is currently not favoured by botanist since few restrictions exist in the journal in which names may be validly published. Furthermore, under the ICNP, a full description of the type of species, (which must be maintained in pure culture) must be submitted. Additionally, subcultures of this strain must be deposited in at least two publicly accessible culture collections in different countries (Oren & Tindall, 2005; Ramos *et al.*, 2017). Under the ICBN, the samples must be permanently preserved. Neither the International Committee on Systematics of Prokaryotes (ICSP) nor the General Committee on Botanical Nomenclature (GCBN) can solely make claims to the nomenclature of cyanobacteria (Pinevich, 2015). Since the rules of the Bacteriological Code are rather different from those of the Botanical Code, the coexistence of the two independent nomenclature systems is highly problematic, making reconciliation between both nomenclature systems quite difficult (Hoffmann *et al.*, 2005). Additionally, the transfer of taxa from Botanical to Bacteriological Code is challenging due to cyanobacteria's unique evolutionary, ecological, and physiological features (Walter *et al.*, 2017).

Therefore, solutions to make both types of nomenclature compatible are essential. The ideal proposed solution is a joint nomenclature and the use of identical methods for the description of species and designation of types (Oren & Tindall, 2005). Symposia held by the International Association of Cyanophyte/Cyanobacteria Research (IAC) have attempted to determine a consensus nomenclature that would be acceptable to both bacteriologists and botanists (Komárek *et al*., 2011), however, to date there still no universally accepted consensus of nomenclature (Oren & Ventura, 2017; Palinska & Surosz, 2014).

Conventionally, cyanobacteria have been classified using morphological and ecological characteristics (Palinska *et al*., 2006). However, this is problematic since cyanobacteria have undergone morphological changes over the period induced by culture environmentally conditions (Hoffmann, 1988; Rippka *et al*., 1979; Stanier *et al*., 1971). Furthermore, selective culturing conditions may suppress the diversity of strains within a culture (Lu *et al*., 1997). The other characteristics such as photosynthetic pigment content, lipid composition and differentiated cell structures that may also change. Moreover, some strains may lose some important features such as gas vesicles or form of the colony during long-term laboratory cultivation, which complicates identification (Rajaniemi *et al*., 2005).

Anagnostidis & Komárek, (1990) and Anagnostidis & Komárek (1988) have estimated that more than 50% of the strains in culture collections are misidentified. Molecular data has provided basic criteria for cyanobacterial taxonomy; however, a correct phylogenetic system can only be constructed by combining genetic data with the last 150 years of cyanobacterial diversity research (Komárek, 2006). Hence, new isolates should be studied by combined "polyphasic" approach. These include both phenotypic information, such as morphological, ecological, staining behaviour, and chemotaxonomic characteristics e.g. cell wall compounds, fatty acids, quinones, *etc*., and genetic properties, such as DDH value, GC content and 16S rRNA gene sequence identity with other closely related species with validated names (Ballot *et al*., 2008; Bravakos *et al*., 2016; Sentausa & Fournier, 2013).

2.3 IDENTIFICATION OF CYANOBACTERIA USING MOLECULAR METHODS

2.3.1 Phylogenetic Marker Genes and Sequence Analysis

Phylogenetic studies have shown that the morphological classification of cyanobacteria occasionally conflicts with genetic analysis (Nowruzi *et al*., 2012; Rajaniemi *et al*., 2005). In recent decades, the use of molecular methods has become necessary for characterisation of cyanobacteria and the assessment of evolutionary relations amongst them. Cyanobacteria possess a ribosomal ribonucleic acid (rRNA) subunit made up of three genes; the 16S small subunit (SSU), 23S large subunit (LSU) and the 5S subunit, each separated by an internal transcribed spacer region (ITS). The 16S rRNA gene is commonly regarded as one of the most commonly used genetic marker and a valid criteria for determining relationships between closely related species or genera (Rajaniemi *et al*., 2005). The 16S rRNA gene can be effectively used to distinguish between broad taxonomic groups as well as individual species. In the latest edition of Bergey's Manual of Systematic Bacteriology, it is the basis for systematic assignment (Sentausa & Fournier, 2013). In 1997, a set of oligonucleotide primers for the specific amplification of 16S rRNA gene from cyanobacteria and plastids by PCR was developed and verified (Nübel *et al*., 1997). The GenBank has been populated with several complete and partial 16S rRNA gene sequences (over 6000) from both axenic and non-axenic cyanobacteria strains. The RDP (Ribosomal Database Project; http://rdp.cme.msu.edu/) is a database that offers an updated and consistent ribosomal related data, largely 16S rRNA sequences of bacteria and archaea (Cole *et al*., 2014). Using the RDP tool Browser, there are 3,356,809 16S rRNA (updated on September 30, 2016).

The 16S rRNA gene sequence identity of two strains with >99% indicates they are members of the same species, whereas <98.7% is regarded as novel taxa and <95% identity potentially representative of a new genus (Sarethy *et al*., 2014; Sciuto & Moro, 2015; Větrovský & Baldrian, 2013). The 16S rRNA gene has several interesting properties which encourages its application in phylogenetic studies which include: (i) rRNAs are universal molecules, present in almost all bacteria; (ii) the nucleotide sequence and secondary structures are highly conserved, thus, it evolves at a different rate in all organisms which is highly useful for comparison closely related strains; (iii) the 16S rRNA gene is a long molecule, containing about 1500 nucleotides and abundant in cells; (v) it is easy to extract, identify and sequence; (vi) there has been no reported

horizontal gene transfer (HGT) ; (vii) it is a multi-copy gene, which increases the detection sensitivity (Janda & Abbott, 2007; Patwardhan *et al*., 2014; Smit *et al*., 2007; Sentausa & Fournier, 2013; Shi & Falkowski, 2008; Ludwig *et al*., 2001).

It has been reported that several organisms with identical 16S rRNA gene sequences have significant sequence divergence in protein-encoding genes (Case *et al*., 2007; Pernthaler & Pernthaler, 2005; Schirrmeister *et al*., 2012). Thus, owing to the limited resolution between closely related species, species definition cannot be based solely on the 16S rRNA gene sequences (Stackebrandt & Goebel, 1994). There is a growing interest in the use of other protein-encoding genes for accurate classification of cyanobacteria. Good marker genes must fulfil the following criteria: (i) universal distribution in all prokaryotes, (ii) in a single copy within a genome, and (iii) appropriate information content. Genome sequences comparisons revealed less than one hundred good marker genes in cyanobacteria (Sentausa & Fournier, 2013a). A useful marker in the taxonomy of cyanobacteria is the 16S-23S ITS region which is more suitable for resolution at the genus level since it possesses enough variability (Boyer *et al*., 2001; Iteman *et al*., 2000). Several other housekeeping genes such as *dnaJ, dnaK, nifH*, *nif*D, *gyrB, recA*, *rop*C1 and *rpoB* have been used in multilocus sequence (MLSA) (Glaeser & Kampfer, 2015; Henson *et al*., 2004; Sciuto & Moro, 2015; Seo & Yokota, 2003). These genes encode core metabolic enzymes and are present in all of the organisms. In MLSA studies, partial sequences of housekeeping genes *i.e.* genes coding for proteins with conserved functions are used to generate phylogenetic trees and subsequently deduce phylogenies. (Dyble *et al*., 2002; Gaget *et al*., 2011). In addition, the *cpcBA*-IGS gene encoding for the blue light-harvesting accessory pigment (C-PC) and intergenic spacer (IGS) between the *cpcB* and *cpcA* have also been targeted for phylogenetic studies of cyanobacteria (Robertson *et al*., 2001). The IGS is selected as a potentially highly variable region of DNA sequence useful for the identification of cyanobacteria to the strain level (Dyble *et al*., 2002). However, phylogenetic analyses based on *cpcBA*-IGS take a substantial amount of time and effort. Even though MLSA has become an accepted and widely used method in prokaryotic taxonomy, this molecular technique also has limitations which have become apparent. In comparison to the 16S rRNA gene database, the sequence database of the other marker genes is limited. Furthermore, the evolutionary history of any single gene may differ from the

phylogenetic history of the whole organism. Therefore, it is evident that full-genome comparisons are essential for the identification of novel taxa (Jones, 2012).

2.4 WHOLE-GENOME SEQUENCING

Genome sequencing aims to determine the entirety of an organism's genetic information, which includes both the coding sequences (genes) and non-coding sequences of the DNA or RNA. Genome sequencing had been started since the seventies of the last century soon after the invention of the Sanger sequencing method (Heather & Chain, 2016). This field of research has rapidly developed and has led to the interdisciplinary scientific field of bioinformatics (Hagen, 2000). Not only do genomes allow for the discovery of more genes but they also help us to understand how genes and genomes are evolving, as this can provide clues to gene function.

The NGS platforms currently commercially available are the high-end instruments and bench-top instruments (Sentausa & Fournier, 2013). The number of reads produced in a given instrument run and the length of those reads is the common criteria used to compare platforms. Other specifications used include the sample preparation and run time, cost per run/ base, sample preparation cost, etc. The high-end instruments can produce long reads and capable of producing thousands of prokaryotic genomes per run and is very costly whereas the bench-top instruments are fast, modestly priced and have lower throughput (Land *et al*., 2015; Loman *et al*., 2012). Currently the smallest, most extensively used benchtop NGS platforms is the MiSeq, owing to the fast turn-around time (4 h to produce 15 Gb of data), high output data (25 M single reads and 50 M paired-end reads) and relatively cheaper cost. Not only does it perform genomic DNA sequencing amplification in a single run, but it is also capable of performing onboard cluster generation and data analysis, including base calling, alignment and variant calling (Ravi *et al*., 2018). Mapping or reference assembly is whereby two strains share high sequence identity across their genome. (Levy & Myers, 2016; Liu *et al*., 2012). When a closely related, fully sequenced genome is available, the assembly can be easily performed by extracting the homologous sequence and assembling it (Chen & Pachter, 2005). However, in many species, it is reported that the 'core' genes that are shared between closely related strains also consists of a significant number of 'dispensable' genes. Therefore, the assembly of the entire genome without a suitable reference strain (known as *de novo* assembly) is a far more problematic (Ricker *et al*., 2012).

2.5 GENOME COMPARISONS METHODS AND SPECIES GENOME CONCEPT

In order to understand gene function and genome evolution comparisons of the sequenced genomes are crucial (Kurtz *et al*., 2004). The pairwise sequence comparison methods using the Basic Local Alignment Search Tool (BLAST) and FASTA have important applications in finding the evolutionary relationships and functions of thousands of proteins from hundreds of different species (Ali *et al*., 2013; Kurtz *et al*., 2004). A new strategy referred to as 'genome blast distance phylogeny' (GBDP) combines various methodologies to produce a phylogenetic tree/ network from a given set of whole-genome data (Henz *et al*., 2005). The GBDP begins with pairwise comparison using BLAST, thereafter, a distance matrix is calculated and finally processed by a distance-based phylogenetic method to produce a phylogenetic tree or network (Henz *et al*., 2005)

A large number of sequenced genomes available resulted in comparative genomics and pan-genome analysis been developed (Guimarães *et al*., 2015). Pan-genome or species genome concept which refers to the full repertoire contained within a species (Duccio & Hervé, 2015). Species genome comprises of all the genes existing in any strain of a species. It is mainly divided into (i) a core set of genes (present in 95% or all strains), (ii) auxiliary or dispensable set of genes, present in only in some strains of the species and (iii) species/strain-specific genes, present in a single genome (Guimarães *et al*., 2015; Haft, 2015). Thus, pan-genome might be orders of magnitude larger than any genome of a single organism when strains of the species have a large number of unique dispensable genes (Tettelin *et al*., 2005). The overall relatedness of the genomes is determined primarily by the similarities in gene content, as well as the nucleotide similarity of shared genes. The DNA base composition is a genotypic character has been used for classification purpose (Wilmotte & Herdman, 2001).

In silico methods based on genome sequencing been founded as an alternative to wet-lab DNA–DNA hybridisation (DDH) (Meier-Kolthoff *et al*., 2013). The whole genomic (DDH) is considered as the standard technique for species identification (Rajendhran & Gunasekaran, 2011). In the last 40 years, it has been the measurement of overall genetic similarity amongst strains, assessed by the degree to which their genomes hybridise under standard conditions (Cho & Tiedje, 2001; Gevers *et al*., 2005). The Committee on Reconciliation of Approaches to Bacterial Systematics

reported that strains that show ≥70% DDH values and <5% difference in their melting temperature (ΔTm) are considered to belong to the same species (Rajendhran & Gunasekaran, 2011; Rosselló-Mora & Amann, 2001; Walter *et al*., 2017). The average nucleotide identities (ANI) and average amino acid identities (AAI) are used to measure the genetic and evolutionary relatedness among strains. It has been proposed as a new standard for defining microbial species (Martens *et al*., 2008; Thompson *et al*., 2013). Two strains are considered to belong to the same species if they share a ≥ 96% ANI value, which is equivalent to the 70% DDH value (Konstantinidis & Tiedje, 2005). Another method used is the genome-to-genome distance calculator (GGDC) has been used. The GGDC determines a set of high-scoring segment pairs (HSPs) or maximally unique matches (MUMs) between the genomes, calculates the genomic distance and converts the distance to percentage similarities (Auch *et al*., 2010). The distance calculation is based on the total length of all high-scoring segment pairs identified by a BLAST search of the genome (Auch *et al*., 2010; Ricker *et al*., 2012).

2.6 CYANOBACTERIA GENOMES

In 1996, *Synechocystis* sp. PCC 6803 became the first cyanobacterium to have its genome published (Kaneko *et al*., 1996). The National Facility for Marine Cyanobacteria, sponsored by the Department of Biotechnology, Govt. of India is devoted to cyanobacterial research, with special attention to marine cyanobacteria. The Cyanobacterial KnowldegeBase (CKB), http://nfmc.res.in/ckb/index.html a freely accessible, comprehensive database resource covering information pertaining to completely sequenced cyanobacterial species (Karp *et al*., 2005; Peter *et al*., 2015). The growing number of cyanobacterial genomes (to date 90 finished genome and several others in progress) in public databases CyanoBase, JGI http://genome.microbedb.jp/cyanobase enables the detailed investigation of the distribution of genes. The availability of genome sequences provides the opportunity to investigate the phenotypical traits of strains amenable to genetic engineering (Thiel, 2006). The increasing number of completely sequenced cyanobacterial genomes allows researchers to reconstruct the metabolic and signalling networks thus, provide a greater opportunity for understanding the metabolic organisation of the cyanobacterial species in diverse environments. Furthermore, the availability of genome sequences allows researchers to create microarrays to analyse gene expression and to easily clone and express any gene (Galperin & Koonin, 2010). Some of the

major resources that provide the basic information about cyanobacteria, current happenings in cyanobacterial research, the methods used in cyanobacteriology include CyanoNews (https://cyanonews.vcu.edu/), Cyanosite (http://www-cyanosite.bio.purdue.edu/) and CyanoDB (http://www.cyanodb.cz/).

Cyanobacteria are diverse in terms of their morphology, physiology, metabolism and functionalities which are also reflected on a genomic level. Sequencing has demonstrated hat genomes within the cyanobacterial phylum vary considerably in several aspects (Sundh *et al*., 2011). Larsson *et al*. (2011) reported that cyanobacterial genomes vary greatly with regards to the size (~1.4-9.1 Mbp), GC content (31-63%), the number of protein-coding genes (1214-8446) and coding nucleotide proportion (52-94%). The list of cyanobacteria genomes and related information is displayed in Appendix 1. The unique characteristics of each cyanobacteria genome also depend on the niche-specific environmental conditions (Prabha *et al*., 2016). Thus, the genome can be either the result of neutral processes or due to the adaptation to the varying environmental factors an organism is exposed to (Alvarenga *et al*., 2017). Two adaptation strategies include (i) broad adaptation through the increases gene families because of genomic expansion, and (ii) genomic reduction due to the removal of dispensable genes required for the adaptation to a specific function (Larsson *et al*., 2011; Zhang *et al*., 2016b).

The genetic features which include genome size, GC percentage, gene number, and evolutionary rates are subjected to change due to selection pressures (Zhang *et al*., 2016b). The core genome is made up of a set of highly conserved, essential genes coding for complex protein structures and indispensable biochemical pathways resistant to HGT (Alvarenga *et al*., 2017). Cyanobacteria predominately acquire novel genes *via* HGT, which also plays a major role in the molecular diversity of cyanobacteria (Ricker *et al*., 2012; Soucy *et al*., 2015). Many cyanobacteria genomes contain a relatively high amount of repeated sequences, which affects completing the assembly of the cyanobacterial genome. The large amounts of repeated sequences pose a great challenge for assembling algorithms, which clarifies the reason why ±90% of the cyanobacteria genomes available are permanent or temporary drafts.

2.7 HALOTOLERANT AND HALOPHILIC CYANOBACTERIA

Cyanobacteria isolated from marine environments are classified based on their major ion requirements for growth. They are classified as halotolerant, moderately halophile and extreme halophile depending upon their salt concentration requirements. Halotolerant isolates tolerate saline environments whereas halophiles require salt and known to grow best in media containing less than 0.2 M sodium chloride (NaCl) (Kanekar *et al*., 2012). Halophiles are further classified based on their optimal NaCl concentration for growth: 20–30% for extreme, 5–20% for moderate and 1–5% slight halophiles (Paul & Mormile, 2017). Other isolates have obligate requirements for increased concentrations of sodium, magnesium, calcium, and chloride that prevent their growth in freshwater media even when supplemented with 0.6 M NaCl (Schneegurt, 2012).

Hypersaline environments are typical extreme habitats found to have high salt concentration, as well as may have low oxygen concentrations, high or low temperatures, and are sometimes very alkaline. Halophiles thrive in environments with high salt thus they have evolved phenotypic traits allowing adaptation and survival under these environmental conditions (Oren *et al*., 2009). Other factors that may affect their biodiversity are low nutrient availability, pressure, light or the presence of toxic compounds or heavy metals (Rampelotto, 2010; Ventosa, 2006; Vera-Gargallo & Ventosa, 2018). Marine cyanobacteria are abundantly found to inhabit in warmer temperate and tropical regions. As frequent colonisers of hypersaline environments, cyanobacteria are found in salt pans and salt marshes and are able to grow in combined salt concentrations as high as 3-4 M (Oren, 2012). Cyanobacteria such as filamentous *Microcoleus* (*Coleofasciculus*) *chthonoplastes* and coccoid cyanobacterium *Aphanothece halophytica* often dominate in microbial mats that are found in higher salinities. Some of the most extreme saline habitats, where cyanobacteria occur include hypersaline lagoons, solar lakes and hypersaline sulphur springs (Farias *et al*., 2017). The Dead Sea (on the border between Israel and Jordan), Great Salt Lake (Utah), Salton Sea (California), as well as some cold hypersaline lakes in Antarctica and alkaline lakes such as Lake Magadi or the lakes of Wadi Natrun in East African have been previously studied as shown in Table 1 (Ventosa, 2006).

Table 1: Cyanobacteria inhabiting hypersaline environments

Name of habitat	Location	Salinity conditions	Cyanobacteria species	Reference
Petukhovskoe Soda Lake	Klyuchevskoi area of Altai Region, Russia	50 - 200 g/L	genera *Geitlerinema* and *Nodosilinea*	(Samylina & Zaytseva, 2019)
Dead Sea	Athalassohaline inland lake on the border between Israel and Jordan	Salinity is around 347 g/L and found to dominant with ions of Mg^2, Ca^{2+}, K^+ and Br^-.	*Aphanothece*, *Microcystis*, *Phormidium* and *Nostoc*	(Jacob *et al*., 2017; Hausler *et al*., 2014)
Lake Magadi,	Kenya	30% w/v and pH values of ~11.5.	*Synechocystis* sp., *Prochlorococcus* sp., *Arthrospira* sp. and *Oscillatoria*	(Muruga *et al*., 2014).
St. Lucia Estuary	largest estuarine lake in Africa	High salinities (>150g/L)	*Cyanothece* sp.	(Carrasco & Perissinotto, 2012; Muir & Perissinotto, 2011),
Saltern Petchaburi	Thailand	90-250 g/L	*Aphanothece* cf. *Cyanosarcina* sp., *Chroococcus halophytica, Coleofasciculus* cf. *chthonoplastes, Halothece* sp., *Oscillatoria lloydiana, and Spirulina subsalsa*	(Chatchawan *et al*., 2011)

Name of habitat	Location	Salinity conditions	Cyanobacteria species	Reference
Guerrero Negro, Baja	California	60 and125 g/L,	*Microcoleus chthonoplastes Phormidium*, *Spirulina*, *Aphanothece* and *Synechococcus*	(Kirk Harris *et al*., 2012; Ley *et al*., 2006)
Lake Vanda	Wright Valley, Antarctica	100 g/L	*Synechococcus* sp. and *Phormidium* typ	(Zakhia *et al*., 2008)
Saltpans	Vedharnyam to Mandapam	48-185 g/L	*Oscillatoria willei, O. salina, O. subbrevis, O. laete-virens, Phormidium tenue, Microcoleus chthonoplastes Spirulina subsalsa and S. labyrinthiformis,*	(Nagasathya & Thajuddin, 2008)
Hamelin Pool at Shark Bay,	Western Australia		*Cyanothece, Leptolyngbya, Plectonema, Pleurocapsa Microcoleus, Nostoc, Synechococcus, Symploca,* and *Xenococcus,*	(Nagasathya & Thajuddin, 2008)
Wadi El Natrun	Sahara Desert, northwest of Cairo,	91 and 393.9 g/L	*Oscillatoria limnetica*, *Aphanothece halophytica*, and *Lyngbya*	(Mesbah *et al*., 2007; Garlick *et al*., 1977).
Lake Bonney	Dry Valleys of Antarctica	Salt concentration of about 100 g/L	*Lyngbya martensiana, Oscillatoria cf. subproboscidea, Nostoc, Synechococcus* and *Phormidium frigidum*	(Laybourn-Parry & Pearce, 2007)

Name of habitat	Location	Salinity conditions	Cyanobacteria species	Reference
The Salton Sea	Inland body of water in California.	Brackish to hypersaline	filamentous *Anabaena*, *Oscillatoria* and *Microcystis,* and the picoplanktonic *Synechococcus*	(Carmichael & Li, 2006).
Salins-de-Giraud	Mediterranean coast of France	70-100 g/L	*Microcoleus chthonoplastes, Halomicronema excentricum, Microcystis, Chroococcus, Gloeocapsa,* and *Synechocystis*	(Fourcans *et al*., 2004)
Solar Lake	Sinai, Egypt	Dependent on the season, the salinity of the lake various from 41 g/L (in autumn-winter) up to ~180 g/L in summer	*Aphanocapsa concharum*, *Aphanothece* spp, *Chroococcidiopsis* sp., *Cyanothece* spp., *Dactylococcopsis* spp, *Entophysalis* sp., *Gloeothece* sp., *Johannesbaptistia pellucida*, *Lyngbya* spp, *Microcoleus chthonoplastes*, *Oscillatoria* spp, *Phormidium* spp, *Pleurocapsa* sp., *Pseudanabaena catenata*, *Spirulina* spp., and *Synechococcus* sp.	(Cohen *et al*., 1980; Wieland & Kühl, 2000).
Lake Hayward	South-West Australia	60-20 g/L	*Cyanothece, Oscillatoria* and *Spirulina* sp.	(Burke, 1995)
Great Salt Lake	Utah, the northern part of USA	Hypersaline northern arm with a salinity up to 300 g/L and a less saline southern arm (<120 g/L)	*Aphanothece halophytica Phormidium* or *Oscillatoria*, *Microcoleus lyngbyaceus*, *Spirulina major* and *Nodularia spumigena*	(Post, 1977)

2.8 GENE REGULATION, STRESS RESPONSE AND MECHANISMS

2.8.1 Salt Acclimation and Responses to Nutrient Stress

Halophiles have adapted cell structures and metabolic functions to suit the harsh conditions found in hypersaline environments. Strict halophilic microorganisms counteract water loss due to high osmolarity by accumulating K^+ ions within their cells (Madern *et al.*, 2000). Through this strategy, these microorganisms have evolved enzymes and other proteins that are stable under extreme saline conditions. An alternative strategy employed by the halophilic and halotolerant species is to accumulate compatible organic solutes, osmolytes, in the form of sugars, amino acids and polyols. In addition to serving as osmotic regulators, these osmolytes also help maintain the stability of halophilic proteins (Roberts, 2005). Besides the impact of constant osmotic pressure, halophilic bacteria must have the ability to adapt to fluctuating salt conditions, as salinity can drastically change with rainfall and evaporation events.

It is extremely valuable to fully understand the salt response as well to as understanding the difficulties associated with the presence of salts at the molecular level in cyanobacteria (Pandhal *et al.*, 2008). Low concentrations of Na^+ ions are required in the cells for various cell functions including pH regulation, ammonia and CO_2 fixation, photosystem II (PSII), water photolysis and even transport of compounds (Pogoryelov *et al.*, 2003). During ionic stress, Na^+ and Cl^- ions enter the cell *via* the chemical and electrochemical gradient due to ion imbalance, affecting enzyme activities and metabolism. Additionally, extrinsic proteins dissociate from both PSII and PSI, with the resultant irreversible inactivation of PSI and PSII machinery (Allakhverdiev & Murata, 2008). Exposure to high salinity initiates immediate activation and/or long-term adaptation of several processes in cyanobacteria: (i) biosynthesis and uptake of solutes; (ii) increase in the (PSI/PSII) ratio, (iii) increase cyclic electron transport activity enhances ATP production used to fuel P-type ATPases; (iv) modifications of membrane lipid composition: and (v) active extrusion of Na^+ ions (Francoise *et al.*, 1996; Hagemann, 2011; Oren *et al.*, 2009).

The immediate response by *Synechocystis* cells to salt stress is well researched, the two strategies are the "salt-in-strategy" and "salt-out-strategy" (Schubert *et al.*, 1993). During the initial stages

of salt shock, increasing Na^+ ion uptake causes membranes to depolarisation thus resulting in the uptake of Cl^- across a chemical gradient *via* passive transport. Immediately afterwards the Na^+ export mechanisms are activated and toxic ions are removed from the metabolically active part of the cell (Hagemann, 2011). Na^+/H^+ antiporters are fundamental membrane proteins that transport Na^+ and H^+ across the cell membrane. The subsequent response is the accumulation of compatible solutes such as sugars, amino acids, polyols, betaines, ectoines and peptides either by synthesis or uptake. The "salt-out-strategy" works by keeping the internal ion concentration low, the cells accumulate compatible solutes in the form of sugars, amino acids and polyols that do not interfere with metabolism at high concentrations and thereafter, they actively export inorganic ions into the cytoplasm (Pade & Hagemann, 2015). In addition to serving as osmotic regulators, these osmolytes also help maintain the stability of halophilic proteins (Roberts, 2005). Compatible solutes largely stabilise proteins and membrane structures by restoring the osmotic potential (Rai *et al*., 2013). The major compatible solute in cyanobacteria strains with low salt tolerance (up to 0.7 M·NaCl) is sucrose and/or trehalose. Cyanobacteria of moderate salt tolerance (up to 1.7 M·NaCl) accumulate mainly glucosylglycerol (GG) and glucosylglycerate (GGA), whereas halophilic strains that tolerate up to 3 M of NaCl, are reported to synthesise glycine betaine and glutamate betaine (GB) (Kolman *et al*., 2015; Sinetova & Los, 2016). Trehalose is commonly found in desiccation-tolerant cyanobacteria strains such as *Nostoc* or *Scytonema* sp. and reported to have superior protective features for membranes (Hagemann, 2011). Marin *et al*. (2004) identified the complete set of salt- and osmo-regulated genes following exposure of *Synechocystis* cells to salt stress. The genes encode proteins for salt acclimation included genes for: (i) enzymes involved in GG biosynthesis (ggpS, stpA, glpK, and glpD); (ii) ABC-type translocator for compatible solutes (ggtABC); (iii) Na+/H+ antiporters (nhaS1–5 and nhaS6) and (iv) DNA-binding stress protein (slr1894) (Tsunekawa *et al*., 2009).

Table 2: Genes induced by stress factors in cyanobacteria

Genes	Protein	Function	Stress						
			Salt	Osmotic	Temperature	Light	UV	Oxidative	Nutrient
hik33	Hik33	Sensory histidine kinase 33			+				
*hik*34	Hik34	Sensory histidine kinase 34	+	+	+		+	+	
hik10			+	+					
hik41			+	+					
hik16			+	+					
hik31	Hik31	Two-component sensor histidine kinase			+				
hik2			+	+					
hik3	Hik 3	Phytochrome-like two-component sensor histidine kinase			+				
rre5	Rre5	Response regulator Rre5			+				
sigB	Sig B	RNA polymerase σ factor B	+	+	+		+	+	
sigC	SigC	RNA polymerase σ factor D			+				
sigD	SigD	RNA polymerase σ factor D	+		+	+	+	+	
rpoA	RpoA	RNA polymerase *α* subunit σ70		+	+	+			
groES	GroES	HSP 10 kDa chaperone	+	+	+	+	+	+	
groEL1	GroEL1	HSP 60 kDa chaperone 1	+	+	+	+	+	+	
groEL2	GroEL2	HSP 60 kDa chaperone 2	+	+	+	+		+	
hspA	HspA	HSP 17 kDa	+	+	+	+	+	+	
dnaK2	DnaK2	HSP 70 kDa	+	+	+	+	+	+	
dnaJ	DnaJ	HSP 40 kDa	+	+	+		+	+	
htpG	HtpG	HSP 90 kDa	+	+	+	+	+	+	

Genes	Protein	Function	Stress						
			Salt	Osmotic	Temperature	Light	UV	Oxidative	Nutrient
clpB1	ClpB1	HSP 100 kDa chaperone	+	+	+	+	+	+	
htrA	HtrA	Serine protease	+	+	+		+	+	
chrR	ChrR	RNA helicase	+	+	+			+	
ctpA	CtpA	Ce-terminal processing Protease			+	+	+	+	
Sll1621	PrxA	Peroxiredoxin	+		+	+	+	+	
smtA	SmtA	S-adenosylmethyonine methyltransferase	+		+	+		+	
slr1674	Slr1674	Involved in thermal defence of PS II	+		+	+	+	+	
Ocp	Ocp	Orange carotenoid-binding Protein	+		+	+	+	+	
sbtA	SbtA	Na-dependent bicarbonate Transporter	+		+				
sodB	SodB	Superoxide dismutase	+	+	+	+	+	+	
sll0528	Sll0528	Metalloprotease (site-2-protease)	+	+	+	+	+	+	
hypA1	HypA1	Hydrogenase synthesis protein	+	+	+	+	+	+	
ssl3044	Fdx	Ferredoxin, hydrogenase Component	+	+	+	+	+	+	+
nblB1	NblB1	Phycobilisome degradation Protein	+	+	+	+	+	+	
isiA		codifies for an additional antenna system around PSI							+
isiB		a gene coding for flavodoxin, which is a flavin-containing protein that replaces ferredoxin							+
idiA		integral subunit of PSII							+

Genes	Protein	Function	Stress						
			Salt	Osmotic	Temperature	Light	UV	Oxidative	Nutrient
dpsA		inducible DNA-binding protein							+
HliA,B,C		inducible protein	+	+	+	+	+	+	+
ndhR		regulator of transcription of the ndhF3 operon							
rnpB		RNase P							
crhR,		encodes an RNA helicase			+				
PhoA,		Alkaline phosphatases	+						+
psaA		PSI P700 Chl a apoprotein A1							
nblB	NblB	Phycocyanobilin lyase	+	+	+	+	+	+	+
ggpS		glucosylglycerol-phosphate synthase							
glpD		glycerol-3-phosphate dehydrogenase							
cbiA	CbiA	Involved in cobalamin biosynthesis			+				
Sll483	*Sll483*	Salt induced periplasmic protein	+	+	+	+	+	+	+

Cyanobacteria have also evolved very efficient mechanisms to deal with nutrient (nitrogen, sulphur, iron and CO_2) limitations. Nutrient deficiencies trigger several responses which include the upregulation of acquisition systems to reduction/substitution of structures/molecules, Fe deficiencies cause a decrease in the quantities of membranes, PBS, cell size, as well as ultrastructural and pigment changes (Sherman & Sherman, 1983). The PSI and PSII contents decrease, however, the PSII/PSI ratios increase and induce the synthesis of a Chl-binding protein (Chen *et al*., 2018). Furthermore, the expression of isiA gene is also induced and flavoxodin in synthesised. Several genes encoding for different pathways including respiration, photosynthesis, nitrogen metabolism, glycolysis, tricarboxylic acids cycle, amino acid synthesis, synthesis of toxins and antioxidant defences are also triggered (González *et al*., 2018).

Sensors transfer the signal to the transducers, which in turn activate stress-responsive genes. Finally, stress-specific proteins and/or metabolites are synthesised to help the cells to adapt or acclimate to the new environment (Los *et al*., 2010). The Hik33-Rre31 TCS regulates the expression of hyperosmotic stress-specific genes *i.e*. fabG and gloA as well as oxidative stress-specific genes (pgr5, nblA1 and nblA2). Hik33 is involved in the sensing of cold, hyperosmotic, oxidative and salt stress, as well as regulates the expression of nblA1 and nblA2 genes involved in PBS degradation during nitrogen starvation (Richaud *et al*., 2001). Hik34 acts as a sensor of signals due to heat, salt, and hyperosmotic stress, it also controls the expression htpG gene which is induced in the presence of H_2O_2 (Kanesaki *et al*., 2007; Suzuki *et al*., 2005). It acts as a positive regulator under salt or hyperosmotic stress, a negative transcriptional regulator during heat shock, and an autoregulator under oxidative stress (Mironov *et al*., 2019). Hik3 (or PlpA – phytochrome-like protein) is equipped with PAS/PAC and GAF sensory domains (Golden, 2004; Kahlon *et al*., 2006). Whereas, Hik31 is involved in the regulation of autotrophic growth and controls photosynthesis and ribosomal proteins as well as responses to light and resistance to cations, Cd^{2+} (Mironov *et al*., 2019).

Chaperone proteins recognise unfolded and aggregated proteins and thereafter try to refold them in their native functional state or assist in their removal. Several types of chaperones have been described which include: hsp60 (groEL), hsp70 (dnaK), hsp90 (htpG), and hsp104 or hsp101 (clpB), groES, clpC/X, and ATPase AAA-2 (Saibil, 2013). The HSP genes and proteases are activated by high temperature, salinity, osmotic, oxidative, and UV-B and light stress (Rajaram *et*

al., 2014). Additionally, major chaperones belonging to the DnaK system, such as dnaJ gene that was shown to respond to various stress conditions *viz*., H_2O_2, high light and iron deficiency (Mironov *et al*., 2019). Two genes that encode alternative subunits of σfactors of RNA polymerase, sigB, and sigD, three hli genes, sodB for superoxide dismutase are also activated by several stress factors. SigA gene encodes the primary sigma factor, essential for cell viability. SigB is involved in the general stress response, and control the stress-induced expression of hspA, which encodes a small heat shock protein (HSP) (Imamura & Asayama, 2009); SigC plays a role in nitrogen regulation and stationary phase transition; sigD is induced by cold, osmotic, salt, high light and inorganic carbon limitation.

2.8.2 Temperature Stress Response

Low temperature is reported to induce regulatory genes hik3 and hik31 and DNA-binding transcriptional regulators *i.e.* rre5 and sfsA. Rre5 belongs to a PatA subfamily of TCS, which are mainly associated with pH homeostasis and involved in CO_2 uptake. SfsA-like protein is involved in the regulation of sugar catabolism (Sinetova & Los, 2016). Low temperature stress induces many genes that are responsible for the maintenance of the membrane fluidity, transcription and translation of the cells. Low-temperature stress activates transcription of three hli genes as well as *rbp*A for RNA chaperone, *rpo*A for RNA polymerase, *sig*D the σ subunits of RNA polymerase, *cyt*M for the alternative form of cytochrome C.

High temperatures suppress genes involved in the biosynthesis of pigments, photosynthesis, and lipid metabolism (Zorina *et al*., 2011). High temperatures stress induces the following genes: htrA for protease; sigB for the σ factor of RNA polymerase; HSPs and chaperones (hspA, groES, groEL1, groEL2, dnaJ, htpG, dnaK2, clpB1); hik34 for sensory histidine kinase and sodB for superoxide dismutase.

2.8.3 Light and Oxidative stress

When cyanobacteria are exposed to high light D1 protein is synthesised te replace the damaged D1 and to help the maintenance of PS II homeostasis. However, prolonged high light intensity results in irreversible photoinhibition. During high PAR or UV radiation exposure, increased expression of desA was reported, related to the unsaturation of fatty acids. In cyanobacteria, reactive oxygen species (ROS) are formed during respiratory metabolism and at the receptor–side of the electron transport chain during photosynthesis (Hsieh & Pedersen, 2014). Electrons that have high energy state are transferred to molecular oxygen (O_2) to form ROS. The ROS include singlet oxygen, superoxide radicals, hydrogen peroxide and hydroxyl radicals (Latifi *et al*., 2009). Chloroplast and microbodies are the sites for the production of ROS. The ROS ($1O_2$, O_{2-} and HO•) are produced in PSII reaction centre. The ROS can damage the PSII by damaging the D1 protein and preventing the repair of damage to PSII (Takagi *et al*., 2016). The reduction site of PSI is also the site of O_{2-} the production *via* the Mehler reaction coupled with the formation of ATP without NADPH. During severe light and oxidative stress conditions, the ROS production is significantly enhanced which causes damage to both PSII and carbon fixation process (Foyer, 2018).

Cyanobacteria have developed efficient defence systems to protect themselves against oxidative stress. The imperative defence mechanisms include the production of: (i) carotenoids and iron stress-induced protein (IsiA) that dissipate the excessive light energy as heat; (ii) antioxidant enzymes complexes such as superoxide dismutase (SOD), catalase (KatG) and peroxiredoxins (Prx) that degrade ROS molecules when cells are metabolically active; (iii) non-enzymatic peroxide detoxifying compounds such as pigments, ascorbate, α–tocopherol and glutathione; (iv) the combination of UV absorbing pigments such as scytonemin which is deposited in EPS sheaths, and intracellular MAA derivatives; (v) D1 protein turnover and PSII repair, and (x) small CAB–like proteins and high light-inducible polypeptides that stabilise PSI and PSII (Birben *et al*., 2012; Latifi *et al*., 2009). Since Chl and PBPs act as photosensitisers *i.e.* they produce ROS, cyanobacterial cells under intensive light may reduce their content by down-regulating pigment synthesis.

2.9 ROLE OF PHYCOBILIPROTEINS IN PHOTOSYNTHESIS

The process of photosynthesis is the conversion of light energy into chemical energy by the reduction of CO_2 and water into glucose and O_2 (Masojidek *et al*., 2013). Green microalgae harvest light by using the Chl in antenna complexes. However, chlorophyll molecules only absorb light in the blue and red region known as the photosynthetically active region (PAR) of the light spectrum. A considerable amount of light-energy is unused *i.e.* "green gap" between ~500-600 nm. By using PBPs to efficiently absorb light in the visible range of 500-660 nm cyanobacteria, red algae and cryptomonads have overcome this limitation (Glazer & Clark, 1986; Sonani *et al*., 2016; Tandeau de Marsac, 2003).

The PBSs transfer absorbed light primarily to PSII with an energy transfer efficiency of >90% (Gantt, 1980). Pigmented PBPs and non-pigmented linker proteins assemble into massive PBS attached in regular arrays to the stromal side of thylakoid membranes as seen in Figure 1. The PBPs make up about 85% of the mass of a PBS, and the colourless linker proteins (LPs) that are and makeup 15% of the mass of a PBS (Tandeau de Marsac, 2003).

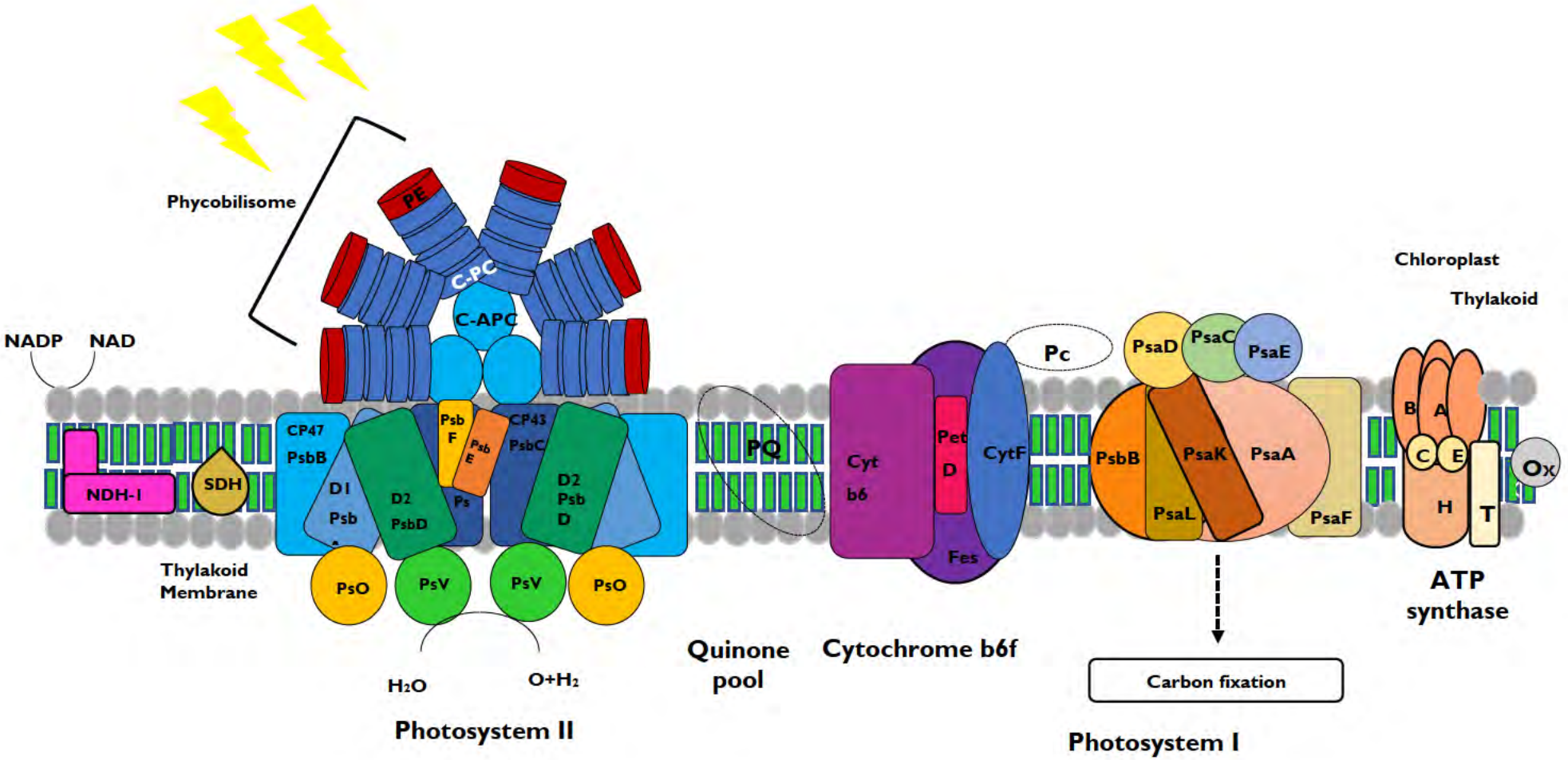

Figure 1: Schematic representation of the intersecting photosynthetic and respiratory electron transport pathways in thylakoid membranes in cyanobacteria. Abbreviations of complex systems: cyt b6f, the cytochrome b6f complex;; NADP(H), nicotinamide – adenine dinucleotide phosphate (reduced form); NDH-1, type 1 NADPH dehydrogenase; Ox, terminal oxidase; PC1, plastocyanin; PQ, plastoquinone; SDH, succinate dehydrogenase. Protein abbreviations is found in Table 1. The enzymes are shown in red, and the compound in black.

2.10 STRUCTURE OF PHYCOBILIPROTEINS

The first structural studies of PBS between the 1960s and 1970s, which has led to insights on PBS function (Bryant *et al*., 1978; Gantt, 1975; Glazer & Clark, 1986; Glazer & Cohen-Bazire, 1971; Glazer & Fang, 1973). Gantt & Conti (1966), coined the term PBS based on their size and shape as visualised by electron microscopy (EM). Structure of PBS can be divided into a central core and peripheral rods with a molecular weight ranging from 7 to 15 MDa to form a fan-shaped structure. The core of the PBS, composed of trimeric $(\alpha\beta)^3$ discs of PBPs stacked into cylinders, located on the cytoplasmic stromal side of the photosynthetic membranes. The basic building block of PBS's are the PBPs consists of the two α- and β-subunits, linker proteins and chromophores (Zhao & Qin, 2006). The monomers made up of the α- and β-subunits covalently binds the chromophores to conserved Cys residues and are further assembled into the core and the rods (Chang *et al*., 2015).

The brilliant colours of PBPs are primarily due to covalently bound open-chain tetrapyrrole chromophores bearing A, B, C and D rings called phycobilins (Kamble *et al*., 2018). The phycobilins include phycocyanobilin (PCB), blue; phycoerythrobilin (PEB), red; phycourobilin (PUB), yellow and phycoviolobilin (PVB), purple (David *et al*., 2014). These chromophores are generally bound to the polypeptide chain at conserved positions either by one cysteinyl thioester linkage through the vinyl substituent on the pyrrole ring A of the tetrapyrrole or occasionally by two cysteinyl thioester linkages through the vinyl substituent on both A and D pyrrole rings (Glazer & Clark, 1986; Sidler, 2004). Phycobiliproteins are divided into four major subgroups depending on their pigment compositions and spectral properties : (i) C-APC in the cores (λmax=652nm), (ii) C-PC in rods (λmax=620nm), and in some cases (iii) C-PE (λmax=560nm) and (iv) phycoerythrocyanin (PEC = λmax 575nm) in the rods, distal to the cores (Liu *et al*., 2005; Watanabe *et al*., 2012). The rods absorb mostly the higher energy photons (500-640nm) and transfer the energy to C-APC in the cores (Oren *et al*., 2009).

The basic monomer component (α- and β-subunits) forms trimers, which are further assembled into a hexamer mostly by interactions between α-subunits. The 3D crystal structures of C-PC and C-APC (Figure 2) show that each α- and β-subunits have eight α-helices namely X, Y, A, B, E, F, G and H with small loops whereby different chromophores can be attached at specific

cysteine residues (Table 3). Each chromophore can act as a light energy acceptor or donor. All PBPs contain the central bilin chromophore at the Cys-84 or equivalent position on both *α*- and *β*-subunits thus have very similar structures (Sidler, 2004). Although C-APC and C-PC have been reported to share high structural homology, they differ significantly with regards to type of PBP and physical structure *i.e.* either rods or core. The C-PC monomer carries three chromophores, while a C-APC monomer carries two chromophores. Rods and core are formed from the association between hexamers mainly due to the interactions between *β*-subunits as seen in Figure 2 (Elanskaya *et al*., 2018).

Table 3: Phycobiliprotein gene and protein names as well as attachment site and lyase

Name	**Symbol**	**Gene**	**Molecular weight (kDa)**	**Attachment site**	**Lyase**
Alpha subunit of C-PC	α^{PC}	CpcA	12-19.2	Cys-84-PCB	CpcE/CpcF
Beta subunit of C-PC	β^{PC}	CpcB	14-21	Cys-82-PCB Cys-153-PCB	CpcS-I/CpcU CpcT
Alpha subunit of C-APC	α^{APC}	ApcA		Cys-81-PCB	CpcS-I/CpcU
Beta subunit of C-APC	β^{APC}	ApcB		Cys-81-PCB	CpcS-I/CpcU
Allophycocyanin subunit beta-18	β^{18}	ApcF		Cys-81-PCB	CpcS-I/CpcU
Allophycocyanin subunit alpha-B	$\alpha^{AP\text{-}B}$	ApcD		Cys-81-PCB	CpcS-I/CpcU
Core-membrance linker protein	L_{CM}	ApcE		Cys-186	Autocatalytic
PC-associated linker	PC L_R	CpcC	24.8–32.6		
PEC-associated linker	PECL_R	PecC	31.3–31.5		
Rod capping linker	PC L_R	CpcD	7.8–9.9		
Rod–core linker	L_{RC}	CpcG	26.8–31.9		
Rod–core linker	L_{RC}	CpcH	30.4–30.8		
Rod–core linker	L_{RC}	CpcI	32.7		
APC–associated linker	L_C	ApcC	7.7–7.8		
Core–membrane linker	L_{CM}	ApcE	76.5–129.8		
PE-associated linker	PE L_R	CpeC	31.8–33.1		
PE-associated linker	PE L_R	CpeD	27.9–28.4		
PE-associated linker	PE L_R	CpeE	27.1–28.4		

Some cyanobacteria species contain C-PE on the end of the rods adjacent to C-PC for more efficient light capture. The central cavities of the rods and core contain additional proteins, *i.e.* LPs. The LPs is able to modify the spectral properties of the pigmented components and expected to have a structural role in mediating the interactions between PBPs (Tal *et al*., 2014). The LPs occupying both the rods and core are highly homologous and have similar structural and functional roles (Pizarro & Sauer, 2001). The PBPs are made of a central globin domain to which the chromophores are bound and a two-helix domain that mediates aggregation of *α*- and *β*-subunits (Figure 2) (Kupka & Scheer, 2008).

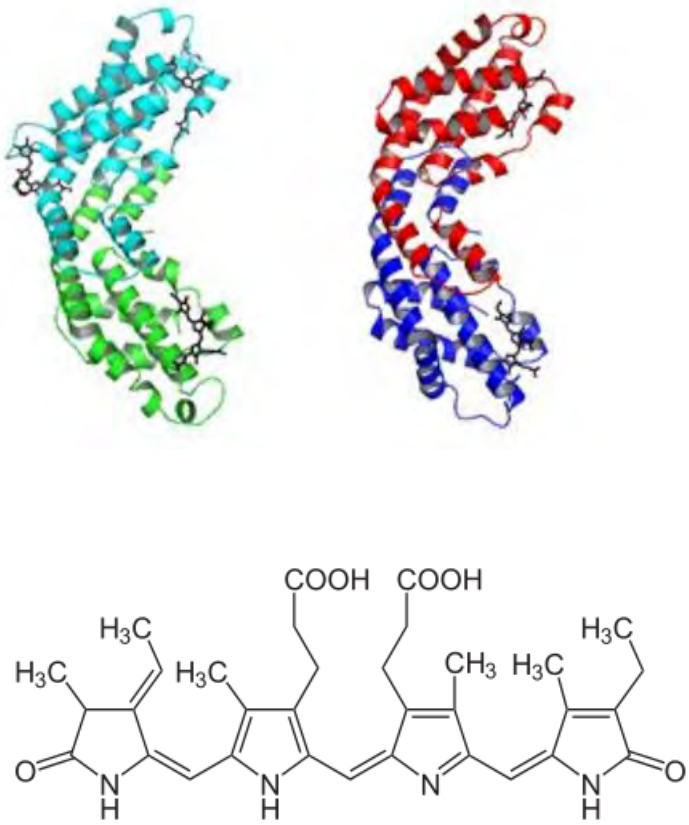

Figure 2: Structural monomers of (a) C-PC (green-cyan) monomer carries three chromophores, while (b) C-APC (red-blue) monomer carries two chromophores, (c) the chemical description of the phycocyanobilin chromophore.

Currently, the widely acceptable PBS structure is 6-8 rods radiating vertically from a central core, which contains 2-5 cylinders (Figure 4). However, the actual positioning of rods on the core, one relative to the other, is still debatable. Furthermore, the exact arrangement of the LPs inside and between the rod and core cylinders is still unsolved. Linker proteins are involved in the assembly and stabilisation of the PBS structure (Tal *et al*., 2014). Chang *et al*. (2015) reported the absorbance characteristics and energy transfer of the PBPs to favour a unidirectional flow of excitation energy from the peripheral rods to the PBS core and finally to the RCs. Depending on the cyanobacterial species, there are different numbers of genes encoding for some of the LP (Pizarro & Sauer, 2001).

Similarly, the number and type of LPs vary between species and can be changed due to of variations in the environment (Adir *et al*., 2006; Chang *et al*., 2015; Mullineaux, 1992). The linkers are classified into four subcategories according to their function and position in the PBS: (i) rod linkers (LR), are involved in rod assembly; (ii) rod-core linkers (LRC), mediates the attachment of rods to the core; (iii) core linkers (LC) are involved in the assembly of the core and (iv) the core-membrane linker (LCM) has multiple roles including attachment of the PBS to membrane and major terminal energy emitter to the PS11. Glazer & Cohen-Bazire, (1971) established a system of abbreviations to characterise the LPs. This widely used classification system defines LPs with regards to their location and molecular masses. L_X^Y refers to a linker polypeptide (L) with a mass kDa of (*Y*), located at position *X* in the PBS, where *X* is either R (rod), C (core), RC (rod–core junction) or CM (core–membrane junction) (Liu *et al*., 2005).

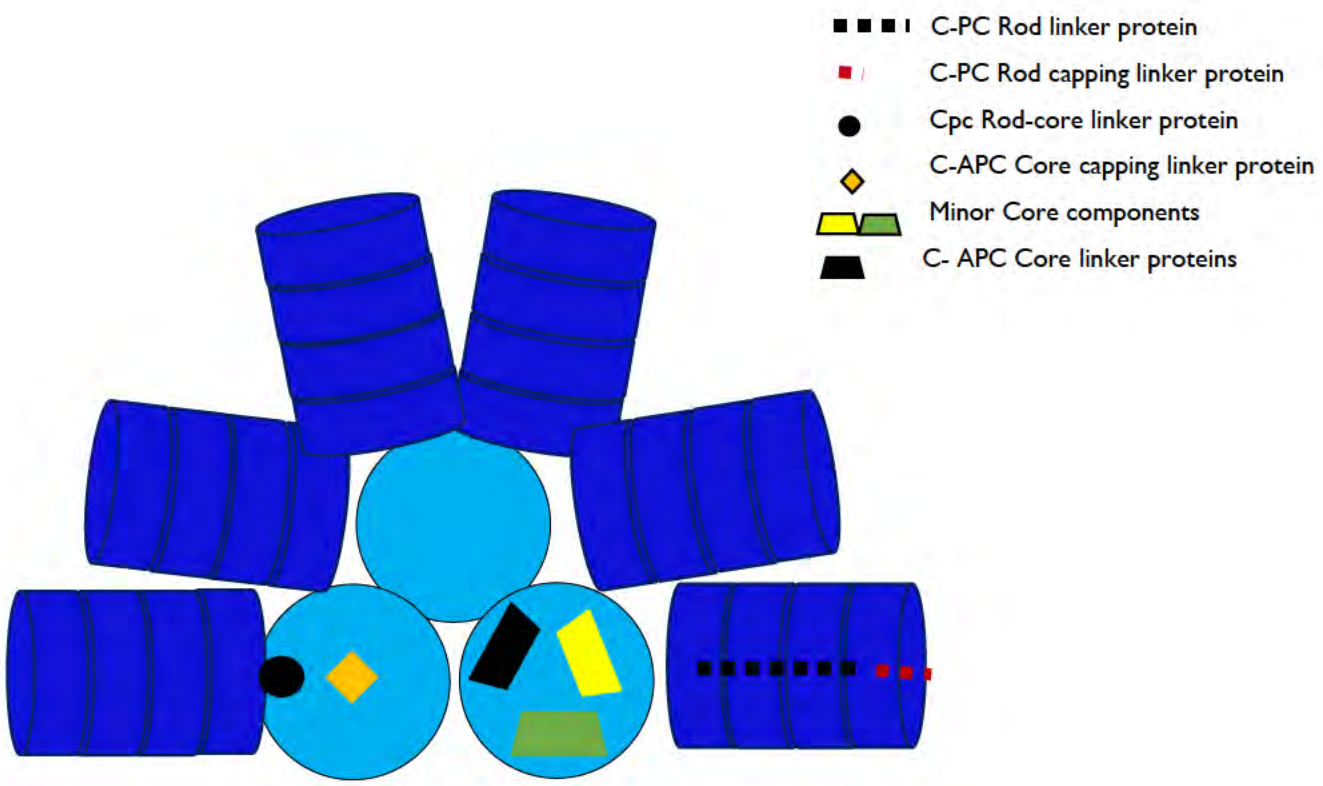

Figure 3: A proposed structural model of the hemidiscoidal PBPS (Adir *et al*., 2001; Liu *et al*., 2005). The three-light blue circles represent the tricylindrical core that is surrounded by an arrangement of six rods. Each rod is composed of a certain number of double-disc-shaped PBPS, shown in bright blue. The LPs are located in the central hole of the hexamers. Rod cylinders side view, core cylinders are in front

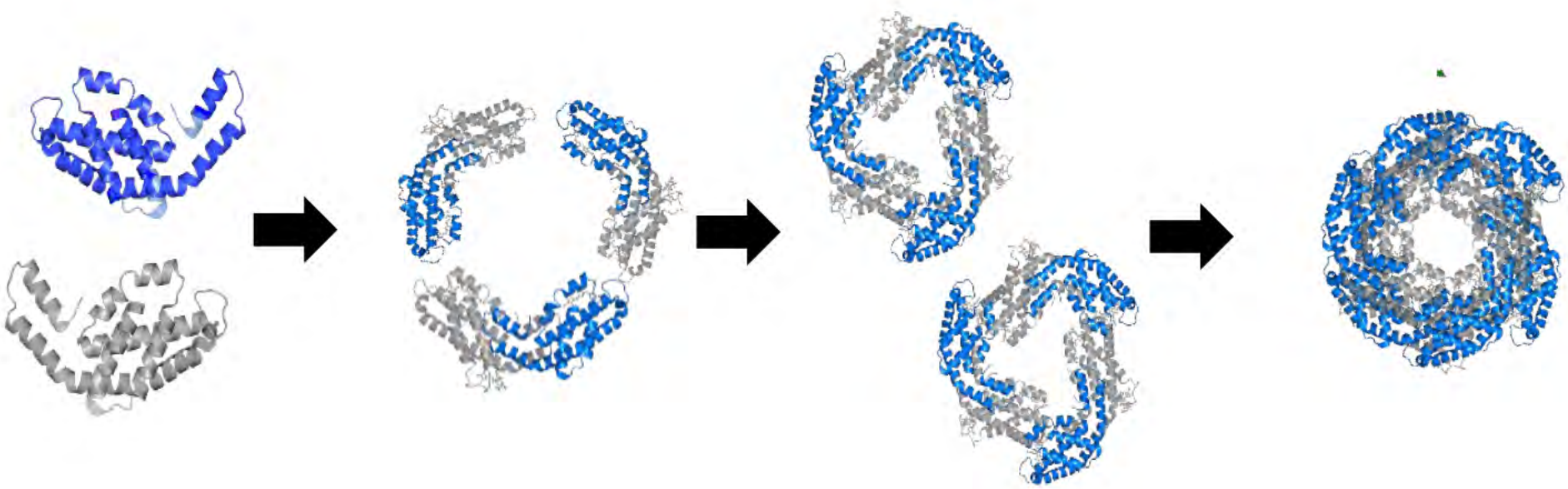

Figure 4: Association of PBP subunits and monomers into the larger aggregates. The *α* subunit is shown in grey colour and the *β*subunit is shown in blue colour. The association of monomers into trimer is and finally into hexamers is shown. (Proteins structures were drawn using SWISS-MODEL (http://swissmodel.expasy.org)

2.11 C-PHYCOCYANIN

2.11.1 Description of C-phycocyanin

C-phycocyanin (C-PC) is the major rod pigment-protein, found in all PBS forms. The C-PC is sub-divided into three types: (i) C-phycocyanin (C-PC, λmax~615-620 nm) exclusively found in cyanobacteria, ii) phycoerythrocyanin (PEC, λmax~575 nm) inducible only in some cyanobacteria, and iii) R-phycocyanin (R-PC, λmax~615 nm) mainly existing in red algae (Adir *et al*., 2001; Chakdar & Pabbi, 2012). These blue or blue-purple coloured PBPs have strong light absorption ability mainly in the range from 580-630 nm and emit intensive red fluorescence at 635-645 nm (Sun *et al*., 2003). Most species possess only one set of C-PC genes, encoding for a single form of ($\alpha\beta$) monomer. This PBP is typically isolated in trimeric $(\alpha\beta)^3$or hexameric $(\alpha\beta)^6$ form demonstrating the stability of these aggregation states (Adir *et al*., 2006). The molecular dimensions of the trimeric rings are a thickness of 3 nm, a diameter of 11 nm and a central hole in diameter of 3.5 nm. C-Phycocyanins commonly occur in disc-shaped hexamers, and a rod linker polypeptide (LR) or a rod-core-linker (LRC) polypeptide are attached to the centre cavity of hexamers to form ($\alpha\beta$) 6LR or ($\alpha\beta$) 6LRC complexes (Bryant *et al*., 1978). The interaction of C-PCs with the linker polypeptides may typically cause a large redshift of about 17 nm in their absorption and fluorescence emission maxima (Ducret *et al*., 1996). C-Phycocyanin is a blue-coloured, deeply red-fluorescent PBPs and a predominant form among C-PCs which is also one of the most studied PBPs. Investigations have shown that three PCBs are attached to Cys α-84, β-84 and β-155. The α-84 and β-155 PCB are found at the periphery of the C-PC complex, whereas β-84 PCB are situated near the central cavity of the trimer and hexamer. Thus, the role of the α-84 and β-155 PCB is to transfer the excitation energy whereas the β-84 PCB are terminal acceptors (Sun *et al*., 2003).

2.11.2 Biosynthesis and Production of C-phycocyanin

The C-PC genes and biosynthetic pathway of C-PC is illustrated in Figure 5. The first committed and rate-limiting step in C-PC synthesis is the formation of ALA from Glutamate (Glu) (Brown *et al*., 1990). Nitrate ions are reduced to ammonium (NH^{4+}) ions catalysed by enzymes nitrate reductase (NR) and nitrite reductase (NiR), thereafter, incorporated into C compounds as the *α*-amino of L-glutamate *via* glutamine synthetase (GS) to form Glu. Two molecules of ALA with the addition of Mg^{2+} is condensed *via* to PBG synthase to form the pyrrole ring of porphobilinogen PBG. Four PBG molecules are oligomerised to form the linear tetrapyrrole intermediate, UPG1 *via* PBGD, followed by a ring closure by UROS to form UPG III. Thereafter, UPG III is converted to PIX *via* three enzymatic steps. In *Euhalothece* sp. PIX is catalysed by oxygen-dependent CPO. The Fe^{2+} are inserted into PIX *via* ferrochelatase to form heme. The HO catalyses the oxidative cleavage of the host heme to BV Ix *α,* which is subsequently reduced by PcyA to PCB.

The final step in PC biosynthesis is the covalent PCB attachment to the apoprotein at Cys residues *via* thioether bonds catalysed by enzymes called billin lyases (Zhao et al., 2007). The bilin lyases included: E/F-type, S-type and T/G-type lyases. CpcE/F lyases are heterodimeric lyases required for specific binding of PCB to the Cys-84 site on the apo-phycocyanobilin *α* subunit *i.e.* PC-*α*-Cys84. The lyase CpcS catalyses the attachment of PCB to the chromophore binding site Cys-*β*84 of CPC (Liu et al., 2005; Wu et al., 2016a; Zhao et al., 2017).

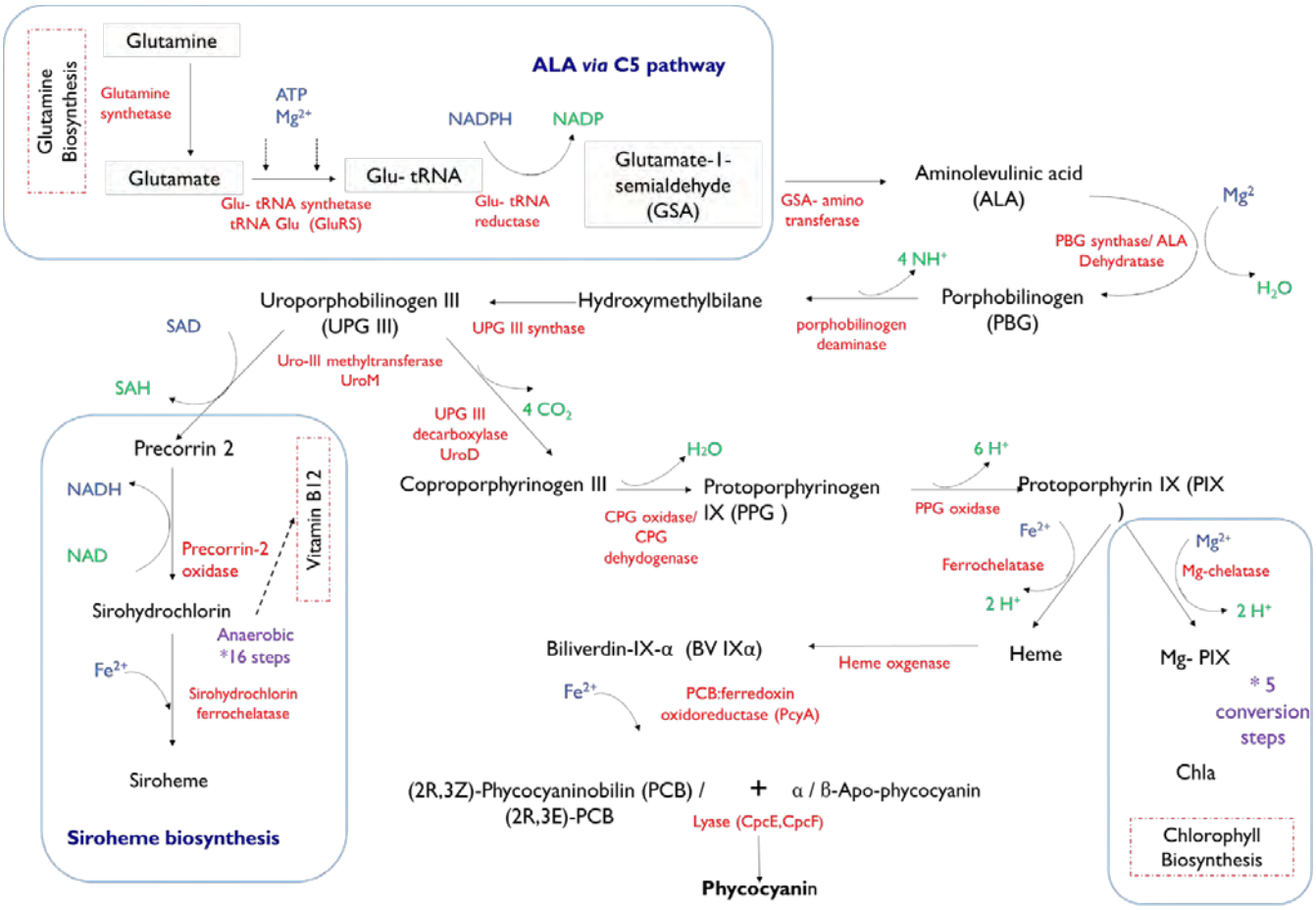

Figure 5: Two molecules ALA is condensed to form PBG, which are oligomerised to form pre-uroporphyrinogen (1-hydroxymethylbilane) *via* PBGD. This molecule undergoes several rounds of modifications, which leads to the formation of PIX. The next key regulatory step is the addition of Fe^{+} ions to PIX catalysed by ferrochelatase to form heme. Heme is converted to BV IX*α via* heme oxygenase, resulting in the formation of carbon monoxide, Fe, and biliverdin IX (BV). Thereafter, the subsequent reduction to PCB by PCB: ferredoxin oxidoreductase (PcyA), which uses four electrons from reduced ferredoxin. The final step in PC biosynthesis is the covalent PCB attachment to the apoprotein at Cys residues *via* thioether bonds catalysed by billin lyases.

There are many different methods of C-PC production including photoautotrophic, mixotrophic, heterotrophic, photoheterotrophic and recombinant production. Table 4 shows the concentration of C-PC obtained when grown in different cultivation conditions. Phoautototrophic growth occurs when the cyanobacteria use sunlight (energy source), and inorganic carbon *i.e.* CO_2 (carbon source) to produce chemical energy through photosynthesis (Benavente-Valdés *et al.*, 2016).

A.platensis grows in warm temperatures between 28 to 40°C with high light intensity in brackish, alkaline (8<pH<11.5) water often in high concentrations of carbonate and bicarbonate (Vernès *et al*., 2015). Photoautotrophic production of *A. platensis* grown in open ponds or raceways for commercial C-PC production in either subtropical or tropical regions (Sonani *et al*., 2016). It is commonly cultivated axenically in open-pond systems for C-PC production. In mixotrophic cultivation, cyanobacteria can use both inorganic carbon (CO_2) and organic compounds such as glucose as their carbon source to undergo photosynthesis. Mixotrophic cultivation of *A. platensis* produces overall higher biomass production (up to 2.3 times more) in any light intensity used compared to autotrophic and heterotrophic cultures. Furmaniak *et al.* (2017) reported a high C-PC production rate of 21.25 mg/L/day from *A. platensis* using mixotrophic condition (urea- 114.74 mg/L and molasses 0.196 mg/L under continuous illumination at 45.5 μmol m^2/s). Setyoningrum & Nur (2015) also found a high C-PC yield of 56.536 mg/g in *A. platensis* FACHB-314 when cultivated using 5mM sodium glutamate and initial nitrate concentration of 30 mg/L, at 28°C with light intensity, 300 μmol/m^2/s in the presence of 2.5% CO_2.

Photoheterotrophic cultivation occurs when the organism use light as the source of energy and organic compounds as the carbon source (Bashan & Perez-Garcia, 2015). A study by Chen *et al.* (1996) sowed C-PC production of 147 mg/L was achieved when a NaCl-tolerant mutant of *A. platensis* was cultivated in a nitrate (40 mM) and bicarbonate (60 mM) sufficient medium at pH 9.0 under phototrophic conditions. (Zhang *et al.* (1998) reported the maximum C-PC production from *A. platensis* of (0.795 g/L) when grown using fed-batch in Zourruk's media with 2 g/L glucose, pH 9.5, at 30°C with a constant light intensity of 80 μmol/m^2/s. In 2015, Xie *et al.* reported the highest C-PC production (1034 mg/L) using fed-batch cultivation of *A. platensis* under a light intensity of 300 μmol.m^2/s. *Synechocystis* sp. 6803 has been reported to grow photoautotrophically with a maximum doubling time of 7~10 h under optimal light conditions as well photoheterotrophically with a shorter doubling time of ~3.5 days (Yu *et al*., 2013).

Table 4: The C-PC content in various cyanobacteria grown under different cultivation conditions

Cyanobacterium species	Growth conditions	C-PC content	References
Arthrospira platensis FACHB-314	Modified SP medium (initial nitrate- 30 mg/L and 5 mM sodium glutamate); operating conditions: 2.5% CO_2 flow rate, 0.2 vvm; 28 °C, 300 μmol/m^2/s	0.34 mg/mL 56.536 mg/g	(Manirafasha *et al*., 2018)
Spirulina sp. *LEB 18*	Green LEDs in partial light photoperiod	126.39 mg/g	(Khan *et al*., 2018b)
Anabaena fertilissima PUPCCC 410.5	Chu-10 medium (supplemented with 2 mM nitrite); 28°C ± 2 °C, 44.5 μmol/m^2/s of blue light for 14 h	696 µg/mg	(Khattar *et al*., 2015)
Cyanidioschyzon Merolae	Autotrophically in mineral medium; pH 2, 40°C with constant illumination	0.55 mg/mL	(Rahman *et al*., 2017)
Geitlerinema sulphureum	Media supplemented 3.5 g of $NaNO_3$ and 6.24 g/L of Na_2CO_3; 30°C, 1000 lux light intensity	0.071 g/L	(Kenekar & Deodhar, 2013)
Geitlerinema sp.	BG11 media; 45 ± 2°C, 40 μmol/m^2/s light	24.45 mg/mL	(Demirel & Sukatar, 2019)
Phormidium ceylanicum	Modified BG11 media (4.5 g/L $NaNO_3$); 27 ± 2°C, 130 μmol/m^2/s of white fluorescent light for 12: 12 h L:D cycles	0.7314 mg/ml	(Singh *et al*., 2009a)
Leptolyngbya. boryana CCALA 084	Z-medium (pH = 8.5); 24±1°C; 75 μmol/m^2/s 15:9 L:D cycle	0.264 mg/mL	(Basheva *et al*., 2018)
Limnothrix sp. 37-2-1	BG-11 media (20mM of $NaNO_3$ and 250mg/ of Se_2O_3); 28°C; white light of 25 μmol/m^2/s	130.02 mg/g	(Patel *et al*., 2016)
Synechocystis sp.	Modified BG1 media (0.058 g/L $CaCl_2$, 0.115 g/L Na_2CO_3,); pH 10, 24 ± 2°C, 75 μmol/m^2/s, 16:8 h L:D cycle	22.6 mg/L	(Deshmukh & Puranik, 2012)
Pseudanabaena catenata USMAC16	BG-11 medium; 15°C, continuous red light	25.8 mg/L	(Khan *et al*., 2018b)
Pseudanabaena mucicola	Wastewater medium; pH 7.5; 25°C, white light 180 μmol/m^2/s	237.01 mg/g	(Khatoon *et al*., 2018)
Nostoc sp.	Modified BG11 medium (75.48 μM Na_2CO_3 and 17.65 mM $NaNO_3$); pH 8, 35°C green light 40 μmol/m^2/s	0.13 g/g	(Johnson *et al*., 2014a)

In the heterotrophic cultivation, organic carbon is used under dark conditions as the sources of both energy and carbon. Heterotrophic production of C-PC is not light-limited (Khan *et al*., 2018a). Thus, this cultivation condition can be an alternative solution to overcome the problem

associated with light limitation (Marquez *et al*., 1993). Schmidt *et al*. (2005) reported the productivity of C-PC in the heterotrophic fed-batch cultures of *Galdieria sulphuraria* was higher than is attained in outdoor cultures of *A.platensis*. In carbon-limited fed-batch cultures, biomass obtained was 80–120 g/L and C-PC yield of 250 and 400 mg/L. *G. sulphuraria* can grow heterotrophically as well as autotrophically in the light, additionally grows at relatively high temperatures >40 C and low pH, (Sloth *et al*., 2006). *G. sulphuraria* was reported to contain a major amount of C-PC and a minor amount of APC. Sloth *et al*. (2017) & Sloth *et al*. (2006) demonstrated that unicellular rhodophyte, *G. sulphuraria*, is a candidate for heterotrophic production of C-PC using glucose in the dark in closed fermenters.

Recombinant production of C-PC is another heterotrophic method and involves gene engineering. The complete synthesis of recombinant PBPs depends on co-expression of α- and β-chains as well as parallel synthesis and insertion of the correct phycobilin chromophores (Eriksen, 2008). The cloning and express of the relevant genes *i.e*. cpcB; cpcS or cpcT; ho1 and pyA from *A. platensis*, *Synechocystis, Synechococcus sp* and *Anacystis nidulans* for production of fluorescent α-CPC in *E. coli* have been reported by several researchers (Cherdkiatikul & Qin *et al*., 2004; Biswas *et al*., 2010; Suwanwong, 2014; Yu *et al*., 2016; Wang *et al*., 2007; Wu *et al*., 2018). Gene engineering has resulted in the production of recombinant C-PC with novel function.

2.12 OVERVIEW OF EXTRACTION AND PURIFICATION METHODS FOR C-PHYCOCYANIN

2.12.1 Extraction of C-phycocyanin

The limited commercial applications of C-PC is often due to their sensitivity to changes in light, temperature, pH, and solvents, which affect their extraction yield and purity. Moreover, C-PC can readily degrade under certain physicochemical conditions (İlter *et al*., 2018). This sensitivity is a major contributor to high production cost as well as reduced biological functions during purification steps (Chakdar & Pabbi, 2015). Hence, rapid and efficient extraction and effective separation/purification methods are essential. Over the years several methods have been investigated to extract and quantify PBPs from various cyanobacteria strains, however, to date, there is no standard technique for quantitative extraction of this valuable pigments (Gutiérrez *et al*., 2016). Extraction of PBPs from cyanobacteria with small size cells and resistant cell wall can be difficult and time–consuming (Kuddus *et al*., 2013).

The C-PC extraction includes cell disruption to release the proteins which are categorised into mechanical and non-mechanical methods. Mechanical methods used include ultrasonication, French pressure, bead mill, high-pressure homogenisation (HPH), pressurised liquid extraction (PLE), supercritical fluid extraction (SFE) and microwave extraction (MW), (Choi & Lee, 2018; Cuellar-Bermudez *et al*., 2015; Kapoore *et al*., 2018; Mittal *et al*., 2017; Ruiz-Domínguez *et al*., 2019; Zhang *et al*., 2019). Non-mechanical methods include chemical osmosis, repeated freeze-thaw, use of enzymes like lysozyme (Moraes *et al*., 2011). The conventional extraction is based on the high solubility of PBPs in aqueous solutions and their polarity, which is accomplished by the addition of either a buffer or solvent to the biomass. The solubilisation is increased by using temperature or by constant shaking of the solution. The enzymatic extraction can be carried out by exposing the cyanobacterial biomass to digestion with lysozymes (Pagels *et al*., 2019).

The extraction of PBPs from wet biomass is preferable because it reduces loss in pigments during drying processes and does not require additional costs on this process. Owing to C-PC peripheral position in PBS on the thylakoid membrane and temperature sensitivity, there is a significant loss of C-PC in dried samples. Selection of suitable buffer for maximum phycobiliproteins extraction is also crucial as this ensures that proteins are not denatured due to a shift in pH. A number of

researchers have reported phosphate buffer (pH 7.0-7.5) to be superior over other buffers with a pH of range of 5.0 to 9.0 (Figueira *et al*., 2018; Hemlata *et al*., 2011) (Benedetti *et al*., 2006b; Sarada *et al*., 1999).

During high-pressure extraction, the cell membranes disassemble irreversibly due to the separation of weak bonds (van der Waals bonds, coupling and hydrogen bonds) thereby inducing morphological and structural changes in macromolecules. Due to application at low-temperatures, extraction of PBP using high-pressure treatments are now to have greater stability and at a higher level of purity (Muthulakshmi *et al*., 2012). Extraction of C-PC from *A. platensis* using hexane in a high-pressure extraction vessel at 5000 bar and 20°C for 15 min resulted in a 3% high yield compared to the conventional enzymatic method. Ruiz-Domínguez *et al*. (2019) found a higher C-PC yield from *A. maxima* was extracted under the HPH technique than the MW and freeze-thaw (FT) methods (Table 6).

Ultrasound based extraction methods can achieved by: i) ultrasound soley is used for cell disruption and enhanced product extraction and ii) ultrasound performed in combination with other cell disruption methods to achieve synergy thus, increasing product yield (Tavanandi *et al*., 2018). The cyanobacteria cells are ruptured by the bursting of cavitation bubbles outside the cells and the development of extremely high pressures (Zhang *et al*., 2019). The C-PC from *A. maxima* under ultrasonication extraction (60 kHz, 3 h at room temperature) was 11.3 mg/mL (Choi & Lee, 2018). However, Santiago-Santos *et al*. (2004) found that the repeated FT was more suitable for the large-scale disruption of *Spirulina* cells than ultrasonication.

The technique of freezing and thawing is mild and non-denaturing. The mechanism behind the FT method is that it causes cells to swell and ultimately break the cell wall and cell membrane, due to sharp ice crystals formed during the freezing process and then contract during thawing (Soni *et al*., 2006). Many researchers have reported that freeze-thaw cycles are one of the most efficient ways to extract C-PC from wet cyanobacterial biomass (Aftari *et al*., 2017; Muthulakshmi *et al*., 2012; dos Santos *et al*., 2019; Lawrenz *et al*., 2010; Salama *et al*., 2015). Lawrenz *et al*. (2010) & Horváth *et al*. (2013) both reported that disruption of cells by the combination of FT and sonication resulted in significantly higher extraction efficiencies than disruption with a tissue grinder and homogenised using a mortar and pestle. ‘

2.12.2 Advantages and disadvantages of different extraction methods

Table 5: Summary of advantages and disadvantages of the different C-phycocyanin extraction methods

Methods	Advantages	Disadvantages	Reference
Mechanical			
Supercritical fluid extraction (SFE)	Non-flammable, non-toxic and relatively inert	Very high investment costs, a lot of energy, resource competencies and more impurities in the extract	(Cuellar-Bermudez *et al*., 2015; King, 2002)
Ultrasonication	Short extraction time, easier operation, less loss, and high yield of the C-PC lower pressure	Denaturing to the protein, more cellular debris and contaminating proteins left in the buffer, generating excessive amount heat, and difficult to scale up	(Ismail *et al*., 2018)
Catalytic ozonation is a process of Advanced Oxidation Processes (AOP)	Electricity consumption for catalytic N ozonation operations is relatively low compared to other technology	Further research is needed	(Rame *et al*., 2018)
Microwave-assisted extraction (MAE)	Significant reduction in extraction time, reduced solvent consumption, and high extraction yields that can be increased from 50 to 500 %, can be performed at low temperature under vacuum	Very high investment costs, a lot of energy and resource competencies	(Juin et al., 2015)

Methods	Advantages	Disadvantages	Reference
High-pressure homogenisation (HPH)	Does not use harmful solvents or chemicals, easily scaled up,	Excessive cell destruction, contaminating chlorophyll	(Ruiz-Domínguez *et al*., 2019)
Pressurised liquid extraction (PLE)	Disrupt species with a high mechanical resistance	Require optimisation	(Herrero *et al*., 2005)
Non-mechanical/ Chemical			
Osmosis	Does not require special equipment, simple operation, less cellular debris,	Longer extraction cycle increased, difficulty of purification process protein denaturation	(Pan-utai & lamtham, 2019)
Aqueous Two-Phase Extraction	Can separate different PBPs concurrently	Optimisation required difficult to separate the C-PC from the polyethylene glycol completely	(Safi *et al*., 2014)
Freeze-thaw	Simple, quick, reproducible, and robust, free of corrosive material	Difficult to scale up energy-intensive	(Horváth *et al*., 2013)
Enzymatic	Gently and efficiently break cell wall, suitable for the large-scale industrial extraction	Relatively expensive releases unpleasant odours	(Bermejo et al., 2007)

Tavanandi *et al*. (2018) also found that ultrasonication in combination with FT resulted in a 30% increase in C-PC extraction efficiency compared to FT alone. More recently, Jaeschke *et al*. (2019) extracted C-PC from *A. platensis* using Pulsed electric field (PEF) treatment and obtained 85.2 ± 5.7 mg/g was at 122 J/mL. Pulsed electric field promotes the electroporation of the cells due to the application of pulses of high voltage and duration (μs to ms) between two electrodes promoting the destabilisation of the cell structure (Martínez *et al*., 2019)

2.12.3 Purification of C-phycocyanin

Various methods have been reported for the purification of C-PC from cyanobacteria. However, in order to obtain analytical-grade C-PC all these methods involve the chromatographic steps. Resin chromatography columns require a higher flow rate to achieve sufficient productivity due to their slow mass transfer rates. Thus, this results in an increase in equipment-related expenses including associated hardware, supporting systems, and facilities. Most purification procedures involve precipitation, centrifugation, dialysis, or aqueous system or c ombinations of these steps, followed by anion exchange, hydroxyapatite, affinity, or adsorption chromatography and finally gel filtration chromatography (Bermejo *et al*., 2003; Santiago-Santos *et al*., 2004). A few procedures have also been reported to use non-chromatographic methods use of chitosan and charcoal, aqueous two-phase in C-PC purification process as well as ultrafiltration, membrane filtration or the use of organic solvents (Patil *et al*., 2006). The downstream process can account for 50-80% of total production costs, depending on the required purity ratio.

One of the standard methods for initially purification involves the precipitation of proteins followed by chromatography for separation. Several precipitating agents such as acetone, polyethylene glycol, Trichloroacetic acid (TCA), chloroform-methanol, ethyl acetate and ammonium sulphate are routinely used for precipitation (Feist & Hummon, 2015). Hemlata *et al*. (2011) compared a number of precipitating agents and found that ammonium sulphate is best for salting out PBPs. Ammonium sulphate maintains the integrity of the protein, readily precipitates PBPs, highly water-soluble at low temperatures and has bacteriostatic effect.

The other precipitating agents like acetone, ethanol or TCA were found to denature the proteins quickly. Different saturation levels of ammonium sulphate precipitate a particular class of protein and for PBPs with 20-55% saturation the mostly used (Chen *et al*., 2017; Moraes & Kalil, 2009; Wingfield, 2001). Fractional precipitation is the process whereby undesired proteins are initially removed at lower saturation levels thereafter followed by a higher level of saturation which precipitates the desired PBPs (Patil *et al*., 2008; Soni *et al*., 2008). Patel *et al*., (2005) reported that 50% saturated $(NH_4)_2SO_4$ solution is required for high purity C-PC from *Spirulina* since at the lower concentration of $(NH_4)_2SO_4$ other proteins were extracted. The precipitation step mainly used to remove contaminant proteins are crucial to obtain a high recovery rate (Moraes & Kalil, 2009). The strategies used in the last decade for the extraction and purification of C-PC from cyanobacteria are presented in Table 6.

Simultaneous purification of all three PBP is very difficult due to similarities in their molecular weights and surface charges. Some recently reported protocols like ATPE demonstrates a new way for separation and simultaneous purification of two PBP (Patil *et al*., 2008); however, it requires tedious downstream processing to remove precipitants from purified proteins. Aqueous two-phase extraction uses the same principle however uses two polymers, a polymer and a salt or two salts. The ATPE has been investigated using PEG and salt by (Patil & Raghavarao, 2007; Zhao *et al*., 2014) and ionic liquids and salt by (Suarez Ruiz *et al*., 2018; Zhang *et al*., 2014). In a study conducted by Singh *et al*. (2009) C-PC purity of 4.1 from *Phormidium ceylanicum* was obtained using ultrafiltration and ion-exchange chromatography. Patil *et al*. (2006) investigated the aqueous two-phase extraction (ATPE) and reported that C-PC purity from *A.platensis* 3.23 was achieved. Furthermore, the combination of ATPE and ion-exchange chromatography increased the purity (6.69). Chakdar *et al*. (2014) reported a lower purity of 2.75 from *Anabaena variabilis* CCC421 after ammonium sulphate precipitation and DEAE-cellulose ion-exchange chromatography. Minkova *et al*. (2003) investigated using rivanol treatment, as well as 40-70% $(NH_4)_2SO_4$ precipitation and gel filtration, a 45.70% C-PC with a purity of 4.30 was recovered from *S. fusiformis.* Soni *et al.* (2006) used $(NH_4)_2SO_4$ precipitation, gel filtration chromatography and DEAE-cellulose column chromatography to obtain C-PC with a purity of 3.31 from *Oscillatoria quadripunctulata*. A purity of 4.78 from *Aphanizomenon flos-aquae* after hydroxy-apatite chromatography was achieved (Benedetti *et al*., 2006). Soni *et al*. (2008) further investigated one

single step hydrophobic interaction chromatography (HIC) for purification of C-PC from *Phormidium fragile* and attained PC with a purity of 4.52. The ATPE combination with ion-exchange chromatography showed a high purity C-PC with 73% recovery, and an increase in product purity (Patil *et al*., 2008). The C-PC (18%) with a n initially purity of 2.0 was extracted dry biomass of *Limnothrix* sp. After using chitosan (0.01 g/L), activated carbon (1% w/v) and 25% $(NH_4)_2SO_4$ saturation purity ratio increase to 4 with final yield of 8% C-PC (Gantar *et al*., 2012). .

Table 6: Summary of extraction and purification methods used for C-PC from different cyanobacterial species

Cyanobacteria strain	Extraction method	Purification procedure	Purity (%)	C-PC Yield		Reference
Aphanizomenon flos-aquae	Homogeniser	Ammonium sulphate precipitation (ASP); Hydroxyapatite (electrostatic interaction) chromatography	4.78	-		Benedetti *et al*., 2006b
Arthronema africanum	Osmotic shock	NaCl precipitation	-	4.52	55	Minkova *et al*., 2007
Arthrospira fusiformis	Freezing and thawing (FT) (-15˚ and 4 ˚C)	Rivanol treatment; ASP; Gel filtration (GF);	4.3	45.7		Minkova *et al*., 2003
Arthrospira platensis	Pulsed electric field (PEF)				85.2 mg/g	Jaeschke *et al*., 2019
Arthrospira platensis	Homogeniser	Chitosan adsorption; Aqueous two-phase extraction (ATPE); Ion exchange chromatography (IEC)	6.69		1.11mg/mL	Patil *et al*., 2006
Arthrospira platensis	Sonication and homogenisation using 0.02 g/mL oven-dried biomass		1.2		86 mg/g	Pan-utai & lamtham, 2019
Arthrospira platensis	homogenise at a pressure range of 200–400 kg/cm^2 for 5 min	ATPE; Ultrafiltration (UF)	4.02			Patil *et al*., 2008

Cyanobacteria strain	Extraction method	Purification procedure	Purity	C-PC Yield (%)		Reference
Arthrospira platensis	Ultrasonic extraction (UE) (20 kHz, acoustic intensity was set at 20–100% for 20 min at 4°C	Stirred fluidised bed IEC	2.7		7.52 mg/mL	Chen *et al*., 2016
Arthrospira platensis	UE in combination with 'Freezing and thawing (FT)		0.7		109.3 mg/g	Tavanandi *et al*., 2018
Arthrospira platensis	UE using freeze-dried biomass, 0.01 M sodium phosphate buffer (pH 7) and biomass-solvent ratio of 1:15		0.6		60 mg/g	Pan-utai *et al*., 2018
Arthrospira platensis	Sonication and repeated FT (-20 and 4°C)	ASP; IEC	4.42	45.6		Patel *et al*., 2005
Arthrospira platensis	Freeze-dried biomass samples suspended in NaCl 0.1 M at 4°C for 24 h	ASP; hydrophobic chromatography (HC)	4.2	67		Rosaria *et al*., 2018
Arthrospira platensis	FT (-20 and 4°C)	Fractional precipitation and IEC	4.33	33		Chen *et al*., 2016
Arthrospira platensis	FT (-20 and 27°C)	Precipitation and HPLC	4.5	80	0.41 mg/mL	Kumar *et al*., 2014
Arthrospira platensis	FT (-20 and 4°C)	ASP; IEC	5.59	67.04	111.83 mg/g	Yan *et al*., 2011
Arthrospira platensis	UE (3% biomass/solvent ratio, at 40 kHz 30% amplitude for 25 min)				98.17 mg/g	İlter *et al*., 2018

Cyanobacteria strain	Extraction method	Purification procedure	Purity	C-PC Yield (%)		Reference
	Solvent- 1.5% $CaCl_2$ (w/v) homogeniser 6237.66 rpm, 15 min				68.12 mg/g	
Arthrospira platensis	Microwave 150 W for 120s using distilled water				215 mg/g	Martínez *et al*., 2017
Arthrospira platensis	Milling in a ball mill	Precipitation, IEC and GF				Moraes & Kalil, 2009
Arthrospira platensis	Soaking with agitation	Chitosan and activated charcoal; IEC	4.3	42.3		Liao *et al*., 2011
Arthrospira platensis	Osmotic shock (continuous mixing with stirrer blade)	Activated charcoal; microfiltration (MF)	1.07	82		Chaiklahan *et al* 2011
Arthrospira platensis	Osmotic shock	ASP, DEAE-Sepharose IEC and Sephacry S-300 size exclusion chromatography.	5.12			Chen *et al*., 2006
Arthrospira platensis	0.5M of ammonium sulphate	Expanded bed adsorption chromatography; IEC	3.64	8.7		Niu *et al*.,2007
Arthrospira maximum	High-pressure homogenisation (HPH) using Na-phosphate at 1400 bar				291.9 mg/g	Ruiz-Domínguez *et al*., 2019
Arthrospira maximum	UE (60 kHz frequency, 3 h, room temperature)				11.3	Choi & Lee, 2018
Anabaena marina	Osmotic shock	Expanded bed adsorption chromatography	4	62		Ramos *et al* 2010
Cyanidioschyzon merolae	FT (−22 and 20°C)				232.8 mg/g	Rahman *et al*., 2017

Cyanobacteria strain	Extraction method	Purification procedure	Purity	C-PC Yield (%)	Reference
Galdieri sulphuraria	FT (-80 and 4°C)	ASP (25-50 %)	4	80	Moon *et al*., 2014
Limnothrix sp. strain	FT (-20 and 4°C)	ASP, activated carbon and chitosan	4.2	8	Gantar *et al*., 2012
Lyngbya sp A09DM	FT (-20 and 4°C)	Triton X-100 mediated ASP; IEC; GF chromatography	5.53	60.23	Sonani *et al*.,2014
Nostoc sp.		IEC; ATPE	3.55	-	Johnson *et al*.,2014a
Oscillatoria tenuis	FT, dialysis	ASP (20%); Sepharose GF	4.88	61.8	Thangam *et al*., 2013
Oscillatoria quadripunctulata	FT (-20 and 4°C)	ASP; GF; IEC	3.31	44.2	Soni *et al*.,2008
Porphyra yezoensis		ASP; Sephadex G-25; hydroxyapatite.	5.10	0.09	Sua *et al*., 2014
Porphyra yezoensis		ASP; HC; IEC; GF	5.32	42	Song *et al* 2013
Phormidium. fragile	Liquid nitrogen in mortal and pestle	ASP; HC	4.52	62.0	Soni *et al*., 2004
Phormidium versicolor	Stirring at 100 rpm, 30°C for 24 h in 0.1 M sodium phosphate buffer	ASP; HPLC		67.45 mg/ g	Gammoudi *et al*., 2019
Lyngbya spp	Sonication FT (-20 and 4°C)	ASP; IEC		36.8	Patel *et al*., 2005
Synechococcus spp	Enzymatic (lysozyme) Digestion	Activated carbon and chitosan	4.27	80	Gupta & Sainis, 2010
Synechococcus	Chaps, 0.3% asolectin combined with nitrogen cavitation	SDS-PAGE		95	Viskari & Colyer, 2003

2.13 PHYSIOCHEMICAL PARAMETERS AFFECTING THE STABILITY OF EXTRACTED C-PHYCOCYANIN

The stability of PBPs varies under different physicochemical stress factors amongst the cyanobacteria exposed to different environmental conditions. The PBPs produced by cyanobacteria growing under high temperatures or high light exposure are expected to have higher stability at high temperatures and light (Chaiklahan *et al*., 2012). Table 9 shows the different physicochemical factors that affect C-PC stability. There is an increasing number of studies that report the main factors affecting C-PC stability are pH and temperature, as well as investigate methods to increase C-PC stability in order to expand their applications (Hsieh-Lo *et al*., 2019). Spectral properties of PBPs are highly pH-dependent. It has been reported that pH is the main factor that affects the aggregation and dissociation of C-PC in monomers, trimers, hexamers and other oligomers in solution. In pH 7.0, the hexameric form dominates. This is the most stable structure and avoids the denaturation of the PBP. It has been reported that at low pH, PBPs easily dissociates into individual subunits decreasing stability. Moreover, extreme changes in pH may disrupt the electrostatic properties and hydrogen bonds involved in protein assembly leading to changes in chromophore structure (Rastogi *et al*., 2015; Tiwari *et al*., 2019).

According to Chaiklahan *et al*. (2012), at pH 7.0 only 18% of C-PC was aggregated in its hexameric form, whereas at a lower pH of 6.0, 77% of C-PC was aggregated. Jespersen *et al*. (2005) also found C-PC to be more stable at pH 5.0 than at pH 7.0. After 24 hours, the C-PC solutions with pH 5 were darker blue whereas the solution with pH 7.0 was found to be almost discoloured after 24 hours. Loss in colour is been reported to be due to either conformational changes of the PCB chromophores and/or changes in the aggregation state of the biliproteins (Böcker *et al*., 2019). Since PBPs are protein pigments and their primary cause of degradation is denaturation they should be handled and preserve at low temperatures. Munier *et al*. (2014) reported that when the temperature rises, the amount of α helix decreases, resulting in the loss of stability of C-PC.

Previously, Pumas *et al.* (2011) reported C-PC extract from *Phormidium* sp., with a thermostability up to 50°C. More recently, Rastogi *et al.* (2015) found that C-PC from *Phormidium rubidum* A09DM showed a thermostability of 41.0% after incubation at 80°C for 1 h. The C-PC isolated from thermophile, *Synechococcus lividus* sp. PCC 6715 exhibited 90% stability after 5h incubation at 50°C and ~70% stability after 2 weeks. And also showed high stability at acidic pH at both low and high temperatures *i.e.* 4 and 50°C, and continued to maintain 100% stability during 4 h incubation at pH 4.0 to 8.0 at 50°C (Liang *et al.*, 2018).

Table 7: Physicochemical factors that affect C-phycocyanin stability

Cyanobacteria	Temperature (°C)	pH	Preservative	Reference
Cyanidioschyzon merolae	80	4.0 – 5.0		Rahman *et al.*, 2017
Phormidium rubidium	40	6.0 – 7.0		Rastogi *et al.*, 2015
Arthrospira sp.	50	5.0 – 7.0	Polyethylene glycol-4000 and sorbitol	Chentir *et al.*, 2018
Arthrospira sp.	47-50	5.5 – 7.0	NaCl 2.5%	Chaiklahan *et al.*, 2012
Arthrospira sp.	57.5 - 62.8	7.0	Honey (fructose, glucose, sucrose, lactose and maltose)	Martelli *et al.*, 2014

Sarada *et al.* (1999) found that C-PC extracted from *Arthrospira* sp. was stable over a pH range of 5–7.5 at 9±1°C, temperature increase above 40°C resulted in the degradation of C-PC. Antelo *et al.* (2008) found that with respect to the degradation of PBPs, pH and temperature are inversely proportional, whereby the extract of C-PC was found to be more stable at high temperature and low pH. At 50 and 55°C, C-PC was more stable at pH 6.0 while at 57 and 65°C, the extract was more stable at pH 5.0. Finally, phycocyanin solution was longer stable at a pH range of 5.5–6.0. In contrast, pH 5.0 leads to low stability. Lawrenz *et al.* (2010) also

studied the effect of time storage on the degradation of phycobilins extracted from *Synechococcus bacillaris* and found that samples can be stored at − 80°C for 6 months without degradation. Different studies have been assessed to increase C-PC extract stability. Chaiklahan and colleagues (2012) also reported at 59°C, the C_R of C-PC from *Arthrospira* sp.was decreased by ~50% over 30 min. After the addition of 2.5% sodium chloride, at 60°C, the C-PC C_R was kept at 76%. The stability of C-PC extracted from *A.platensis* at pH values of 5.0, 6.0 and 7.0 and temperatures at 50 and 65 °C was evaluated. The C-PC extract was more stable at pH 6.0 between 50-55°C and between 57-65°C at pH 5.0. Furthermore, at pH 7 an increased temperature led to unstable C-PC. The addition of sorbitol between 10 and 50% (w/w) in the treatment at 62°C for 30 min increased the half-life values of the phycocyanin extract. Martelli *et al*. (2014) also found that C-PC is slightly more stable at pH 5.0 (Tm 61.8°C) whereas at pH 9 the stability of C-PC strongly reduces (Tm 49.9°C).

To preserve the colour and prevent C-PC denaturation due to the adverse chemical changes, stabilising agents are often used as preservatives to protect the structure of the protein chains. The thermostabilisation of C-PC could be enhanced by modification of the chemical environment *via* the addition of various additives. Indeed, among the most used additives, sugars (glucose, sucrose, fructose), polyols (sorbitol), salts (NaCl) and acids (ascorbic acids or citric acids) Mishra *et al*. (2008) investigated the effect of edible preservatives which included citric acid, sucrose and calcium chloride on the stability of C-PC at 0 ±5°C and 35 ± 5°C. The citric acid (4 mg/mL) was observed to be one of the best preservatives for C-PC at 35 ± 5°C for 45 days with negligible loss when compared to the stability of C-PC at 0 ±5°C Chaiklahan *et al*. (2012) reported after incubation at 74°C for 1 min that the C_R value of the C-PC solutions at pH 5.0, 6.0 and 7.0 was in 96–100%. Furthermore, C-PC solution was more stable at 4°C. The maximum stability at 50°C was observed at pH 6.0, with an increase in temperature up to 60°C the maximum stability was at pH 5.5. From this study, it was found that glucose (20%), sucrose (20%) and sodium chloride (2.5%) were considered suitable for prolonging the stability of the C-PC extract

Martelli *et al*. (2014) tested the effect of different monosaccharides sugars such as fructose, glucose or sucrose and disaccharides (lactose and maltose) on the stability of C-PC by mixing one part of the purified protein solution with four parts of saturated solutions. The thermal stability of C-PC at 80°C increases slightly using the sucrose solution (54%), and a significant increase in the stability of C-PC at 80°C in fructose solution (62%) was observed, in contrast,

glucose solution (37%) did not significantly increase the stability of C-PC at 80°C. Lactose does not stabilise C-PC, only 5% of the protein was in solution after 30 min at 80°C. The presence of 42% maltose also increases the thermal stability of C-PC. Results showed that is not the type of sugar that stabilise C-PC but rather its concentration.

Pan-utai *et al*. (2018) reported that the addition of citric acid increased the thermal stability of food-grade C-PC extracted from *A. platensis*. These results indicated that citric acid as the preservative improved colourant stability during heating. The stability of C-PC from *A.platenis* decreased by increasing the storage time at various temperatures. The highest stability of C-PC was observed at 18°C followed by 4°C. The stability of C-PC drastically decreased in a pH of 5.5, thus, the best conditions for the minimum concentration loss of C-PC were in a pH of 4.5 at -18°C stored for 30 days. Three additives, PEG-4000 and sorbitol were tested to improved C-PC stability considerably. The C-PC values in the presence of PEG-4000, sorbitol, and sucrose were 85.71, 76.17 and 57.14 % respectively (Chentir *et al*., 2018).

2.14 COMMERCIALISATION AND APPLICATIONS OF C-PHYCOCYANIN

The global market for PBPs was estimated at more than US$ 50 million in 1997. At present, the prices of PBPs products are 3 to 25 US$ per mg for native pigment and can reach 1500 US$ per mg for certain cross-linked PBPs (with antibodies or other fluorescent molecules). C-Phycocyanin divides into different grade depending on its purity ratio (A_{620nm} /A_{280nm}): (i) food/ cosmetic grade, only as a dye (0.50-2.50); (ii) reagent level used as dye and Biomarker (2.50-3.50); (iii) analytical/ antibody grade used in therapeutics, for biomarkers, and treatment (>4) (Chen *et al*., 2017; Pan-utai *et al*., 2018; Song *et al*., 2013).

The market size for PBPs is difficult to determine since there is still no reliable published statistics on the C-PC market size and price (Leu *et al*., 2013). In 2013, Borowitzka estimated the total market of PPBs s as bigger than 60 million US$. According to the Global Phycocyanin Market Report (FDA, 2017), the C-PC market size was estimated at 15.6 million US$ and maintained a growth rate of 26.39% to reach 31.5 million US$ in 2016.

In 2016, (Global One-Stop Reports Center, 2016), projected the C-PC market to reach US$ 97 million by 2019 (dos Santos *et al*., 2019). Furthermore, analysts expect that by 2021 the C-PC market size will increase up to 186.7 million US$. A report from Future Market Insights indicated that Western Europe is the biggest consumer of C-PC of ~ 33% with 80% of C-PC produced is used in the food industry (Pagels *et al*., 2019). Several Biotechnology companies sell cyanobacterial C-PC products as summarised in Table 8. Flogen® is Febico's brand for PBPs, which include R-PE, APC, CL-APC, PerCp, B-PE, Cr-PE, R-PC, and its relevant conjugates. Several other companies are commercialising different products based on C-PC like – C-PC from Cyanotech; PhycoLink® Biotinylated C-PC from PROzyme; PhycoPro™ C-PC from Europa Bioproducts Ltd.; C-PC from Sigma Aldrich etc. (Chakdar & Pabbi, 2012). Phyco-Biotech company is a supplier of natural fluorescent tags APC, APCXL, C-PC, R-PE and B-PE, for LifeTech and CisBio Bioassays.

Table 8: Companies and the commercialised PBPs products (Eriksen, 2008; Kuddus et al., 2013; Sekar & Chandramohan, 2008)

Name of the company	Products	Application
Dainippon Ink and Chemicals (DIC) Cooperation	Linablue	Food dye
Japan Algae	Spi-Blue	Food dye for coating, confectionery, capsule, candy, bean paste, gum, jelly, ice cream, powdered juice, sugar, rice cake, noodles, wasabi
Parry Nutraceuticals		
Earth Rise Nutritional		
Natura4Eva	NaturaBlue®	Food supplement- antioxidant
Zhejiang Binmei Biotechnology	BINMEI PC	Food and cosmetic dye
Cyanotech	Fluorescent tags, markers	Food and cosmetic colouring
		Flow cytometry, fluorescence immunoassay,
Prozyme	Fluorescence tags, markers	Multicolour fluorescence applications, fluorescence resonance energy transfer (FRET)

Name of the company	Products	Application
Febico's (Flogen)	Fluorescence tags,	Immunostaining, Fluorescence tags, flow cytometry, fluorescence in situ hybridisation, FACS, receptor binding in fluorescence resonance energy transfer (FRET), fluorescence immunoassays, fluorescence microscopy, multi-colour immunofluorescence and other imaging techniques
Martex Bioscience Corporation	SensiLightTM Dyes -PBXL-1, PBXL-3 and P3L Streptavidin−CryptoFluor™	Flow cytometry, fluorescence immunoassay
Phyco-Biotech	C-APC, APC-XL, C-PC, R-PE and BPE,	Medical diagnosis, flux cytometry, immunohistochemistry, DNA microarrays, FRET,
Sigma Aldrich	C-PC, R-PE, C-APC,	Biochemicals and Reagents, Fluorescent Labels, Fluorescent Probes
SETA BioMedicals		
Xi'an Pincredit Bio-tech Co., Ltd	C-PC	
Anaspec	C-PC, CL-APC, R-PE, B-PE	Flourescent dye
AAT Bioquest	C-PC	
ABBIOTEC	C-PC antibody	
Norland Biotech		
Columbia Bioscience		

2.14.1 Fluorescent Agents

A large number of patents on fluorescence-based applications of PBPs reflect their growing demands in the industry (Sekar and Chandramohan, 2008). Depending on the purity and intended application, the price of PBPs may go up to thousands of US$ per mg (Sekar and Chandramohan, 2008). The major fluorescent protein complex in cyanobacteria the PBS. The presence of covalently attached chromophores on PBPs makes them highly fluorescent. There are several unique properties of PBPs compared to other fluorophores such as fluorescein, tyrosine, tryptophan and Green Fluorescence proteins (GFP) which make them ideal

candidates for various biological applications including very powerful and highly sensitive fluorescent reagents. These properties include: (i) high molar absorbance coefficients, (ii) high fluorescence quantum yield(~ 0.65-0.98), (iii) a wide range of absorbance spectra (490-650 nm), (iv) large Stokes shift which provides a greater signal to noise ratio compared to other small fluorophores, (v) high oligomer stability (vi) fluorescence is free of interference from biological molecules (vii) and high photostability and (viii) stable at a wide pH range (4.5-8.0) (Li *et al*., 2019; Sun *et al*., 2003). Purified native PBPs and their subunits fluoresce strongly thus have been widely used as probes for fluorescence-based assays including cell sorting (Tooley *et al*.,2001; Wu *et al*., 2018).

The C-PC may be conjugated to monoclonal and polyclonal antibodies for use in multicolour flow cytometry analysis. C-PC can be applied in the counting of nucleated cells and measuring the proliferative activity of the cell in case of malignancy (Singh *et al*., 2009b). The stabilised PBPs designated PBXL-3L was applied as a fluorochrome for flow cytometric immunodetection of surface antigens on immune cells (Telford *et al*., 2001). Glazer & Clark (1986) conjugated PBPs to immunoglobulins, protein A and avidin to develop fluorescent probes. These conjugates have been widely used in histochemistry, fluorescence microscopy, flow cytometry, fluorescence12 activated cell sorting and fluorescence immunoassays (Glazer and Stryer 1984; Glazer 1994; Sun & Wang *et al*. 2003).

Trimers of C-PC can be stabilised by chemical cross-linking of polypeptide chains (Fukui, Saito *et al*. 2004; Sun, Wang *et al*. 2006). Another important use of PBP is in Fluorescence immunoassay technique (FIT), a process used for the identification of various proteins or enzymes in diseased cells. Artificial photosynthesis is currently a hot topic in science and technology. Consequently, there are growing demands for designing photoelectron-chemical (PEC) cells, capable to perform artificial photosynthesis. In PEC devices, light-harvesting proteins (such as C-PC) are used to "sensitise" metal and semiconductor surfaces. BioPEC solar hydrogen generator with a hematite-phycocyanin hybrid photoanode was designed. In order to obtain PEC cells with higher performances, the stability of immobilised C-PC needs to be improved.

2.14.2 Food Colourant and Dye in the Cosmetic Industry

In recent years there has been rising costs of health care and an increase in chronic diseases and due to changing lifestyles. As a result, people are becoming more health-conscious and more interested in health-promoting products to improve their quality of health. This has lead to an increased demand for natural nutraceuticals, dietary supplements, functional food ingredients and additives (Dragana Stanic-Vucinic, 2018).

The PBPs as natural colourants are gaining importance over synthetic colours as they are environment-friendly, non-toxic and non-carcinogenic. Furthermore, the protein component of C-PC adds nutritive value to food products, In 2013, the food and drug administration (FDA) first approved *Spirulina* extract as a food additive for applications in gum and candy. The following year, the list expanded to dessert coatings, frosting, frozen desserts, ice cream, beverage mixes and powders, yoghurts, cottage cheese, custards, puddings, gelatin, breadcrumb, and ready-to-eat cereals (Dragana Stanic-Vucinic, 2018). In 2015, the applications continue to grow, whereby coatings in dietary supplements and pharmaceuticals were also approved. Dainippon Ink & Chemicals (Sakura, Japan) has developed a product called "Linablue" (C-PC extract from *A. platensis*) which is used in chewing gum, ice sherbets, popsicles, candies, soft drinks, dairy products and wasabi (Nag Dasgupta, 2015). Linablue® is currently only approved as a natural blue colourant in the US, Europe, and Asia (Table 8).

In 2018, DIC Corporation further invested US$13 million for C-PC production expansion project for Linablue® of its California-base subsidiary Earthrise Nutritionals, LLC. C-Phycocyanin also becomes a popular component of different wellness bioactive drinks such as Ocean Mist by Allgalio Biotech, B Blue by B blue, Bloo tonic by Cidererie Nicol, Holy water by Juice Generation, Natura blue by Natura4Ever, Smart chimp by Smart chimp (Dragana Stanic-Vucinic, 2018). Blue Majik is a C-PC extracted from *A. platensis* by E3Live used in many of these drinks to provide an attractive blue colour and nutraceutical properties. C-Phycocyanin can be combined with natural yellow and red pigments to create another food colouring that imparts more vibrant greens and purples.

Accordingly, the demand for these applications is also growing. The DIC Group currently has over 90% of the global market share for *Spirulina*-derived natural blue food colouring. Despite its lower stability to heat and light, C-PC is considered more versatile than gardenia and indigo, showing a bright blue colour in jelly gum and coated soft candies (Lone *et al*., 2005). Use of PCB in cosmetics like lipstick, eyeliners *etc*., is also gaining momentum. Studies have

addressed the functionality of C-PC in foods with regards to colour stability and rheological properties. C-PC can potentially be used as an edible coating, thus, acts as a carrier of bioactive compounds to improve the quality of food products.

2.14.3 Biomedical, Pharmaceutical and Nutraceutical Applications

Several investigations have also shown the health-promoting properties and a broad range of pharmaceutical applications of PBPs. Evidence has shown that C-PC has more than one specific target and therefore, it has a diversity of effects. The pharmacological properties like antioxidant, anti-inflammatory, neuroprotective and hepatoprotective activity have been attributed to C-PC (Benedetti *et al*., 2006; Chen *et al*., 2015; Gammoudi et al 2019; Lee *et al*., 2018; Madamwar *et al*., 2015; Pleonsil *et al*., 2013; Young *et al*., 2016; Yu *et al*., 2017). Owing to the unique properties of C-PC such as being biodegradable, biocompatible, photosensitive, and poor immunogenic protein it can be used as a carrier for preparation of protein-based nanoparticles for drug delivery (Samydurai *et al*., 2016).

2.14.3.1 Antioxidant properties and effects

Cyanobacteria produce antioxidants to protect themselves from oxidative stress mainly due to the accumulation of reactive oxygen species (ROS). Both enzymatic and non-enzymatic antioxidant mechanisms assist in the neutralisation of ROS. C-Phycocyanin acts by scavenging the free-radicals of ROS, neutralising the reactive molecules and decreasing the level of oxidation by a non-enzymatic antioxidant mechanism (Pagels *et al*., 2019). The antioxidant and radical scavenging activities of C-PC from different cyanobacteria are well researched and studies have reported that C-PC is very efficient free radical scavengers and exhibit the high antioxidant activity (Bermejo *et al*., 2008; Fernández-Rojas *et al*., 2014; Hossain *et al*., 2016; Suzery *et al*., 2017). The apoprotein *i.e.* α and β subunits and PCB are involved in the stabilisation of the ROS. Furthermore, under different light conditions, C-PC is bi-functional, it can generate •OH, whereas in the dark it traps them. The ROS production is counteracted when the concentration of PC increased.

2.14.3.2 Anti-inflammatory and anti-cancer properties

The anti-inflammatory activity of C-PC is primarily due to the action of the compound in different mechanisms of action in enzymes expression and activation as well as in the modulation of macrophages function, inhibiting the pro-inflammatory signals. Reports have shown that the anti-inflammatory effect of C-PC is related to a reduction in the release of

histamine, the activity of myeloperoxidase (MPO), level of prostaglandin E2 (PGE2), level of phospholipase A2 (PLA2) and inhibition of the expressions of cyclooxygenase-2 (Cox-2), interleukin-6 (Il-6) and Stat3 genes. Prescription Cox-2 inhibitors can damage the liver, however, C-PC is shown to help the liver (Hao *et al*., 2018; Jensen *et al*., 2015; Romay *et al*., 2003).

The therapeutic potential of C-PC in cancer treatment has been reported by several researchers whereby it exerts its anti-cancer effect by modulating apoptosis and cell proliferation. C-PC has a potent anticancer effect both *in vitro* and *in vivo* on a variety of cancer cell types, including lung cancer, colon cancer, breast cancer and bone marrow cancer (Li *et al*., 2015; Pan *et al*., 2015). Studies have shown that C-PC exhibits a significant inhibitory effect on the growth of cancer cells through various mechanisms including the induction of apoptosis, cell cycle arrest, inhibition of DNA replication and generation ROS (Safaei *et al*., 2019). The advantage of applying C-PC is that it is toxic to the cancer cells however is not toxic to the normal cells (Jiang *et al*., 2017; Pagels *et al*., 2019).

C-Phycocyanin has shown to induce apoptosis in tumour cells through the production of ROS. By down-regulating the expression of the anti-apoptotic Bcl-2 molecule12, by inducing cytochrome c release from mitochondria into the cytosol and PARP cleavage13. C-Phycocyanin can also induce apoptotic cell death by upregulation of Caspase 3 and Caspase 8 activities (Liao *et al*., 2016).

2.14.3.3 Antimicrobial activity

C-phycocyanin, from *Porphyridium aerugineum* was reported to inhibit the growth of the Gram-positive *S. aureus* with a MIC of 7 *μg*/mL (Najdenski *et al*., 2013). Also, *in vitro* studies proposed that *Spirulina* possesses antiviral activities (Daoud & Soliman, 2015; Hernandez-Corona *et al*., 2002; Karkos *et al*.,2011); The most susceptible bacteria to *A. maxima* were *Streptococcus* sp. and *Bacillus. subtilis* with highest inhibition zones ranged 6–13 mm at 100–400 μL/disk (Soni *et al*., 2005). Mohammadi-Gouraji *et al*. (2019) evaluated the effects of purified C-PC on the physicochemical and microbial properties of yoghurt during 21 days of storage. *Streptococcus thermophilus* and *Lactobacillus bulgaricus* count decreased significantly on days 21 and 14, respectively. C-phycocyanin has also demonstrated *in vitro* antimalarial activity against the chloroquine resistant of *Plasmodium falciparum* strains (Biswas, 2001).

CHAPTER 3 : CHARACTERISATION OF A NOVEL INDIGENOUS EURYHALINE *EUHALOTHECE* SP.

3.1 INTRODUCTION

St. Lucia Estuary part of the iSimangaliso Wetland Park, South Africa's first UNESCO World Heritage Site represents one of the largest estuarine lakes in Africa. From 2001-2012, this lake experienced high salinities up to 100 g/L due to prolonged mouth closure, high water evaporation rates and severe extended droughts (Carrasco & Perissinotto, 2012). Increased salinity levels up to 60 g/L resulted in the disappearance of many planktonic and benthic microorganisms within Lake St Lucia (Muir & Perissinotto, 2011). Few organisms are able to tolerate or grow in hypersaline environments owing to harsh ecological conditions such as low nutrients, oxygen availability, high salt concentrations, extreme pHs and temperatures. (Wong *et al*., 2016), however, some can flourish. At higher salt concentrations above 120 g/L in Lake St Lucia, a few halophilic microorganisms were found to persist under these hypersaline conditions (Carrasco & Perissinotto, 2012). In 2011, we isolated and studied the bloom-forming cyanobacteria belonging to the genus *Cyanothece* sub-cluster *Euhalothece* from Lake St Lucia. The isolated strain of cyanobacterium was found to tolerate temperatures up to 45°C, salinity >120 g/L, pH range between 6.0-9.0, survive in varying nutrients levels and naturally produce a high quantity of C-PC (45 mg/g) (Mogany, 2013). *Cyanothece* strains have been investigated for their robust circadian rhythms, hydrogen production, nitrogen fixation, fermentative abilities and other biotechnological applications (Bandyopadhyay *et al*., 2011b; Stockel *et al*., 2011; Welsh *et al*., 2008a). Hence the characterisation and accurate identification of the isolated cyanobacteria based on ecological studies and biotechnological techniques has become an essential step to fully understand and exploit the organism. The traditional classification of cyanobacterial taxa has been performed by a comparison of phenotypic features. However, this method does not reflect the evolution and the degree of relationship among different taxa (Kim *et al*., 2014b; Komárek *et al*., 2011). In recent decades the use of molecular taxonomy based on nucleotide sequence homology of marker genes (usually 16S, 23S, 16S–23S intergenic spacer regions or cpcBA-IGS region) has been employed for accurate identification (Bravakos *et al*., 2016; Rajendhran & Gunasekaran, 2011). Although comparative studies based on a single gene analysis are acceptable, they have only partly resolved relationships among the cyanobacterial lineages. Furthermore, the phylogeny derived from single-gene comparison showed inconsistency with each other due to different factors such

as horizontal gene transfer (HGT), paralogy and highly variable rates of evolution (Chrismas *et al*., 2015; Larsson *et al*., 2011; Snel *et al*., 2002). It is important to focus on multiple genes from many species are to be carried out to accomplish a reliable phylogenetic resolution. Consequently, whole-genome sequencing (WGS) has emerged as a powerful tool to identify and resolve the functional characteristics of cyanobacterial species for species-level identification (Tan *et al*., 2016). Since these cyanobacteria are prevalent in extremely mineralised waters, they are expected to have higher genomic diversity between different strains. Recent advancements in cyanobacterial genome sequencing have enabled large-scale, multi-gene phylogenetic analyses (Kim *et al*., 2014a). This has provided a robust framework to resolve deep branching relationships, understand the evolutionary history of these organisms and identify the different factors such as vertical descent, gene transfer, gene and genome duplication, gene invention, gene loss and degradation that affect the tree lineage (Chrismas *et al*., 2015). Therefore, WGS appears to be a more accurate tool for the generation of reliable phylogeny and identification, as it allows for the comparison of entire genome content.

This chapter focused on a polyphasic approach for identification of an indigenous euryhaline cyanobacterium based on both the phenotypic and genotypic characteristics. Both 16S rRNA based phylogenetic analysis and whole-genome sequencing were performed to better differentiate the isolate from its closest relatives.

3.2 MATERIALS AND METHODS

3.2.1 Cyanobacterium Cultivation

The cyanobacterial strain used in the study was previously isolated by the Institute of Water and Wastewater Technology from False Bay region at Lister's Point (Lake St. Lucia, South Africa, 27.976S 32.362E) (Mogany *et al*., 2018b) (the site location and parameters of sample collected are available in Appendix 2). Isolation and purification of the isolate was carried out using serial dilutions and repeated streak-plating on 1% Blue-Green 11+ sodium chloride (BG11+NaCl) agar medium (Stanier et al., 1971) medium, pH 7.0. Wet mounts were prepared and examined using light microscopy (Zeiss Axio microscope) to ensure purity of the culture. Single colonies were picked from agar plates and inoculated into liquid 10 mL BG 11 medium containing 100g/L NaCL. Cultures were illuminated by Sylvania® Gro-Lux® lightbulbs (80

μmol/m^2/s),16 h light: 8 h dark cycles at 29 ± 2°C. Cultures were maintained in 5 L Erlenmeyer flasks containing 3.5 L media under continuous aeration. Cyanobacteria strain was deposited in the Culture Collection of Algae and Protozoa (CCAP) under the GenBank reference KF017202. The CCAP reference for the strain is CCAP 1435/1. Microscopy (as per section 3.2.2.1 was conducted to determine if the strain was axenic.

Previous research conducted was performed to maximise the biomass and C-PC production by optimising the cultivation conditions and media. The modified BG11media contained (120 g/L of NaCl, 1.67 g/L of $NaNO_3$, 0.10 g/L of $MgSO_4$, 0.09 g/L of iron-EDTA and citric acid).

3.2.2 Phenotypic Characterisation

3.2.2.1 Light microscopy

To examine the morphological characteristics, wet mounds were prepared and observed using a Zeiss Axio microscope equipped with transmitted light and phase contrast illumination (Axio Imager A1; Carl Zeiss, Germany). Micrographs were taken with a digital camera (Axiolab) using the Zen software. The major characteristics examined were cell shape, cell dimensions (diameter, length), the type of cell division, colour of cells and motility. Tentative identification was done following Bergey's Manual of Systematic Bacteriology taxonomy (Castenholz, 2001) as well as the classification made by Komárek & Cepák, (1998) and Komárek, (2014).

3.2.2.2 Epifluorescence microscopy

A modified method by Mukherjee & Ray (2015) was used to stain the DNA structures with 4′,6-diamidino-2-phenylindole (DAPI). Exponentially growing cells (100 mg) were harvested by centrifugation 8000 x g for 10 min and washed with phosphate buffer and thereafter, stained with 100 μL of 20 μg/mL of DAPI for 30 min. To visualise the exopolysaccharides (EPS), samples were filtered onto a 0.4 μm pore size filter and stained for 30 min with a 0.02% w/v Alcian Blue solution in 0.06% v/v acetic acid (pH 2.0±5), followed by rinsing with DdH_20 water (Sohm *et al.*, 2011). The stained cells were examined with an epifluorescence microscope (Axiolab, Carl Zeiss, Germany) applying a mercury source (HBO 50) interfaced with a Zeiss Filter set 49 (excitation 365, beam splitter FT 395 and emission 445/505 nm). Subsequent images were taken with Axiovision imaging v8.0.

3.2.2.3 Scanning electron microscopy (SEM)

Scanning electron microscopy was conducted to examine the surface topology (presence of a sheath, polymeric substances) and distribution of specimens at high magnification (Żyszka *et al*., 2017). For SEM analysis exponentially growing cyanobacterial cells were harvested and samples were fixed in 2.5% glutaraldehyde in 0.1 M sodium phosphate buffer (pH 7.2) overnight, followed by a post-fixation step, whereby the sample was immersed in 0.5% OsO4 for 1 h and thereafter, rinsed twice with sodium phosphate buffer (pH 7.2). This was followed by a series of dehydration steps using 30, 50, 75, 85, 95 and 100% ethanol for 5 min and drying at a critical point for 3 h under a CO_2 environment. The samples were subsequently mounted on stubs (Ø12.7mm) and sputter-coated with gold, using Quorum (Q 150R ES). The coated samples were then examined with a ZEISS LEO 1450 scanning electron microscope operated at 10 or 20 kV and with working distances of 7–9 mm.

3.2.2.4 Ultrastructure characterisation using transmission electron microscopy (TEM)

Ultrastructure analysis of cyanobacterial cells was analysed using TEM. Preparation of slides for electron microscopy was done according to the method by Loza *et al*. (2013) with some modification. Cells from 10 mL of culture were collected by centrifugation at room temperature (8000 x g, 5 min) and washed with DdH_2O, and transferred into 2% bacteriological agar in 0.1 M phosphate buffer (pH 7.2). Thereafter, fixed in 3% glutaraldehyde in 0.1 M phosphate buffer (pH 7.2) and incubated for 24 h at 4°C. Subsequently, the samples were washed using 0.1 M phosphate buffer (pH 7.2), and post-fixed in 1% osmium tetroxide made up in 0.1 M phosphate buffer for 2 h at 4°C. Samples were then dehydrated in increasing concentrations of ethanol (30-100% v/v). Thereafter, samples were progressively infiltrated then embedded in Spurr's resin and allowed to polymerise at 65°C for 72 h (Spurr, 1969). Ultra-thin sections were cut with an ultramicrotome using glass knives and stained with uranyl acetate and lead citrate. Visualisation and photography were performed using a JEOL 1010 transmission electron microscope (JEOL MA, USA) operated at 100 kV.

3.2.3 Genotypic Identification

3.2.3.1 DNA isolation

Genomic DNA extraction was done using a FastDNA™ SPIN Kit for soil according to the manufacturer's instructions. (MP Biomedicals, Thermo Fisher Scientific) (Detailed protocol in

Appendix 3). Briefly,10 mL of exponentially growing cyanobacteria was centrifuged (857 x g, 15 min) and re-suspended in 2 mL Eppendorf microtubes. Samples were washed twice with DdH_2O and transferred to the 2 mL Lysing Matrix E tube™ (containing ceramic and silica particles) and PBS and MT buffer™. Thereafter, samples were lysed using bead beating (Mini bead beater, Biospec Products, USA) for 60 s and centrifuged (14 000 x g, 10 min). Subsequently, the DNA was precipitated and re-suspend in the binding matrix. Approximately 500 µL of the mixture was transferred to a SPIN™ Filter, centrifuged at 14 000 x g for 1 min and was gently resuspended in the concentrated SEWS-M following centrifugation (14 000 x g, 10 min). Finally, the precipitated DNA was re-suspended in DNase/ Pyrogen-Free Water).

3.2.3.2 DNA quantification and purity analysis

The quantity and purity of the extracted DNA were assessed spectrophotometry (Qubit® 2.0 Fluorometer, Thermo Fisher Scientific). The overall purity was assessed by calculating the absorbance ratios $A_{260\ nm/280\ nm}$ and $A_{260\ nm/230\ nm}$. High values > 1.8 and > 2 for ratio $A_{260\ nm/280\ nm}$ and $A_{260\ nm/230nm}$ respectively are commonly accepted as good indicators for pure DNA (Simbolo *et al*., 2013). A low $A_{260\ nm/23\ 0nm}$ value indicates the presence of organic compounds such as phenolates, thiocyanates, carbohydrates, or salts in the extract, whereas low $A_{260\ nm/280\ nm}$ ratios indicate a protein and/or phenol contamination within the sample.

The molecular weight and the integrity of the extracted genomic DNA were determined using agarose gel electrophoresis. Approximately 4 μL of the sample was loaded on a 0.8% w/v agarose gel stained with ethidium bromide (final concentration 100 μm/L, Sigma-Aldrich) and electrophoresed at 80 V for 1 h. A 100 bp DNA ladder (Invitrogen™) was used as a reference to evaluate the size of the DNA. The results can be seen in Appendix 4.

3.2.3.3 Genome sequencing and assembly

Multiplexed paired-end libraries (2 x 300 bp) were prepared using the Nextera XT DNA sample preparation kit (Illumina, San Diego, CA, USA). Sequencing was performed on an Illumina MiSeq instrument at the NICD Sequencing Core Facility, Johannesburg (Figure 6).

The genome sequencing workflow was divided into five logical sections: assembly, ordering of (contiguous sequence) contigs, annotation, genome comparison and typing. The resultant paired-end reads were quality trimmed and *de novo* assembled using CLC Genomics Workbench version 8 (CLC Bio-Qiagen, Aarhus, Denmark). The fragments are aligned and

joined together using a computer program called an assembler, thereafter, the sequence quality was checked and the reads regions containing bases of low-quality scores or unknown bases (represented as "N" in the datasets) were removed. After assembly, a collection of contigs were obtained. A scaffolder was used to link distant sequences together based on the distance between the two ends of the original template. After the ordered set of contigs was obtained, the next step was to annotate the draft genome.

All resultant contigs were then submitted to GenBank, where gene annotation was implemented using the NCBI Prokaryotic Genome Annotation Pipeline (PGAP) (Tatusova *et al*., 2016). PGAP combines HMM-based gene prediction methods with a sequence similarity-based approach, which combines comparison of the predicted gene products to the non-redundant protein database, Entrez Protein Clusters, the Conserved Domain Database, and the COGs (Clusters of Orthologous Groups).

3.2.2.4 Genome comparisons analysis

The 16S rRNA gene sequence of the cyanobacterial isolate extracted from genome data was compared against the sequences from GenBank, National Center for Biotechnology Information (NCBI) (www.ncbi.nlm.nih.gov) using Basic Local Alignment Search Tool (BLAST). Closely related sequences from GenBank were retrieved and used for phylogenetic analysis. Nucleotide sequences obtained were edited and aligned using BioEdit V7.26. The overview of the sequencing process is shown in Figure 7.

Phylogenetic analyses were used to estimate the evolutionary relationships of cyanobacteria. Genome comparisons were based on 16S rRNA gene sequence, 23S rRNA gene sequence, ITS region gene sequence, a highly conserved C-PC operon and full genome. The sequences were first compared using Basic Local Alignment Search Tool (BLAST) (Donkor et al., 2014). NCBI BLAST (http://blast.ncbi.nlm.nih.gov) is a shared public resource that is simple to use, produces results quickly, and requires only a web browser. The blastn tab for nucleotide sequences was selected, thereafter, the FASTA sequence was uploaded into the query sequence identifier and BLAST button clicked. The BLAST algorithm either megaBLAST or BLASTN was selected. The megaBLAST is a nucleotide-nucleotide search, optimised for very similar sequences (in the same or in closely related species), it first looks for an exact match

of 28 bases, and then attempts to extend that initial match into full alignment. The BLASTN is nucleotide-nucleotide search looks for more distant sequences.

Sequence analyses included alignment of gene sequences followed by the construction of a phylogenetic tree. ClustalW was used for multiple alignment process, whereby the sequences from different strains were organised by inserting gaps so that homologous positions of the sequences are placed in the same columns of the data matrix (Chenna *et al*., 2003).

The steps follow to construct the tree was done according to (Hall, 2013) in MEGA X software (Kumar *et al*., 2008).The Neighbor-joining method (Ludwig *et al*., 2001; Saitou & Nei, 1987) with 1,000 bootstraps and Maximum Likelihood method T was used to construct the phylogenetic tree. The bootstrap method was used to estimate the reliability of a phylogenetic tree. The similarity matrix was built comparing the 16S rRNA sequences using BioEdit.

Genome relatedness indices (OGRI) used in this study were DNA–DNA hybridisation (DDH) and average nucleotide identity (ANI). The *in-silico* DDH estimate and the difference in the average GC content were calculated using the Genome-to-Genome Distance Calculator 3 (GGDC V 2.0) http://ggdc.dsmz.de/distcalc2.php (Meier-Kolthoff *et al*., 2013). The Average Nucleotide Identity by Orthology (OrthoANIu) between the pair of genome sequences was done online using http://www.ezbiocloud.net/tools/ani (Yoon *et al*., 2017).

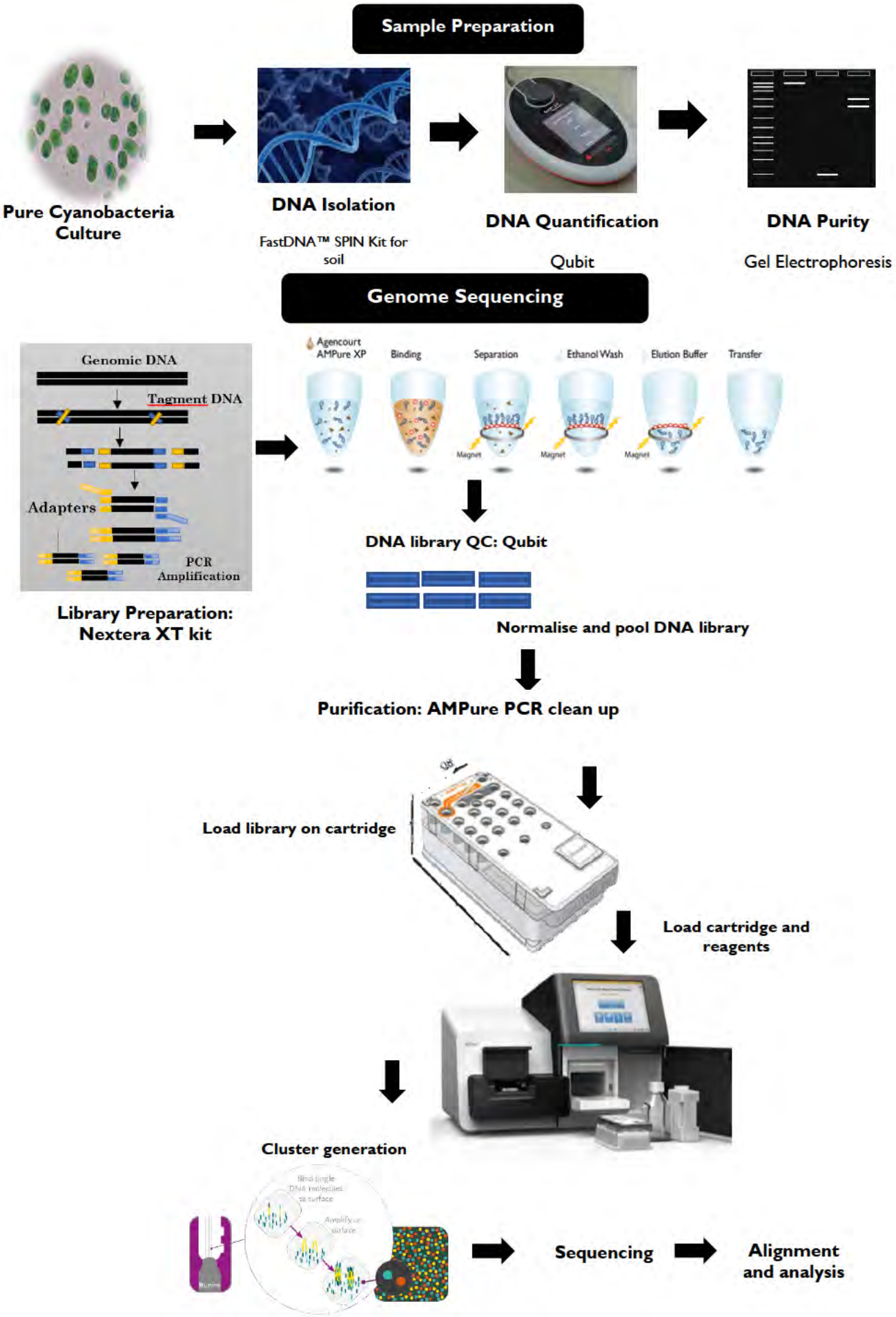

Figure 6: Overview of sample preparation and genome sequencing

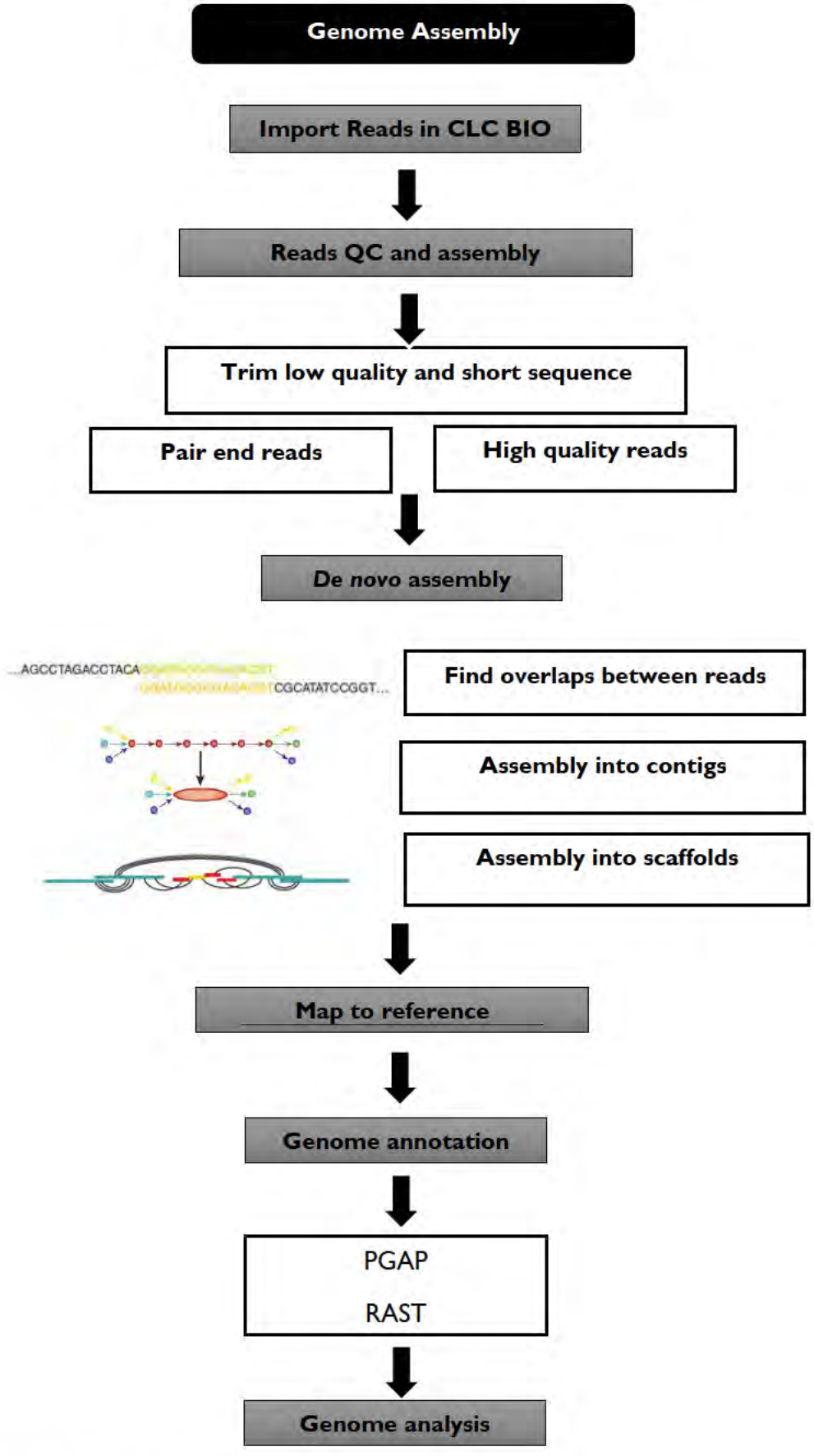

Figure 7: Overview showing steps carried out for genome assembly.

3.3 RESULTS AND DISCUSSION

3.3.1 Colonial Morphology of Isolate

After six weeks visible colonies appeared, the colonies purity was checked under the light microscope. Purified isolated appeared to be blue-green, lustrous, circular, raised smooth colonies with straight edges shown in Figure 8. The axenic cultures were inoculated into BG11 agar slant for maintaining the culture and inoculated into 10 mL of BG11+NaCl liquid medium

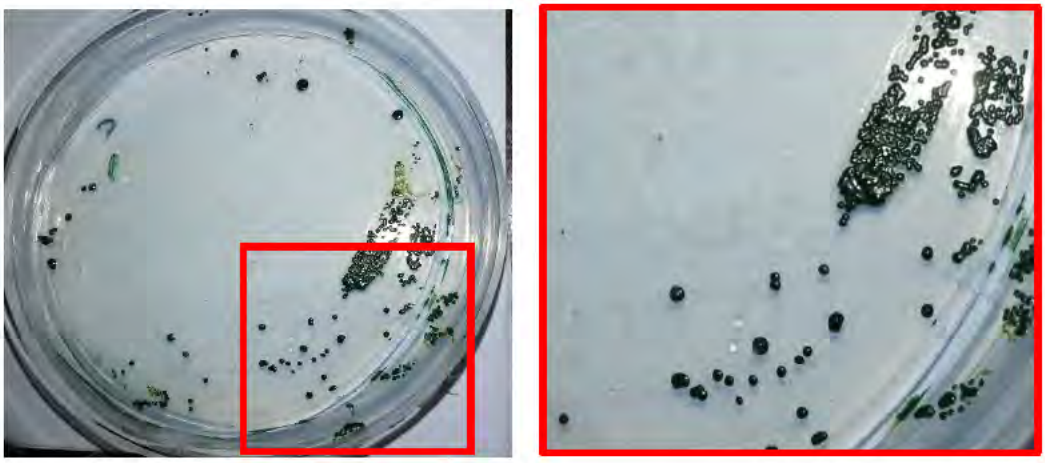

Figure 8: Growth of isolate on 0.8% agar after incubation for six weeks.

3.3.2 Phenotypic Characterisation of the Isolate

The Bergey's Manual of Systematic Bacteriology classifies the cyanobacteria in 'form genera' which, in turn, are divided into clusters or sub-clusters, however not an 'official classification' (Ramos *et al.*, 2017). Members of Subsection I (formerly order Chroococcales) are unicellular, spherical, ellipsoidal or rod-shaped cyanobacteria that reproduce by binary fission or budding (Ludwig *et al.*, 2001). The classification and general features of the isolated strain of cyanobacterium are summarised in Table 9.

Table 9: Morphological features and characterisation of isolated cyanobacterium strain

Classification	
Domain	Bacteria
Phylum	Cyanobacteria
Class	Cyanophyceae
Sub-Section / Order	Sub-Section I /Chroococcales
Family	Cyanobacteriaceae
Genus	*Cyanothece*
Cluster	Cluster 3: *Halothece*
	Subcluster: *Euhalothece*
Conditions at the time of sampling	
Habitat	St Lucia, False Bay (Hypersaline)
Water depth	±40 cm
Cell description	
Cell shape	Cylindrical- oval cells
Cell size (stationary phase of growth)	16 μm
Cell content	Granular
Biomass	2-4 g/L
Growth rate	0.76 g/day
Optimum cultivation conditions	
Growth media	Modified BG11
Salinity	120 g/L
Temperature	35°C
pH range	7-9
Pigment	PPBs and Chl

The cyanobacterial cells were found to be unicellular, blue-green and oval with a cylindrical shape, depending on the stage of the cell division cycle. At the time of isolation, the cells were 8-9 μm. However, after inoculation and incubation in BG 11 medium for ± 5 weeks, the cells reached stationary phase and had a width of > 14 μm and length of > 18 μm (Figure 9A). Cell division was always perpendicular to the longer axis of oval cells. Actively dividing younger cells appeared to be smooth and had a very thin mucous layer around them.

Microscopic observation of cells stained with Alcian Blue showed the presence of EPS which stained blue (Figure 9C). It was observed that these polysaccharides were associated with the cells but did not form a well-defined capsule (Figure 9F). In addition, some material was secreted into the medium and was not associated with the cell. Capsular polysaccharides (CPSs), surround cells and are differentiated based on their thickness and consistency. "Slime" is a less condensed form of EPS which are loosely attached to cells and does not reflect the

shape of the cells (Rossi & De Philippis, 2015). These polysaccharide external layers can be partly released in the surrounding medium, termed released polysaccharides (RPSs). Marine *Cyanothece* sp. have been reported to be efficient EPS producers. *Cyanothece* ATCC 51142 produces high levels of EPS (4.5% w/v NaCl pH 7.0, and $NaNO_3$) (Shah *et al*., 2000). The EPS released reached 1.8 g/L in *Cyanothece* sp. CCY 0110 grown in high light intensity in the presence of combined N (Mota *et al*., 2013). *Cyanothece* sp. 113 produced 18.4 g/L of EPS when cultivated in modified F_2 medium with 70 g/L of NaCl, 0.9 g/L of $MgSO_4$.

The presence of nucleic acids in cells, when stained with DAPI, was observed as a blue colour, with a mosaic of red (Chl) (Figure 9E), whereas polyphosphate bodies were observed as greenish-yellow dense granules in the cells (Figure 9D) (Cepák & Komárek, 2010). The DNA was spread unevenly across the entire cell cytoplasm, with no distinct nucleus. The nucleoid has a netlike structure - numerous skeins of DNA without visible DNA threads (Figure 9D).

The SEM images confirmed the presence of a thin, fine slime layer around the cells and this layer was found to be loosely associated with the cell surface (Figure 9F). Older cells had an irregular net-like granule appearance and were buoyant due to the presence of internal gas vesicles. Furthermore, the cyanobacterium was found to adjust buoyancy, accordingly, to achieve access to re-mineralised nutrients and float to obtain light energy for photosynthesis.

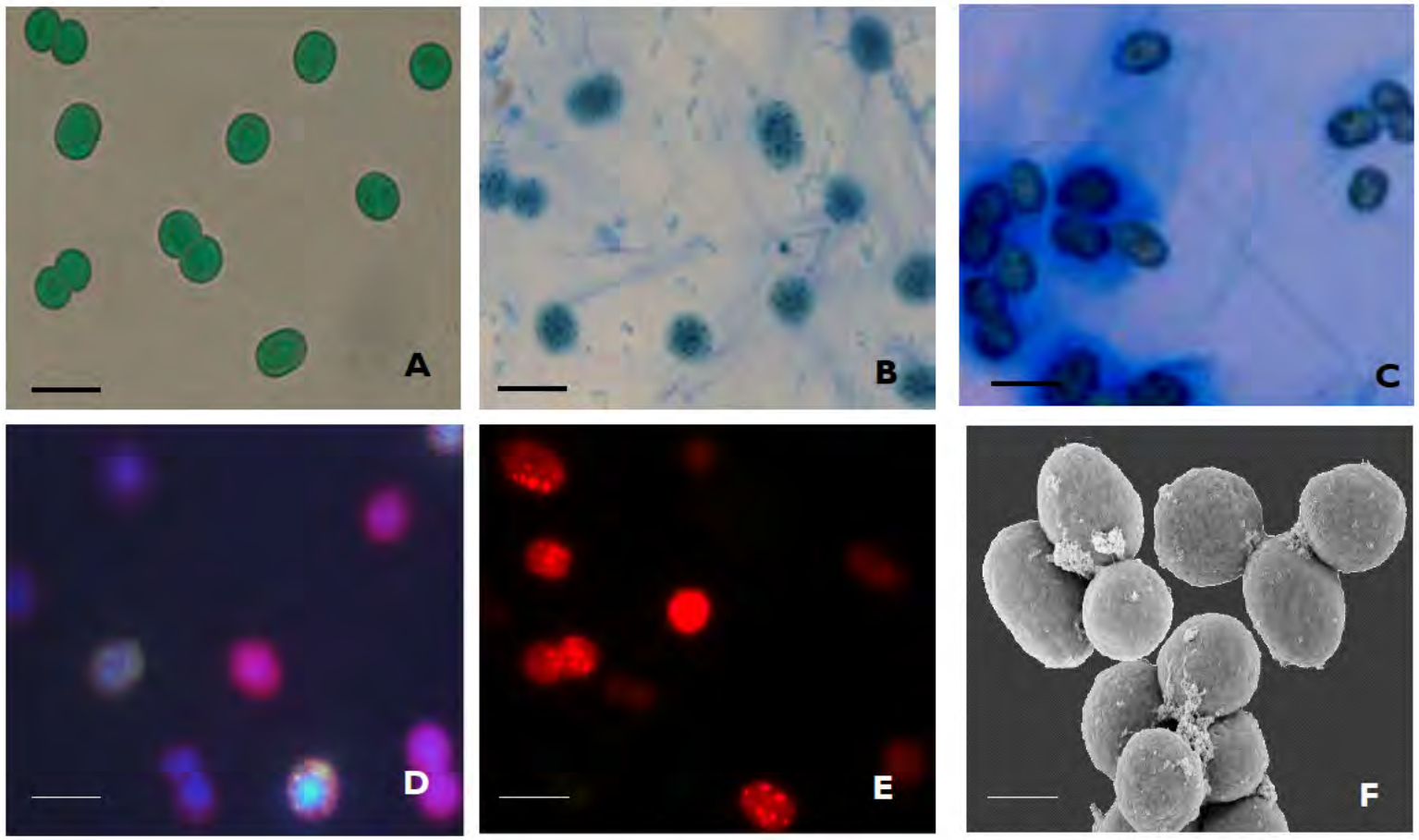

Figure 9: Micrographs of *Euhalothece* sp. (A) Light micrograph showing spherical to ovoid (14 to 18 μm) cells in singles and undergoing binary fission (1000 x), (B) Light micrograph of methylene blue stain showing polyphosphates (cy), scale bars = 15 μm. (C) Light micrograph of Alcian stain showing EPS stained blue, (D) Epifluorescent micrograph of showing DAPI stained cells, whereby DNA fluoresces blue and cytoplasm is pink, (E) Epifluorescent micrograph showing red autofluorescence of pigments (Chl and PBPs), scale bars = 10 μm. (F) SEM showing slime surrounding cell aggregates (micrograph 7.26 kx, scale bars = 1 μm) .

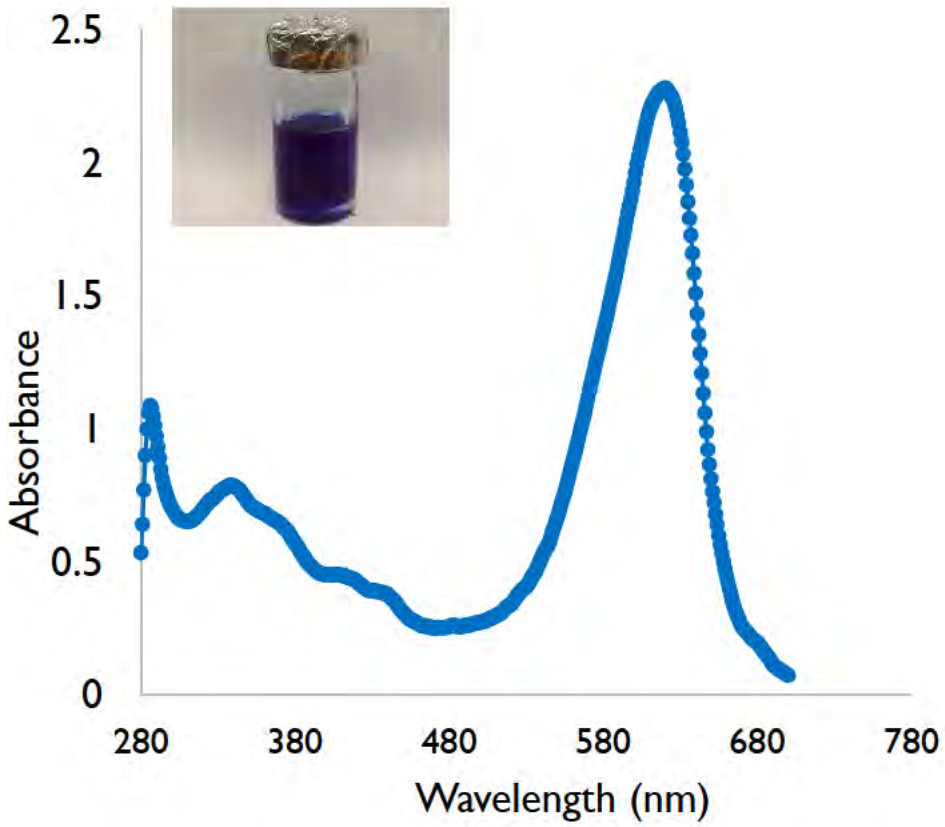

Figure 10: Absorption spectra of C-PC extract from the isolate. Insert shows blue C-PC extract.

Transmission electron micrographs showed the presence of a thick outer cell wall. The external layer (EL) surrounded the cell walls, consisted of thin fibres known as pili that emanated from the outer membrane and were arranged perpendicular to the cell (Figure 11A). Pili aid motility of the cyanobacterial cells Cyanobacteria are Gram-negative prokaryotes that possess an envelope thicker than typical Gram-negative bacteria. These organisms have a wall consisting of exopolysaccharides (S-layer), an outer membrane (OM), and a thin peptidoglycan layer (PG) adjacent to the plasma membrane (PM). As observed after methylene blue staining, the cell also contained numerous polyphosphate (p) granules that store phosphate. Moreover. the cell contained various other cellular inclusions, including and glycogen granules (g), which store carbon and carboxysomes (cb), which are nitrogen storage compounds that are membrane-bound. Cyanophycin (cy) granules that store nitrogen were also present; these appeared to be bodies of globular-like appearance with varied size after

±5 weeks (Figure 11B). The photosynthetic machinery of the isolate was made up of numerous irregular thylakoids (the) radiating all over the cell, partly in fascicles (Figure 11E).

The blue-green colour of the cells (Figure 9A) are due to the major PBP, *i.e.* C-PC occurring in the PBS rods. The bright blue crude C-PC can be observed in Figure 10. The cytoplasmic surface of the thylakoid membranes is separated by the PBS. The cross-section of the cell illustrating the side view of the PBS as a typical hemi-discoidal structure (blue box), as well as PBS with a 'grape' pattern or blackberry-like appearance (Figure 11C). Phycobilisomes are hemi-discoidal pigment-bound protein complexes that are attached to the cytoplasmic side of the thylakoid membrane. The PBSs are composed of a core and clusters of rods made up of short stacks of discs (Liu *et al*., 2005). The appearance of the PBS in thin sections electron micrographs is dependent upon the plane of sectioning of the samples (Cosner, 1978). When the rows of PBS are cut in cross-section in a plane perpendicular to the thylakoid surface, the PBS displays an irregular semi-circular outline with the flat side attached to the thylakoid membrane, therefore, appearing in face view (Bryant *et al*., 1978). A close examination of the micrograph presented in Figure 11C exhibits the predicted typical hemi-discoidal organisation of the PBS (red box shows the face view), whereby rods can be seen radiating outwards. The PBS rods formed by four to five hexamers, showing the arrangement of the hexamers. In Figure 11F the PBS are dense structures lying on the thylakoid membrane of the cyanobacterial isolate. The shape and organisation of the structures resemble the PBS.

These results are in agreement with previous observations by Adir *et al*. (2001); Chang *et al*. (2015) & Dagnino-Leone *et al*. (2017). Due to the tight packing of the PBS components, a distinction between core cylinders and rods cannot be seen. Additional, grape-like structures seen in Figure 11F (yellow box), also represented the PBS, in the bottom view. (Glauser *et al*., 1992) and (Ducret *et al*., 1996) found that in electron micrographs, the PBS of *Anabaena* sp. PCC 7120 and *Mastigocladus. laminosus* appear to be a compact body exhibiting roughly the form of a grape pattern. Distortion of PBS shapes within cells could be caused by close contact with the abundant α-granules which compete for the same stromal space (Gray *et al*., 1973). It is known that PBS naturally has a rectangular shape and stands upright on the thylakoid membrane in the cell (Collins *et al*., 2012). The PBS is seen in edge view standing on the thylakoid surface, when the rows of PBS are either cut in longitudinal section in a plane normal to the thylakoid surface or tangential section *i.e.* when the plane of sectioning is parallel to the thylakoid surface (Glauser *et al*., 1992). The PBS appear as electron-dense cords running at

an angle to the long axis of the cells. As seen in transversal sections, PBS appears to be dense structures that are anchored on the thylakoid membrane. Similarly, Porta *et al.* (2000) found that in *Cyanothece* PCC 8303, the alternative distribution of the PBS between two thylakoids gave the PBS a zipper-like appearance.

Based on the phenotypic and morphological characteristics, the isolated strain resembled members of Subsection I. The genus *Cyanothece* was suggested by Komárek (1976) Taxonomic review of the genera *Synechocystis* Sauv.1892, *Synechococcus* Näg. 1849, and *Cyanothece* gen. nov. (Cyanophyceae). Arch. Protistenkd. , 118, 119 -179., 1976.) and elaborated by (Rippka *et al*., 1979) to accommodate the cyanobacteria that were inaccurately placed in genus *Synechococcus*. These two genera are distinguished based on the following features: *Cyanothece* is present in single cells or pairs, and able to fix nitrogen whereas, *Synechococcus* can be found in chains and unable to fix nitrogen (Reddy *et al*., 1993).

Subsequently, Waterbury and Rippka (1989), proposed that the coccoid to rod-shaped cyanobacteria with cells larger than 3 μm in diameter, dividing by binary fission and lacking a sheath should be provisionally placed in the *Cyanothece* group. Strains assigned to the *Cyanothece* genus fall into three different clusters based on their characteristics such as salt tolerance, cell size, and DNA base compositions. *Cyanothece* strains (PCC 7424, PCC 7425, PCC 7822, PCC 8801, and PCC 8802) were sequenced at the Joint Genome Institute, U.S. Department of Energy (Appendix 5). The strains were collected from different geographical locations and exhibited considerable diversity with respect to cell size and pigment composition. A comparison of the genomes of the different *Cyanothece* strains revealed that members of this genus are metabolically versatile, each member having acquired unique metabolic capabilities Table 10 (Bandyopadhyay *et al*., 2013; De Philippis & Vincenzini, 1998; Margheri *et al*., 1999) Generally, Cluster 1 and 2 comprise of strains isolated from freshwater environments that possess the pigment phycoerythrin, whereas strains belonging to cluster 3 '*Halothece*' grow at higher salinities > 3% (Castenholz, 2001). The common features of strains belonging to the *Halothece* cluster are extreme halotolerance (optimal growth at salinities between 5-20 %), moderate thermophiles, and only contains the C-PC pigment (Garcia-Pichel *et al*., 1998).

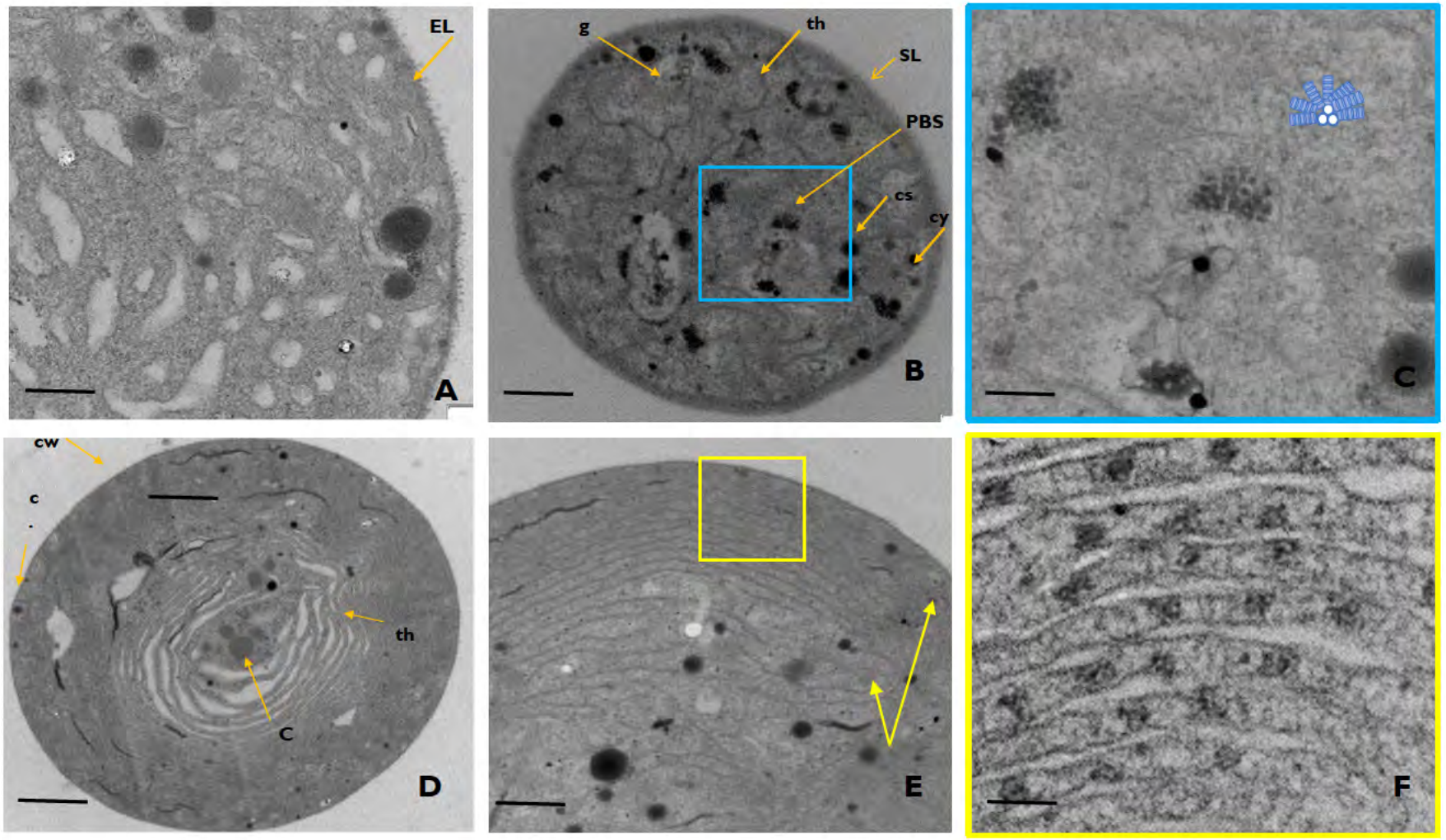

Figure 11: Transmission electron microscopy showing (A) serrated external layer (EL) thin fibres that emanated from the outer membrane; (B) ultrathin cross-section of cell showing glycogen (g), phycobilisomes (PBS), carboxysomes (cs), cyanophycin granules (cy); (C) enlargement of section of micrograph B showing PBS structure; (E) longitude section of cell showing the irregular thylakoids (th) arrangement, inter thylakoid spaces (inter.sp) and (G) gas vesicles (indicated by the arrow), scale bars = 100 nm (F) magnification of the ; scale bars = 100 nm

Table 10: Comparison of the characteristics (morphology, ultrastructural and genome) features of the isolate and marine/halophilic related cyanobacterial strains

	***Euhalothece* sp.**	***Dactylococcopsis salina* PCC 8305**	***Cyanothece* 115**	***Euhalothece* sp. Z-M001**	***Halothece* PCC 7418**
Site of isolation	Lake St Lucia, South Africa	Solar Lake, Sinai, Egypt	Sea water off China's Coast	Soda Lake Magadi	Solar Lake, Sinai, Egypt
Tolerance	Halophile	Halophile	Marine	Extreme natronophile (180 g/L Na_2CO_3)	Halotolerant
Salinity (%)	6-12	5-20	1-5	3-10	3-6
Temperature (°C)	25-45	30-34	28	35	25-37
Gas vesicles	Yes	Yes	No	-	Yes
Thylakoid Organisation	Irregular arrangement	Irregular position of widened thylakoids	-	Thylakoid membranes densely packed at the cell periphery	Numerous, radially oriented thylakoids
Cell morphology	Oval - cylindrical	Long, spindle-shaped	Rod-shaped	Round	Round oval-rod
Cell size (μm)	8-14	4–8 × 35–80	2.5-5 x 7.5-10	2.7–4	5 -7.4
Cell division	Binary fission divides into two identical cells	Divides in one plane	Binary fission in a single plane.	Divides into two daughter cells	Single plane
Size Genome (Mbp)			N/A	N/A	3.1
Isolated by	In this study	(Walsby *et al*., 1983)	(Zhang *et al*., 2007)	(Mikhodyuk *et al*., 2008)	(Cohen & Golden, 2015)

Although all strains belonging to the *Halothece* genus were unicellular, there were noticeable differences amongst them especially with regards to cell size and shape (Table 10). '*Dactylococcopsis*' (*Myxobakton salium*) PCC 8305 has distinct spindle-shaped cells and a different ultrastructure from the other *Euhalothece* sp. cells. PCC 8305 a fusiform, forms (4-8 x 35-80 μm) with many gas vacuoles at the periphery of cells. Our isolate morphology was distinctively different from PCC8305, however; both strains sustained growth in standard seawater and preferred a higher salinity (15%), therefore, they are considered true halophiles, whereas the other stains were considered halotolerant.

Furthermore, PCC 8305 and the isolate *Euhalothece* cells were filled with densely gathered gas vesicles, this contributes to their strong buoyancy ability. Buoyancy helps maximise photosynthetic light capture Abundant nutrients have been reported to promote buoyancy, whereas, nutrient limitation decreases the cyanobacteria's buoyancy ability allowing the organism to migrate and scavenge for nutrients (Brookes & Ganf, 2001). Strain PCC 7418 was reported to have a low number of gas vesicles, whilst the other two strains (Z-M001 and 115) were not reported to produce gas (Margheri *et al*., 1999). The thylakoid arrangement amongst the strains was also different. Strain PCC 8305 has enlarged thylakoids and PCC 7418 had numerous radially oriented thylakoids. However, numerous irregular thylakoids were present in the *Euhalothece* cells.

3.3.3 Phylogenetic Identification of Cyanobacterial Isolated using Phylogenetic Marker Genes and WGS.

The full genome sequencing yielded a total of 2,030,980 paired end reads. After filtering the impurities and reads of length smaller than 15 nucleotides, approximately 99% of the raw reads were retained (QC report shown in Appendix 6). *De novo* assembly of the high-quality reads (without the aid of a reference genome) led to 4983 contigs. The genome sequence is available in NCBI (https://www.ncbi.nlm.nih.gov/nuccore/1334780654?report=fasta). The annotated genes showed sequence similarity (>90%) to a planktonic gas-vacuolated cyanobacterium genome known as *Dactylococcopsis salina* PCC 8305 (CP003944.1). This was confirmed by mapping the reads and the contigs to the PCC 8305 genome. Results showed that ±50 % of the reads and 90.4% of the contigs mapped to the reference genome. The draft genome of *Euhalothece* sp. with a total of 5.11 Mbp from 1408 contigs, contains 46.7% GC content. A total of 5247 genes were predicted. Of these 4332 were annotated as protein-coding genes, with 69 for RNA genes (9 for rRNA, 4 for tRNA and 4 other nc RNA). There were five clustered regularly interspaced short palindromic repeat (CRISPR) arrays. General genome features and assembly statistics of the cyanobacterium are provided in Table 11. The circular map of the genome can be seen in Appendix 8.

The 16S ribosomal genes have all the characteristics of phylogenetic marker genes due to the universal distribution in prokaryotes, presence of variable and conserved regions and the high

information content (Sarma, 2013). Thus, this region has been used extensively for phylogenetic studies in prokaryotes including cyanobacteria (Nübel *et al*., 1997).

Table 11: Genome features of *Euhalothece* sp. draft genome

Attributes	**Values**
NCBI Bioproject	PRJNA335957
NCBI Biosample ID	SAMN05467874.
NCBI genome accession number	MDVL00000000
Assembly size (bp)	5,113,178
Total number of contigs	1408
G + C content (%)	46.7
Genes (total)	5247
Number of coding sequences	4332
Number of rRNAs	3,3,3 (5S, 16S, 23S)
Number of tRNAs	56
Number of ncRNAS	4
Number of Pseudogenes	846
CRISPR Arrays	8

Due to its too low taxonomic resolution, sometimes cyanobacterial lineages are not easily discriminated by the 16S rRNA gene marker. The other useful markers widely used for phylogenetic analysis of cyanobacteria include RNA polymerase gamma subunit (*rpoC1*), the 16S-23S internal transcribed spacer region (ITS) (*nifH*) and the C-PC operon (*cpc*BA-IGS) (Dall'agnol *et al*., 2012; Dyble *et al*., 2002; Robertson *et al*., 2001). However, the sequence data available for some of these genes are rather limited and inconsistency of phylogenetic results when using single genes have been reported (Nubel *et al*., 1997; Tan *et al*., 2016).

Based on the 16S phylogenetic analysis, the isolated strain examined in this study appeared to be closely related (99% similarity) to representatives of the not yet legitimate but widely studied genus *Halothece* (*Euhalothece* sub-cluster). The other conserved genes showed various degrees of similarity (96 to 99%). Similarity matrix calculations of the 16S rRNA sequences of the 12 strains are shown in Table 12. The sequences were aligned using the multiple sequence alignment tool in the ClustaW package in BioEdit (Appendix 7). Phylogenetic relationships of

the isolate and other reported cyanobacteria based on 23S rRNA and C-PC gene analysis is presented in a tree calculated by applying the maximum likelihood method.

The NCBI BLAST analysis showed that among all the matches for the 16S rRNA gene sequences from Genbank, the strain showed the highest similarity to *Dactylococcopsis salina* PCC 8305 (AJ000711) and *Cyanothece* 115 (DQ243690.1) isolated from seawater off China's coast (Zang *et al*., 2007). These two sequences shared 99% identity, with 100% coverage to the isolate and formed a stable clade. Strain PCC 8305 was originally wrongly designated as *Dactylococcopsis salina* (Walsby *et al*., 1983), which is a type species of a green alga that was reclassified to the genus *Myxobactron salinum* (Koma´rek & Anagnostidis 1998). The isolate also shared a 98% identity (99% coverage) to *Cyanothece* sp. GSL007 (FJ546715.1) isolated from Great Salt Lake, Utah.

Among the other cultured representatives of the genus, *Euhalothece* strains Z-M001 isolated from Lake Magadi and *Euhalothece* sp. BAA002 (DQ457013), isolated from Libyan hypersaline lake, Qabar-Onn were the closet (99% identity, 96% coverage). Our isolate also shared identities to sequences of uncultured bacteria (KU309088.1) from Salt flats United Arab Emirates (Mckay *et al*., 2016). The isolate was related (showing 96% similarity) to *Halothece* sp. PCC 7418 isolated from Solar Lake on the eastern shore of the Sinai Peninsula in 1972. The *Euhalothece* sp. was distantly related (showing > 90% similarity) to freshwater *Cyanothece* sp. belonging to cluster 2. The low salt tolerance, among the other properties, distinguishes these strains from members of the *Halothece* genus.

Currently, the cyanobacteria isolates belonging to genus *Euhalothece* have not been assigned to species level, therefore, the interpretation of the similarity levels of the 16S rRNA gene sequences could not reveal the intra-species and inter-species relatedness (Mikhodyuk *et al*., 2008). Thus, the branches of the phylogenetic tree inside the *Euhalothece* cluster indicate the high genetic heterogeneity within the *Euhalothece*. Only very few names of cyanobacteria have been validly published under the bacteriological nomenclature system. Even though *Halothece* is not a validated genus, to date there are approximately 45 isolates that are assigned to *Halothece*, subcluster *Euhalothece*. Garcia-Pichel *et al.* (1998) described the characteristics of 13 extremely halotolerant strains of unicellular cyanobacteria, isolated from various hypersaline environments, including hypersaline and solar evaporation ponds.

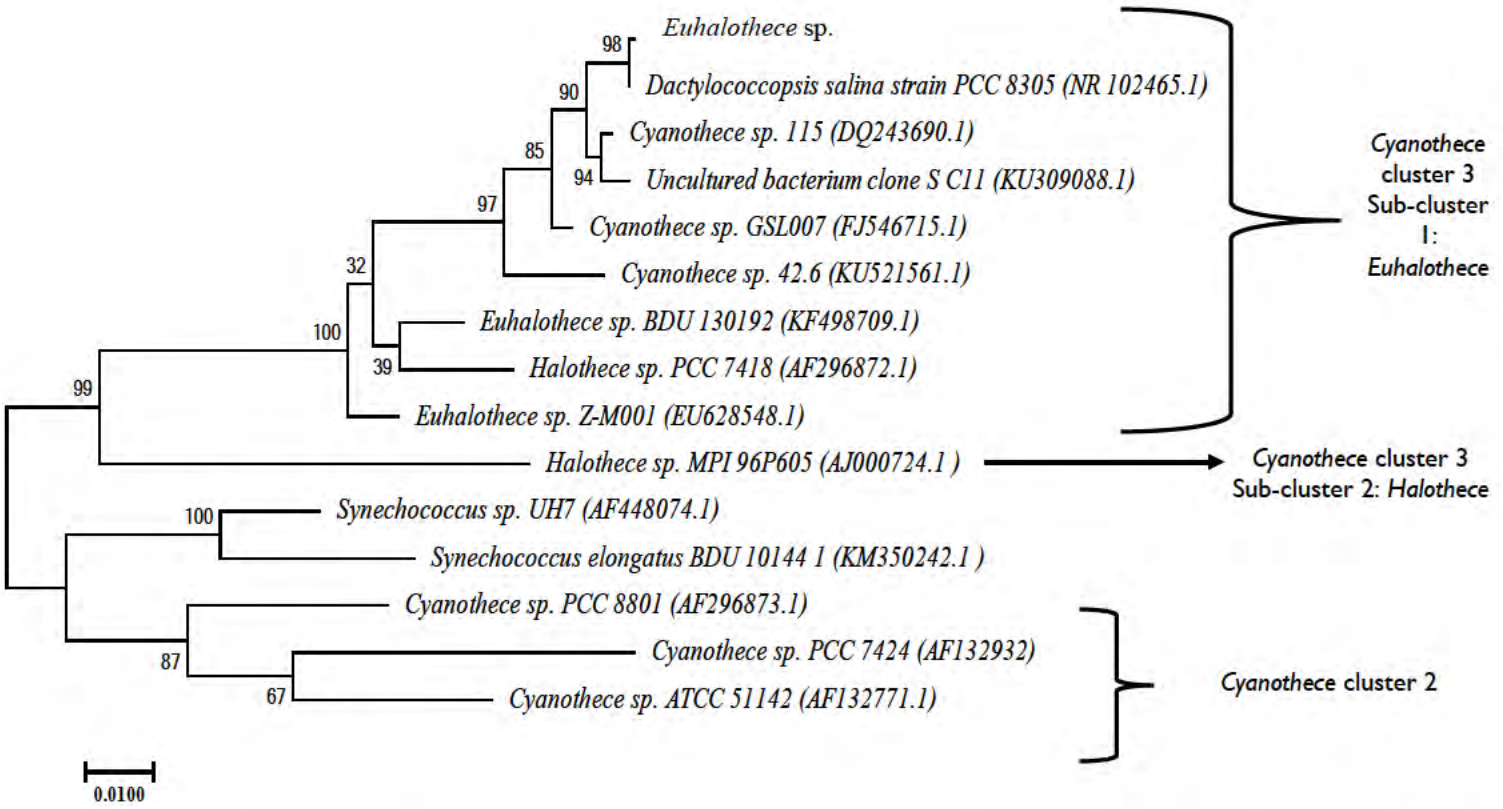

Figure 12: Reconstructed phylogenic tree of *Euhalothece* sp. and 12 related cyanobacteria that were aligned based on 16S rRNA sequences using the neighbour-joining method (with 1000 bootstrap replicates). All sequences were extracted from the NCBI database. GenBank accession numbers for each strain are shown in parentheses. Multiple sequence alignments were performed using the BioEdit sequence alignment editor. The evolutionary distances were computed using the Kimura 2-parameter method. Sequence alignment, as well as tree building, were performed using MEGA X. The tree is drawn to scale, with branch lengths in the same units as those of the evolutionary distances used to infer the phylogenetic tree. All positions containing gaps and missing data were eliminated. There was a total of 348 positions in the final dataset.

Two distinct sub-clusters of *Cyanothece* were acknowledged: (1) '*Euhalothece*', comprising 12 closely related strains of similar morphology and were originally identified as members of three traditional genera *Aphanothece*, '*Dactylococcopsis*' (*Myxobakton*) and *Cyanothece* (Kormárek *et al*., 2004), and (2) 'true *Halothece*', consisting of only a single strain, MPI 96P605, which was isolated from a benthic gypsum crust in a solar evaporation pond (Eilat, Israel). Cepák and Komárek, 2010, reported that strains belonging to *Halothece* can be further divided into two groups based on cytomorphological and ultrastructural characteristics. a) *Euhalothece* cells divide only by binary fission, forming identical daughter cells and they do not form any chains, whereas b) true *Halothece'* strains form chains or pseudofilaments under selected environmental conditions. Similarly, using 16S rRNA sequence analysis Margheri *et al*. (1999) confirmed 11 new halotolerant strains that formed a monophyletic cluster previously proposed '*Halothece*' genus. Although the strains belonging to this cluster are supported by a molecular phylogeny, the establishment of the new genus of *Halothece* subsequently stirred up the opposition.

To date, the form-genus *Halothece* is taxonomically invalid and has no standing under either the International Code of Nomenclature for algae, fungi, and plants (ICN) or International Code of Nomenclature of Prokaryotes (ICNP) (Komárek 2014). The *Halothece* genus was not validated owing to the absence of the diagnosis in Latin and the description of the new genus based on the difference of physiological character concerning halotolerance (Oren, 2009). The isolate also had a high percentage (16%) of pseudogenes (846) in their genome in comparison to PCC 7418 (126 pseudogenes). Pseudogenes are presumably inactivated, non-functional genes that can accumulate in the genomes, especially those organisms undergoing processes such as niche selection or host specialisation (Williams *et al*., 2009).

To date, cyanobacterial genomes reported vary greatly in size and sequence diversity. The high degree of diversity between the cyanobacterial strains is likely related to its capability to adapt to different environmental niches (Tamagnini *et al*., 2007; Welsh *et al*., 2008; Kalaitzis *et al*., 2009). The plasticity of the *Cyanothece* genomes is evident from the fact that the strains have acquired many novel metabolic capabilities, which is reflected in their diverse genotypes and phenotypes (such as cell size, shape, and pigment composition) (Bandyopadhyay *et al*., 2011). Currently, only two *Halothece* genomes *i.e.* strain PCC 8305 and PCC 7418 have been sequenced. The annotated genes of *Euhalothece* sp. in this study showed sequence similarity (90.4%) with a planktonic gas-vacuolated cyanobacterium genome PCC 8305.

Table 12: Pairwise nucleotide similarity matrix of the16S rRNA genes for the 14 strains. Strain percentages in bold indicate the closely related strains (>97%)

	Percentage similarity											
	***Euhalothece* sp.**	**PCC 8305**	**115**	**S_C11**	**BDU 130192**	**PCC 7418**	**GSL007**	**PCC 7424**	**PCC 8801**	**ATCC 51142**	**42.6**	**MPI 96P605**
Dactylococcopsis salina PCC 8305 (NR_102465.1)	**99,7**											
Cyanothece sp. 115 (DQ243690.1)	**98,6**	98,8										
Uncultured bacterium clone S_C11 (KU309088.1)	**98,4**	98,6	99,2									
Euhalothece sp. BDU 130192 (KF498709.1)	**96,8**	96,9	96,3	96,7								
Halothece sp. PCC 7418 (AF296872.1)	**96,1**	96,1	96	96,1	97,2							
Cyanothece sp. GSL007 (FJ546715.1)	**98,5**	98,7	98,6	98,5	96,3	95,9						
Cyanothece sp. PCC 7424 (AF132932)	73,2	73,4	73,2	73,3	73,5	72,9	73,2					
Cyanothece sp. PCC 8801 (AF296873.1)	89,5	89,8	89,5	89,7	89,5	88,9	89,6	74,4				
Cyanothece sp. ATCC 51142 (AF132771.1)	89,2	89,5	89,2	89,2	89,8	89,7	89,4	74,5	93,6			
Cyanothece sp. 42.6 (KU521561.1)	93,1	93,1	93,2	93,2	92,2	91,4	93,8	70,2	85,4	85,1		
Halothece sp. MPI 96P605 (AJ000724.1)	90	90	90	90,2	90	89,7	90,3	73,5	89,2	88,9	86,9	
Synechococcus sp. UH7 (AF448074.1)	90,6	90,7	90,7	90,7	91	90,6	91	85,8	73,9	92,6	92,1	86,4
Synechococcus elongatus BDU 10144 (KM350242.1)	89,3	89,4	89,4	89,6	89,9	89,6	89,6	84,9	73,1	91,5	91,7	85,5

The isolate also had shown a high GC content of ± 50% and a genome size of 5.11 Mbp, similar to freshwater *Cyanothece* PCC 7425 (Bandyopadhyay *et al*., 2011b). Whereas halophiles, PCC 7418 and PCC 8305 both have only 42.5% GC content, and genome size of 4.18 and 3.78 respectively (Boone *et al*., 2001).The relatedness of our isolate, *Euhalothece* sp. and whole-genome sequences of the two other *Halothece* PCC 7418 and PCC 8305 using ANI and DDH by pairwise comparisons were determined. The ANI was 78.41 and 97.15%, whereas the percentage DDH was 25.1 and 70.6% for comparisons of PCC 7418 and PCC 8305, respectively. The determined same-species cut-off for DDH is 70% (Goris *et al*., 2007). It has been reported that values of 95-96% for ANI correspond to 70% of the DDH analysis. Thus, results from genome relatedness using ANI, correlated well with the DDH values and 16S rRNA sequence similarity. This indicates the close relationship between *Euhalothece* sp. and PCC 8305, and a distinct difference from the other *Halothece* strains, including PCC 7418.

The 16S rRNA gene phylogeny and comparative genomic analysis, indicated the same pattern, highlighting that the high salinity has contributed to the genetic relatedness of the *Euhalothece* sp. and *Dactylococcopsis salina* PCC 8305. It is interesting to note that although the phylogenetic analysis indicates that our isolate and PCC 8305 is highly similar, this does not corroborate to the morphological data (Table 10). Therefore, the isolate cannot be classified as a strain *Dactylococcopsis salina*.

CONCLUSIONS

A novel euryhaline species of cyanobacterium was isolated from a hypersaline estuary in Kwa-Zulu Natal, South Africa. A comprehensive polyphasic approach *i.e.* cell morphology, pigment composition and complete genome sequence analysis was conducted to elucidate the taxonomic position of the isolated strain. The blue-green oval to rod-shaped cells is found to be 14–18 μm in size, and dominant in C-PC pigments. Based on 16S rRNA gene sequence similarities, the strain is related to members of the form-genera '*Euhalothece*' subcluster (99%). The annotated genes from the whole-genome sequence shows sequence similarity of 90% to the gas-vacuolate, spindle-shaped *Dactylococcopsis salina* PCC 8305. The size of the genome is 5,113,178 bp with 4332 protein-coding genes and 69 RNA genes with a GC content of 46.7%. With the information obtained from the 16S rDNA analyses, whole-genome sequencing, and the morphological analyses, it appears that this isolate is likely a novel species within the genus *Euhalothece*.

CHAPTER 4 GENOME ANALYSIS OF *EUHALOTHECE* SP.

4.1 INTRODUCTION

Cyanothece strains have been investigated for their robust circadian rhythms, hydrogen production, nitrogen fixation, fermentative abilities and other biotechnological applications (Al-Haj *et al*., 2016; Skizim *et al*., 2012; Stockel *et al*., 2011; Welsh *et al*., 2008). It has been reported that the genus *Cyanothece* maintains a plastic genome, by acquiring new metabolic capabilities while concurrently retaining archaic metabolic traits. This provides the cyanobacteria with the flexibility to adapt to various ecological and environmental conditions (Bandyopadhyay *et al*., 2011a). Halophilic cyanobacteria have adapted to high salinities owing to their unique physiological properties and metabolic capabilities (Kanekar *et al*., 2012). During the last decade, there has been increasing interest in survival mechanisms of halophiles, which require high internal salt concentrations for their metabolism (Plemenitas *et al*., 2014). The mechanisms including photosynthetic activities, nutrient metabolism and salt acclimation allowing *Euhalothece* sp. (genome ID: MDVL00000000) to persist during hypersaline conditions was of great interest. Owing to the extreme environmental conditions such as high ionic concentrations, high pressure, variable temperatures, low light and nutrient availability, marine-derived secondary metabolites are structurally complex with unique functionalities and possess prominent biological activity. Roberts, (2005) reported that enzymes and protein complexes encoded by halophiles often display better stability compared to non-halophilic cyanobacteria. Thus, the discovery of unique genes and compounds from cyanobacteria inhabiting hypersaline environments has attracted much interest due to the potential for the discovery of new enzymes that may have extended functional capacity (Ventosa, 2006).

Genome sequencing aims to determine the entirety of an organism's genetic information, which includes both the coding sequences (genes) and non-coding sequences of the DNA or RNA (Mardis, 2013). Cyanobacteria genomes can be divided into two parts, a 'stable core' and a 'variable shell'. The stable core consists of conserved genes coding for proteins involved in genome replication and expression. The variable shell also known as the pan-genome includes metabolically non-essential genes that may be important environmental adaptations, and exposed to evolution and loss/acquisition of genes *via* HGT (Shi & Falkowski, 2008). Genome-scale models are built from an annotated genome sequence that allows the

prediction of metabolic reactions and aids a better understanding of several key pathways (Shi *et al*., 2010). Genome-scale modeling of cyanobacteria can also assist in the creation of synthetic strains with necessary characteristics for the overproduction of metabolites. Moreover, genomics has revealed that cyanobacteria have a greater potential to produce secondary metabolites. However, biosynthetic gene clusters (BGCs) that encode proteins responsible for the synthesis of certain compounds are "cryptic" thus not expressed under laboratory cultivation conditions (Gupta *et al*., 2017; Rutledge & Challis, 2015). Furthermore, comparative genomics provides an understanding of the known cyanobacterial natural product diversity and facilitated the discovery of novel natural products.

The number of completed or nearly completed genome sequences of halophiles is rapidly increasing, which provides new information regarding the genetic diversity and metabolic potential. Currently, there are approximately 376 cyanobacterial genomes available in public databases among complete (86), draft (142) and (148) incomplete genomes (https://gold.jgi-psf.org/index, accessed on January 13, 2018). Of the complete genomes sequenced, 8 genomes belong to cyanobacteria from the genus *Cyanothece*, 6 freshwater strains exist; namely PCC 7424, 7425, 8801, 8802, 7822 and ATTC 51142; and 2 marine strains (PCC 7418 and PCC 8305) belonging to subcluster *Euhalothece* (Beck *et al*., 2012). As mentioned previously the indigenous, halophilic cyanobacterium *Euhalothece* sp. KZN 001 (MDVL00000000) (hereafter referred to as *Euhalothece* sp.) was found to have several traits that made it an attractive target for genome investigation. The cyanobacterium can grow at high salinity (120 g/L), proliferate under varying nutrient conditions, has a fast growth rate and is capable of naturally producing high quantities of C-PC (75mg/g). We determined the nucleotide sequence of the entire genome *Euhalothece* sp. and compared with the available genomes (*Dactylococcopsis salina* PCC8305 and *Halothece* PCC 7418) in Genbank.

The focus of this chapter was to sequence the genome of the halophilic *Euhalothece* sp. to better understand the physiology and other metabolic processes particularly adaptation mechanisms that allow the cyanobacterium to dominate hypersaline and varying nutrient environments, as well as gain insight in C-PC synthesis.

4.2 MATERIALS AND METHODS

4.2.1 DNA Extraction and Genome Sequencing

Cyanobacterial DNA extraction was done using FastDNA™ SPIN Kit for soil, refer to the protocol in Chapter 3, section 3.2.3.2. Multiplexed paired-end libraries (2 x 300 bp) were prepared using the Nextera XT DNA sample preparation kit as per manufacturer's instructions (Illumina, San Diego, CA, USA). Sequencing was performed on an Illumina MiSeq instrument at the NICD Sequencing Core Facility (Figure 6). The resulting paired-end reads were quality trimmed and *de novo* assembled using CLC Genomics Workbench version 8 (CLC Bio-Qiagen, Aarhus, Denmark).

4.2.2 Genome Annotation and Analysis

The genome was annotated using the NCBI Prokaryotic Genome Annotation Pipeline (PGAP) (Tatusova *et al.*2016) and further uploaded to Rapid Annotation using Subsystem Technology (RAST) (http://rast.nmpdr.org/) for subsystems-based annotation Aziz *et al.* 2008; Brettin *et al.* 2015; Overbeek *et al.* 2014). RAST is a fully-automated online service for annotating bacterial genomesThe steps followed by the RAST pipeline to annotate a prokaryotic genome is shown in Figure 13. RAST uses the SEED framework for the comparative genomics approach.The first step for the annotation process was to import the genome using GenBank format into the RAST pipeline. Once the files were uploaded, they were first normalised by removing duplicate copies of sequences and then a unique internal ID is generated for each of the sequences. These unique sequences were then screened for PEG's (Protein Encoding Genes) against the SEED comprehensive nonredundant database *via* BlastX as well as other rDNA databases, including GREENGENES RDP-II and the European 16S RNA database. The SEED (http://pubseed.theseed.org/) also houses subsystems (collections of functionally related protein families) and their derived FIGfams (protein families).

The 'Compare Regions View', tool on the SEED is used to compare the genomic neighbourhood of a given gene across genomes. The CGView Server is a comparative genomics tool used for visualisation of the circular genome analysis (Grant & Stothard, 2008), The CGView Server can be accessed at http://stothard.afns.ualberta.ca/cgview_server/index.html.

To determine the role of gene candidates that were not assigned to the subsystem, using SEED program, a search for proteins in the genome, which match proteins in other genomes, that have been annotated with this role was done. Thereafter, were compared to the 30 closest neighbours using BLASTP, and included if they are similar to any protein. Enzyme Commission (EC) numbers reported in the Tables below were based on the recommendations of the Nomenclature Committee of the International Union of Biochemistry and Molecular Biology (IUBMB) (Bairoch, 2000).

The protein sequences are also available on (https://www.ncbi.nlm.nih.gov/protein?linkname=bioproject_protein&from_uid=335957).

4.2.3 Secondary Metabolite Analysis

By using antibiotics & Secondary Metabolite Analysis SHell (antiSMASH) software https://antismash.secondarymetabolites.org secondary metabolite biosynthesis gene clusters in the genome were identified. The program aligns the identified regions at the gene cluster level to their nearest relatives from a database containing all other known gene clusters (Medema *et al.* 2011).

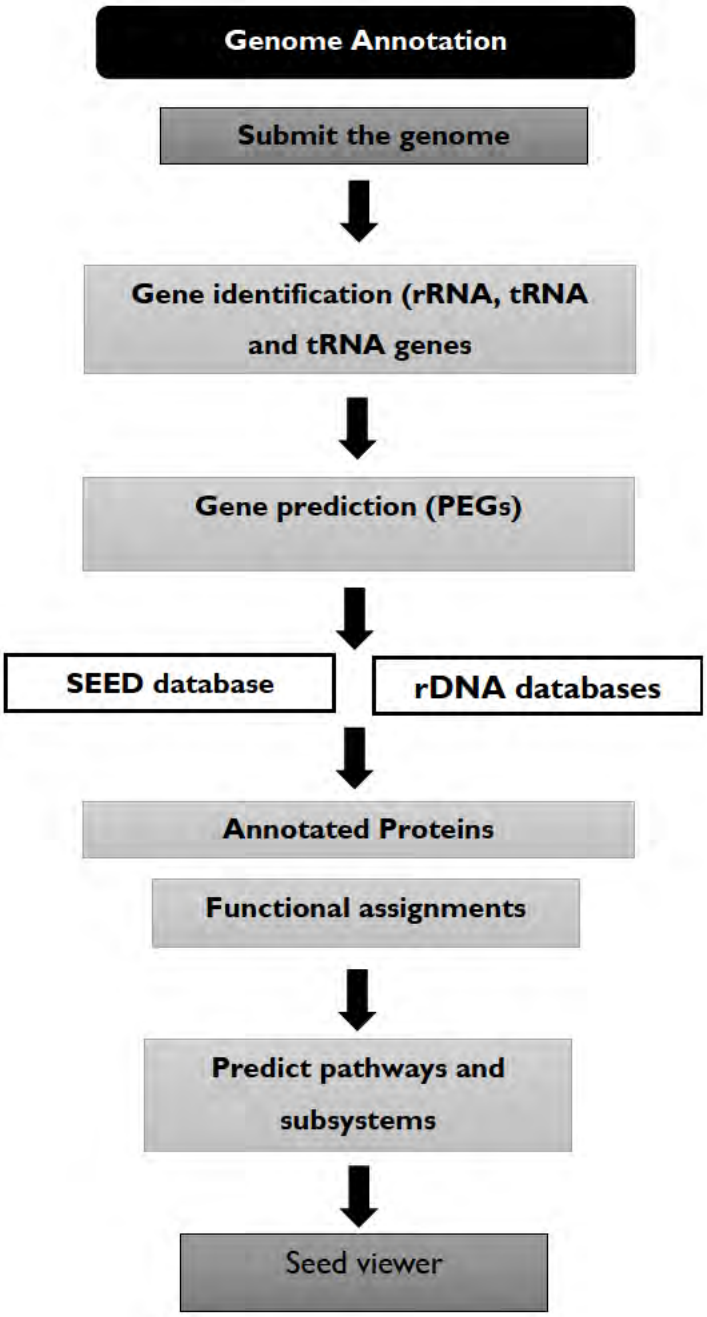

Figure 13: Annotation using the Rapid Annotation using Subsystem Technology.

4.3 RESULTS AND DISCUSSION

4.3.1 Overview and Comparison of Genes in *Euhalothece* sp.

As previously mentioned in Chapter 3, the genome is 5,113,178 bp and contains 5178 CDS, and 4332 protein-coding genes. Analysis *via* RAST revealed a total of 381 subsystems covering 39% of the protein-coding genes classified into 27 categories also known Clusters of Orthologous Groups (COGs) (Table 13). Amongst these, category 1 (cofactors, vitamins, prosthetic groups, and pigments) featured the largest number (348) of the assigned coding sequences (CDS). Within subsystem 1: folate and pterines consisted of 129 genes including vitamin B9 (37 genes), pterin synthesis (40 genes), molybdenum cofactor biosynthesis (21) and 5-FCL-like protein (23); tetrapyrroles biosynthesis (103 genes) consists of genes encoded for Chl (14 genes), bilin (6), cobalamin synthesis (21), heme and siroheme 21) and coenzyme B_{12} biosynthesis (32); riboflavin (29); quinone cofactors (29); thiamine biosynthesis (9); biotin (3); vitamin B6 (9); NAD and NADP (21); lipoic acid (4).

The second most abundant functional category of genes was Amino Acids (299) and followed by Protein Metabolism (293), and Carbohydrates (293). Genes of categories involved in 'Membrane transport' and DNA (139) and RNA (158) metabolism, 'Cell Wall and Capsule,' 'Virulence (135), Disease and Defense'" and Stress response were also abundant. These genes are linked to the characteristics that may have provided a competitive advantage to the organism for survival in extreme environmental conditions (Prabha *et al*., 2016). The genes of the category 'Membrane transport' aids in the uptake of the trace metals critical for the survival, as the availability of these metal such as iron in hypersaline environments may be limited. Genes involved in 'Virulence, Disease and Defense (57) and 'Stress response' (107) helps enhance the adaptability of the *Euhalothece* sp. and the cyanobacteria's defence mechanisms. Since extreme environmental conditions may lead to DNA damage, the presence of multiple copies of genes involved in DNA/RNA and protein replication and repair improves the robustness of the repair systems within the *Euhalothece* sp. Additionally, presence of extra copies of genes involved in cell motility and cell wall may also be advantageous, making movement easier. The graphical representation of the distribution of the non-hypothetical genes in the subsystem is illustrated in Appendix 8. *Euhalothece* sp. genome contained 2649 hypothetical proteins.

Table 13: Genes connected to subsystems and their distribution in different categories. Total non-hypothetical genes in the subsystem were 2683

	Subsystem/Categories/COGs	Genes
1	Cofactors, Vitamins, Prosthetic Groups, Pigments	348
2	Cell Wall and Capsule	135
3	Virulence, Disease and Defense	57
4	Potassium metabolism	20
5	Photosynthesis	65
6	Phages, Prophages, Transposable elements, Plasmids	33
7	Miscellaneous	62
8	Membrane Transport	92
9	Iron acquisition and metabolism	8
10	Protein Metabolism	293
11	RNA Metabolism	58
12	Nucleosides and Nucleotides	69
13	Cell Division and Cell Cycle	60
14	Motility and Chemotaxis	14
15	Regulation and Signaling	76
16	Secondary Metabolism	9
17	DNA metabolism	139
18	Fatty Acids, Lipids, and Isoprenoids	115
19	Nitrogen Metabolism	40
20	Dormancy and Sporulation	2
21	Respiration	72
22	Stress Response	107
23	Metabolism of Aromatic Compounds	9
24	Amino Acids and Derivatives	299
25	Sulfur Metabolism	28
26	Phosphorus Metabolism	60
27	Carbohydrates	303

Since unique genes are not conserved among related cyanobacteria, a high percentage of unique genes are often annotated as a protein of unknown function. Unique genes are found in a single genome only. The main characteristic of unique genes makes their functional classification challenging. The determination of the function of newly discovered genes is based on the comparison to already known genes. Where the functional annotation of unique genes is possible, it reveals a high percentage of genes related to phage genes, HGT and mobile genetic elements (Ding *et al*., 2018). Since different species of cyanobacteria are exposed to a variety of niche-specific competitive conditions, they are often found to possess unique characteristics.

Genes that have been horizontally acquired and encode extrachromosomal functions are commonly underrepresented in the core genome. Even though the core genome is conserved in cyanobacteria, over time the core genome does change by HGT and natural selection (Shi & Falkowski, 2008). Hence, cyanobacterial taxa show significant differences in the functional distribution and amount of their genes. Accessory genes are found in at least two genomes and all the genes that are neither core nor unique genes. They are assumed to not be involved in essential metabolic functions however, they provide an important tool for genetic variability. Considerable variation in genomic amino acid identity occurred between closely related cyanobacteria. The annotated genes of the isolate showed a 90.4% sequence similarity to *Dactylococcopsis salina* PCC 8305, the remaining repetitive sequences are predicted to bring plasticity into the genome.

A comparison of the COGs for *Euhalothece* sp. *Halothece* PCC 7418, *Dactylococcopsis salina* PCC 8305, and *Cyanothece* ATCC 51142 can be seen in Figure 14. Genes that were present only in *Euhalothece* sp. and not the other strains were prophages. *Euhalothece* sp. contained nitrogen-fixing genes similar to *Cyanothece* ATCC 51142, whereas the genome of *Dactylococcopsis salina* PCC 8305 does not contain any nitrogen-fixing genes. The complete genome of *Euhalothece* sp. has revealed some interesting features of the genetic inventory of this strain. These characteristics will be discussed in the sections to follow.

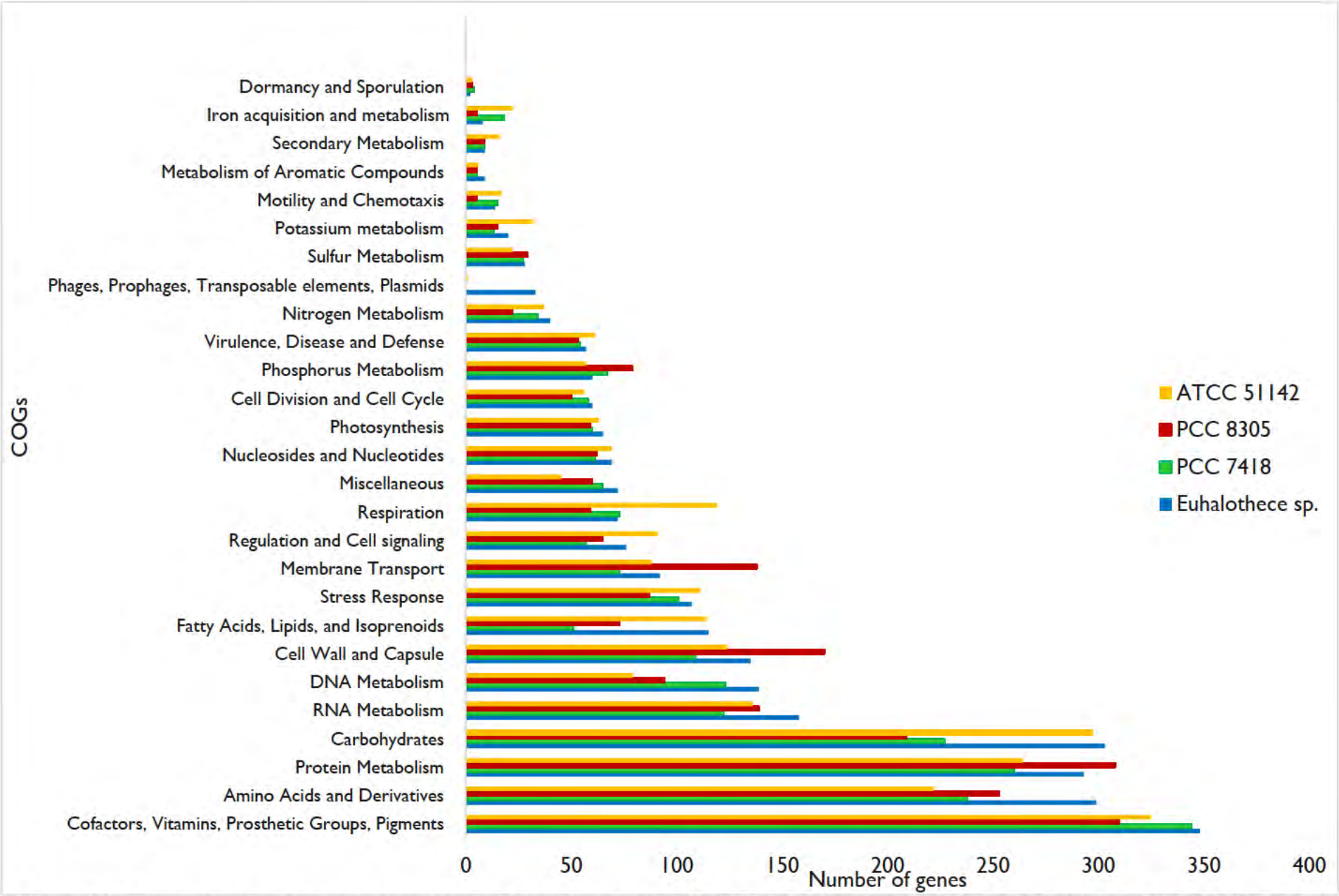

Figure 14: Comparison of gene numbers between the *Euhalothece* sp., *Halothece* PCC 7418, *D. Salina* PCC 8305, and *Cyanothece* ATCC 51142. Each bar indicates number of genes in each functional category in descending order.

4.3.2 Phages and CRISPR-Cas System

Mobile genetic elements include transposons, insertion sequences and phage-related proteins (Vandecraen *et al*., 2017). Phage's play an important role in the exchange of genetic information between different bacteria. Interestingly, in comparison to the *Dactylococcopsis salina* PCC 8305 genome, *Euhalothece* sp. had 33 phage-related genes comprised of phage replication, phage packaging machinery and phage tail fibre proteins as seen in Table 14. Prophages are known as the main contributor to microbial diversification that assists in the survival of the cyanobacteria under various environmental conditions, genomic rearrangements, and mediating transfer of virulence factors (Prabha *et al*., 2016).

Table 14: List of genes related to phages, integrons and CRISPRs regions

Gene Name	Description
Phage replication (4)	
DNAP11192	DNA polymerase III alpha subunit (EC 2.7.7.7)
Hel1	DNA primase/helicase, phage-associated
Phage packaging machinery (4)	
P01	Phage terminase, small subunit
P03	Phage terminase, large subunit
Phage tail fibre proteins (25)	
TFP1,2	Phage tail fiber protein 1 and 2
SaTFP	Tail fiber protein / SA bacteriophages 11, Mu50B
TFAP	Phage tail fibre assembly protein
LTFPS	Phage long tail fibre proximal subunit
LTFPC	Phage long tail fibre proximal connector
IM30	Phage shock protein A
FsxA protein	protein affecting phage T7 exclusion by the F plasmid)
	Phage antirepressor protein
	Phage integrase
	Phage protein
CRISPR associated proteins (27)	
CRISPR repeats	
Csx	
Cas1,2,3,4,6	
Csc 2,3,4	
Csm6	
Cmr2,3,6	
Tm1812	
Other	
Group II intron-associated genes (26)	
Mobile elements (36)	

Moreover, the genome contained 36 contigs identified as mobile elements, 2 transposons, and 26 Group II intron-associated genes. Group II introns are mobile catalytically active intron RNA (ribozymes) that self-splicing *via* transesterification which then invades new genomic DNA sites by reverse splicing (Lambowitz & Zimmerly, 2011).

The *Euhalothece* sp. genome contained five CRISPR arrays as shown in Table 14. In addition to CRISPR repeats, 19 CRISPR associated proteins (Cas1, Cas2, Cas3, Cas4, Cas6, Csc2, Csc3, Csc4, Cmr2, Cmr3, Cmr6, Csm6 and TM1812). CRISPR-Cas systems exchanged *via* HGT provides adaptive immunity against invading cyanophages, this is a possible indication of cyanophage infection. Small portions of viral DNA are incorporated into the host cyanobacteria genome which also contains nucleases downstream, hence, if the same cyanophage attacks the same host, the host can activate the CRISPR arrays so that nucleases are secreted to cleave the cyanophage DNA. Horizontal gene transfer plays a significant role in the evolution of cyanobacterial genomes and has contributed to the remarkable diversity of the species (Mohanta *et al*., 2017). The presence of phage genes and CRISPR region in the *Euhalothece* sp. genome suggest phages may have previously posed a threat.

4.3.3 Photosynthesis and Respiration

Cyanobacteria are unique in that the internal thylakoid membrane system houses the components of both the photosynthetic and respiratory electron transport chains (ETC), and that components of these processes overlap (Liu, 2016). The photosynthetic reactions are divided into two steps: light reactions and CO_2 fixation. The *Euhalothece* sp. genome contained all the genes related to photosynthesis, including the genes necessary for a functional cytochrome b6f complex, which is shared between photosynthesis and respiration. In total, more than 100 genes are found to be dedicated to the synthesis and regulation of the photosynthetic apparatus (Table 15). *Euhalothece* sp. genome had the homologs of the complete sets of genes coding for PSI, *i.e.* total of 14 genes (psaA,-B,-C,-D,-E,-F,-J,-K,-L,-I, Ycf3,-4,-37 and BtpA) with 1 additional Chl-binding protein, homolog (IsiA). There were three copies of psaA that encodes the reaction centre D1 complex, two copies of psaC and D genes, encodes for CP43 protein and D2 protein. Photosystem II consisted of 19 protein-encoding single genes (psbA,-B,-C,-D,-L,-J,-O,-P-K,-U,-V,-N,-I,-X,-Z,-27,-28), two cytochrome genes (psbEF), two genes for assembly factors (ycf39 and ycf48) and two additional homologs.

The psbA and psbD genes encode the two PSII core reaction centre proteins, D1 and D2 (Kiss *et al*., 2012). Tetrapyrrole pigments include Chls, cobalamin, hemes and bilins are involved in photosynthesis, respiration and various metabolic reactions in cyanobacteria. The biosynthesis of these pigments includes more than 19 enzymatic steps with a core common pathway from glutamate to protoporphyrin IX (Proto) (Fujita *et al*., 2015).

Both photosynthetic capacity and respiratory activity have shown to exhibit strong diurnal oscillations in *Cyanothece.* The sequencing data also indicated the presence of a complete set of genes necessary for circadian clock genes function. This included kaiABC (4 genes), cluster that encodes the components of the central oscillator; cikA (4ngenes and ldpA (1 gene) required for the input pathway components; key output pathway components, sasA (1 gene) and its cognate response regulator gene rpaA (2); as well as other genes: pex (1 gene), cpmA (2 genes), and group 2 sigma factors (PSF) (2 genes). Circadian rhythms have intensively been studied in cyanobacteria, and genes involved in various processes of circadian timing and regulation have been identified in many species of cyanobacteria (Cerveny *et al*., 2013). A clock system consists of an input pathway whereby environmental signals are transmitted to the oscillator. The important redox-sensitive proteins required for synchronising the circadian oscillator are circadian input kinase A (CikA) and light-dependent period A (LdpA). Information from the oscillator is transmitted *via* an output pathway comprised of sensor kinase A (sasA) and regulator of phycobilisome association A (RpaA) that is important for driving rhythms of biological activities such as the timing of cell division and gene expression (Cohen & Golden, 2015

Table 15: List and number of genes related to photosynthesis and respiration present in *Euhalothece* sp.

Gene Name	Description
Photosystem I (15)	
PsaA	P700 chlorophyll a apoprotein subunit Ia
PsaB	P700 chlorophyll a apoprotein subunit Ib
PsaC	Iron-sulfur centre subunit VII
PsaD	Subunit II
PsaE	I subunit IV
PsaF	I subunit III precursor, plastocyanin (cyt c553)
PsaJ	I subunit IX
PsaK	Reaction centre subunit X (psak2)
PsaL	Subunit XI
PsaI	Subunit VIII
PsaM	Subunit XII
PsaX	4.8K protein
PsaH	Subunit VI
Ycf3	Assembly related protein Ycf3
Ycf4	Assembly related protein Ycf4
Ycf37	Assembly related protein Ycf37
Ycf39	Assembly related protein Ycf39
BtpA	Biogenesis protein btpa
IsiA	Chl a(b) binding protein, PS II CP43 protein (psbc)
Photosystem II (26)	
PsbD	Protein D2 (psbd)
PsbC	CP43 protein (psbc)
PsbC_h	Chl a(b)binding protein, CP43 protein (psbc) homolog
PsbB	CP47 protein (psbb)
PsbE	Cytochrome b559 alpha chain
PsbF	Cytochrome b559 beta chain
PsbJ	Protein psbj
PsbL	Protein psbl
PsbK	Protein psbk
PsbU	12 kda extrinsic protein (psbu)
PsbV	Protein psbv, cytochrome c550
PsbO	Manganese-stabilising protein (psbo)
PsbI	Protein psbi
Psb28	13 kda protein Psb28 (psbw)
PsbX	Protein psbx
PsbY	Protein psby
PsbZ	Protein psbz
Psb27	Protein Psb27
ycf39	Chaperon-like protein Ycf39
ycf48	Stability/assembly factor HCF136/Ycf48
petH	Ferredoxin-NADP oxidoreductase
pntA	Pyridine nucleotide transhydrogenase alpha subunit
pntB	Pyridine nucleotide transhydrogenase beta subunit

Gene Name	Description
Other Electron transport (6)	
crtE	Geranylgeranyl pyrophosphate synthase
ctaB	Cytochrome c oxidase folding protein
ccsA	C-type cytochrome synthesis protein
ccs1	C-type cytochrome synthesis protein
ccdA	Putative c-type cytochrome synthesis protein
Soluble carriers (17)	
petF	Ferredoxin, pet f
pet I	Cytochrome c553
pet J	Cytochrome c553
Cytochrome oxidase (3)	
cox A	Cytochrome c oxidase subunit I
cox B	Cytochrome c oxidase subunit II
cox C	Cytochrome c oxidase subunit II
Chlorophyll (13)	
ChlD (E.C.6.1.1)	Mg protoporphyrin IX chelatase subunit D
ChlI (E.C.6.1.1)	Mg protoporphyrin IX chelatase subunit I
ChlH (E.C.6.1.1)	Mg protoporphyrin IX chelatase subunit H
ChlL (EC 1.18.-.-)	Light-independent protochlorophyllide reductase Fe protein subunit
ChlM (E.E.2.1.1.11)	Mg protoporphyrin IX methyl-transferase
ChlN (E.C. 1.3.1.33)	Light-independent protochlorophyllide reductase subunit N
ChlEAe	Mg protoporphyrin IX monomethyl ester oxidative cyclase
ChlB (EC 1.18.-.-)	Light-independent protochlorophyllide reductase subunit B
DVR (EC 1.3.1.75)	Divinyl protochlorophyllide a 8-vinyl-reductase
BchP (EC 1.3.1.83)	Geranylgeranyl hydrogenase; Geranylgeranyl reductase
ho1	Heme oxygenase
Phycobilisomes (18)	
apcA	APC alpha chain
apcB	APC beta chain
apcC	Apoprotein (core components of the phycobilisomes
apc D	APC alpha-B chain
Apc E	PBP core-membrane linker polypeptide
cpcA	C-PC alpha subunit
cpcB	C-PC beta subunit
cpcC	PBP rod linker polypeptide
cpc D	C-PC linker protein
cpc E	PBP maturation protein
cpc G	PBP rod-core linker polypeptide
cpc F1	C-PC alpha-subunit phycocyanobilin lyase
cpc F2	C-PC alpha-subunit phycocyanobilin lyase
cpc T	C-PC beta-subunit phycocyanobilin lyase
cpeS	C-PE linker protein
nbl B	C-PC alpha phycocyanobilin lyase related protein
PBS related hypothetical proteins	

Gene Name	Description
APCB	APC-b
PCC	PBP core component
LRsm	PBS small rod capping linker polypeptide
PEac	C-PE alpha chain
PEbc	C-PE beta chain
LPE	PBS phycoerythrin-associated linker polypeptide
LCpeR	Cper homolog, phycoerythrin linker-proteins region
PECac	Phycoerythrocyanin alpha chain
PECbc	Phycoerythrocyanin beta chain

The number of transcriptional units encoding PBPs components varies in different cyanobacteria (about 5-9 units), and the distribution of genes within these units are also variable. The C-PC protein is encoded by cpc operon containing mainly two genes cpcB (~518bp) and cpcA (~488bp) separated by an intergenetic spacer region igsB-A. Furthermore, C-PC operons are composed of genes encoding PBS rod components and polypeptides that are involved in chromophore attachment to the C-PC *α*-subunit (cpcE and cpcF genes). The cpcG gene (s), encoding the LRC p upstream sequence. In all cyanobacteria studied till date, the cpcA gene coding for the *α* subunit of PC is located downstream from the cpcB gene encoding *β*-subunit of C-PC.

The rod–core linker cyanobacterial C-PC protein G (CpcG), which connects the rod to the core, plays a key role in the assembly of the PBS. The genome of *Euhalothece* sp. contained at least 25 open reading frames (ORFs) encoding genes with similarity to proteins involved in phycobilin biosynthesis, assembly of PBS, ligation and regulation. This included homologs of genes coding for PBPs, including PBS core component (PCC), lyase subunits (PLabs), as well as core and rod linker polypeptides (LCM, LC LRpc and LRCpc), Apc ABCD homologs are present in the genome , where the APC cores is made up of two types of *α*-chains (*α* and *α-B*) and *β*-chains (*β* and *β*-18), as well as LC and LCM linker polypeptides. One cpcG homolog encoding rod-core linker polypeptides (LRC), as well as PC rod linker (LR) genes cpcC or cpcD were also identified in the genome. In addition, the genome had homologs for PBS degradation protein (nblB) were found. However, the strain lacked other genes required for phycoerythrocyanin and phycoerythrin biosynthesis. Apart from light absorption and transduction, PBS act as an emergency source of nutrients in case of nitrogen, sulphur or carbon starvation (Singh *et al*., 2015).

4.3.4 Carbon Fixation, CO_2 Concentrating Mechanism

The complete set of genes required for the Calvin cycle (12 genes; some with additional homologs) along with the presence of key enzymes Rubisco (RbcL and Rb), phosphoribulokinase (PRK), and sedoheptulose-1,7-bisphosphatase (SBP) were present. Cyanobacteria are capable of acclimating and growing under a wide range of ambient CO_2 concentrations. They have carboxysomes, intracellular microcompartments formed by a protein shell that encapsulates the enzymes carbonic anhydrase and ribulose-1,5-bisphosphate carboxylase/oxygenase (RuBisCO). Carbonic anhydrase converts HCO_3 to CO_2, in turn RuBisCO utilises this CO_2 molecule to synthesise phosphoglycerate. The compartmentalisation enhances the efficiency of carbon fixation by elevating the levels of intracellular CO_2 around RuBisCO (Rae *et al*., 2013).

Table 16: Carbon fixation genes found in *Euhalothece* sp.

Gene Name	Description
CO_2 fixation (29)	
ccmK1,3,4	Carbon dioxide concentrating mechanism protein
ccmL	Putative carboxysome assembly protein
ccmM	Putative carboxysome assembly protein
ccmN	Putative carboxysome assembly protein
rbcR	Rubisco operon transcriptional regulator
cbbT	Transketolase
cbbF	Fructose-1,6-/sedoheptulose-1,7-bisphosphatase
cbbE	Pentose-5-phosphate-3-epimerase
pepC	Phosphoenolpyruvate carboxylase
cbbP	Phosphoribulokinase
cbbK	3-phosphoglycerate kinase
cbbJ	Triosephosphate isomerase
cbbA	Class II fructose-1,6-bisphosphate aldolase
rbcL	Ribulose bisphosphate carboxylase large subunit
rbcS	Ribulose bisphosphate carboxylase small subunit
cbbI	Ribose 5-phosphate isomerase
cbbG	Glyceraldehyde 3-phosphate dehydrogenase (NADP+)
Cp12	Putative cp12 protein
NADH dehydrogenase (19)	
ndhD	Subunit 4
ndhC	Subunit 3
ndhK	Subunit ndhk
ndhI	Subunit ndhi
ndhJ	Subunit 1
ndhL	Subunit ndhl

The Carbon-dioxide Concentrating Mechanism (CCM) enables cyanobacteria to increase the CO_2 level at the carboxylating sites, *i.e.* carboxysomes, and thus overcome the large difference between the concentration of dissolved CO_2 and the Km (CO_2) of the RubisCO enzyme (Burnap *et al*., 2015; Yeates *et al*., 2008). In addition, the essential genes involved in CMM which included both *α* and *β* carboxysomes (28 genes) were also present in the genome. The proteins of CCM operon in *Euhalothece* sp. consisted of -K,-L,-N,-M and O as well as 7 orthologs of high-affinity carbon uptake proteins (Hat/HatR) (Table 16).

4.3.5 Nitrogen Fixation

Cyanobacteria are known to assimilate N from atmospheric nitrogen, nitrate, nitrite, ammonia, hydroxyl amine and amino acids. In non-heterocystous forms, the oxygenic photosynthesis was found to be separated from nitrogen fixation either spatially or temporally. In temporal separation, nitrogen fixation predominantly occurs during the dark period and photosynthesis during the light; whereby during spatial separation, the central non-photosynthetic cells are involved in nitrogen fixation, whereas, the outer green cells are photosynthetically active. Nitrogen fixation has a great influence on cellular metabolism in *Cyanothece* since the nitrogenase enzyme is synthesised, functions, and is then degraded during each diurnal period, a process that consumes considerable cellular resources (Welsh *et al*., 2008). This *Euhalothece* sp. isolated was capable of N_2 fixation thus had access to a virtually unlimited source of nitrogen, in the form of atmospheric N_2. The adaptation of *Euhalothece* to a N-limited marine environment is reflected at the genomic level.

The nitrogen fixation (Nif) gene cluster in *Euhalothece* sp. consisted of the 21 genes, similar to other nitrogen-fixing species in *Cyanothece* ATTC 51142 (Table 17). This Nif cluster is made up of structural genes encoding for nitrogenase molybdenum-iron (Mo-Fe) reductase enzyme (nifH) and Mo-Fe protein (nifDK); genes involved in Mo-Fe cofactor biosynthesis which included nifB, fdxN, nifS, nifU, nifX and nifV; as well as the Mo-Fe cofactor assembly (nifE and nifN) and nitrogenase stabilising protective protein (Figure 15). Additionally, other genes such as (NifW and NafY) nitrogenase cofactor carrier protein, (modB, and modc) molybdenum transporter genes and (nif T and nif Z) genes of unknown function were found (Welsh *et al*., 2008).

Table 17: Name and description of nitrogen-fixing genes present in *Euhalothece* sp.

Gene Name	Description
Nitrogen fixation (24)	
NifS (EC 2.8.1.7)	Cysteine desulfurase NifS subfamily
Nif A	Nitrogenase (molybdenum-iron)-specific transcriptional regulator
NifU	Iron-sulfur cluster assembly scaffold protein nifu
NifB	Nifb-domain protein
frdN	4Fe-4S ferredoxin, nitrogenase-associated
NifX	Nitrogenase femo-cofactor carrier protein nifx
NifX2	Nifx-associated protein
NafY	Nitrogenase cofactor carrier protein nafy
NifE	Nitrogenase femo-cofactor scaffold and assembly protein nife
NifN	Nitrogenase femo-cofactor scaffold and assembly protein nifn
NifV (EC 2.3.3.14)	Homocitrate synthase
NifK (EC 1.18.6.1)	Nitrogenase (molybdenum-iron) beta chain
NifD(EC 1.18.6.1)	Nitrogenase (molybdenum-iron) alpha chain
NifH	Nitrogenase (molybdenum-iron) reductase and Maturation protein nifh
NifT	Nift protein
NifZ	Nifz protein
NifW	Nitrogenase stabilising/protective protein nifw
IscA	Probable iron binding protein from the hesb_isca_sufa family in Nif operon
CysE (EC 2.8.1.7)	Cysteine desulfurase
modB	Molybdenum transport system permease protein
FeoB	Ferrous iron transport protein B
FeoA	Ferrous iron transport protein A

The close proximity of the genes CysE; Nif D, K,E, U, B, H; frdN and Nif Z,V, T strongly suggests that all genes in this cluster are involved in nitrogen fixation. Notably, the genes associated with nitrogen fixation genes are found as multiple copies. Thus, it is possible this represents a mechanism for efficient control of gene expression and, together with the capability to store metabolic products in inclusion bodies, provides an advantage for unicellular marine strain in their natural nutrient-poor habitats. *Euhalothece* sp. and PCC 7408 both had similar nitrogen-fixing genes however, PCC8305 does not contain any nitrogen-fixing genes. Although both strains share many genomic similarities, the N requirements differentiate them from each other.

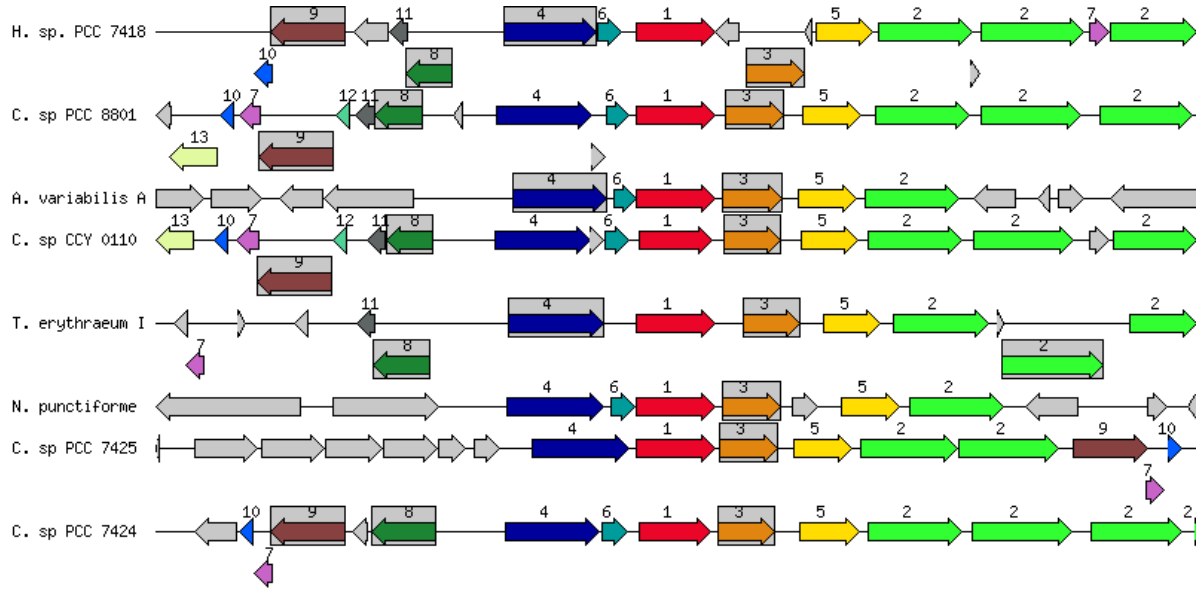

Figure 15: Clusters of some of the N_2-fixation-related genes. Shown are genes between *Euhalothece* and other nitrogen-fixing cyanobacteria. Coloured arrows represent genes assigned to functional categories: (1) CysE; (2) Nif D, K,E; (3)Nif U; (4) Nif B; (5) Nif H; (6) frdN; (7) Nif Z; (9)Nif V and (10) Nif T. Grey arrows correspond to hypothetical genes and genes of unknown function. The cyanobacteria sequences used are as follows: *Cyanothece* sp. PCC 8801; *Anabaena. variabilis* ATCC 29413; *Cyanothece* sp CYY 010; Trichodesmium erythraeum IMS101; *Nostoc punctiforme* PCC 73102, CP001037; *Cyanothece* PCC 7452 and *Cyanothece* PCC 7424.

4.3.6 Cell wall and Extracellular Polysaccharides

The synthesis of the EPS layer that covered the cells is a protective mechanism that *Euhalothece* sp. developed to help protect the cells from unfavourable environmental conditions such as high salt stress. Distribution of the genes found in the subsystem related to capsular, extracellular polysaccharides and cell wall components can be seen in Figure 16. These substances also play a significant role against desiccation, microbial invasion and protozoan predation. Polysaccharides often form hydrogen bonds with DNA, lipids and proteins, hence the water that usually surrounds these macromolecules are replaced. Due to the hydrophilic/hydrophobic characteristics, EPS are able to trap and accumulate water, creating a gelatinous layer around the cells that regulates water uptake and loss, and stabilises the cell membrane during periods of desiccation Furthermore, the sheath was found to in harbour UV absorbing substances, thus protecting the cyanobacterial cells from the deleterious effects of UV radiation.

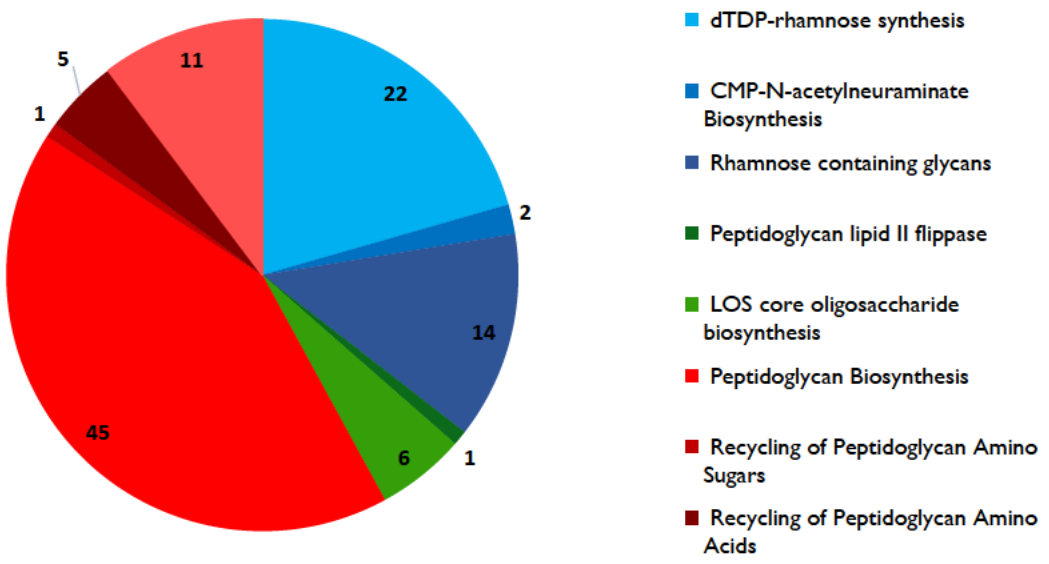

Figure 16: Distribution of genes in subsystem 3: cell wall and capsule

Peant *et al.* (2005) reported that extracellular polysaccharides can be attached to cell membrane components as lipoteichoic acids and lipopolysaccharides (LPS), they can form a capsule layer around the cell as capsular polysaccharides (CPS), or they can be released as exopolysaccharides (EPS). Some of the proposed functions of EPSs are that they (i) absorb nutrients, (ii) create a protective microenvironment and (iii) a sink of excess fixed C during growth imbalance (Sohm *et al.*, 2011). Excretion of EPS is thought to be a physiological response to fluctuations in environmental conditions, allowing cyanobacteria to continue growing (Rossi & De Philippis, 2015). As seen in Figure 7C and Figure 9 (shown in Chapter 3), the *Euhalothece* sp. produced a copious amount of EPS. The particular characteristics of these EPS, namely the presence of 2 different uronic acids, sulphate groups and a high number of different monomers, make them promising for biotechnological applications such as the removal of heavy metals from polluted waters.

Genetic components required for EPS production include genes encoding regulation, chain-length determination, repeat-unit assembly, polymerisation and export. Biosynthesis of heteropolysaccharides also known as heteroglycans begins with the intracellular formation of EPS precursors, the sugar nucleotides uridine-59-diphosphate (UDP)-glucose, UDP-galactose and deoxythymidine diphosphate (dTDP)-rhamnose. The genetic organisation of the EPS gene clusters showed very important differences from those of the gene clusters involved in the synthesis of capsular and free EPS.

Table 18: Genes involved in capsular and extracellular polysaccharides biosynthesis in *Euhalothece* sp.

Gene Name	Description
deoxythymidine diphosphate (dTDP)-rhamnose (37)	
RfbF (EC 2.7.7.33)	Glucose-1-phosphate cytidylyltransferase
RfbG	dTDP-rhamnosyl transferase
galE (EC 5.1.3.2)	UDP-glucose 4-epimerase
TagH (EC 3.6.3.40)	Teichoic acid export ATP-binding protein
rmlB (EC 4.2.1.46)	dTDP-glucose 4,6-dehydratase
rfbA (EC 2.7.7.24)	Glucose-1-phosphate thymidylyltransferase
RmlC (EC 5.1.3.13)	dTDP-4-dehydrorhamnose 3,5-epimerase
Glucose/ Glycogen other related (18)	
UGDH (EC 1.1.1.22)	UDP-glucose dehydrogenase
[EC:2.4.1.-]	UDP-glucose:tetrahydrobiopterin glucosyltransferase
bscA	UDP-glucose-beta-D-glucan glucosyltransferase
(EC 2.7.7.27)	Glucose-1-phosphate adenylyltransferase
GH-13-type (EC 2.4.1.18)	1,4-alpha-glucan (glycogen) branching enzyme
PYGL (EC 2.4.1.1)	Glycogen phosphorylase
MalQ (EC 2.4.1.25)	4-alpha-glucanotransferase (amylomaltase)
GH-57-type (EC 2.4.1.18)	Glycogen branching enzyme
GlgA (EC 2.4.1.21)	Glycogen synthase, ADP-glucose transglucosylase
amsG3 (EC 2.7.8.6)	Undecaprenyl-phosphate galactosephosphotransferase
	Galactose mutarotase and related enzymes
(EC 1.1.1.122)	L-fuco-beta-pyranose dehydrogenase
Gtf (EC 2.4.1.-) (6)	Glycosyltransferase
Sialic Acid Metabolism (14)	
ManM (EC 5.4.2.8)	Phosphomannomutase
NagB(EC 3.5.99.6)	Glucosamine-6-phosphate deaminase
NagA (EC 3.5.1.25)	N-acetylglucosamine-6-phosphate deacetylase
NeuC (EC 5.1.3.14)	UDP-N-acetylglucosamine 2-epimerase
NeuB (EC 2.5.1.56)	N-acetylneuraminate synthase
NeuA (EC 2.7.7.43	N-Acetylneuraminate cytidylyltransferase
AGE (EC 5.1.3.8)	N-acylglucosamine 2-epimerase
GlmM (EC 5.4.2.10)	Phosphoglucosamine mutase
GlmU2 (EC 2.7.7.23)	N-acetylglucosamine-1-phosphate uridyltransferas
Other	
	putative polysaccharide export protein
RfbA (2)	ABC transporter permease protein
RfbB (5)	ABC transporter ATP-binding protein

These are responsible for the structural organisation of the heptasaccharide repeating unit as well as involved in the polymerisation and export of the EPS. Several genes involved in the carbohydrate modification of the cell envelope including glycosyltransferases (six genes), and

homologues of genes involved in the synthesis of sialic acid were found (Table 18). *Dactylococcopsis salina* PCC 8305 was found to contain several more genes related to "capsule and exopolysaccharides" compared to *Euhalothece* sp. The strain also has Gram-Positive cell wall components such as teichuronic acid biosynthesis genes.

It was reported that >90% Na+ was removed extracellularly and trapped in the mucopolysaccharide sheath halotolerant *Anabaena torulosa* (Apte & Thomas, 1997). These polymers are also known to harbour both water-soluble and lipid-soluble UV-absorbing pigments (Potts, 1999), furthermore, other roles include protection against desiccation, salinity, UV-irradiation; increase the availability of light, nutrient uptake, nitrogen fixation (Rossi & De Philippis, 2015).

4.3.7 Regulation and Signal Transduction

Since the *Euhalothece* sp. was found to proliferate the Estuary during fluctuating nutrient, and hypersaline conditions, the cyanobacterium was expected to possess numerous signal transducers and stress sensors and various mechanisms to help deal with these stress factors. *Euhalothece* has 65 genes involved in regulation and cell signalling. Two-component signal transduction systems are used to sense and adapt to various environmental stresses. Two-component signalling systems is made up of sensor histidine kinases (HK) and response regulators (RR) (Mitrophanov & Groisman, 2008). Environmental signal interacts with the membrane-bound sensor kinase, which regulates the phosphorylation of a cytosolic response regulator protein, which in turn either represses or activates the expression of specific genes (Izumitsu *et al*., 2007).

The numbers of signal transduction proteins vary widely among cyanobacterial genomes, which is probably related to the genome size and living environment. Prabha *et al*. (2016), reported that cyanobacteria in the nutrient-limited environment prefer to produce only those proteins which are essential for their survival since the biosynthesis of proteins are energy-intensive, thus to ensure this occurs, the cyanobacteria follow signal-dependent regulation. The signal transduction pathways are crucial in sensing signals both outside and inside cells and controlling cellular activities. Twenty-two genes for the histidine kinases (Hiks), 2 genes for serine-threonine protein kinases (Spks), 35 response regulator genes (Rres) and 4 genes for RNA polymerase σ factors were identified in *Euhalothece* sp. (Table 19).

SigB is an autoregulated heat-shock sigma (σ) factor, which is reported to recognise the hspA promoter. HspA key role is minimising the negative effects of light during heat-stress through stabilisation of the PS II complex and PBS (Imamura & Asayama, 2009). It also plays a role during salt- or osmotic-stress, and nitrogen deprivation. During N-deprived conditions, C-PC acts as a source of N released from degraded PBPs for the synthesis of polypeptides. SigB may be a σ factor sensing the status of the PS II complex and PBS. The degradation of PBS is also considered to be useful for minimising the absorption of excess excitation energy under stressful conditions. These genes may provide a competitive advantage to the organisms for adaptation against the salt and nutrient stress. Members of the HflX Guanosine triphosphatase (GTPase) are widely conserved and serve crucial roles in signal transduction. Cyclic-diGMP is a second messenger controlled by antagonistic activities of diguanylate cyclases (DGC) and phosphodiesterases (Reinders *et al*., 2016).

Furthermore, Motile cyanobacteria use a phototaxis signalling system to move away from high levels of detrimental UV radiation. Bacteria synthesise cyclic-diGMP from two molecules of guanosine triphosphate (GTP) using a diguanylate cyclase (Kalia *et al*., 2013). Cyclic-diGMP is also been linked to the regulation of various cellular processes, including regulation of virulence and persistence factors, motility and chemotaxis, surface colonisation, the formation of communities, progression biofilm formation, pathogenicity, and cell mobility (Nesbitt *et al*., 2015). Owing to its medical role, it is currently being explored as an anti-infective agent, as well as a vaccine adjuvant. *Euhalothece* sp. was found to have 13 copies of DGC-PDEs. Bacteria evolved multiple DGCs and PDEs to be able to rapidly respond to a diverse range of signalling inputs. Furthermore, this enzyme family is specialised for specific cellular tasks and only single genes are expressed under the specific environmental condition at any given time.

Type IV pili and type II secretion systems are involved in the uptake of DNA and natural transformation in cyanobacteria. Type IV pili are also associated with gliding motility, phototaxis, pathogenesis-related bacterial virulence, cell-cell interaction, communication, and aggregation (Schuergers & Wilde, 2015). Ten genes associated with the pilus system of motility proteins were observed, including two twitching motility proteins (homologs of pilT), pilus assembly and biogenesis proteins (homologs of pilB, -C, -D, -Q, -O, -N and two genes of PilA that encode for prepilin. The PilB encodes the motors for pilus extension and retraction, which encodes the prepilin peptidase/ N-methyltransferase. SigF plays a key role in motility

by controlling the formation of pili and is also possibly the regulation of other features of the cell surface (Imamura & Asayama, 2009).

Table 19: Name and description of signal regulators and transduction genes present in *Euhalothece* sp.

Gene Name	Description
Signal regulators and transduction	
CheA (EC 2.7.3.-) (8)	Signal transduction histidine kinase
CheW (1)	Positive regulator of chea protein activity
CheY (2)	Chemotaxis regulator - transmits chemoreceptor signals to flagelllar motor components
CheB (EC 3.1.1.61)	Chemotaxis response regulator protein-glutamate methylesterase cheb
CheR (EC 2.1.1.80)	Chemotaxis protein methyltransferase
MalE (2)	Maltose/maltodextrin abc transporter, substrate binding periplasmic protein male
HflX	Gtp-binding protein hflx
RR (25)	Two-component response regulators
ARS	Sulphur deprivation responsive response regulator
NrrA	Nitrogen-responsive response regulator
Type IV pili	
PilT	Twitching motility protein
PilN	Type iv pilus biogenesis protein
PilO	Type iv pilus biogenesis protein
PilQ	Type iv pilus biogenesis protein
PilB	Type iv fimbrial assembly, atpase
PilA	Type iv pilin
PilC	Type iv fimbrial assembly protein
	Leader peptidase (prepilin peptidase)

Toxin-antitoxin (TA) systems encoded on chromosomes are made up of a stable toxic protein and its unstable cognate antitoxin. They are responsible for plasmid maintenance, programmed cell death, or stress response (Kopfmann *et al*., 2016). There are several types TA families which include ccdAB, mazEF, pemIK, vapBC, phd/doc, parDE, and higBA (Hayes & Van Melderen, 2011). Thirty-seven genes in the TA have been identified in the *Euhalothece* sp. genome. They belong to vapBC (5 genes), higBA (4 genes), phd/doc (11 genes), relBE (5 gene), YoeB (2 genes) and parDE (6 genes) families (Table 19). RelBE TA system comprises of antagonist RelB antitoxin and RelE toxin, which bind together to form the non-toxic system (Gronlund & Gerdes, 1999). The HigBA TA system inhibits cellular growth and consists of

the HigA antitoxin and HigB toxin. The parDE TA system functions in plasmid maintenance by a post-segregation killing mechanism and consists of the ParD antitoxin and ParE toxin (Johnson *et al*., 1996). The VapBC TA system is involved in plasmid maintenance and hypothesised to function in response to stress (Cooper *et al*., 2009; Garcia-Pino *et al*., 2010). *Euhlaothece* sp. also has a larger number of genes coding an antitoxin system. These results indicated that isolate may potentially need to export 'toxins' produced by other microorganisms. Six genes for repeats-in-toxin (RTX) and Ca^{2+} binding proteins were present. RTX protein family are exotoxins reported to form pores in cytoplasmic membranes of erythrocytes, leukocytes, and other cells, leading to the modification of cellular functions and/or lysis of host cells. Moreover, RTX proteins have also shown to be necessary for cell motility in cyanobacteria. Thus, there may be a functional diversity of RTX proteins in cyanobacteria (Sakiyama *et al*., 2006).

4.3.8 Salinity, Nutrient, Light and Temperature Stress-Related Genes

In a previous study that we conducted, (Mogany *et al*., 2018a) *Euhalothece* sp. cells were able to regulate their intracellular osmolality to levels similar to that of the external media over the salinity range of 30- 150 g/L. Accessory genes of a species' genome are often involved in adaptation to a specific niche or manifestation of a specific phenotype, such as host adaptation or pathogenicity. Salinity stress-related genes were common genes found in both *Euhalothece* sp. and *Dactylococcopsis salina* PCC 8305. The whole-genome results of *Euhalothece* sp. revealed a common shock protein (csp) that is known to be expressed during stress and is followed by specific regulations in response to either heat shock or osmotic shock. Salt stress can be divided into two types: i) osmotic water stress which is high salt concentration and ii) matric water or salt stress *i.e.* the increase in intracellular salt concentration as water evaporates (Hershkovitz *et al*., 1991). Hyperosmotic stress results in an increase in solutes concentrations due to the efflux of water from the cytoplasm. Whereas, salt stress decreases the cytoplasmic volume to a small degree, while rapidly increasing cytoplasmic concentrations of Na^+ and Cl^- ions *via* an influx of NaCl (Los *et al*., 2010). Cyanobacteria have developed two effective strategies for osmotic acclimation, *i.e.* the "salt-in-strategy" and the "salt-out-strategy". For the "salt-in-strategy," very large numbers of inorganic ions (2–3 M, mainly KCl) are accumulated in the cytoplasm to ensure water uptake and turgor pressure (Pade &

Hagemann, 2015). Cyanobacteria use the "salt-out-strategy" to acclimate to high or changing salt concentrations; whereby the internal ion concentration is kept low, *via* the accumulation of small organic molecules called compatible solutes (Klahn *et al*., 2010). The osmotic solutes produced by cyanobacteria under extremely high salt concentration are glycine betaine as well as mycosporine-like amino acids, MAAs, whereas marine cyanobacteria produce glycerol. *Euhalothece* sp. genome as encoded genes are involved in the synthesis of compatible solutes such as glycine betaine (GB), sucrose and trehalose (Table 20). These are compatible solutes that accumulate in halophilic strains to grow in saturated salt concentrations.

Both *Euhalothece* sp. and *Dactylococcopsis salina* PCC 8305 were found to have the genes to take up and transport GB from glycine. However, *Euhalothece* sp. also has choline-sulfatase (3 betC genes) and high-affinity choline protein uptake proteins (9 genes), thus these species not only have the ability to actively take up glycine betaine from the environment but also synthesised from choline by a two-step pathway with betaine aldehyde as intermediate. *Dactylococcopsis salina* PCC 8305 is unable to synthesised GB from choline.

Similar to *Dactylococcopsis salina* PCC 8305, *Euhalothece* sp. was found to be buoyant In the natural environment, gas-filled structures allow the cells to float to the water surfaces and position themselves under optimal light and oxygen conditions needed for growth (Mlouka et al., 2004). GvpA is the major component and assembles to form the ribbed wall of the GV. GvpC protein being a structural element of the size of the gas vesicles shown to strengthen the resistance. However, the *Euhalothece* sp. genome had only 11 of the 14 gas vesicle (GV) proteins. Besides, to gvpA gene cluster, *Euhalothece* sp. GV gene cluster encoded homologs of gas-vesicle proteins gvpA, C, J, N, M and W. However, *Dactylococcopsis salina* PCC 8305 had additional gens such as gvpF, K and G.

The mrp-like clusters have been reported to be involved in salt stress tolerance. Genes mrpB,E was found in the genome, which, together with other antiporters function as an Na^+/H^+ antiporter for salinity stress tolerance (Tang *et al*., 2019). The other mechanisms of salt adaptation in cyanobacteria involve the active export of Na+ and accumulation of K+. The existence of rather large gene families for antiporters possibly indicated that these proteins fulfill many important functions in cyanobacterial cells. The Na^+/H^+ antiporters are primarily involved in Na^+ efflux and thus inhibits the adverse effects of raised Na+ levels within the cytoplasm. These Na^+/H^+ antiporters promote salt tolerance as well as enhance growth under

alkaline conditions (Billini *et al*., 2008). The genome sequence revealed that the cyanobacterium *Euhalothece* sp. contains eight putative Na^+/H^+ antiporters.

Table 20: Name and description of stress-related genes present in *Euhalothece* sp.

Gene Name	Description
Detoxification (9)	
HMG-DH (EC 1.1.1.284)	S-(hydroxymethyl)glutathione dehydrogenase
FGH (EC 3.1.2.12)	S-formylglutathione hydrolase
Heat shock	
DnaJ (13)	Chaperone protein DnaJ
DnaK (7)	Chaperone protein DnaK
GS (EC 6.3.2.3)	Glutathione synthetase
GroEL	
GroES	
GrpE (4)	Heat shock protein GrpE
Hsp 20	Heat shock protein
HrcA	Heat-inducible transcription repressor
ClpB	Heat shock protein HSP 100
SAM-HSP	Hypothetical radical SAM family enzyme in heat shock gene cluster, similarity with CPO of BS HemN-type
RsmE (EC 2.1.1.-)	Ribosomal RNA small subunit methyltransferase
L11+m (EC 2.1.1.-)	Ribosomal protein L11 methyltransferase
LepA	Translation elongation factor
RsmI	rRNA small subunit methyltransferase I
SmpB	tmRNA-binding protein SmpB
RdgB (EC 3. 6.1.15)	Nucleoside 5-triphosphatase RdgB (dHAPTP, dITP, XTP-specific)
Osmotic Stress	
Betaine biosynthesis from glycine (12)	
m2G-MT	Dimethylglycine N-methyltransferase
S-MT	Sarcosine N-methyltransferase
G-MT(EC 2.1.1.20)	Glycine N-methyltransferase
Choline and Betaine Uptake and Betaine Biosynthesis (7)	
ProV (TC 3.A.1.12.1)	L-proline glycine betaine ABC transport system permease protein ProV
ProW (TC 3.A.1.12.1)	L-proline glycine betaine ABC transport system permease protein ProW
ProX (TC 3.A.1.12.1)	L-proline glycine betaine binding ABC transporter protein ProX
BetT	High-affinity choline uptake protein BetT
PsaE	I subunit IV
Pro U	
Trehalose	
TPS1 (EC 2.4.1.15)	Alpha,alpha-trehalose-phosphate synthase [UDP-forming]
TPP	Maltooligosyl trehalose synthase
TreZ (EC 3.2.1.141)	Malto-oligosyltrehalose trehalohydrolase
UDPG (EC 1.1.1.22)	UDP-glucose dehydrogenase

Gene Name	Description
sucrose	
SUS (EC 2.4.1.13)	sucrose synthase
SPP (EC 3.1.3.24)	Sucrose-phosphate phosphatase
Oxidative stress (23)	
AhpC (5)	Alkyl hydroperoxide reductase subunit C-like protein
FeZn	Fe2+/Zn2+ uptake regulation proteins
Furp	Ferric uptake regulation protein
FUR	Ferric uptake regulation protein FUR
Fr (3)	Ferroxidase (EC 1.16.3.1)
Dps (3)	Non-specific DNA-binding protein Dps
IBP	Iron-binding ferritin-like antioxidant protein
	Peroxide stress regulator
ZUR (3)	Zinc uptake regulation protein ZUR
Crp (3)	transcriptional regulator, Crp/Fnr family
ROS	
sodB (EC 1.15.1.1)	Superoxide dismutase [Fe]
Sod A	Magnesium dismutase
Rubrerythrin	
AHR (5)	Alkyl hydroperoxide reductase subunit C-like protein
Rdx	Rubredoxin
Periplasmic Stress Response	
DegB (3)	HtrA protease/chaperone protein
Universal stress	
USP (7)	Universal stress protein family 3
Mycosporine-like amino acid (MAA) (12)	
mysB	O-methyltransferase MysB
mysC	ATP-grasp ligase forming mycosporine-glycine, MysC
mysT	Predicted sodium/serine symporter MysT
mysD	D-alanine--D-alanine ligase (EC 6.3.2.4) MysD
NRPSm	Mycosporine-producing nonribosomal peptide synthetase
High-light induce proteins (5)	
CAB/ELIP/HLIP	High-light induce CAB/ELIP/HLIP superfamily

High intensity of PAR, desiccation, nutrient deficiency, exposure to heavy metals as well as the limited capacity of the cyanobacteria to use absorbed light energy results in the imbalance in functions of PSI and PSII (Asada, 2006). Cyanobacteria can adapt rapidly to the metabolic demands and/or changing light conditions by regulating the distribution of absorbed light energy between PSI and PSII (Chukhutsina *et al*., 2015; Joshua & Mullineaux, 2004). *Euhalothece* sp. contains four psbA genes encoding two different forms of DI (Table 15). The

psbA1 encodes the constitutive form D1:1, whereas psbAII genes encode an alternate form D1:2, which differs at 25 residues. It is reported that the D1:2 form transiently replaces D1:1 upon shifts to high light, allowing the cyanobacteria to overcome photoinhibition damage to PSII (Campbell *et al*., 1998; Latifi *et al*., 2009). Thus, it is proposed that the strain could have responded to photoinhibition by a transient exchange in the form of D1 to more resistant isoforms of this protein.

The excess photons may lead to increased production of ROS (Hakkila *et al*., 2014). Moreover, ROS has also been shown to be signalling molecules involved in the activation of the stress response and defence pathways. Some of the defence mechanisms developed by cyanobacteria include enzymatic *i.e.* catalases, SOD and peroxidases, as well as non-enzymatic such as glutathione, vitamin A, C, E, PBPs carotenoids, *etc* to protect themselves against ROS damage (Latifi *et al*., 2009). *Euhalothece* sp. genome contained 2 important genes encoding for protection against oxidative stress *i.e.* manganese superoxide dismutase (sodA) and superoxide dismutase (sodB). Additionally, 23 oxidative stress genes were present which include: Fe-stress and redox related genes (BphO, PCh, IBP, Dps, Fr, FUR, Irr Rex, HemO), H_2O_2 stress response genes (PRP, OxyR, PerR), fumarate and nitrate reduction regulatory protein (Fnr), alkyl hydroperoxide reductase subunit C-like protein (AhpC), zinc uptake regulation protein (ZUR) and a non-heme iron protein rubrerythrin (RTH) that protects against oxidative stress and reactive nitrogen species (Table 20). Glutathione plays a role in the maintenance of cellular redox homeostasis as well as an antioxidant (Cameron & Pakrasi, 2010). *Euhalothece* sp. contained 25 genes from glutathione biosynthesis. Putative haemoglobin plays a role in the protection against nitrogen reactive species.

Hence, cyanobacteria respond to a sudden increase in temperature by inducing the synthesis of a specific group of polypeptides known as heat shock proteins (HSPs) (Rajaram *et al*., 2014). *Euhalothece* sp. comprised of 38 heat shock response (HSR) genes. The genome encoded 8 Hsp70 (DnaK), 13 Hsp40 (DnaJ); 4 GrpE, proteins together with 2 (Hsp20), 9 GroeL, 2 GroeS and 1 HtrA chaperones. Heat shock proteins have multiple roles including folding of proteins, stabilisation of thylakoid and periplasmic membranes (Rajaram *et al*., 2014). Chaperons are essential for proper folding of denatured proteins and for protecting proteins from stress-induced unfolding and aggregation (Kampinga, 2006). In addition, five genes for typical single membrane-spanning proteins of CAB/ELIP/HLIP superfamily which is involved in tolerance against high light stress was found. The PBSs can also be photo-damaged under heat stress.

The periplasmic chaperone and serine protease (HtrA) are important for bacterial stress responses and protein quality control (Asadulghani. *et al*., 2004).

The MAAs are highly hydrophilic and consist of an aminocyclohexenone or aminocyclohexene imine structure as the basic chromophore structure, on which various kinds of amino acids such as valine, glutamic acid, serine, threonine, and glycine are substituted (Wada *et al*., 2013). The synthesis of MAAs are enhanced by PAR, UV-A (315-400 nm), and UV-B (280–315 nm) light radiation. Additionally, UV-A irradiation has a negative effect on DNA, initiates ROS production and induces direct damage to PS II. Whereas, UV-B radiation affects the physiological and biochemical processes, including photosynthesis, growth, pigmentation, nitrogen metabolism, CO_2 uptake and RuBisCO activity (Moon *et al*., 2012). Garcia-Pichel *et al*. (1998) found that the 13 unicellular halophilic cyanobacteria *Euhalothece* sp. isolated from the upper layer of a gypsum crust developing on the bottom of a hypersaline saltern pond had two types of MAAs, having absorption maximum at 331 and 362 nm when grown at high light intensities. Similarly, *Euhalothece* sp. had genes encoding for these UV-absorbing compounds were also evident in the genome. The *mys* biosynthetic gene contains the three genes required for the biosynthesis of mycosporine-glycine, the precursor compound for shinorine biosynthesis. Cyanobacteria are well known for producing high amounts protective and photoreceptor pigments pteridines, owing to their chemical and photophysical properties (Moon *et al*., 2012). *Euhalothece* sp. genome contained 40 genes encoding for pteridines.

Euhalothece sp. genome has multiple channels for transporting major seawater ions and multiple transporters or ABC-type solute binding proteins for several major nutrients. Although the isolate may not require zinc detoxification, several zinc/manganese transporters were detected in the genome. Multiple copies of amino acid and oligopeptide transporters (22 genes) were found in the genome displayed in Table 21, suggesting that *Euhalothece* sp. may have the ability to use these ubiquitous compounds in hypersaline water. Phosphorus is a crucial component of the cell membrane, required for energy metabolism as well as the storage and recovery of DNA/RNA. During phosphate (P) limitation cyanobacteria have evolved several strategies. Firstly, they store polyphosphate bodies to overcome short periods of P-starvation. As per Chapter 3 (Figure 9) *Euhalothece* sp. was found to accumulate polyphosphate granules. Polyphosphate granules are used as an intracellular P-reserve and are commonly found in exponentially growing cells under P-rich conditions and are degraded in

P-deficient cells. Secondly, cyanobacteria synthesise enzymes alkaline phosphatases (APases) in response to P-deficiency in their external environment (Pandey & Tiwari, 2003). These enzymes hydrolyse dissolved organic P thus releasing dissolved inorganic phosphorus that the cells are able to readily utilise.

The Pho regulon are a group of genes that control the acquisition of P. It is composed several elements which include: (i) high-affinity phosphate transport is comprised of the periplasmic binding protein (PstS) and membrane-bound ABC transport system (PstC, PstA, and PstB) and low-affinity phosphate transport, (ii) APases, and (iii) polyphosphate metabolism (PpK)(Fernández-Juárez *et al*., 2019). *Euhalothece* sp. genome has two gene clusters encoding for 23 genes of the high-affinity phosphate transporter system, 30 APases genes, and 7 APase transporter genes. Kageyama *et al*. (2011) reported that APases was induced by salt stress in *Aphanothece halophytica* and was found to be secreted out of the cells. The cyanobacterium was also found to have high-affinity transport systems which are involved in the active transport of solutes across the cytoplasmic membrane. genes for the transport of phosphonates (compounds with C–P bonds) are present in the genome.

Under iron-limiting conditions, some cyanobacteria can enhance iron uptake by secreting (siderophores) to complex environmental iron. The siderophore-iron complexes are bound by receptor proteins (TonB-dependent transporters) in the outer membrane transferred to the cytoplasm. This process is dependent on TonB which provides the energy required for the translocation of siderophore-iron complexes across the outer membrane. Iron specific transporters (10 genes), as well as low-molecular-weight iron chelators *i.e* siderophore synthesis and uptake were present in the *Euhalothece* sp. genome. The Ton and Tol transport systems genes were unique to *Euhalothece*, and not found in PCC8305.

IsiA is a Chl storage protein (Table 15), which is not present in all cyanobacteria. The presence of isiA is a natural biomarker for cyanobacteria found in iron-limited, high-nutrient environments (González *et al*., 2018). Cyanophycin, is a polymer of arginine and asparagine, that plays a role as a nitrogen reserve molecule in cyanobacteria. Catabolism of L-arginine can serve as a source of nitrogen, carbon, and energy for the cells (Bandyopadhyay *et al*., 2011a). *Euhalothece* sp has an arginine decarboxylase that catalyses the conversion of arginine to agmatine, then converts agmatine into putrescine and urea. The genomes six genes encode urease and its accessory proteins, as well as genes involved in the conversion of putrescine into spermidine.

Table 21: Name and description of basic phosphate metabolism, high-affinity phosphate uptake, iron, amino acid and oligotide transporter genes present in *Euhalothece* sp.

Gene Name	Description
Phosphate metabolism (95)	
IPP (EC 3.6.1.1)	Inorganic pyrophosphatase
THb (EC 1.6.1.2)	NAD(P) transhydrogenase alpha subunit
THa (EC 1.6.1.2)	NAD(P) transhydrogenase subunit beta
PhoHv	Phosphate starvation-inducible protein phoh, predicted atpase
SAP (EC 2.3.1.51)	Secreted alkaline phosphatase
	Asga 1-acyl-sn-glycerol-3-phosphate acyltransferase
ALPT (EC 2.3.1.-)	Apolipoprotein N-acyltransferase
corC	Magnesium and cobalt efflux protein corc
MH	Metal-dependent hydrolase
YbeY	Involved in rrna and/or ribosome maturation and assembly
AP (EC 3.1.3.1)	Alkaline phosphatase
LAT	Low-affinity inorganic phosphate transporter
PPK (EC 2.7.4.1)	Polyphosphate kinase
phoP	Alkaline phosphatase synthesis transcriptional regulatory protein phop
API	Alkaline phosphatase like protein
High affinity phosphate transporter and control (23)	
PhoUh	Phosphate transport regulator (distant homolog of phou)
PhoR (EC 2.7.13.3)	Phosphate regulon sensor protein phor (sphs)
PhoB	Phosphate regulon transcriptional regulatory protein
PhoU	Distant similarity with phosphate transport system regulator
ptsS (TC 3.A.1.7.1)	Phosphate ABC transporter, periplasmic phosphate-binding protein
ptsA (TC 3.A.1.7.1)	Psta Phosphate transport system permease protein
ptsC (TC 3.A.1.7.1)	Pstc Phosphate transport ATP-binding protein
ptsB (TC 3.A.1.7.1)	Phosphate transport ATP-binding protein
OprO	Pyrophosphate-specific outer membrane porin
OprP	Phosphate-specific outer membrane porin
PhoR (EC 2.7.13.3)	Phosphate regulon sensor protein
(SphR) (3)	Phosphate regulon transcriptional regulatory protein phob
PPiase (EC 3.6.1.11)	Exopolyphosphatase
Phosphonates (9)	
PhnK	Phosphonates transport ATP-binding protein
PhnL	Phosphonates transport ATP-binding protein
phnE1 (TC 3.A.1.9.1)	Phosphonate ABC transporter permease protein
phnE2 (TC 3.A.1.9.1)	Phosphonate ABC transporter permease protein
Iron transporter (10)	
FeoA	Ferrous iron transport protein A
FeoB	Ferrous iron transport protein B
sfuC	Iron(III)-transport ATP-binding protein
FecB (TC 3.A.1.14.1)	Iron(III) dicitrate transport system, periplasmic iron-binding protein

Gene Name	Description
(FeCT)	Iron chelate uptake ABC transporter family, permease protein
FecE (TC 3.A.1.14.1)	Iron(III) dicitrate transport ATP-binding protein
EfeO	Ferrous iron transport periplasmic protein
FUR	Ferric uptake regulation protein
Fbp	Ferric iron transporter
Piu	Iron uptake factor
Ton and Tol transport systems (9)	
TonB	Ferric siderophore transport system, periplasmic binding protein TonB
TonR	TonB-dependent receptor
*TolQ_ExbB	Ferric siderophore transport system, biopolymer transport protein ExbB
*TolR_ExbD	Biopolymer transport protein ExbD/TolR
*TRP	TPR domain protein, putative component of TonB system
TolB	tolB protein precursor, periplasmic protein involved in the tonb-independent uptake of group A colicins
HTAS	4-hydroxybenzoyl-CoA thioesterase family active site
IUP	Iron-chelator utilization protein
HasA	Hemophore HasA
TolC	Type I secretion outer membrane protein, TolC precursor
piamt	Protein-L-isoaspartate O-methyltransferase (EC 2.1.1.77)
Antiporters (19)	
Na+/H+ antiporter (15)	Multiple resistance and ph antiporter
Mrp subunits A-G (3)	
K+/H+ antiporters	
Subunit E (2)	PH adaptation potassium efflux system protein E
Subunit G	PH adaptation potassium efflux system protein G
YrbG	predicted calcium/sodium:proton antiporter
	Multi antimicrobial extrusion protein (Na(+)/drug antiporter), MATE family of MDR efflux pumps
GltT (EC 2.3.2.2)	Gamma-glutamyltranspeptidase
GshB	Glutathione synthetase
GltT (EC 2.3.2.2)	Gamma-glutamyltranspeptidase
GshB	Glutathione synthetase
Glutaredoxins (4)	
GR2	Glutaredoxin 2
GR3 (2)	Glutaredoxin 3
MTGR	Uncharacterised monothiol glutaredoxin ycf64-like
ABC transporter oligopeptide (10)	
OppA (TC 3.A.1.5.1)	Oligopeptide ABC transporter, periplasmic oligopeptide-binding protein
OppB (TC 3.A.1.5.1)	Oligopeptide transport system permease protein
OppC (TC 3.A.1.5.1)	Oligopeptide transport system permease
OppF (TC 3.A.1.5.1)	Oligopeptide transport ATP-binding protein

Gene Name	Description
Amino acid transporters (12)	
LivF (TC 3.A.1.4.1)	Branched-chain amino acid transport ATP-binding protein
LivG (TC 3.A.1.4.1)	Branched-chain amino acid transport ATP-binding protein
LivM (TC 3.A.1.4.1)	Branched-chain amino acid transport system permease protein
LivH	High-affinity branched-chain amino acid transport system permease protein
LivK (TC 3.A.1.4.1)	High-affinity leucine-specific transport system, periplasmic binding protein
Zinc/Maganese/Urea transporter	
ZnuC	Zinc ABC transporter, ATP-binding protein
ZnuB	Zinc ABC transporter, inner membrane permease protein
ZnuA	Zinc ABC transporter, periplasmic-binding protein
SitD	Manganese ABC transporter, inner membrane permease protein
SitB	Manganese ABC transporter, ATP-binding protein
UrtE	Urea ABC transporter, ATPase protein
UrtD	Urea ABC transporter, ATPase protein
UrtC	Urea ABC transporter, permease protein
UrtB	Urea ABC transporter, permease protein
UrtA	Urea ABC transporter, substrate binding protein
	Urea carboxylase-related ABC transporter, permease protein
	Urea carboxylase-related ABC transporter, periplasmic substrate-binding protein
	Urea carboxylase-related ABC transporter, ATPase protein
Magnesium/Cobalt	
CorC (5)	Magnesium and cobalt efflux protein
CorA (2)	Magnesium and cobalt efflux protein
MgtE (4)	Mg/Co/Ni transporter

4.3.9 Other Essential Genes

4.3.9.1 Heavy metal resistance

Euhalothece sp. also has efflux pumps for metals (Table 22). The primary intracellular process for regulating an excess of metals is based on transporting the metals through the cytoplasmic membrane (Intorne *et al*., 2012). These cations are transported into the cell by Mg^{2+} transport systems. High concentrations of divalent cations of cobalt (Co^{2+}), zinc (Zn^{2+}), and nickel (Ni^{2+}) are toxic to cyanobacteria. Hence, during heavy metal stress, uptake of the toxic ions cannot be reduced by a simple down-regulation of the transport activity (Nies, 1992). Thus, when metal ions are in excess, specific ion efflux protein complexes are synthesised in response to metal toxicity to assist in the elimination of these non-essential metals. Together with other genes, CzcA forms the Czc determinant, which encodes a multi-protein complex associated

cadmium, cobalt and zinc resistance. The membrane bound CzcD protein is also essential for induction of Czc. Moreover, the isolate *Euhalothece* sp. also contained additional genes encoding cobalt, zinc, cadmium, mercury and arsenic resistance, as well as resistance to chromium compounds and fluoroquinolones.

Table 22: Name and description of heavy metal resistance present in *Euhalothece* sp. Enzyme Commission (EC) numbers are based on the recommendations of the Nomenclature Committee of the International Union of Biochemistry and Molecular Biology (IUBMB) (Bairoch, 2000).

Gene Name	Description
Arsenic resistance (8)	
ArsC (EC 1.20.4.1)	Arsenate reductase
ArsH	Arsenic resistance protein
ArsA (EC 3.6.3.16)	Arsenical pump-driving ATPase
ARC	Arsenical resistance operon repressor
ARC3	Arsenical-resistance protein ACR3
Beta-lactamase and fluoroquinolones	
BL (EC 3.5.2.6)	*β*-lactamase
BLA	*β*-lactamase class A
BLI	Metal-dependent hydrolases *β*-lactamase superfamily I beta-lactamase domain protein metallo-beta-lactamase-related protein
(PBP-2)	Penicillin-binding protein 2
gyrA(EC 5.99.1.3)	DNA gyrase subunit A
gyrB (EC 5.99.1.3)	DNA gyrase subunit B
Cobalt-zinc-cadmium resistance	
CzcA	Cobalt-zinc-cadmium resistance protein
CzcD	Cobalt-zinc-cadmium resistance protein
CusA	Cation efflux system protein CusA
TR	Probable Co/Zn/Cd efflux system membrane fusion protein
CadC	Cadmium efflux system accessory protein
ZUR	Zinc uptake regulation protein ZUR
COG0523	Putative metal chaperone,
FolE1(EC 3.5.4.16)	GTP cyclohydrolase I type 1
PryC(EC 3.5.2.3)	Dihydroorotase
Copper, chromium and mercury	
CIA (EC 3.6.3.4)	Copper-translocating P-type ATPase
MO	Multicopper oxidase
CopG	CopG protein

Some cyanobacterial strains were described as resistant to some antibiotics, including penicillin and amplicilin (Dias *et al*., 2015). Resistance to *β*-lactam antibiotics is mediated by production either of a *β*-lactamase that hydrolyzes and inactivates or of an altered target *i.e.* penicillin-binding proteins. Genes encoding for Beta-lactamase as well as penincilin-binding protein were present in *Euhalothece* sp. however, were not found in either PCC7408 or PCC

8305. Beta-lactamase is an enzyme that provides multi-resistance to *β*-lactam antibiotics such as penicillins, cephalosporins, cephamycins, and carbapenem. class B the metallo-beta lactamases that require a bivalent metal ion, usually Zn^{2+} for their activity. Therefore, if necessary, during cultivation the above-mentioned antibiotics can be used to control grow of contaminating bacteria.

4.3.9.2 Isoprenoids

Isoprenoids are group compounds with remarkable chemical and functional diversity, consisting of 70 000 compounds (Vickers *et al*., 2014). Owing to their diversity they are exploited in varied essential and non-essential biological functions including carriers for electron transport, hormones, photosynthetic and non-photosynthetic pigments, regulation of transcription and post-translational processes, defence molecules, vitamins, protein-targeting components, virulence factors glycoprotein biosynthesis, protein degradation, modification of tRNAs, antioxidant activities (Lange *et al*., 2000). In addition, isoprenoids are imperative for cell wall biosynthesis, stabilisation of cell membranes and structural components of organelle membranes. Thus, this diverse group of compounds have extensive applications as biofuels, chemical precursors, pharmaceutical and in aromatherapy. Overall, horizontal gene transfer appears to have contributed substantially to the distribution across prokaryotic genomes of genes for isoprenoid biosynthesis.

Isopentenyl pyrophosphate (IPP) and dimethylallyl pyrophosphate (DMAPP) are the universal precursors of natural products called isoprenoids. *Euhalothece* sp. produced IPP and DMAPP *via* the non-mevalonate pathway, also known the 1-deoxy-D-xylulose-5-phosphate (DOXP) or 2C-methyl-D-erythritol-4-phosphate (MEP) pathway. The DOXP pathway consists of eight reactions catalysed by nine enzymes, all of the genes were be identified (Table 26). This nonmevalonate pathway is absent in humans, thus, there is a great interest in targeting these enzymes for broad-spectrum antimicrobial drug development (Hunter, 2007). Furthermore, these enzymes also are attractive targets for herbicide development by inhibiting chloroplast function.

An abundant group of isoprenoids found in cyanobacteria are the carotenoids. These are tetraterpenes formed from the condensation of two geranyl geranyl diphosphate (GGDP) molecules (Kultschar & Llewellyn, 2018). When comparing the genome of *Euhlaothece* sp. to *Dactylococcopsis salina* PCC 8305 and *Halothece* PCC 7408, the isolate was found to have all

the genes required for carotenoid synthesis. Phytoene dehydrogenase is an enzyme of carotenoid biosynthesis that converts phytoene into zeta-carotene.

Table 23: Name and description of isoprenoid biosynthesis genes present in *Euhalothece* sp.

Gene Name	Description
Isoprenoids	
STM474_3911	Putative Zn-dependent hydrolase
(EC 2.3.1.16)	3-ketoacyl-CoA thiolase
ACAT (EC 2.3.1.9)	Acetyl-CoA acetyltransferase
HepT2 (EC 2.5.1.30)	Heptaprenyl diphosphate synthase component I
GGPS (EC 2.5.1.29)	Geranylgeranyl diphosphate synthase
DMAT (EC 2.5.1.1)	Dimethylallyltransferase
IPDDI (EC 5.3.3.2)	Isopentenyl-diphosphate delta-isomerase
IPDDIf (EC 5.3.3.2)	Isopentenyl-diphosphate delta-isomerase, FMN-dependent
IspA(EC 2.5.1.10)	(2E,6E)-farnesyl diphosphate synthase
IspB (EC 2.5.1.90)	Octaprenyl diphosphate synthase
ISPD (EC 2.7.7.60)	2-C-methyl-D-erythritol 4-phosphate cytidylyltransferase
ISPC (EC 1.1.1.267)	1-deoxy-D-xylulose 5-phosphate reductoisomerase
IspE (EC 2.7.1.148)	4-diphosphocytidyl-2-C-methyl-D-erythritol kinase
ISPF (EC 4.6.1.12)	2-C-methyl-D-erythritol 2,4-cyclodiphosphate synthase
ISPG (EC 1.17.7.1)	1-hydroxy-2-methyl-2-(E)-butenyl 4-diphosphate synthase
ISPH (EC 1.17.1.2)	4-hydroxy-3-methylbut-2-enyl diphosphate reductase
DXS (EC 2.2.1.7)	1-deoxy-D-xylulose 5-phosphate synthase
GTT (EC 2.5.1.10)	(2E,6E)-farnesyl diphosphate synthase
UppS (EC 2.5.1.31) (3)	Undecaprenyl diphosphate synthase
CrtN (EC 1.14.99.-)	Dehydrosqualene desaturase
CrtM (EC 2.5.1.96)	Dehydrosqualene synthase
CrtQ (EC 2.4.1.-)	4,4'-diaponeurosporenoate glycosyltransferase
(EC 2.7.7.60)	2-C-methyl-D-erythritol 4-phosphate cytidylyltransferase
Sds (EC 2.5.1.11)	Solanesyl diphosphate synthase
Carotenoid/other (20)	
crtB(EC 2.5.1.32)	phytoene synthase
crtD(EC 1.14.99.-)	phytoene desaturase
(EC 1.14.99.-)	Phytoene dehydrogenase
crtEb (EC 2.5.1.-)	Lycopene elongase
CrtISO	Carotenoid cis-trans isomerase
crtL	Neurosporene desaturase
	Pro-zeta-carotene desaturase
crtR	beta-carotene hydroxylase
crtE	geranylgeranyl pyrophosphate synthase

4.3.10 Natural Products

Diversity of cyanobacteria in terms of morphology, biochemical and physiology increases the amount, type and function of secondary metabolites produced. Due to their complex structures and varied bioactivities these secondary metabolites can be utilised in drug discovery. The majority of cyanobacterial natural products are non-ribosomal peptides, polyketides or hybrid peptidepolyketide compounds. Non ribosomal peptides are synthesised by nonribosomal peptide synthetases (NRPS) and polyketides are biosynthesised by polyketide synthases (PKS) (Micallef *et al*., 2015). *Euhalothece* sp. contained gene clusters belonging to the NRPS/PKS, PRPS (specifically bacteriocin gene clusters), UV-absorbing (MAA and scytonemin) and terpene classes of natural products

Apart from the above, seven biosynthetic gene clusters (BGC) were identified, of which 2 were non ribosomal peptides (NPRS), 3 were terpenes and 1 polyketide synthase (PKS) and 1 ladderane were found in the genome. Non-ribosomal peptides are a very diverse family of natural products with an extremely broad range of pharmacological properties and biological activities. When compared with known gene cluster for secondary metabolites, *Euhalothece* sp. was predicted to synthesis puwainaphycins, a cytotoxic cyanobacterial lipopeptides, (Mareš *et al*., 2014). Puwainaphycins are reported to exhibit cytotoxic, anti-fungal, antibiotic, anti-proliferative activities, and a widely used immunosuppressant agent (Cheel *et al*., 2017). Analysis of gene cluster 5 predicted T1pks, which predicted cryptophycin and dkxanthene, a yellow pigment biosynthetic gene cluster showing a 17 and 11% gene similarity, respectively. Cryptophycin, is a potent cytotoxin used as a natural anticancer drug (Costa *et al*., 2012). The above observation indicated that the isolated strain, *Euhalothece* sp. has great potential to produce important secondary metabolites, and novel bioactive compounds with potential pharmaceutical applications. Based on the above observations, it can be concluded that the novel strain of cyanobacterium, *Euhlaothece* sp. displayed a genotypic plasticity by gaining new metabolic capabilities in comparison to the other two strains while concurrently retaining the major archaic metabolic traits.

4.4 CONCLUSIONS

The genomic study reveals that this cyanobacterium has developed unique strategies to adapt to environments exposure high salinities and nutrient fluxes, as well as mechanisms involve the uptake and utilisation of excess nutrients and metals, regulatory systems and motility. It likely employs the storage compounds, glycogen, and cyanophycin, can produce the osmolytes, trehalose, and glycine betaine, as well has EPS. According to the genome analysis, *Euhalothece* sp. also has the potential to produce products of biotechnological interest such the suncreens mycosporines, as well as isoprenoids. With respect to C-PC production, initial comparisons of the genetic architecture and sequence of relevant genes, and a comparative model of protein structures revealed differences that could explain its C-PC producing capacity. Overall, this study provides a better understanding of the functional profile of this cyanobacteria inhabiting hypersaline environment.

CHAPTER 5 : EXTRACTION AND RECOVERY OF ANALYTICAL GRADE C-PHYCOCYANIN FROM A NOVEL *EUHALOTHECE* SP.

5.1 INTRODUCTION

Phycobiliproteins are antennae-protein pigments involved in light-harvesting in cyanobacteria (Sonani *et al*., 2014). These brilliantly coloured, proteins are divided broadly into three classes based on their spectral properties: C-PE (λmax ~565 nm), C-APC (λmax ~650 nm) and C-PC (λmax ~620 nm) (Khattar *et al*., 2015; Singh *et al*., 2009a). C-phycocyanin is characterised by light blue colour, absorbs orange and red light, has an absorption maximum between 615 and 622 nm, and emits fluorescence at about 650 nm. This compound is composed of two different kinds of polypeptides *i.e.* α (MW- 12-19 kDa) and β (MW- 14-21 kDa) and is generally organised as trimeric ($\alpha\beta$) 3 or hexameric ($\alpha\beta$) 6 discs (Kumar *et al*., 2014).

To date, *Arthrospira* sp. is the main source for C-PC, with a yield and purity ratio ranging from 39.2- 67.8 mg/g, and 0.31- 4.4. (Chen *et al*., 2016; İlter *et al*., 2018; Manirafasha *et al*., 2018; Moraes *et al*., 2011; Taufiqurrahmi *et al*., 2017). Research has shown the potential of other cyanobacteria to replace *Arthrospira* sp. in C-PC production such as *Cyanidioschyzon merolae* (Rahman *et al*., 2017); *Polysiphonia urceolata* (Wang *et al*., 2014); *Galdieria sulphuraria* (Moon *et al*., 2014*); Phormidium ceylanicum* (Singh *et al*., 2009a). The isolated halophilic*, Euhalothece* sp. in this study appeared to be particularly interesting for the production of this high-value pigment. A major advantage of using this cyanobacterium for C-PC production is the low risk of bacterial and fungal contamination due to the requirement of high salt (120 g/L) in the growth medium. Furthermore, the cyanobacterium was also found to tolerate temperatures up to 45 °C and pH range 6.0-9.0. A comparable yield (45 mg/g) and good quality C-PC (purity >2.0) from this *Euhalothece* sp. strain make it a possible candidate to produce high-grade C-PC (Mogany *et al*. 2018b).

Phycobiliproteins are primarily utilised in the food and cosmetic industries as natural colourants replacing current synthetic dyes. Because of their unique structural characteristics, PBPs have intrinsic fluorescence properties that make them highly sensitive fluorophores for various fluorescence-based techniques such as immunofluorescence, fluorescence-activated

cell sorting, microplate assays and immunology, and as photosensitisers in photodynamic therapy for cancer treatment and other therapeutic benefits (Chaiklahan *et al*., 2011; Cherng *et al*., 2007; Eriksen, 2008; Kuddus *et al*., 2013; Sonani *et al*., 2014). Thus, the design and application of bioprocesses for the production, recovery and purification of these protein-based pigments are one of the most attractive segments of the biotechnological industry (Pagels *et al*., 2019). The commercial value of highly purified C-PC obtained ranges from 30–150 US$/depending on the nature of the final product. The current total market value for PBP products (including fluorescent agents) is estimated to be greater than 60 million US$ (Chaiklahan *et al*., 2011; Martínez *et al*., 2017). C-phycocyanin with a purity ratio ($A_{620\ nm}/A_{280\ nm}$) of at least 0.7 is considered to be of food-grade, while the purity of 3.9 is considered to be of reagent grade, and > 4 regarded as analytical grade (Sekar & Chandramohan, 2008).

The application of C-PC in diagnostics, nutraceutical and pharmaceutical industries are limited by the high cost of the purified protein, mainly related to the cost of extraction and purification. To fully exploit and improve the feasibility of the application of this valuable molecule, it is necessary to employ simple and cost-effective protocols that allow recovery of high yield and purity C-PC (Manirafasha *et al*., 2018). Extraction and purification of PBPs are one of the essential steps required for their accurate characterisation and quantification (Viskari & Colyer, 2003). Thus, the development of rapid and efficient extraction and purification methods at a minimum cost for obtaining C-PC is of great interest. The process of C-PC isolation involves various steps, namely, cell disruption, extraction and purification. In recent years, many authors have reported freeze-thaw (FT) as an effective cell lysis method for cyanobacteria (Lawrenz *et al*., 2010; Minkova *et al*., 2007; Mogany, 2013; Moraes *et al*., 2011). This method is advantageous since it is simple, quick, reproducible and robust. When cells are frozen, there will be intracellular ice formation, which causes cells to swell and contract during thawing which ultimately leads to damaged cell walls promoting better extraction of intracellular substances (Tangtua, 2014). The other factors that could influence C-PC extraction include the type of buffer/solvent, time, pH and temperature (Silveira *et al*., 2007). Chaiklahan *et al.* (2012) reported that the control of pH and ionic strength are essential for the stability of C-PC during extraction and purification processes.

Purification processes to provide C-PC in different degrees of purity, using a minimum number of steps, are important for industrial and commercial value. At present, several studies have

evaluated the development of a process with multiple scalable steps to obtain C-PC of different purities. However, in order to obtain high purity C-PC, the purification method often used include fractional precipitation with ammonium sulphate followed by ion-exchange chromatography and gel filtration (Bermejo *et al*., 2007; Kumar *et al*., 2014; Soni *et al*., 2006; Viskari & Colyer, 2002). All these methods are expensive, comprises of multiple steps and are time-consuming, which may lead to an increase in production costs and limit widespread application. Thus, in order to improve the economics, there is a need for low-cost extraction and purification technologies that are simple, fast, efficient and result in high yield and purity C-PC. More recently the use of chitosan and charcoal treatment has been investigated and shown to improve the quality of the C-PC (Gantar *et al*., 2012; Fekrat *et al*., 2019; Patil *et al*., 2008).

Therefore, the objectives of this chapter were to first optimise the freeze-thaw extraction parameters which included type, concentration and pH of buffer; biomass ratio; and freezing and thawing times and temperatures in order to find the best protocol for primary extraction of crude C-PC from wet biomass of *Euhalothece* sp. Secondly to establish the best conditions for high purity C-PC, purification and recovery *via* simple precipitation, adsorption and UF was conducted.

5.2 MATERIALS AND METHODS

5.2.1 Gel Electrophoresis

Sodium dodecyl sulphate–polyacrylamide gel electrophoresis (SDS-PAGE) analysis was performed to determine the C-PC size (molecular weight) and yield according to Laemmli (Laemmli, 1970) using a MiniProtean II apparatus (Bio-Rad®). Briefly, a stacking gel of 5% and resolving gel of 15% acrylamide concentration was used. The prepared gel was 1.0 mm thick. Prior to loading the gels, samples were pre-incubated at 90°C from 10 min with sample buffer [62.5 mM Tris-HCl (pH 6.8), 2% SDS, 25% glycerol, 0.01% Bromophenol Blue] (He, 2011). The optimal separation range for these conditions is between 10 - 200 kDa. Unstained protein standards, of a broad range (10–250 kDa) (Bio-Rad®) were used as molecular weight markers. The detailed protocol is available in Appendix 9.

5.2.2 Preparation and Estimation of Crude C-phycocyanin

Wet biomass (1.50 mg/mL) of *Euhalothece* sp. were harvested during the exponential phase of

their growth by centrifugation at 8000 x g (Heraeus Biofuge Fresco, LabCare, England) for 10 min at 4°C. The cell pellet was washed with deionised water (pH 7.0) and subjected to freezing at -20°C overnight and thawing at 4°C for 2h. Thereafter, the samples were centrifuged at 17000 x g for 30 min and the supernatant collected for further analysis.

Absorbance spectra (200-700 nm) of C-PC were measured using a UV–Vis spectrophotometer (Spectroquant Pharo 300). The extraction purity of C-PC is given by the ratio of A_{620nm}/A_{280nm}, whereby A_{620nm} is the maximum absorbance of C-PC and $A_{280\ nm}$ is the absorbance of total proteins. The concentration of C-PC was calculated using the following equations:

C-PC mg/mL = $\frac{A_{620\ nm} - 0.7\ (A_{652\ nm})}{7.38}$ **Equation 1**

Yield mg/g = $\frac{C-PC\ (mg/mL) * volume\ of\ buffer\ (mL)}{Dry\ cell\ weight\ (g)}$ **Equation 2**

5.2.3 Extraction of Crude C-phycocyanin

5.2.3.1 Experimental design for the screening of extraction parameters

The schematic representation of the overall experimental protocol is shown in Figure 17 and the methods are explained in detail in the subsequent sections. Single-factor experiments were used to determine the preliminary range of the factors investigated. The extraction protocol was firstly optimised for the ideal extraction buffer for C-PC. The buffers investigated included: acetate pH-6.0, potassium phosphate (PPB) pH-7.5, sodium phosphate (SPB) (pH-7.5), phosphate-buffered saline (PBS) pH-7.5, Tris-chloride pH-7.4 and double distilled water (control) (Recipes for buffers in Appendix 10). The pH was adjusted with 0.1 M HCl. The concentration of the selected buffer was varied from 10 mM – 1 M.

Cell lysis was carried out by freezing the cells at different temperatures *viz*., at -196, and -80, and -20°C, and by thawing at 4 and 25°C. The freezing and thawing time was varied from 0.5-24 h. The other factors investigated were biomass: buffer ratio (0.005-0.550 g/mL) and enzyme (lysozyme) concentration (0-0.1 mg/mL). The cell suspension with enzyme was incubated at 37°C in a water bath for 2 h, thereafter the solution was incubated at 4°C. To protect C-PC from photo-denaturation all steps were performed in the dark.

Table 24: Screening of extraction parameters using single-factor experiments

Thawing temperature (°C)	Freezing temperature (°C)	Enzyme Concentration (mg/mL)	Freezing Times (h)	Thawing Times (h)	Biomass: buffer ratio (g: mL)
4	-196	0	1	0.5	0.0050
25	-80	0.1	2	1	0.0100
	-20		4	1.5	0.0150
			6	2	0.0200

5.2.3.2 Optimisation of extraction conditions

Response surface methodology (RSM) was used to optimise the extraction factors *i.e.* thawing temperature, enzyme concentration and biomass-buffer ratio on the C-PC yield and purity. In a 2^3 central composite design (CCD), these factors were varied systematically at high (+1) and low (-1) levels (Table 25). A total of 20 experiments were performed. The order of the experiments was fully randomised. The experimental design, mathematical model and analysis of data were carried out using Design Expert Version 9.0 (Stat-Ease Inc., Minneapolis, Minnesota, USA) statistical software. The accuracy of the model was further tested by conducting confirmation experiments.

C-PC and purity were selected as the responses, which can be calculated using the following general formula:

$$y = \beta_0 + \sum_i^K \beta_I X_i + \sum \sum_{i<j} \beta_{ij} x_i x_j + \in \qquad \textbf{Equation 3}$$

where y is the predicted response, β_0 is the intercept of the plane, βi is the constant coefficient of the equation, and x_i and x_j are coded independent factors, and ϵ is the random error term.

5.2.3.3 Validation of experiments

In order to confirm the reliability of the developed RSM model, the predicted results were compared with the experimental values (actual C-PC yield). The validation experiment which predicted error between the actual and predicted values is very small, which shows a good agreement between the developed RSM model and experimental data.

Table 25: Detailed experimental central composite design with actual values of the three variables tested showing C-PC yield and purity

Std	Run	X_1: Biomass: buffer ratio (g/L)		X_2: Enzyme digestion time (h)		X_3: Freezing time (h)		C-PC yield (mg/g)			C-PC Purity		
		Actual	Coded	Actual	Coded	Actual	Coded	Actual	Predicted	Residual	Actual	Predicted	Residual
1	10	0.020	-1	1	-1	4	-1	29.63	29.00	0.64	1.916	1.92	0.010
2	17	0.035	1	1	-1	4	-1	54.79	54.28	0.51	2.125	2.13	0.008
3	7	0.020	-1	4	1	4	-1	37.06	35.68	1.39	2.001	2.01	0.002
4	13	0.035	1	4	1	4	-1	56.11	54.07	2.04	2.166	2.16	0.004
5	5	0.020	-1	1	-1	6	1	55.92	56.65	-0.73	2.041	2.05	-0.008
6	18	0.035	1	1	-1	6	1	70.53	70.61	0.08	2.125	2.13	-0.042
7	12	0.020	-1	4	1	6	1	58.08	57.28	0.79	2.083	2.07	0.052
8	8	0.035	1	4	1	6	1	65.02	64.35	0.671	2.083	2.09	0.003
9	15	0.015	-1.682	2.5	0	5	0	31.88	32.49	-0.61	1.958	1.96	-0.005
10	4	0.040	1.682	2.5	0	5	0	58.46	59.69	-1.23	2.166	2.16	0.010
11	2	0.028	0	-0.023	-1.682	5	0	56.92	56.49	0.43	2.083	2.07	0.003
12	16	0.028	0	5.023	1.682	5	0	54.57	56.84	-2.08	2.125	2.13	0.0083
13	14	0.028	0	2.5	0	3.318	-1.682	40.57	42.66	-2.28	2.041	2.05	-0.0079
14	20	0.028	0	2.5	0	6.682	1.682	74.79	74.55	-2.39	2.125	2.12	0.0081
15	3	0.028	0	2.5	0	5	0	75.19	71.03	4.16	2.372	2.35	-0.014
16	6	0.028	0	2.5	0	5	0	75.46	71.03	4.43	2.375	2.35	-0.014
17	9	0.028	0	2.5	0	5	0	69.92	71.03	-1.11	2.333	2.35	-0.014
18	1	0.028	0	2.5	0	5	0	69.14	71.03	-1.89	2.374	2.35	-0.014
19	11	0.028	0	2.5	0	5	0	68.75	71.03	-2.28	2.376	2.35	-0.014
20	19	0.028	0	2.5	0	5	0	68.03	71.03	-3.00	2.333	2.35	-0.014

5.2.4 Purification of C-phycocyanin using Precipitation, Activated Charcoal and Ultrafiltration

C-phycocyanin was sequentially precipitated from the crude extract by stepwise addition of finely powdered AR grade $(NH_4)_2SO_4$ (Sigma-Aldrich, South Africa) with continuous stirring for 1 h at 4°C followed by centrifugation at 9500 x g for 20 min (Heraeus Biofuge *fresco,* Germany). The pellet obtained after each centrifugation was re-suspended in SPB (pH 7.0) and analysed using the spectrophotometer. Percentage (%) saturation concentrations of $(NH_4)_2SO_4$ assessed were 0, 10, 20, 30, 40, 50, 60, 70, 80 and 95 % w/v. Percentage (%) saturation concentration of $(NH_4)_2SO_4$ in solution as % of maximum solubility at the given temperature (Wingfield, 2016). The equation used to calculate the % saturation is below:

$(NH_4)_2SO_4$ weight (g/L) = $\frac{Sat\ (M1-M2)}{[SatM-\left(\frac{Vol}{1000}x\ MW\ x\ SatMxM2\right)]}$ **Equation 4**

Sat = number of grams/Liter in a saturated solution of $(NH_4)_2SO_4$,

M_2 = the molarity you want to achieve,

M_1 = starting molarity, SatM = molarity of a saturated solution of $(NH_4)_2SO_4$,

Vol = specific volume of $(NH_4)_2SO_4$, which is the amount of volume 1g will add to an aqueous solution, which is ~0.54 mLs,

MW= the molecular weight of $(NH_4)_2SO_4$ is 132.14.

The modified activated charcoal method was done according to the protocol by (Liao *et al*., 2011). The activated charcoal powder was washed with distilled water, dried in the oven at 60°C until all moisture was removed. Thereafter 10 mg/mL of activated charcoal powder was added to the crude extract of C-PC (pH 7.5) and continuously stirred with a magnetic stirrer every 15 min. The samples were centrifuged (8000 x g, 10 min, 4°C), then the supernatant was dissolved in SPB. The C-PC was concentrated by ultrafiltration using Amicon with MW cut off ~ 50 kD (Millipore, USA).

5.2.4.1 Statistical analyses

Significant differences between the C-PC yield and purity under the different conditions were determined by one-way ANOVA and a Tukey's *post-hoc* test using the GraphPad Prism software version 5.0 (Californa, USA). Values were considered statistically significant when $p < 0.05$.

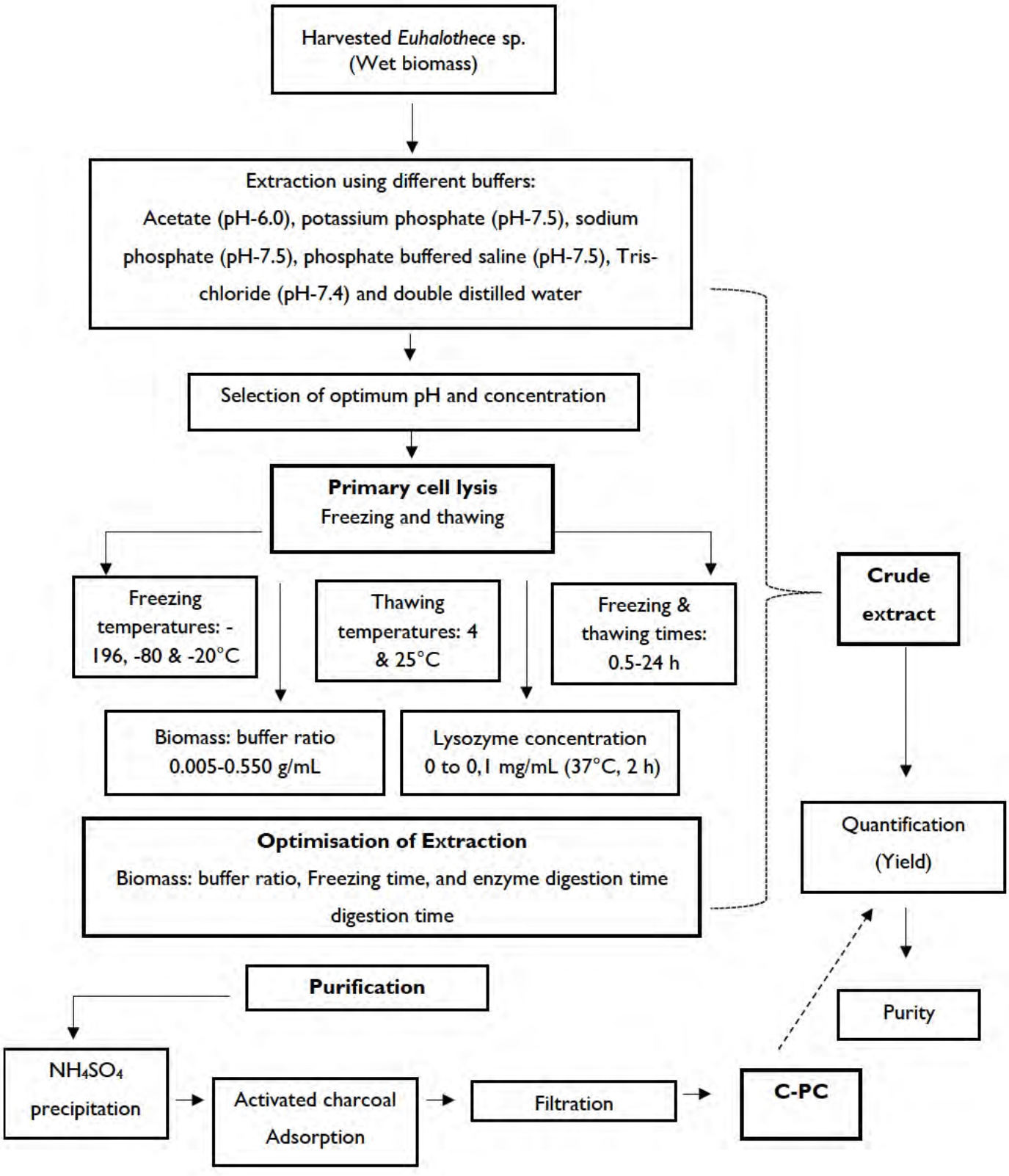

Figure 17: The schematic representation of the overall experimental protocol.

5.3 RESULTS AND DISCUSSION

5.3.1 Screening of Extraction Parameters Using a One-Factor-At-A-Time Approach

5.3.1.1 Selection of suitable buffer

In this study, the preliminary one-factor-at-a-time approach was adopted to investigate which factors played a significant role in the extraction of C-PC. Several factors such as buffers, temperature, pH and lysis method are known to influence C-PC extraction (Silveira *et al.*, 2007). Since C-PC is water-soluble, deionised water could be used. There was no statistically significant difference ($p > 0.05$) in the C-PC yield when comparing the control *i.e.* ultrapure water (18.2 MΩ) to the phosphate buffers (SPB, PPB and PBS).

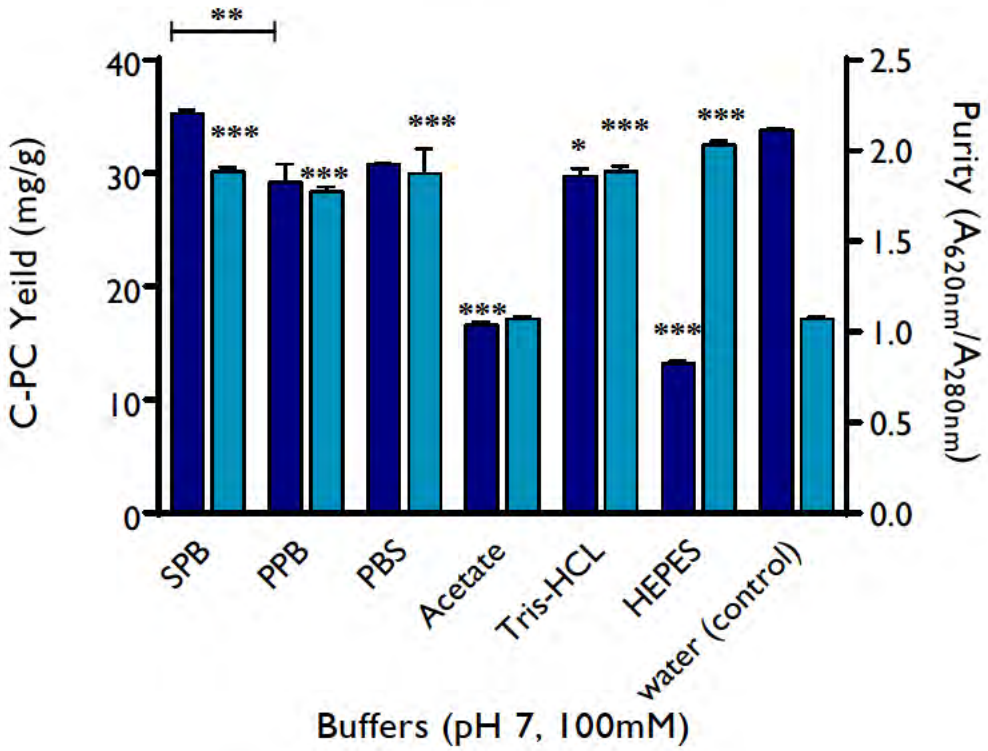

Figure 18: Yield (●) and purity (■) C-PC extracted using six different buffers *i.e.* acetate, potassium phosphate, sodium phosphate, phosphate-buffered saline, Tris-chloride and double distilled water (100 mM pH 7.5±2) Asterisks indicate significant differences between control and variables ($p < 0.05$). The number of * indicates the level of significance. Error bars indicate standard deviations of the means ($n = 3$).

This was probably due to mechanical disruption of cells of freezing which caused the release of the C-PC However, amongst the phosphate buffers, sodium phosphate buffer resulted in significantly higher C-PC yield (35.32 mg/g) ($p < 0.05$). Nevertheless, when analysing the purity, a significantly lower C-PC purity *i.e.* 1.074 ($p < 0.05$) compared to the buffers investigated was achieved in the ultrapure water (18.2 MΩ) owing to increased impurities that flowed into the water during extraction (Figure 18). Phosphate buffers have been reported to be a suitable buffer for extraction of PBPs, ensuring that proteins are not denatured due to a shift in pH (Kamble *et al*., 2012; Ramos *et al*., 2010; Silveira *et al*., 2007; Sudhakar *et al*., 2015).

5.3.1.2 Effect of buffer pH and concentration on C-PC extraction

Since PBS are assembled in subunits composed of trimers of PBPs, pH control helps to maintain the aggregation of PBPs and prevent dissociation of monomers, trimers or hexamers, in solution (Sun *et al*., 2009). Sua *et al*. (2014) reported that a higher pH increases the extraction rate and equilibrate concentration, while a lower pH leads to protein denaturation. C-phycocyanin has isoelectric point (pI) value of 4.1- 6.4, pH value in which there is a balance between the positive and negative charges of the ionic groups of a protein (Jiang *et al*., 2017).

The maximum yield and purity of C-PC were extracted when using SPB with a pH range between 6.0 and 8.0 (Figure 19). When comparing the C-PC yield and purity at pH 6.0, 7.0 and 8.0, there was no significant difference ($p > 0.05$). A significant decrease in C-PC yield was found at pH 5.0 and 9.0 ($p < 0.05$). Similarly, Hemlata *et al*. (2011) showed that the C-PC extracted using a pH 7.0 SPB remained stable for several weeks at 4°C. Extreme changes in pH cause a disturbance of electrostatic properties and hydrogen bonds involved in protein association that can induce changes in chromophore structure (Liu *et al*., 2009).

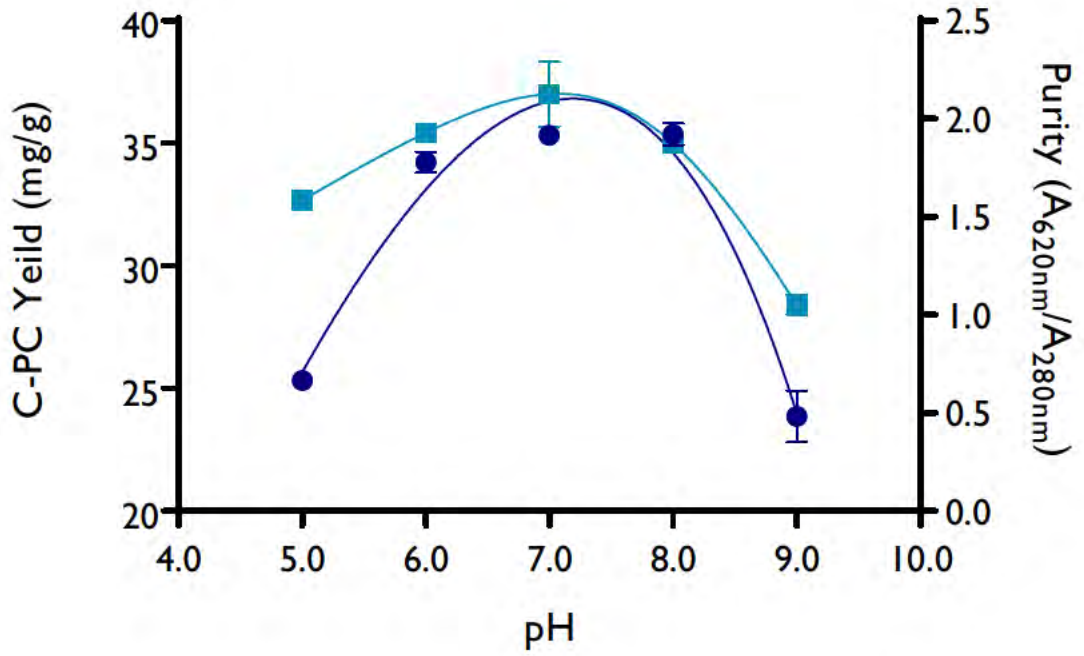

Figure 19: Yield (●) and purity (■) C-PC extracted using 100 mM sodium phosphate buffer with varying pH values (5.0-9.0), Error bars indicate standard deviations of the means (n = 3).

Moreover, the solubility of compounds is directly dependent on the pH. Near pI, proteins interact less in water, reducing the extraction amounts. Thus, pH and ionic strength similar to intracellular conditions could lead to improved extraction. An increase in ionic strength from 50 mM up to 1 M, did not show a significant increase in the C-PC purity or yield. There was a significant decrease ($p < 0.05$) in C-PC yield when the lowest concentration (10 mM) of SPB was used for extraction Figure 20. Thus, 50 mM was the optimal concentration for SPB. At a low ionic concentration, there was a significant decrease ($p < 0.05$) in C-PC yield whereas an increase in ionic strength from 50 mM up to 1 M, did not have a significant effect or effect on the C-PC or yield, thus 50 mM was considered to be the optimal buffer concentration. Similarly, Furuki *et al.* (2003) reported that phosphate buffer at low concentrations *i.e.* < 0.1 M dissociates PBS and can maintain the pH value at 7.0. In addition, using a dilute phosphate buffer for extraction, the resulting osmotic shock can cause the breakage of cell walls (Sekar & Chandramohan, 2008).

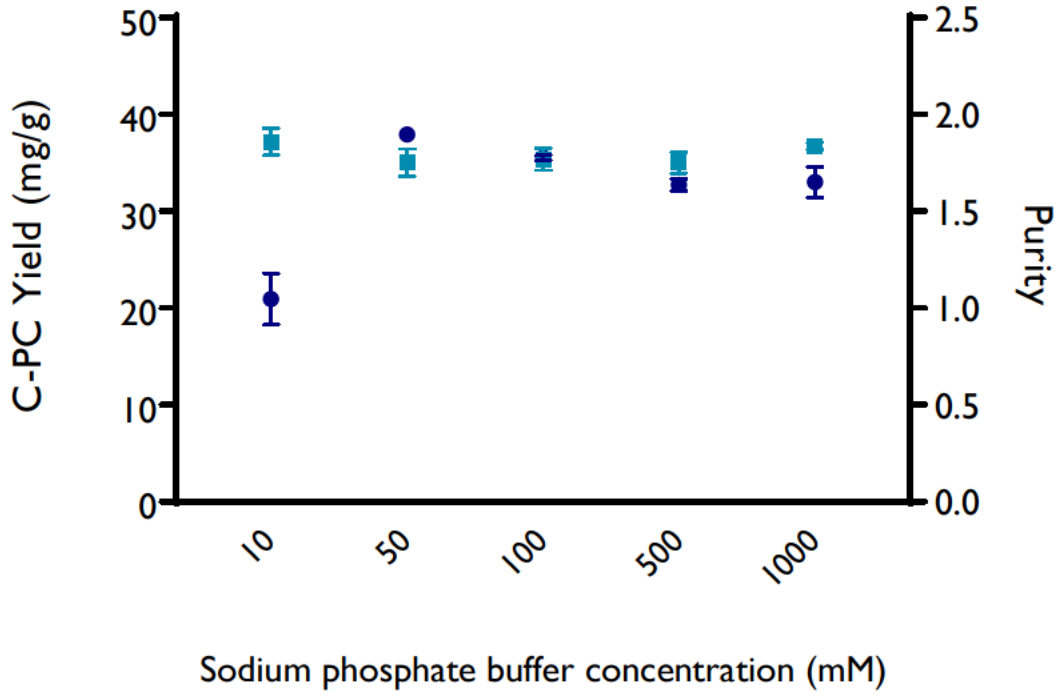

Figure 20: Yield (●) and purity (■ C-PC extracted phosphate at varying concentrations. Error bars indicate standard deviations of the means (n = 3).

5.3.1.3 Effect of freezing and thawing on C-PC extraction

Freeze-thawing uses the effect of ice crystal formation in the cells during the freezing process. When cells are frozen, there is inevitable intracellular ice formation, resulting in damage to the cell, promoting a better extraction of intracellular substances (Moraes *et al.*, 2011). Cell lysis achieved by rapid freezing at -196°C, resulted in the significantly lower yield and purity of C-PC ($p < 0.05$) Martínez-Maqueda *et al.* (2013) reported that cells in liquid nitrogen results in ice crystal formation in the outer parts of cells, which causes the interior of the cells to expand, pushing against the plasma membrane until the cell bursts. A combination of three freezing temperatures (-196, -80 and -20°C) and two thawing temperatures (4 and 25°C) was investigated. Results of this study indicated that low freezing temperatures resulted in the least amount of C-PC being extracted as well as a lower purity due to rapid freezing. Slow cooling allows water to leach out and reduce ice crystal formation, however, it can also cause cell rupture due to an imbalance in osmotic pressure. Freezing and thawing at -20 and 4°C

proved to be the most effective temperatures for lysing the cyanobacterial cells. This could be as a result of its peripheral position in PBS on the thylakoid membrane which may attribute to its sensitivity to temperature (Chaiklahan *et al*., 2011).

Table 26: Effect of varying freezing and thawing temperatures on C-PC yield and purity

Freezing temperature (˚C)	**Thawing temperature (˚C)**			
	4		25	
	C-PC Yield (mg/g)	Purity	C-PC Yield (mg/g)	Purity
-196	22.23 ±0.47	1.19±0.34	18.77±0.13	1.06±1.03
-80	26.85±0.44	1.27±0.54	24.73 ±0.05	1.18 ±1.01
-20	37.16±0.23	1.93 ±0.58	34.37± 1.08	1.81±1.02

This finding is consistent with other studies by Soni *et al*. (2006) and Singh *et al*. (2012) who reported higher C-PC yield when subjecting the cyanobacterial cells to repeated FT cycles of -25 and 4°C and -30 and 4°C respectively. Minkova *et al*. (2007) also reported on the efficiency of the FT method using *A. fusiformis* cells which were frozen at −15°C, heated at 30°C for 1 h, and incubated overnight at 4°C. A significantly lower PC yield ($p < 0.05$) was evident at 25˚C, due to the sensitivity of C-PC to elevated temperature. Additionally, more variability of C-PC yield was observed in the samples extracted at 25°C than the samples extracted at 4°C. These results were similar to the studies by Sarada *et al*. (1999) where they have related the variation in C-PC extraction to uncontrollable fluctuations in room temperature. Overall results indicated that slow freezing at -20 and thawing at 4°C was the best combination,

Using SPB, the freezing times were tested from 1 to 24 h. The yield of the C-PC ranging from 17.62 to 46.58 mg/g and the purity of the C-PC ranging from 1.5 to 2.5 is displayed in Figure 21. The C-PC yield increased with an increase in freezing time up to 4 h, followed by a decrease in C-PC yield, thereafter the yield remained constant with no significant difference ($p < 0.05$) from 8 to 24 h. The purity of C-PC was highest when the cells were frozen for 4 h, thereafter it started to decrease. This infers that freezing for 4 h is enough time to lyse the *Euhalothece* sp. cell walls and extract most of the C-PC. A longer freezing time partially denatures C-PC (Seo *et al*., 2013). Therefore, the optimal freezing time to obtain maximum C-CP yield and purity was between 4-6 h.

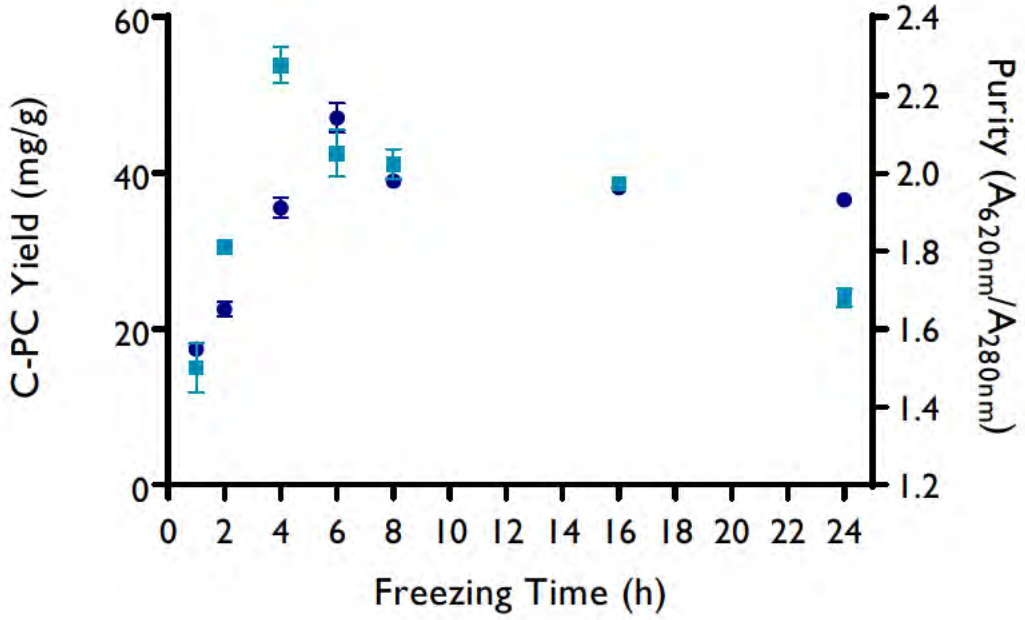

Figure 21: C-phycocyanin yield (●)and purity (■) with varying freezing times from 1 to 24 h.. Error bars indicate standard deviations of the means (n = 3).

It can be seen from Figure 22 that with an increase in thawing time, the yield of C-PC increased, and then gradually stabilised. A minimum thawing for 4 h at 4°C is required for recovery of maximum C-PC yield (41.41 mg/g). Tukey's *post-hoc* analysis showed that there was no significant difference in the C-PC yield and purity after 4 h. however, a significantly lower C-PC yield was found when samples were thawed for < 2h ($p < 0.05$).

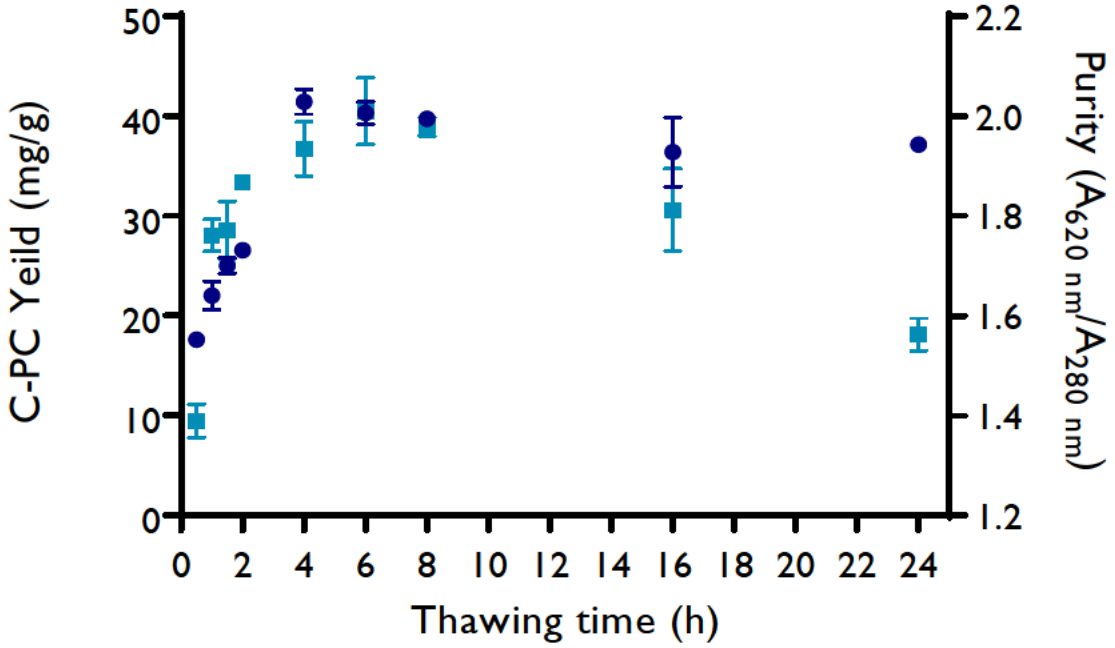

Figure 22: C-phycocyanin yield (●)and purity (■) with varying thawing times from 0.5 to 24 h. Error bars indicate standard deviations of the means (*n* = 3).

5.3.1.4 Effect of biomass: buffer ratio on C-PC extraction

Cuellar-Bermudez *et al.* (2015) reported that a low extraction buffer volume was insufficient to extract the C-PC from the cells completely. However, a larger buffer volume resulted in more impurities been released from the cell. This inhibits the C-PC dissolution and decreases the purity of the C-PC. Our results agreed and showed that increasing the biomass-buffer ratio increases the C-PC yield. A higher biomass concentration contained more cells thus, a higher C-PC content, therefore increasing the biomass-buffer ratio increased the C-PC yield. The highest extraction yield and purity for both were achieved when the biomass-buffer ratio was 0.0300 g/mL Figure 23. More importantly, less buffer can reduce the extraction cost and decrease time consumption for separation.

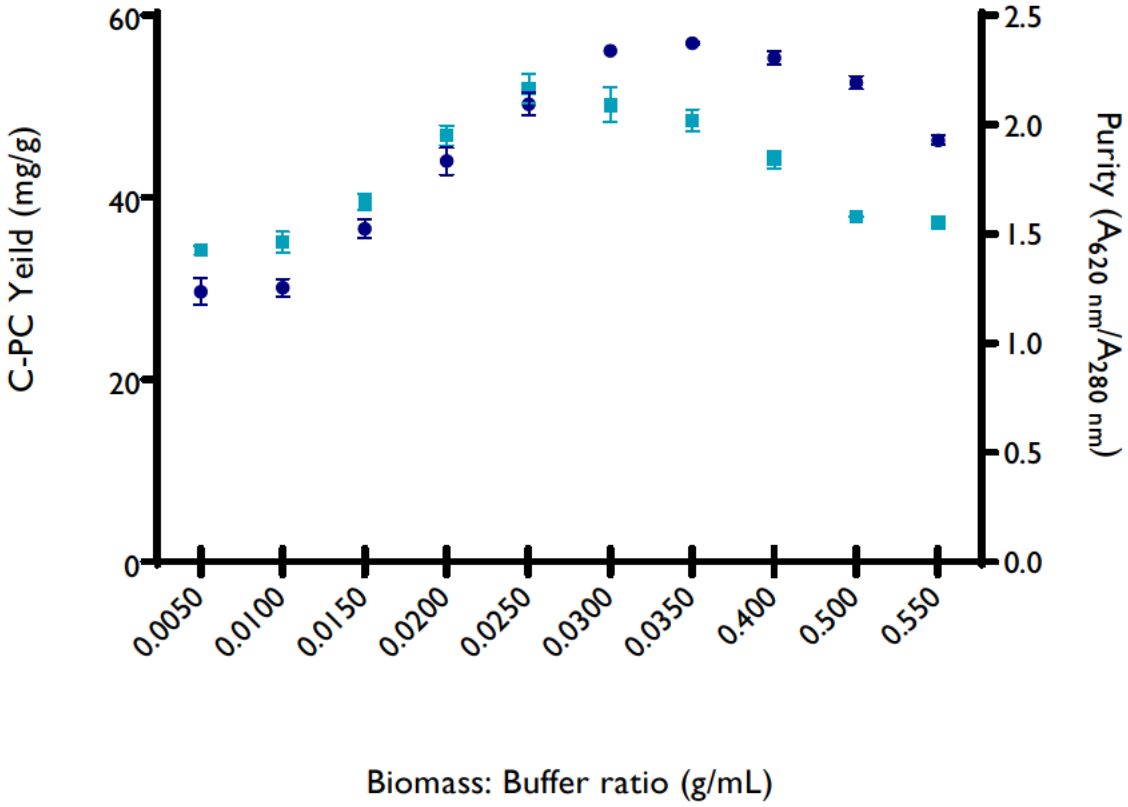

Figure 23: C-phycocyanin yield ( )and purity ( ) with varying biomass-buffer ratios. Error bars indicate standard deviations of the means (n = 3).

5.3.1.5 Effect of lysozyme on C-PC extraction

The freeze-thaw method is an effective method to break the cell wall and extract high C-PC yield, however depending on the cell wall, sometimes the method is not effective enough to lyse the cells. Therefore, the use of enzymes *viz*., lysozyme could be used to improve digestion of the cell wall to a greater extent. The efficiency of the lysozyme treatment on C-PC extraction was monitored at different concentration (Figure 24). It can clearly be seen that the use of lysozyme increased C-PC yield, however, the concentration of lysozyme did not have a significant effect on C-PC yield ($p > 0.05$). Therefore, the lowest concentration (0.0025 mg/mL) of the enzyme was chosen since a lower enzyme concentration will overall cost less. By adding the lysozyme to SPB, the cells (0.0250 g/mL) were effectively lysed releasing all the C-PC into the solution, thus a second freeze-thaw cycle was not necessary. Gupta & Sainis

(2009) reported that *Anacystis nidulans* BD1 appeared to be more susceptible to lysozyme treatment compared to *Synechococcus* 7942 and *Synechocystis* 6803 strains.

Lysozymes, also known as muramidase or N-acetylmuramide glycanhydrolase, are glycoside hydrolases. These enzymes damage bacterial cell walls by catalysing the hydrolysis of 1,4-beta-linkages between N-acetylmuramic acid and N-acetyl-D-glucosamine residues in a peptidoglycan and between N-acetyl-D-glucosamine residues in chitodextrins. Large amounts of lysozyme can be found in egg white and its price range from 0.1 to 20 g per US$ depending on quality (Yoshimura *et al.*, 1988). Lysozymes break the algal cell walls gently and efficiently and are potentially suitable for the large-scale industrial extraction of the C-PC. However, use of this enzyme can be expensive and releases unpleasant odours (Singh *et al.*, 2009b).

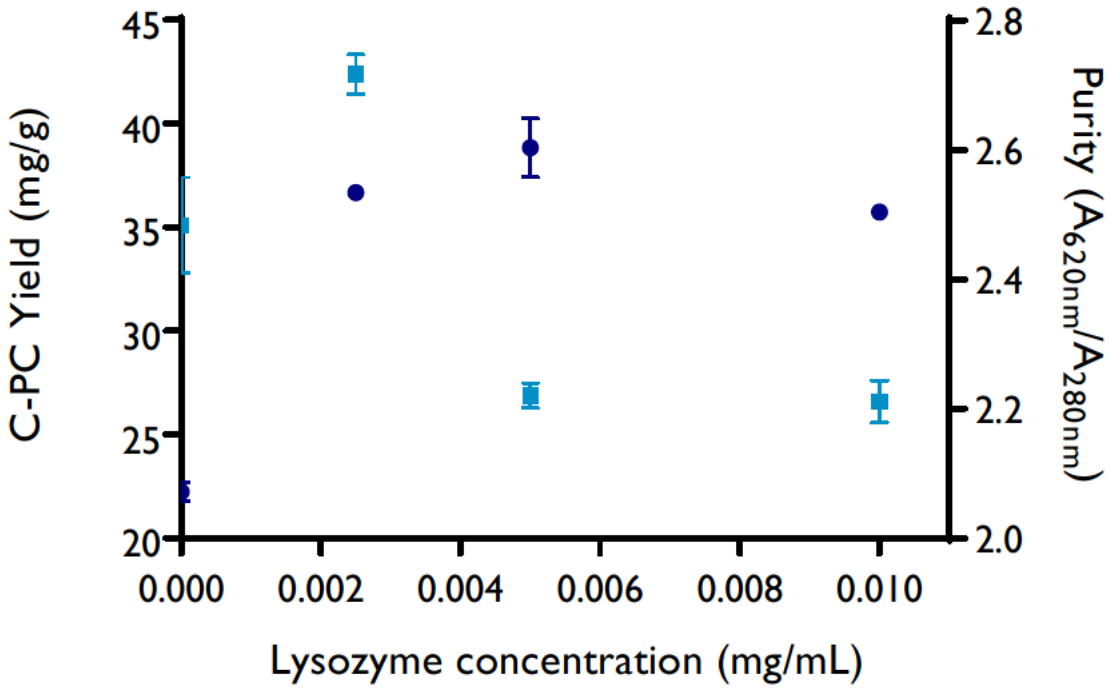

Figure 24: C-phycocyanin yield (●)and purity (■)with varying lysozyme concentrations (white square, purity and black circle is yield). Error bars indicate standard deviations of the means (n = 3).

5.3.2 Optimisation of C-phycocyanin using Response Surface Methodology

Based on the single factor experiments, the optimum conditions used for C-PC extractions were freezing the cells at -20°C for 4 h and thawing cells at 4°C in SPB (50 mM of pH 7). In addition, freezing time, biomass-buffer ratio and lysozyme concentration were also contributed to high yield and purity. Thus, response surface methodology (RSM) was used to estimate the effect of independent factors, (X_1) biomass-buffer ratio, enzyme digestion time (X_2) and freezing time (X_3) on the C-PC yield and purity. The central composite design was chosen to study the interactions among the three factors and to determine the optimal level of each of the factors required for maximum C-PC yield and purity in *Euhalothece* sp.

The mathematical model relating to the yield and purity of C-PC are described in Equation 5 and 6 respectively. The equation provides an estimate of the level of C-PC (Y) as a function of biomass: buffer ratio (X_1), freezing time (X_2) and enzyme digestion time (X_3). The C-PC yield response equation from the above set of experiments can be written as:

C-PC (mg/g) = 71.0293 + 8.08753 * X_1 + 0.105258 * X_2 + 9.48221 *X_3 +optimum -1.7212 * X_1X_2 + -2.83106 * X_1X_3 + -1.51245 * X_2X_3 + -8.81802 * X_1^2 + -5.07852 * X_2^2 + -4.39293 * X_3^2 **Equation 5**

While, the purity response equation from the above set of experiments can be written as:

Purity = 2.36107 + 0.0592162 * X_1 + 0.014284 * X_2 + 0.0194151 * X_3 + -0.015625 * X_1X_2 + -0.0364583 * X_1X_3 + -0.015625 * X_2X_3 + -0.105316 * X_1^2 + -0.0905851 * X_2^2 + -0.0979508 * X_3^2 **Equation 6**

Analysis of variance (ANOVA) of C-PC yield and purity which also including the main effect of the factors, regression coefficient, F values, and p values of factors are shown in Table 27 and Table 28 respectively. The model F values of 54.93 for C-PC yield and 42,23 for purity implies that both design models are significant and there is only 0.01% chance that this large value could occur due to noise; in addition, both pre-determined R^2 values were in reasonable agreement with the adjusted R^2 values. C-PC yield results indicated that biomass: buffer ratio (X_1) and freezing time (X_3); interactions between X_1X_3, and X_1^2, X_2^2, X_3^2 were significant model terms ($p < 0.005$), whereas for purity results, all three factors were significant model terms. The interactions between X_1X_2, X_1X_3 X_2X_3 were also found to be significant model

terms. The predicted optimised factors for maximum C-PC yield and high purity *i.e.* 0.030 g of biomass, 5.33 h freeze time and 2.4 h lysozyme digestion.

Table 27: Analysis of variance for the response surface model for C-PC yield

Source	**Sum of Squares**	**df**	**Mean Square**	**F-value**	***p*-value**	
Model	3749.62	9	416.62	54.93	< 0.0001	Significant
A-biomass:buffer ratio	893.27	1	893.27	117.77	< 0.0001	
B-lysozyme digestion time	0.1513	1	0.1513	0.0199	0.8905	
C-freeze thaw	1227.92	1	1227.92	161.89	< 0.0001	
AB	23.70	1	23.70	3.12	0.1076	
AC	64.12	1	64.12	8.45	0.0156	
BC	18.30	1	18.30	2.41	0.1514	
A^2	1120.59	1	1120.59	147.74	< 0.0001	
B^2	371.69	1	371.69	49.00	< 0.0001	
C^2	278.11	1	278.11	36.67	0.0001	
Residual	75.85	10	7.58			
Lack of Fit	20.03	5	4.01	0.3589	0.8574	not significant
Pure Error	55.82	5	11.16			
Cor Total	3825.47	19				

Table 28: Analysis of variance [TYPE III] for quadratic model for C-PC purity

Source	Sum of Squares	df	Mean Square	F-value	*p*-value	
Model	0.3577	9	0.0397	42.23	< 0.0001	significant
A-biomass: buffer ratio	0.0479	1	0.0479	50.89	< 0.0001	
B-lysozyme digestion time	0.0028	1	0.0028	2.96	0.1160	
C-freeze thaw	0.0051	1	0.0051	5.47	0.0414	
AB	0.0020	1	0.0020	2.08	0.1802	
AC	0.0106	1	0.0106	11.30	0.0072	
BC	0.0020	1	0.0020	2.08	0.1802	
A^2	0.1338	1	0.1338	142.15	< 0.0001	
B^2	0.0960	1	0.0960	102.00	< 0.0001	
C^2	0.1141	1	0.1141	121.24	< 0.0001	
Residual	0.0094	10	0.0009			
Lack of Fit	0.0006	5	0.0001	0.0682	0.9948	not significant
Pure Error	0.0088	5	0.0018			
Cor Total	0.3671	19				

The contour plots of regression equations provide a crucial contribution to understanding the interactions amongst factors and finding their optimum levels (Myers & Montgomery, 1995). The association between biomass-buffer ratio and freezing time, an increase both in biomass: buffer ratio and freezing time resulted in higher C-PC yield can be seen in Figure 25A. The significant interaction between freezing time and biomass concentration for purity can be observed in Figure 26C. When biomass was 0.029 g, an increase in freezing time resulted in an increase in purity up to a limited degree, however, a further increase in this ratio resulted in a consequent drop in purity. Cuellar-Bermudez *et al.* (2015) described that a low volume of extraction buffer is insufficient to completely extract the C-PC from the cells. Whereas, too much buffer results in more impurities been released from the cell, which inhibits the C-PC dissolution and decreases the purity of the C-PC. Our results were in agreement with the above observations showing that increasing the biomass-buffer ratio increases the C-PC yield, with the highest extraction yield and purity been achieved when the biomass-buffer ratio was 0.0300 g/mL. More importantly, less buffer can reduce the extraction cost and decrease time consumption for separation. Seo *et al.* (2013) found that too long

freezing time partially denatures C-PC. This infers that freezing for 5 h was sufficient time to lyse the *Euhalothece* sp. cell walls and extract the highest purity of crude C-PC.

A similar pattern was observed when the freezing time was 5 h and lysozyme digestion time increased from 2 to 4 h (Figure 25C). The use of enzymes *viz*., lysozyme could be used to improve digestion of the cell wall to a greater extent. It can clearly be seen that the use of lysozyme (0.0025 mg/mL) increased C-PC yield. By adding the lysozyme to SPB, the cells were effectively lysed releasing all the C-PC into the solution, thus a second freeze-thaw cycle was not necessary. The predicted optimised factors for maximum C-PC yield and high purity were 0.030 g of biomass, 5.33 h freeze time and 2.4 h lysozyme digestion.

The combined factors were analysed by performing validation experiments in triplicates. The validation experiment for C-PC and purity was found to be 75 mg/g and 2.4 respectively, which was in close agreement with the predicted values suggesting that Equation 5 and 6 were valid for predicting the C-PC yield and purity (Appendix 11).

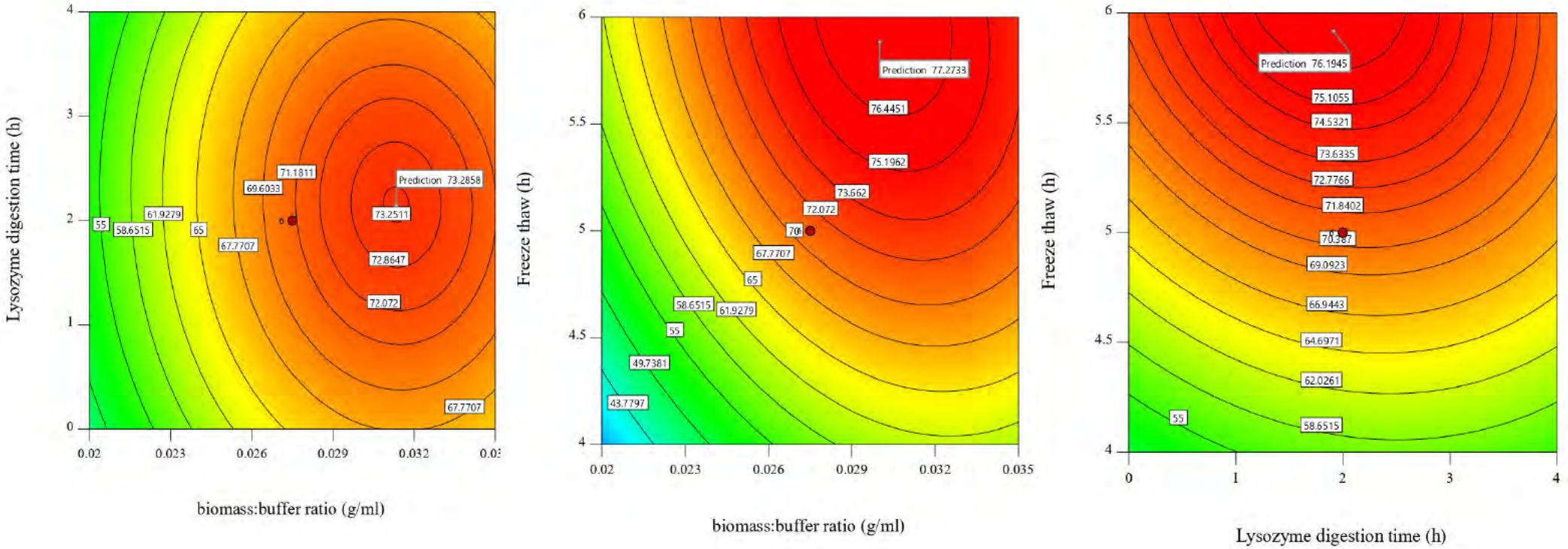

Figure 25: Response surface contour plots for the interactions between different significant selected factors (A) lysozyme digestion time and biomass: buffer ratio ($p < 0.05$), while the freezing time is kept constant, (B) freezing time and biomass: buffer ratio ($p < 0.05$) while lysozyme digestion time was kept at a constant level, and (C) lysozyme digestion time and freeze time ($p > 0.05$) on C-PC yield.

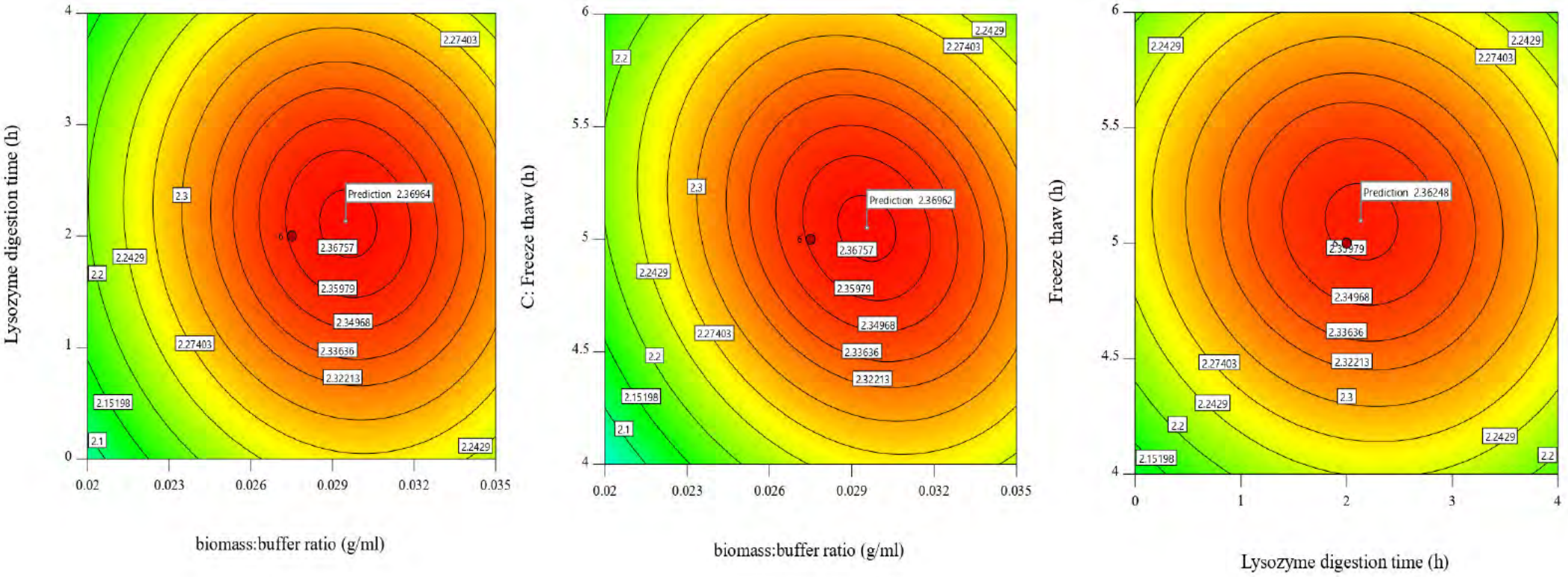

Figure 26: Response surface contour plots for the interactions between different significant selected factors (A) lysozyme digestion time and biomass: buffer ration while the freezing time is kept constant (B) freezing time and biomass: buffer ratio while lysozyme digestion time was kept at a constant level ($p < 0.05$) and (C) lysozyme digestion time and freeze time on C-PC purity.

5.3.3 Purification of C-phycocyanin Using Simple Techniques

5.3.3.1 Precipitation of C-phycocyanin

The cost of the downstream process is dependent on the purification steps employed to achieve the desired purity. Thus, to improve the economics, minimal capital investment and consumables are required (Ruiz-Ruiz *et al*., 2013). Ammonium sulphate precipitation is a simple and cheap method that can be applied to a large-scale and requires basic equipment (Silva *et al*., 2009). The effectiveness of different salts used for precipitation relies on the Hofmeister series. Based on previous literature the effectiveness of the salts was shown to be sulphate > phosphate > chloride (Manirafasha *et al*., 2017; Wingfield, 2001; Zhang, 2012). Moreover, $(NH_4)_2SO_4$ is considered more efficient in comparison to other precipitating agents since it helps to maintain the integrity of protein and found to readily precipitate C-PC (Wingfield, 2001). Report by Soni *et al.* (2006) have shown that it is also highly water-soluble a low temperature, has a bacteriostatic effect and helps to reduce the quantity of sample handling

The effect of varying $(NH_4)_2SO_4$ concentrations (in terms of percentage saturation) on C-PC purification was examined. Addition of 20 and 30% $(NH_4)_2SO_4$ did not result in precipitation of C-PC and thus ±100% of C-PC was still retained in the supernatant. The C-PC began to precipitate when the concentration of $(NH_4)_2SO_4$ increased up to 40%. Furthermore, the highest C-PC purity of 3.5 was observed at 40%. At 60% $(NH_4)_2SO_4$ concentration, the majority of the C-PC was precipitated, but the purity of the precipitate decreased with increasing concentration of $(NH_4)_2SO_4$ (Figure 27). Similarly, Chen *et al.* (2017) reported at higher $(NH_4)_2SO_4$ concentration there could be simultaneous precipitation of other proteins or impurities. In this study in order to recover maximum C-PC, a two-step $(NH_4)_2SO_4$ fractionation was adopted. The first step in the precipitation was with 30% saturated $(NH_4)_2SO_4$ which mainly precipitated unwanted proteins with an improvement in the purity from 2.5 to 3.1. This was then followed by fractionation with 60% $(NH_4)_2SO4$ which resulted in > 80% of C-PC being recovered (Table 32).

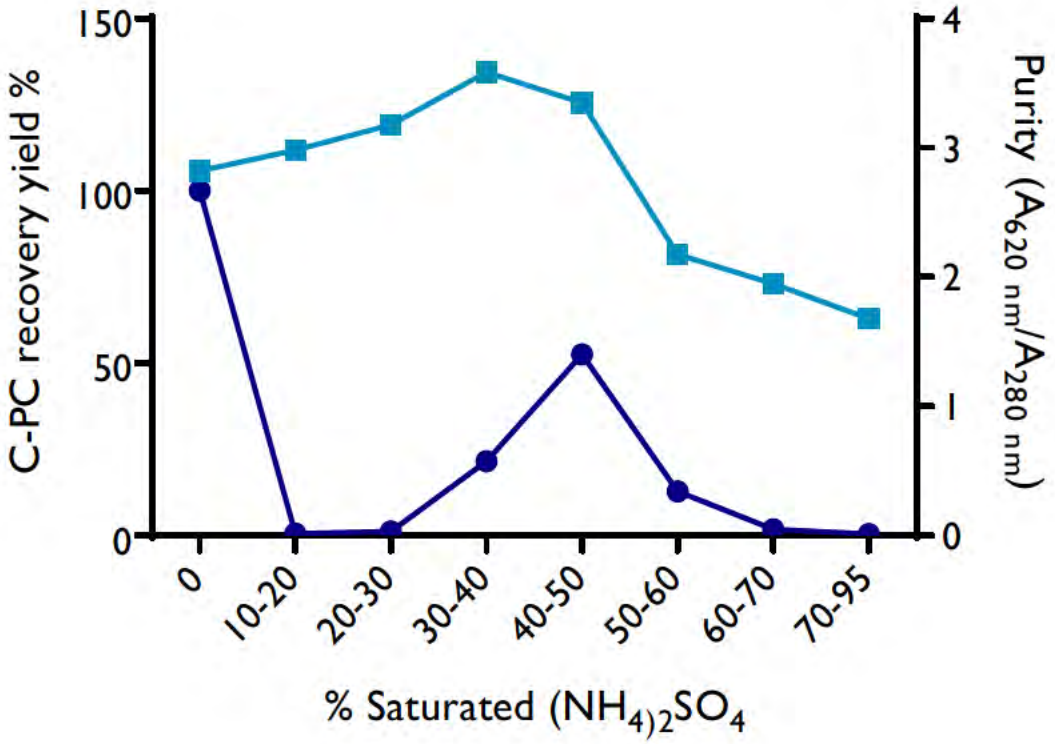

Figure 27: C-Phycocyanin recovery yield (●) and purity (■) at different ammonium sulphate saturation concentrations.

5.3.3.2 Activated charcoal adsorption

Activated charcoal powder has a high specific surface area, fine pore structure, low cost, and does not affect the bioactivity of the extract. The addition of activated charcoal to the C-PC solution results in a gradual decrease in the yield of C-PC. It can be seen in Figure 28, that 8.0% w/v activated charcoal resulted in the highest C-PC purity, however, a significant decrease in C-PC yield was found ($p < 0.05$). Similarly, Fekrat *et al.* (2019) found that maximum C-PC purity and yield of 3.14 and 0.27 mg/mL from *A. platensis* were attained under the optimisation conditions of 0.24% w/v chitosan, 8.4% w/v activated charcoal, and 10.2 min stirring time).

Whereas, Safaei *et al.* (2019) reported a higher concentration of 12.0% activated charcoal resulted in the maximum purity and yield of C-PC (0.065 mg/mL) from *Limnothrix* sp. Pan-utai & lamtham, (2019) reported a purity index of 1.2 and C-PC yield of ~80%, when using activated charcoal (70–80 g/L for 24 h) for purification. Patil *et al.* (2006) used charcoal–chitosan adsorption and aqueous two-phase extraction for purification of C-PC from *S.*

platensis and reported a high purity of 3.96. It has a low binding capacity for high molecular weight polymers thus provides excellent recoveries when employed for the purification of higher molecular weight proteins (Stone & Kozlov, 2014). Furthermore, by using the differences insolubility, a further separation of substances from each other become possible.

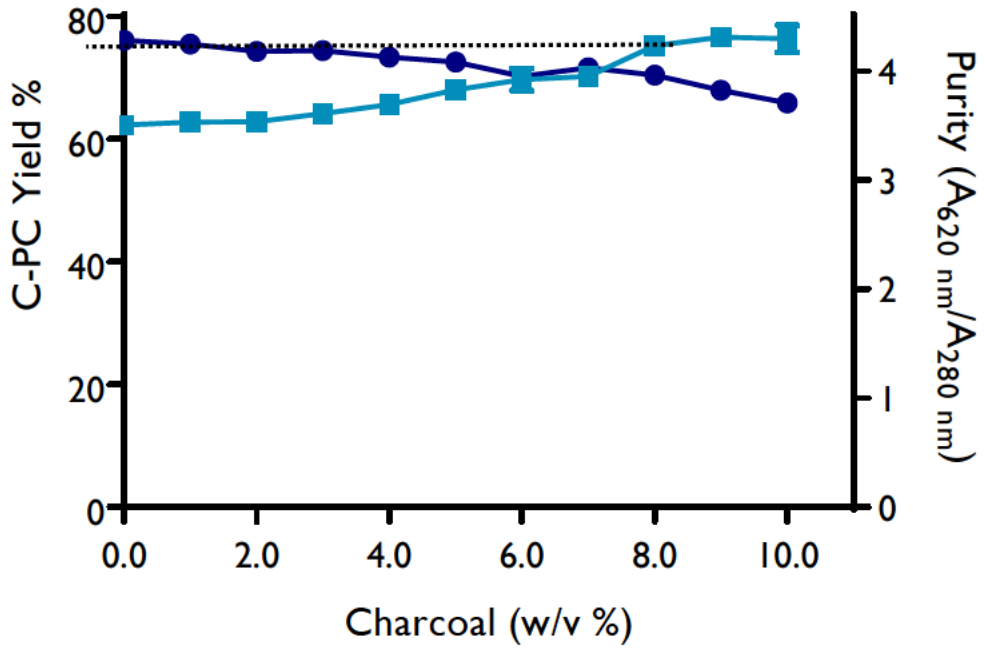

Figure 28: C-Phycocyanin recovery yield (●) and purity (■) at different ammonium sulphate saturation concentrations.

Thus 6.0% w/v was chosen as the optimal concentration for high purity and maximum C-PC yield. Factors reported influencing the separation of lower molecular weight (LMW) proteins include protein size and effective charge. Activated carbon was reported to have its highest binding capacity for the LMW proteins when the solution pH was closest to their pI (Stone & Kozlov, 2014). Therefore, to ensure the removal of the small-sized impurities, the pH value of the activated charcoal used was far from the pI of C-PC. Thus. owing to the adsorption of other low-molecular-weight proteins by the activated charcoal, the solution resulted in a bright blue colour. The remaining debris and impurities in the solution were efficiently removed by UF. This also resulted in an improvement in the overall purity (3.8) of the extracted C-PC.

Ultrafiltration is a membrane separation process used extensively in protein separation, which possesses several characteristics that ensure minimum denaturation, deactivation, and /or degradation of highly labile biological products. When ammonium sulphate fractionation was combined with other methods, *i.e.* activated charcoal and ultrafiltration C-PC could be recovered with a purity of 4 and recovery of up to 60% of the amount of C-PC originally present in the crude extract (Table 29). By using the optimised extraction and purification method analytical grade C-PC was recovered. It just took about <10 h to finish the entire process while the traditional method takes 4-5 days. Moreover, this method uses activated carbon which is cheap to purify the C-PC and need less equipment to produce C-PC.

Table 29: Phycocyanin recovery and purity at different purification methods

	Steps	**Volume mL**	**C-PC % recovered**	**C-PC mg/mL**	**Purity**
1	Crude protein	100	100	146	2.5
2	Ammonium sulphate fraction (0-30 and 30-60%)	20	71	397	3.5
3	Activated charcoal (6% w/v)	20	51	197	3.8
4	Combined activated charcoal + AS precipitation	20	82	319	4.5
5	Ultrafiltration	10	61	472	5.0

It has been established that C-PC with a purity ratio of 4 and above is of analytical grade (Gantar *et al*. 2012). Owing to the relatively high purity of the crude extract, a high-quality C-PC was obtained without the use of chromatography. This will significantly reduce the cost of C-PC production and would increase commercial value. The crude extract and purified C-PC fractions at each step were analysed using SDS-PAGE (Figure 29). C-Phycocyanin is made up of two dissimilar polypeptide chains namely *α*- and *β*-subunit, confirmed by the SDS–PAGE analysis. This data indicated that the purified C-PC was trimer (*αβ*)3. With the current optimised purification procedure, the purity ratio (A_{620nm}/A_{280nm}) achieved was 5, therefore the C-PC is considered pure for biochemical studies and fluorescent label applications.

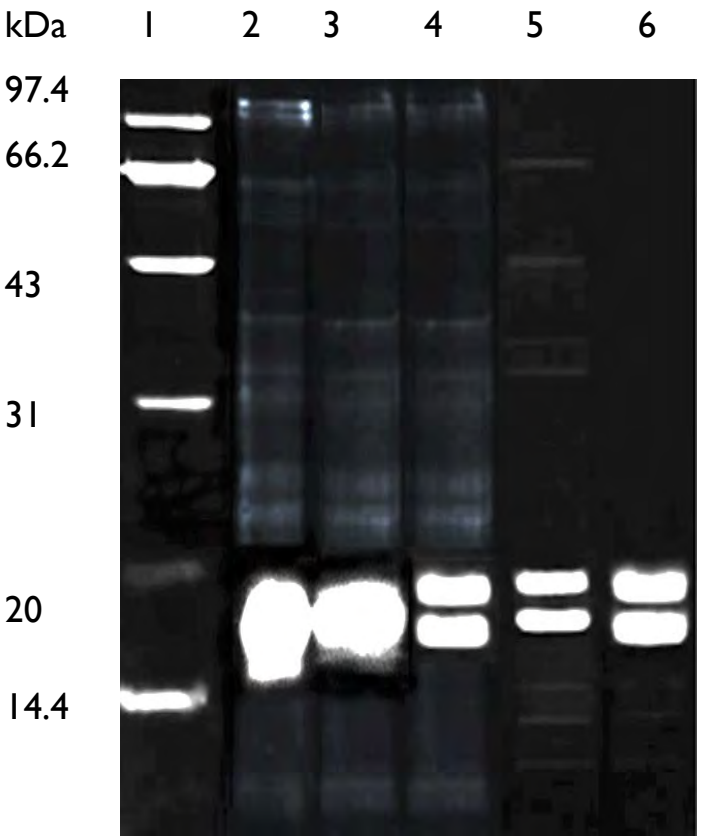

Figure 29: SDS-PAGE analysis of C-PC during different steps of purification. Lane 1: molecular standard. Lane 2: crude PC. Lane 3: 30-60% ammonium sulphate precipitation. Lane 4: activated charcoal+ precipitation. Lane 6: PC dialysed. The molecular weights of subunits *α* and *β* correspond to the ~17 and ~20 kDa bands, respectively.

5.4 CONCLUSIONS

In conclusion, the optimised protocol for the extraction and purification of analytical grade C-PC (purity ratio A_{620nm}/A_{280nm} = 5) from *Euhalothece* sp. includes: subjecting biomass (0.03 g/mL) to -20°C for 5h, thereafter re-suspending the cells in 50 mM SPB (pH 7) containing 0.0025 g/mL of lysozyme, incubation of the cell suspension for 2 h at 37°C in a water bath, following incubation at 4°C for at least 4h, thereafter, stepwise precipitation using 20-50% NH_4SO_4, active charcoal adsorption and ultrafiltration. The optimised extraction protocol resulted in high yield (78 mg/g) of analytical grade C-PC. *Euhalothece* sp. and has the potential to be used as a source of valuable C-PC. The extraction and purification strategy described here is considerably efficient to purify analytic grade C-PC and can be scaled up for commercial exploitation.

CHAPTER 6 : CHARACTERISATION OF C-PHYCOCYANIN FROM *EUHALOTHECE* SP.

6.1 INTRODUCTION

It is also important to determine the stability of the purified protein when exposed to different stress conditions such as temperature, pH, oxidation, etc. Denaturation results in disruption of the tertiary structure of proteins which in turn affects the secondary structure leading to the unfolding of the protein. Upon denaturation of the PBP, the covalently attached chromophore undergoes a conformational change, leading to a significant alteration of the absorption spectrum. However, the primary structure of the protein remains unchanged (Hsieh-Lo *et al*., 2019). The unique fluorescence properties of C-PC are due to the presence of covalently linked linear PCB chromophores (Rastogi *et al*., 2015). Exposure of C-PC to different physicochemical stress factors can provide vital insight towards understanding the structural stability of C-PC. Temperature, light, pH and protein concentration are important factors controlling the stability of C-PC (Chaiklahan *et al*., 2012). The application of C-PC in different fields has been hindered by its sensitivity to treatment and storage conditions, which can easily cause denaturation, precipitation, and discolouration. Various preservatives have been evaluated to improve the stability of PBPs based on the down streaming applications (Martelli *et al*., 2014). Preservatives such as citric acid, sodium chloride, and sucrose are mostly used to stabilise and help maintain the thermostability of food-grade C-PC, whereas antimicrobial agent sodium azide (NaN_3) and protein reducing agent dithiothreitol (DTT) are the most commonly used as to enhance the storage stability and maintain the quality of C-PC for analytical purposes (Wu *et al*., 2016b).

Elucidation of the composition and structure of the polypeptides and protein subunits of C-PC is crucial for the characterisation of the compound (Offner *et al*., 1981). Furthermore, the function of a protein is determined by its structure, which depends on the conformation *i.e.* the way in which the protein is folded. C-Phycocyanin structures are composed of two different subunits, *α*- and *β*-, which make up an *αβ* monomer. The *α*-subunit has a molecular weight between 10-19 kDa and *β*-subunit has between 14-21 kDa (Moon *et al*., 2014; Patel *et al*., 2005). The monomers are arranged around a threefold symmetry axis in the trimer $(\alpha\beta)^3$, while two trimers are assembled face to face to form a hexamer (Jiang *et al*., 2001). Thus,

depending on their source, concentration, and isolation conditions, PBPs exist in many forms *in vitro*, mostly as $(\alpha\beta)^3$ and $(\alpha\beta)^6$.

Each *α*- and *β*-subunits of PBPs are covalently attached to cysteines of the apoprotein *via* a thioether bond to C-3 on ring A and in some cases by an additional thioether bond to C-18 on ring D (Ducret *et al*., 1996). Chromophores are generally bound to the polypeptide chain at the conserved position either by one cysteinyl thioester linkage through the vinyl substituents on the pyrrole ring A of the tetrapyrrole or occasionally by two cysteine linkage through the vinyl substituents on the both A and D pyrrole rings (Glazer & Clark, 1986). The properties of light-harvesting of PBPs in photosynthetic cyanobacteria are mainly dependent on chromophore assembly held in well-defined geometries inside the core of proteins. C-phycocyanin carries three phycocyanobilin (PCB) chromophores in the heterodimeric (*αβ*) protomer, at cysteines *α*-84, *β*-84 and *β*-155. The Asp87 residue is a key amino acid that determines the electronic state of the chromophore (Kikuchi *et al*., 2000).

A number of cyanobacteria from marine habitats are capable of producing a high quantity of PBPs (Parmar *et al*., 2011; Singh *et al*., 2015b), However, the knowledge of the structural or functional stability properties of C-PC from marine cyanobacteria is limited (Mishra *et al*., 2010; Pumas *et al*., 2011). This chapter focused on the analysis of the amino acid sequences of each protein and linker peptide, also the secondary structure of each sequence was calculated and compared to the known structures, followed by a comparative analysis of the C-PC tertiary structures. Secondly, the structural and functional integrity (stability) of C-PC isolated from *Euhalothece* sp. to variations in temperatures, pH and an oxidising agent (H_2O_2). Thirdly, the optimal conditions for maintaining stable C-PC and antioxidant potential were investigated. Finally, the use of preservative on the C-PC yield and purity was examined to determine their potential use in the production of fluorescing reagents, cosmeceuticals and other pharmaceutical products.

6.2 MATERIALS AND METHODS

6.2.1 Multiple Sequence Alignments of C-Phycocyanin Amino Acid Sequences

The amino acid sequence of C-PC obtained from the genomic sequence data was analysed with reference to other C-PC by multiple sequence alignment. The amino acid sequences of C-PC subunits and linker proteins of *Euhalothece* sp were analysed and compared using FASTA (https://www.ebi.ac.uk/Tools/sss/fasta/). The amino acid sequences of the α- and β-subunits of the other cyanobacteria were also retrieved from UniProtKB server (https://www.uniprot.org/).

Multiple sequence alignments were performed using the ClustaW package in BioEdit 7.2 with Clustal W (Wang et al., 2014). The Clustal W alignment file was imported into the BoxShade V 3.21 sequence alignment editor (http://sourceforge.net/projects/boxshade/).

6.2.2 *In Silico* Analysis and Homology Modeling of C-Phycocyanin Subunits and Linker Proteins

6.2.2.1 Primary and secondary structure prediction

The primary structure was predicted by online software ProtParam of the Expasy proteomics server, a tool which allows the computation of various physical and chemical parameters (http://www.expasy.org/tools/protparam.html). The physiochemical parameters such as the molecular weight, pI, extinction coefficient, half-life, aliphatic index, amino acid property, instability index, Grand Average of Hydropathicity (GRAVY) were determined. Stability of a protein can be calculated using the aliphatic index according to (Ikai 1980). The aliphatic index values of cyanobacterial proteins were normalised between 0 and 10 to predict the structural stability. The hydropathy value for a protein *i.e.* hydrophilic and hydrophobic properties of each amino acid side chain in a protein was calculated based on a formula developed by (Kyte and Doolittle 1982). Positive hydropathy value was indicative of a polar protein and negative value indicates a non-polar protein.

Additional amino acid sequences were submitted at I-TASSER internet service dedicated to function and binding sites predictions (http://zhang.bioinformatics.ku.edu/I-TASSER/)The

translated protein sequences were analysed for secondary structure prediction. The query sequence was uploaded in an alignment box and the query was submitted to GOR secondary structure prediction method version IV for structural analysis. This method identifies the ten best regions of similarity between the query sequence and each sequence from the search set and sets up a matrix. Thereafter, the "best" regions are then rescored using a scoring matrix and checked to see if some of these initial highest-scoring diagonals can be joined together. Finally, the set of sequences with the highest scores is aligned to the query sequence for graphical display. The structure was predicted and compared with their models. The secondary structure prediction from the amino acid sequence of a protein and their accuracy is typical -70%.

Sequences for the *α*- and *β*-subunits of the C-PC were submitted to the Multiple Em formMotif Elicitation (MEME) available on http://meme-suite.org/tools/meme to predict the sequence motifs(Bailey & Elkan, 1994). MEME discovers novel, ungapped motifs (recurring, fixed-length patterns) the sequences. The maximum width was set as 50 for each motif and the maximum number of motifs was 5.

6.2.2.2 The three-dimensional model of C-Phycocyanin

SWISS-MODEL (http://swissmodel.expasy.org) is a server for automated comparative modelling of three-dimensional (3D) protein structures. Template search with BLAST and HHBlits were performed against the SWISS-MODEL template library. An initial HHblits profile has been built using the procedure outlined in (Remmert *et al.* 2012). For each identified protein template, the template's quality was predicted from features of the target-template alignment. The templates with the highest quality were selected for model building. Models are built based on the target-template alignment using ProMod3, and PROMOD-II (Waterhouse *et al*., 2018). Insertions and deletions were remodelled using a fragment library, and side-chains were then rebuilt. Finally, the geometry of the resulting model is regularised by using a force field (Guex *et al*., 2009). The quaternary structure annotation of the template is used to model the target sequence in its oligomeric form. The method (is based on a supervised machine learning algorithm, Support Vector Machines (SVM), which combines interface conservation, structural clustering, and other template features to provide a quaternary structure quality estimate (QSQE) (Bertoni *et al*., 2017).

6.2.3 Spectral Analysis of C-Phycocyanin

The absorbance spectrum was measured out using the Spectroquant Pharo 300 (Merck, S.A). The C-PC sample (2 mL) was placed in a 10 mm quartz cuvette and measured using sodium phosphate buffer as a blank. The emission spectrum was recorded for the diluted samples of C-PC in a 10 mm quartz cuvette in a Varian Cary Eclipse (Agilent, Santa Clara, CA, USA) fluorometer. Emission was scanned from 600 to 750 nm at 1-nm intervals and 10-nm bandwidth.

6.2.4 Stability Experiments

To determine the thermostability, 3 mL of purified C-PC solution was incubated at different temperatures from 25 to 65°C (intervals of 5°C) in a water bath for 1h. Furthermore, the effect of storage temperatures 4 and 25°C of purified C-PC was also monitored over 42 days. The yield and antioxidant activity were determined.

To assess the effect of pH on C-PC stability, the pH of the solution was adjusted to the desired value (4.0-9.0 ± 0.1) using 100 mM solutions of basic or acidic phosphate buffer. Samples were taken at regular intervals up to 24 h. Based on a previous study by Munier *et al.* (2014) after 1 h incubation, C-PC yield and antioxidant activity were determined for both studies.

To determine the stability of C-PC under oxidative stress, different concentrations of H_2O_2 solutions *i.e.* 0.1, 0.2, 0.4, 0.8 and 1.0% were added to 1 mg/mL of C-PC. After 2 h the yield and antioxidant activity were analysed.

6.2.5 Effect of Stabilising Agents/ Preservatives on C-phycocyanin

The thermal stability of C-PC with the addition of stabilising agents/ preservatives, citric acid (0.4%), 1 mM EDTA + NaN_3 (0.005%), and sodium chloride (20%) were studied. The C-PC samples with and without preservatives were incubated at two temperatures *i.e.* 4 and 25°C. Samples were taken weekly for analysis for up to six weeks.

6.2.6 Antioxidant Assays

6.2.6.1 DPPH assay (2, 2-diphenyl-1-picrylhydrazyl)

The radical scavenging activity of C-PC extracts was determined by using DPPH assay according to Chang *et al.* (2001). The decrease in the absorption of the DPPH solution after the addition of an antioxidant was measured at 517 nm. Ascorbic acid (10 mg/mL) in methanol was used as a reference. A 0.01 M stock solution of DPPH was prepared by dissolving 39.4 mg of DPPH in 100 mL of methanol. For the assay, 1 mL of 0.01 mM DPPH was added to 1 mL of C-PC sample and the mixture was left to stand for 30 min in the dark at room temperature. The absorbance of the resulting mixture was measured at 517 nm using UV-visible spectrophotometer. Methanol 90% (1 mL) and C-PC sample (1mL) were used as a blank. DPPH solution (1mL) plus 90% methanol (1 mL) was used as a negative control. L-ascorbic acid solution (0.01-0.1 mg/mL in methanol) was used as positive control [*i.e.* standard/reference]. The percentage inhibition was calculated using Equation 7.

$$\%\ \boldsymbol{Inhibition} = \frac{\boldsymbol{A\,(control) - A\,(Test)}}{\boldsymbol{A(control)}}\ \boldsymbol{x\ 100} \qquad \textbf{Equation 7}$$

The IC_{50} values (concentration of sample required to scavenge 50% of free radicals) were calculated based on regression equation below.

$$\boldsymbol{y = 15.496x - 7.6491} \qquad \textbf{Equation 8}$$

6.2.6.2 Reducing power (RP) assay

The reducing power of C-PC was determined as described by (Berker *et al.*, 2007) using the L-ascorbic acid as standard. Different concentrations of C-PC (0.01-0.1 mg/mL) were prepared. The C-PC (0.5 mL) was mixed with 0.5 mL EtOH (96%), 5mL H_2O, 1.5mL of 1MHCl, 1.5mL of ferricyanide solution [$K_3Fe\ (CN)_6$] (1%), 0.5mL of SDS (1%), and finally 0.5mL of $FeCl_3 \cdot 6H_2O$ (0.2%) so that the final volume would be 10 mL. The mixture was

incubated at 50 °C in a water bath for 20 min, thereafter, let cool to room temperature prior to the absorbance been measured at 700 nm ($A_{700\ nm}$) against a reagent blank.

6.2.7 Quantification of C-Phycocyanin

The relative concentration C-PC (C_R) was determined as the remaining C-PC concentration as a percentage of the initial concentration using;

$$\mathbf{C_R = \frac{Cf}{Co} x 100} \qquad \textbf{Equation 9}$$

where C_R is expressed as a percentage (%), and C_f and C_0 are the remaining and initial C-PC concentration (mg/mL), respectively.

6.2.8 Statistical Analyses

All analyses were performed in triplicate. Mean and standard deviations were calculated for each experiment. Statistical analyses *i.e.* one-way analyses of variance (ANOVA) were conducted with the GraphPad Prism 8. Significant difference at $p < 0.05$ between the samples was determined by Tukey's *post hoc* multi-comparison test.

6.3 RESULTS AND DISCUSSION

6.3.1 Physiochemical characteristics of amino acid sequences of C-PC from *Euhalothece* sp.

Elucidation of the composition, structure and physicochemical properties of the amino acid sequence of the C-PC protein subunits is of great importance for understanding and improving the stability of these compounds when exposed to various stress factors (Pan-utai *et al*., 2018; Patel *et al*., 2018). Genes encoding C-PC *α*- and *β*-subunits and linker proteins were extracted from the recently sequenced *Euhalothece* sp. genome (accession number MDVL00000000) (Mogany *et al*., 2018a) and translated into amino acids. The analysis of the amino acid composition of C-PC can help explore the structure and active groups as well as also provide a theoretical basis for other properties (Liu *et al*., 2016). Protein primary structure is the linear amino acid sequence usually represented by a one-letter notation. The complete primary structure *α*- and *β*-subunits and linker protein from *Euhalothece* sp. can be seen in Table 30.

Identical to C-PC from other cyanobacteria, the *α*- and *β*-subunits are found to be composed of 162 and 172 amino acid residues respectively (Table 31) and each *αβ* monomer binds to three phycocyanobilin (PCB) chromophores at positions *α*-Cys84, *β*-Cys82 and *β*-Cys153 (Liu *et al*., 2016; Patel et al., 2018; Wang *et al*., 2001). The hydropathy value for a protein *i.e.* hydrophilic and hydrophobic properties of each amino acid side chain in a protein is calculated based on a formula developed by (Kyte and Doolittle 1982). The overall amino acid sequences of the C-PC subunits had a negative value hydropathy, this indicates a non-polar protein (Table 2). The *α*-subunit had 15 negatively charged residues (Asp+ Glu) and positively charged residues (Arg+ Lys) 17. Whereas the *β*-subunit had 17 and 20 negatively and positively charged residues. Thus, *α*-subunits exhibit a higher content of charged residues than *β*-subunits, however, *α*-subunits globally appear to be the least stable of the two subunits.

Table 30: Amino acid sequences of subunits and linker proteins that make up the PBPs in *Euhalothece* sp.

Gene	Protein name	Amino acid sequences					
cpcA	C-PC *α* subunit	MKTPITEAIA KFPYTTQMQG FELSPSWYIE	ADSQGRFLGN PQYAHDQRGK ALKHIKANHG	TELQSANGRF DKCARDIGHY LNGQAANEAN	ERALASMEAA LRMVTYCLIA TYLDYAINALS	RGLTQKSNDL GGTGPMDEYL	INGAANAVYQ IAGLDEINRT
cpcB	C-PC *β* subunit	MFDAFSRVVS ADQPQLVQPG LGVPGASVAA	QADSRGEFLS GNAYTNRRMA GVQKMKEEAV	TEQLDALTQM ACLRDMEII RLASDPNGIT	VKDGNKRLDT LRYVTYATLA QGDCSQLMS	VNRMTSNSAS GDASVLEDRC EVASYFDRAAA	IVTNAARGLF LNGLRETYQA AVA
cpcC	LRpc -32.1 kDa	MKTLVASNLA SAESLLRQG EWAYHTGLC QLYRGYGSSD QSARMYRVE	NAGRLGLESF NLTVRGLVRA EEKGVDAEI RAQAGGKEA VSGQIGRKIR	SGDPVELRWN IAKSDLYKE DSYLDSEEYV RLTWELGKN PVIRYSNNAY	ASEDDLQTVI KFFYPNSNQR SKFGEEIVP EASTIVEPST LVPYDQLSQ	RAAYRQVLGN FVELNFKHL YYTGFQVGLG STEEGTSRTP RLQQIVRQGG	DYVMESERLI LGRPPYDEE ARTTNFTRMF QTAYGGVGN KVVSVRPA
cpcD	LRpc - 8.9 kDa	MYGQTTVTT QMRRINRMG	PSSAASRMY GKIVNIEPLN	RIEVEGMRQS TEPETESSEN	SESDKQSYAI	RKSGSVFFT	VPYSRMNE
cpcG	LRC -28.5 kDa	VSLPLLNYTT ASNRQRFLES EAEKIAWSIV RYGPYYRQQL IDYDKKVPYR	SSQNQRVEG QLRYGQITVK VGTKGINGFV GFPQIVWQNQ KFN	YEVPGEEQLR DFIFGLLTSD EDLLNSEEYL VRRFIPQEKQP	PTPGMMNSEE PFRRWNYEPN NNFSEDTVPY KAGDPTLFLN	DAEATIWAAY SNYRFVELCV QRRRVLPQKA VARGLSSAKG	RQIFSEHQML QRALGRDVYN QGETPFNLKTP NALPKVSAMN
apcC		MRMFKITAC KVQLATGK	VPSQTRIRT PGTNTGLV	QRELQNTY	FTKLVPYEN	WFTEQQRI	MKMGGKIV
ApcE	LCM	MISASGGSS ITRNSELIVSR	VARPQLYQTV AANRIFTGGS	PLSKLSQAEQ PWLTLKNRE	QDRFLEKGE KKPQQWSQP	LQELNTFFQL MAKNRILVAK	GTKRIEIAQI CNWEQLAIKK

Gene	Protein name	Amino acid sequences					
ApcE	LCM	AAVAVSKDY LQVIPILSPLT PLPLPPNSVN LTVSRFLINPK ISPLSLMADFQL LTLNIIVLWRIN *KMAKLPFVSL MR*WMPFWT KFLKNAANPM KRSLPT*KV RR*IRRRFKSI TPKACTIS*R *LDR*TLPKR GKQLFSQVIV PRKGFTPSLIT	DLYLASLVA CVGYGKSSKM VPVATNKGN LKTVKFPRNLS *LMR*WIVKN IPTEAAMIL*RF FGCWRSRSYS PQSTAKPLARI FSIASNKGLISV SSEMVRLLL INFWQVKGF SRMTSWLF YKKAPLGFSA PCASW*KPLL SSMVLNTIVS	VVFLSHQASV LVPVMPQLLL CLKVTLTRQK AVWVNLPFIG TPITLARKQSPT NLGQFSRKKLA VNSTGLLFMS QFPMNVI*PQ GNKPSSLSSRI RSLLKG*VV GRL*RRW*T PVLKPLDRS ILPKPTAAKP SLRYINSVL*F SVTWLFPTPKET	PLMCPVMVP GKCKPPPVTS IVRNTRSLDSL NSSTNPISTVAL FAV*EKKRKNV TPVKAQRRLVR PSPLNTSIVVC* VGYSYALAPITY CMIRLRLKL*S LISM*KSST VWNIPKCLG WIMVSYR* KK*LMRCML LTQIRKLWKR	KICRNRCGTY VKTKTLALTS TRKNKRRKQR *NWRSVTSSD VTGECSKTCLIT IPVGF*LIVVRLP VVRLMVVKKS GKMWEQRCK ARRIVRYLN RLILIRR*LS RMLFPIVVI RLKPMAQM NC*MCLKHK SIDIC*GAPPA	LGCCVMPMRS NTSKFSTNLK IVKSLNGTSLA GVPLLAKKYKP APLSAKFLNLSP ITKLETRKHGD TNTLIFVRRKGF KRLLLVILSWV GILNPMW* WERSIS*DE PRSQLRISP AREKPLGIWS CQMSSVYSH RSKSTK*PDS*

Table 31: Physico-chemical properties of the selected C-phycocyanin protein genes

Physicochemical parameters	***α***	***B***	**LRpc32**	**LRpc8.9**	**LRC 28.5**
Length (total no. of amino acids)	162	172	286	84	254
Isoelectric point	6.06	5.00	6.25	8.07	9.03
Molecular weight (MW)	17764	18480	32172	9561	29478
Negatively charged residues(-R)	17	20	36	10	28
Positively charged residue(+R)	15	17	35	11	32
Extinction coefficient (EC)	19035	7575	41830	5960	42860
Instability index (II)	27.25	38.83	36.28	85.76*	40.65
Aliphatic index (AI)	75.56	81.22	77.03	48.69	72.52
GRAVY	-0.436	-0.166	-0.551	-0.864	-0.686

*unstable

The extinction coefficient (EC) of the proteins was found ranging from 7575 to 42860 (Table 31) with respect to their concentration of aromatic amino acids and Cys (disulfide bonds). These EC values can be used to calculate protein concentration in a solution which in turn help in the quantitative study of biochemical interactions between the protein-protein and protein-ligand (Punjabi *et al*., 2018).

C-Phycocyanin has been reported to be highly stable near-neutral pH (Chaiklahan et al., 2011). As the pH increases from the isoelectric point (pI), the C-PC becomes more soluble due to the increase in electrostatic repulsion that decreases the aggregation and subsequent precipitation of the compounds (Orta-Ramirez *et al*., 2000). The pI is an important property since the protein is least soluble at the pH near this point and thus unstable. The net charge on a protein is zero at the pI, positive at pHs below the pI, and negative at pHs above the pI (Shaw et al., 2001). The pI of c-pcA and c-pcB was 6.0 and 5.0 respectively, which is a high value. Linker peptides are positively charged with an pIs are >pH 9.0 (Table34). In contrast, the C-PC are extremely water-soluble and are negatively charged at physiological pH. The *β*- and *α*- subunits both have the lowest pI of 5.00 and 6.06 respectively. Of the three linker

proteins, LR pc32 has the lowest calculated pI = 6.25. In contrast, the rod linker LR pc 8.9 and rod-core linker both have an extremely high pI of 8.07 and 9.03 respectively. The pI is an important property since the protein is least soluble at the pH near this point and thus unstable. Thus, both below and above the pI the protein will be soluble.

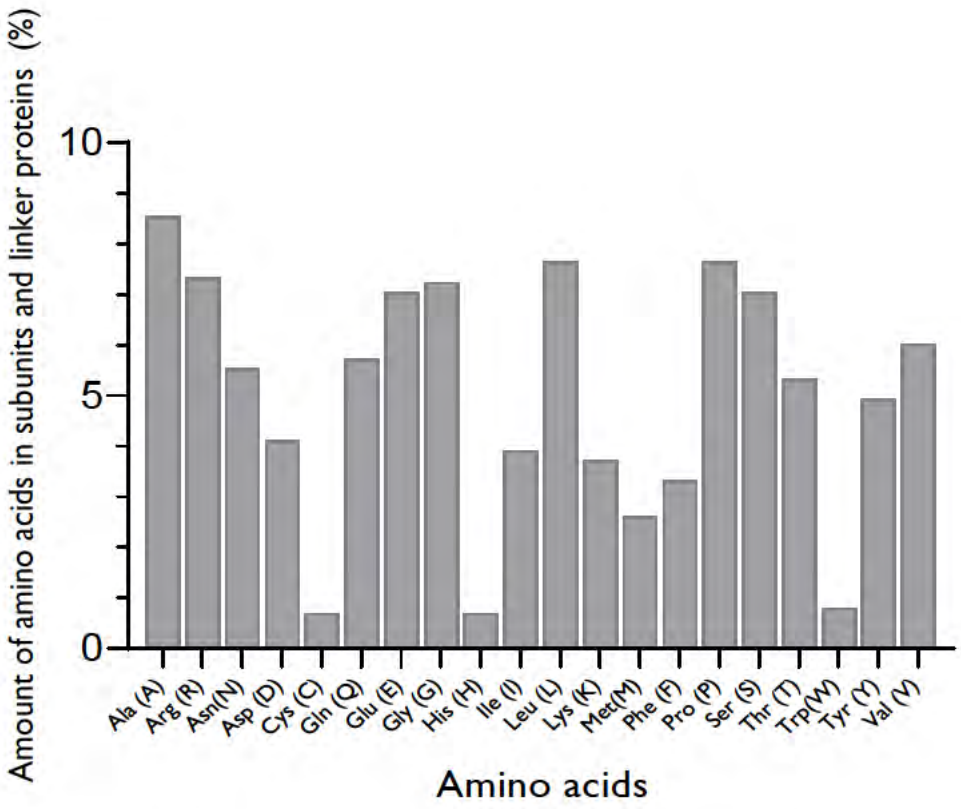

Figure 30: Graphical representation average percentage of 20 amino acid presents C-PC.

The compositions and percentage of all 20 amino acids in *αβ* subunits and linker proteins of *Euhalothece* sp. was displayed in Table 32 and Figure 30 respectively. The most abundant amino acids in *α*-subunit were Ala with 14%, followed by Gly, Leu, Asn and Ile with the percentage of 8.6, 8.6, 6.8 and 6.2% respectively (Table 32). Similar results were observed in the *β*- subunits were non-polar hydrophobic amino acids, Ala and Ile made up 14 and 8.7%,

however, a difference observed was a high content of Arg and Ser (7.6% each). Arg, Glu, and Gly contributed the highest abundance residues in the linker proteins.

Table 32: Amino acid composition of C-phycocyanin subunits and linker proteins from *Euhalothece* sp.

Amino Acids	**α -subunit**	**β -subunit**	**LRpc32**	**LRpc8.9**
Polar (Acidic)				
Asp (D)	8	12	11	1
Glu (E)	9	8	25	9
Polar (Basic)				
Arg (R)	8	13	24	8
His (H)	4	0	2	0
Lys (K)	7	4	11	3
Polar (Hydroxy acids)				
Ser (S)	7	13	23	12
Thr (T)	10	10	15	7
Non-polar (Aliphatic)				
Ala (A)	23	25	20	3
Gly (G)	14	12	26	5
Asn(N)	11	8	13	5
Ile (I)	10	4	10	5
Leu (L)	14	15	25	1
Cys (C)	2	3	1	0
Met(M)	5	7	4	6
Pro (P)	5	4	10	40
Gln (Q)	9	10	15	4
Val (V)	2	14	22	5
Trp(W)	1	0	3	0
Aromatic				
Phe (F)	4	5	9	2
Tyr (Y)	9	5	17	4
Total	162	172	286	120

6.3.2 Molecular characteristics of C-Phycocyanin from *Euhalothece* sp.

Previous studies have shown a high similarity in the amino acid composition of related cyanobacteria, however different biochemical and biophysical properties were found amongst cyanobacterial strains isolated from different environments (Satyanarayana *et al*., 2005). In order to unveil possible differences in the molecular conformation of PBS's resulting from adaption to the temperature and high salinity, we compared the *Euhalothece* sp. C-PC subunits from this study to thermophilic and mesophilic cyanobacteria isolated from hypersaline, marine and freshwater cyanobacterial strains.

The C-PC subunits from *Euhalothece* sp. were similar to other halotolerant and thermotolerant marine cyanobacteria. The amino acid sequences of the *α*- and *β*-subnunits showed 100 and 99.42 % sequence similarity to cyanobacteria, *Dactylococcopsis salina* PCC8305 (WP_015228331.1) isolated from hypersaline, Great Salt Lake, Utah. It also showed similarity (up to 95% for the *α*- and *β*-subunits) with two other strains isolated from other hypersaline environments *i.e. Halothece* PCC 7418 (WP_015227201.1) and *Euhalothece natronophila* (WP_146295844.1) (Mikhodyuk *et al*., 2008). A lower similarity percentage (< 89) was observed for *α*- and *β*-subunits in marine thermophilic cyanobacteria such as *Spirulina subsalsa* (WP_017305690.1) (Kuroiwa et al., 2014), *Rubidibacter lacunae* (WP_022605817.1) (Choi et al., 2008), *Chroococcidiopsis* sp. strain TS-821 (WP_104546962.1) (Hayashi et al., 1997) and *Gloeocapsa* sp. PCC 7428 (WP_015190910.1). Freshwater mesophile, *Synechococcus* sp. PCC 6301 (Q5N4S9.3) displayed only a >67% similarity. The phylogenetic tree of the amino acid sequences of cpcA and cpcB for *Euhalothece* sp. and some of thr selected strains is available in the Appendix 12.

Alignment results indicate that the primary sequences of linkers are less conserved than those of their associated C-PC subunits. The *α*-subunit of C-PC has an average molecular weight of 17764 kDa (Table 31), with Met and Ser the NH_2- and carboxyl-terminal amino acids. The protein sequence revealed that Met-85 is conserved in *Euhalothece* sp, as well as in other marine cyanobacteria including *Cyanothece* whereas position 162 is occupied by Ser residues

(Figure 31). The Asp87 residue is a key amino acid that determines the electronic state of the chromophore (Kikuchi et al., 2000). The *β*-subunit is made up of 172 amino acids, with methionine and arginine and the average molecular weight of 18480 kDa. Cysteine residues are found on position 84 for the *α*- subunit and positions 82, 110 and 154 for *β*-subunit (Figure 32). Conserved Arg and Asp acid residues in close vicinity to the Cys attachment sites also interact with the chromophores. It was also observed that position 129 is occupied by Ala residues (Guan *et al*., 2007). Alignment results indicate that the primary sequences of linkers are less conserved than those of their associated C-PC subunits. Among all linker polypeptide, LC shows a comparatively high level of sequence identity in different cyanobacteria, indicating possible conservation among ancestral linker polypeptides (Guan *et al*., 2007). Motifs with less than 2 e-values were considered as the most significant motifs (Figure 33).

Further analyses of the *Euhalothece* sp. C-PC subunits showed that *α*- and *β*- amino acid sequences exhibited a number of conserved characteristics but relatively close to the other hypersaline strains deposited in databases. The C-PC amino acid sequences from *Euhalothece* sp. had several significant amino acid substitutions in the *α*- and *β*-subunits in comparison to the mesophilic cyanobacteria inhabiting marine and freshwater. This can be seen in the multiple sequence alignments of the *α*- and *β*-subunits sequence of C-PC. The substitutions in the *α*- and *β*-subunits are potentional due to additional evolutionary pressure. The first substitution is located on the *α*-20 residue, *Euhalothece* sp. and cyanobacteria from hypersaline environments contain Gly whereas the marine and freshwater cyanobacteria have Ser. Gly contributes to the hydrophobic interaction and help to maintain conformational stability and flexibility in the inner part of protein (Liang *et al*., 2018).

The overall percentage of amino acids sequences of C-PC α*β*-subunits and linker proteins are displayed in Figure 30. Siglioccolo *et al.* (2011) reported that halophilic proteins are characterised by a general decrease in hydrophobic amino acids. It was observed that in *Euhalothece* sp. from this study and the other halotolerant cyanobacteria were several replacements of hydrophobic amino acids with polar amino acids. *Euhalothece* sp. had *α*Ser26, *α*Asn28, *α*Asn148, *β*Trp21, *β*Gln29 and *β*Trp40 whereas the marine and freshwater cyanobacterial strains contained either *α*Ala26/*α*Val26, *α*Val28, *β*Gly21/ *β*Asp21, *β*Val29 and *β*Val40/ *β*Ala40 respectively.

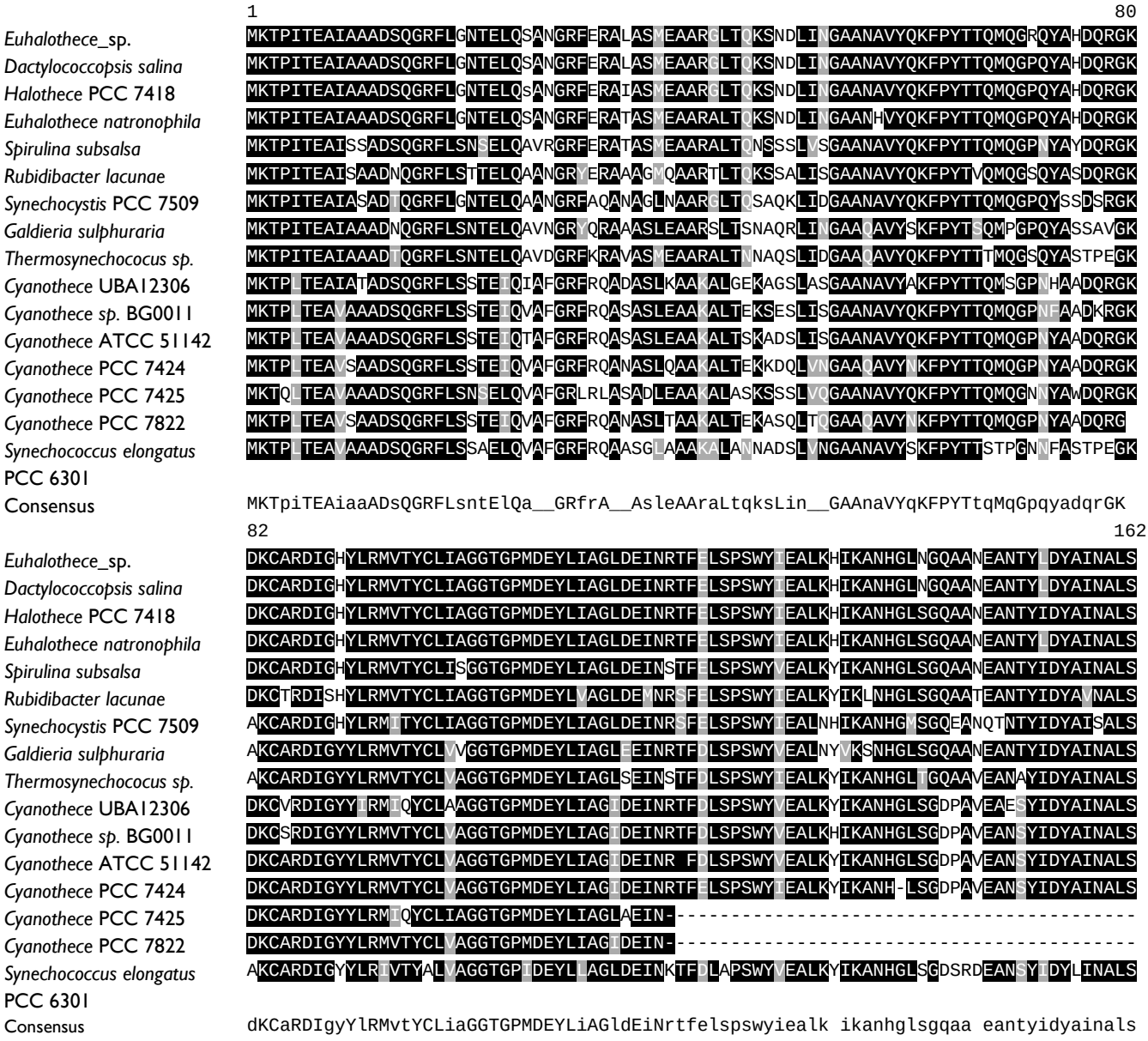

Figure 31: Multiple sequence alignment of α-subunits of C-phycocyanin genes. Potential amino acid substitutions and differences between thermotolerant and mesophilic cyanobacteria from hypersaline, marine and freshwater environments are presented as single-shaded boxes. Similarity can be seen in black shaded boxes.

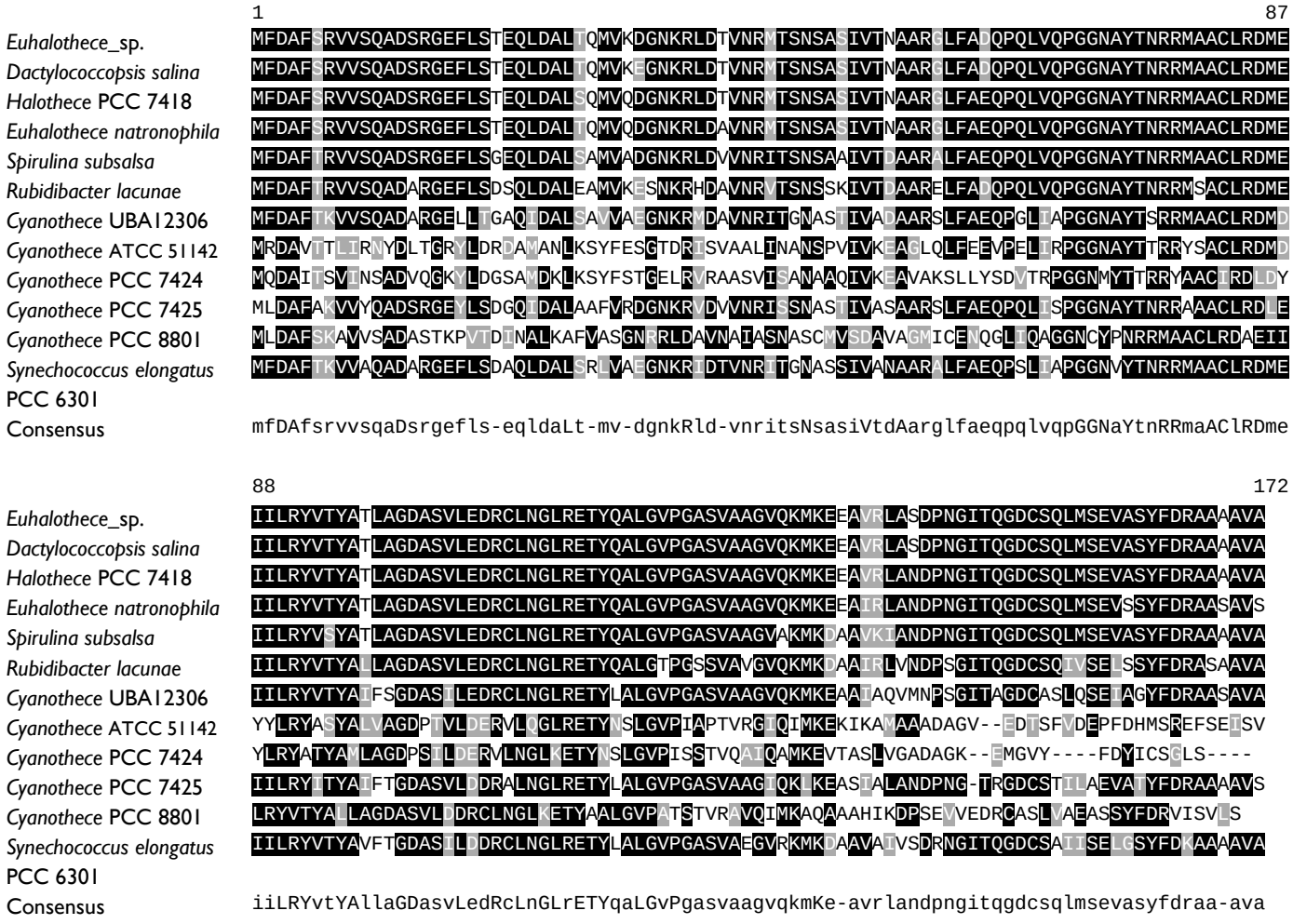

Figure 32: Multiple sequence alignment of *β*-subunits of C-phycocyanin genes. Potential amino acid substitutions and differences between thermotolerant and mesophilic cyanobacteria from hypersaline, marine and freshwater environments are presented as single-shaded boxes. Similarity can be seen in black shaded boxes.

Ala and Val are hydrophobic amino acids, whereas Ser is a polar amino acid known as the best residues for interacting with the water surrounding protein. Asn and Gln are known as thermolabile amino acids due to their tendency to undergo deamination at high temperature. Fukuchi *et al*. (2003) reported for proteins from halophiles, a biased amino acid composition also exists in thermophiles.

In both *α*- and *β*- subunits, several potential salt bridges that are known to stabilise the structure were found in the halotolerant cyanobacteria and not present in freshwater cyanobacterial strains. The first salt bridge form in the α-subunit was between *α*Glu32 and *α*Lys47 present in *Euhalothece* sp. from this study, cyanobacteria from the hypersaline environment *i.e. D. salina*, *Halothece* PCC 7408 and *E. natronophila* as well as the thermotolerant marine cyanobacteria (*S. subsalsa* and *R. lacunae*). In the freshwater strains compared, there are no such salt bridges because *α*Glu32 has been replaced with *α*Arg32. In all *α*-subunit sequences, the corresponding salt bridge residues *α*Lys2 and *α*Glu7, *α*Arg17 and *α*Glu23 and *α*Arg119 and *α*Glu117 are conserved. Similarly, there were two *β*-subunit salt bridges (formed with *β*lys22 and *β*Glu22; *β*Arg139 and *β*Asp145) only found in *Euhalothece* sp., *D.salina* and the two marine thermophiles (*R. lacu*nae and *Gloeocapsa sp*.).

The non-polar amino acids are characterised by having no polar atoms (only carbon and hydrogen) in their side chains was include Gly, Ala, Val, Leu, Ile, Pro and Met. Among hydrophobic residues, Ala, Val, Leu, and Ile belong to the aliphatic amino acids (Table 32). The proteins of the thermophilic cyanobacteria are found to have higher residue hydrophobicity, more charged amino acids (especially Glu, Arg, and Lys), and fewer uncharged polar residues (Ser, Thr, Asn, and Gln) [8]. Hydrophobic interactions also play an important role in the stability of proteins. The hydrophobic aliphatic amino acid residues (Ala, Val, Leu, and Ile) content in *Euhalothece* sp. found to be high and makeup 32.06% of the subunits (Figure 30). Furthermore, it is reported that in halophiles there is an excess number of acidic residue on the protein's surface which increases the negative charge thus, allows the proteins to retain their functional state at higher salt concentrations (Lenton *et al*., 2016; Reed *et al*., 2013). The comparison of the *α*- and *β*- amino acid composition of *Euhalothece* sp. to other thermophilic and mesophilic cyanobacteria inhabiting hypersaline, marine and freshwater are shown in Appendix 13.

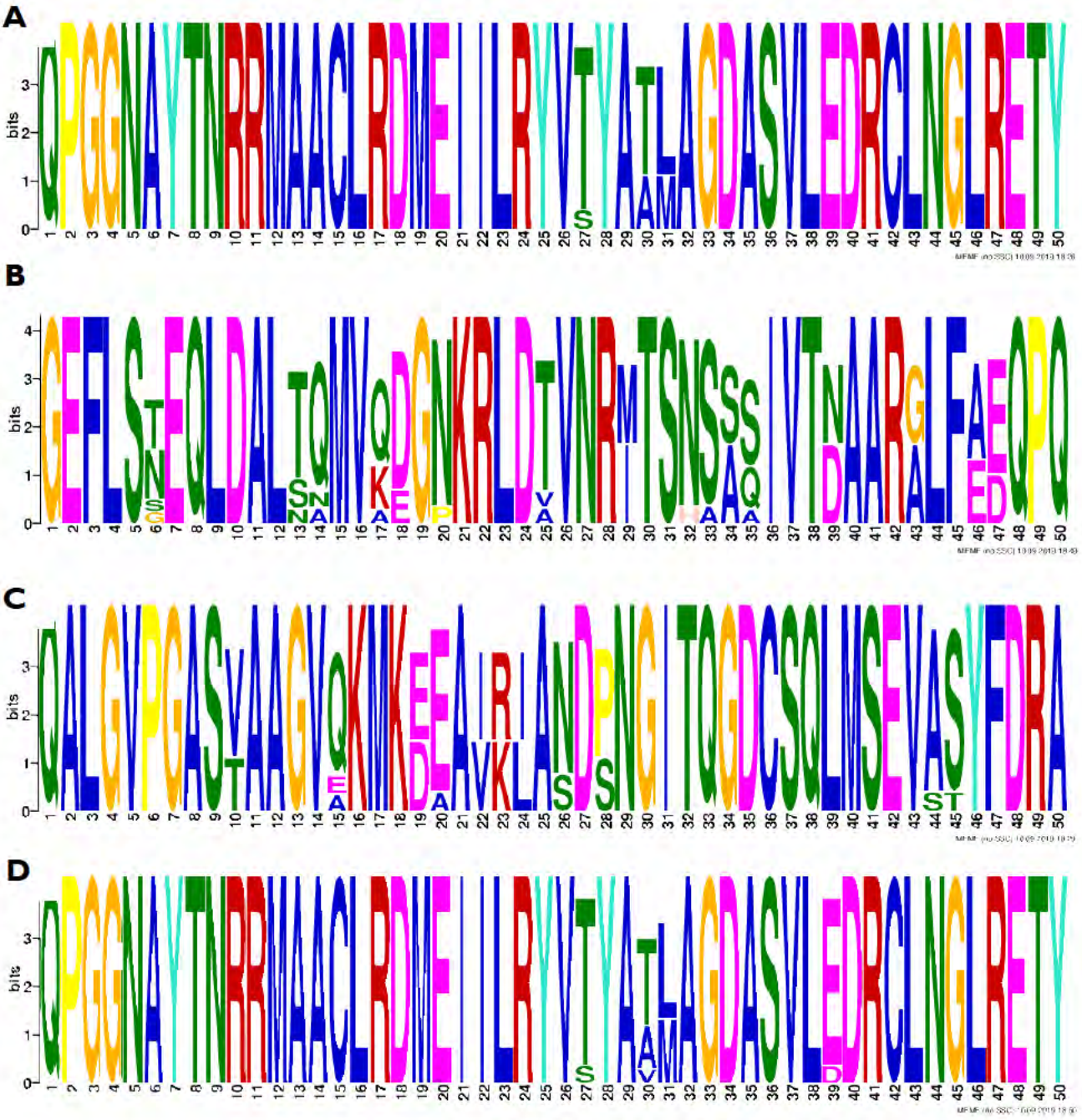

Figure 33: The sequence logos of the 1motifs predicted by MEME showing (A) α subunits with 1.5e-282, (B) α subunits with 1.6e-258, (C) *β* subunits with 2.1e-283 and (D) *β* subunits with 2.3e-328 .The total height of the stack is the "information content" of that position in the motif in bits. The height of a letter indicates its relative frequency at the given position (x-axis) in the motif.

6.3.3 Secondary and Three-Dimension Structures of C-phycocyanin

Stretches of polypeptide chains consist of *α* helices, *β* sheets and loops that form the secondary structure. Even though *α*- and *β*-subunits differ in their primary structure, their tertiary structures exhibit extensive similarity. The secondary structure of a protein is more conserved than its nucleotide sequence, hence, is highly valuable for understanding its function, molecular evolution, and interaction with macromolecules. Secondary structure predicts the structure of proteins and nucleic acid sequences based only on the knowledge of their primary structure (Punjabi *et al*., 2018). The secondary structure helps to determine the exact structure of the gene which was predicted using GOR IV software (Reehana *et al.* 2013). The protein secondary structure prediction for three structural states (*α*-helix, P-strand, loop) was applied to each of the sequences. The secondary structure predictions for both C-PC subunits. A large number of *α*-helices and fewer *β*-strands are displayed in Figure 34 and Figure 35. In the trimer, the *α*-84 chromophore in one monomer and the *β*-84 chromophore in an adjacent monomer are in close contact and energy is transferred from the *α*-84 chromophores to the *β*-84.

The estimate of the secondary structure of C-PC *α* subunit was 50% a helix, 13.58 % extended strand, 36.42% turn. The *β*-subunit was 54.07% a helix, 9.03 % extended strand, 36.63% turn, which indicated the dominance of helix followed by coil structure in both sequences. This structural state is due to the rich content of highly flexible glycine and kink inducing proline amino acid residues. Although the *α* and *β* chromophores are close in proximity to each other as observed in Figure 37C, this is not necessarily sufficient for complete energy transfer. Thus, the environment (*i.e.* buffer concentration and pH) plays an important role in the native trimer structure, whereby the chromophore configuration and polypeptide conformation affect each other to give the most favourable structure for efficient energy transfer (Bermejo *et al*. 2000). The trimers are quite stable and only in the presence of high concentrations of chaotropic agents (such as urea), very acidic solutions, or elevated temperatures induces monomerisation, followed by the separation between the subunits (Marx & Adir, 2014).

```
         10        20        30        40        50        60        70
         |         |         |         |         |         |         |
MKTPITEAIAAADSQGRFLGNTELQSANGRFERALASMEAARGLTQKSNDLINGAA
NAVYQKFPYTTQMQ

ccccceeehhhhhhhccccccchhhhhcchhhhhhhhhhhhhhhhhhchhhhhhhhhheeeccccccccc

GPQYAHDQRGKDKCARDIGHYLRMVTYCLIAGGTGPMDEYLIAGLDEINRTFELSP
SWYIEALKHIKANH

ccccccccccccchhhhhhceeeeeeeeeeecccccchhhhhhchhhccceeecccchhhhhhhhhhhhc

GLNGQAANEANTYLDYAINALS

Ccccchhhhhhhhhhhhhceec
```

Alpha helix	(Hh):	81 is 50.00%
310 helix	(Gg) :	0 is 0.00%
Pi helix	(Ii) :	0 is 0.00%
Beta bridge	(Bb) :	0 is 0.00%
Extended strand	(Ee) :	22 is 13.58%
Beta turn	(Tt) :	0 is 0.00%
Bend region	(Ss) :	0 is 0.00%
Random coil	(Cc) :	59 is 36.42%
Ambiguous states	:	0 is 0.00%

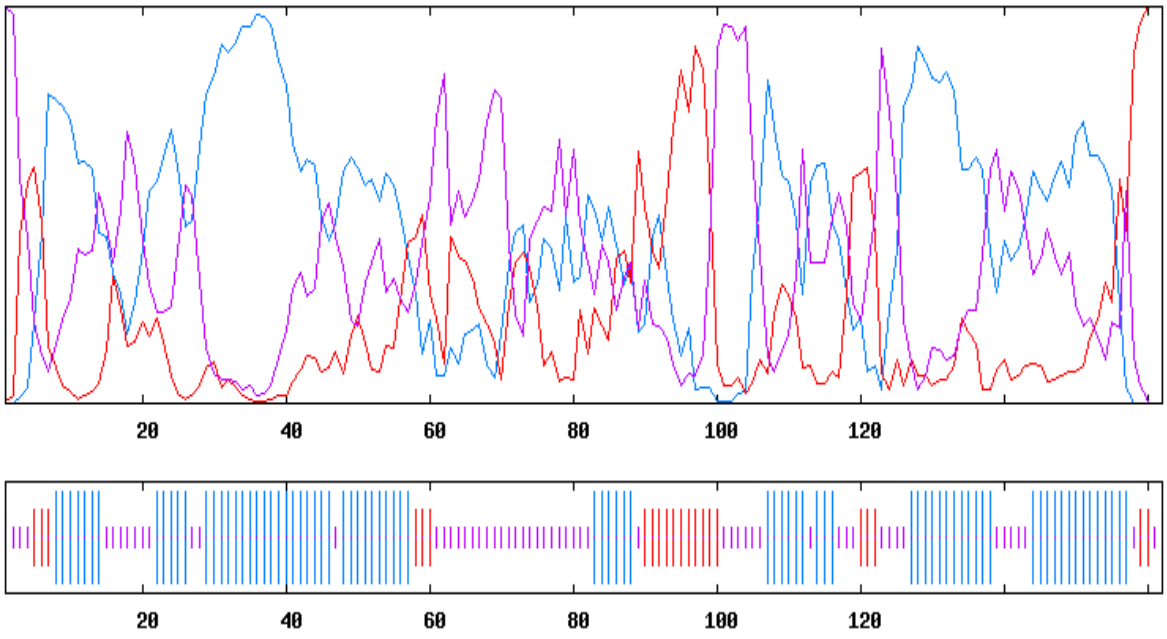

Figure 34: The secondary structure of the C-phycocyanin alpha subunit. H represent the alpha helix, e represent the extend strand and c represent the random coil.

10 20 30 40 50 60 70

| | | | | | |

MFDAFSRVVSQADSRGEFLSTEQLDALTQMVKDGNKRLDTVNRMTSNSASIVTNA ARGLFADQPQLVQPG

ccccccceeeecccccchhhhhhhhhhhhhhhhccccceeeeeecccccchhhhhhhhcccccccceeccc

GNAYTNRRMAACLRDMEIILRYVTYATLAGDASVLEDRCLNGLRETYQALGVPGA SVAAGVQKMKEEAVR

ccccchhhhhhhhhhhhhhhhhhhhhhhhcccchhhhhhhhhcccchhhhhhccccccchhhhhhhhhhhhhhh

LASDPNGITQGDCSQLMSEVASYFDRAAAAVA

Hccccccccccchhhhhhhhhhhhhheeeec

Alpha helix	(Hh) :	93 is 54.07%
310 helix	(Gg) :	0 is 0.00%
Pi helix	(Ii) :	0 is 0.00%
Beta bridge	(Bb) :	0 is 0.00%
Extended strand	(Ee) :	16 is 9.30%
Beta turn	(Tt) :	0 is 0.00%
Bend region	(Ss) :	0 is 0.00%
Random coil	(Cc) :	63 is 36.63%

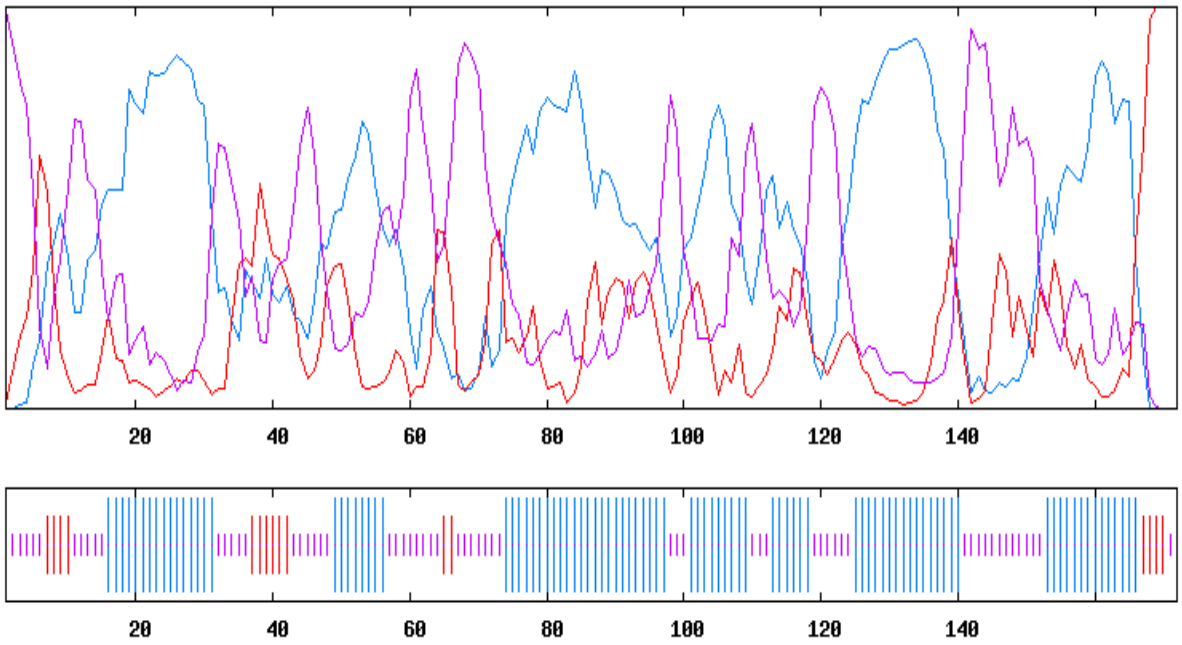

Figure 35 The secondary structure of the C-phycocyanin beta-subunit. H represents the alpha helix, e represent the extended strand and c represent the random coil.

The homology modelling approach was carried out to build the theoretical model of C-PC in order to derive structural information about the protein. The accuracy of a comparative model is correlated to the percentage of sequence identity *i.e.* the number of residues that match exactly between two different sequences. A >50% sequence identity with their templates indicates that comparative models are accurate (Pearson, 2013). Global Model Quality Estimation (GMQE) reflects the expected accuracy of a model built with that alignment and template and the coverage of the target (Benkert *et al*., 2010; Waterhouse *et al*., 2018). The closest homologous sequence for c-pcA (three sequences) showed 80.25% sequence identity with a (GMQE) of 0.91-0.93 indicating high reliability. For cpcB, the closet sequence showed a 77.33% identity and GMQE 0.83, which indicates a reasonably reliable structure, three other sequences with higher GMQE (0.93) had a ~75% sequence identity. Both *α*- and *β*-subunits adopted very similar helical globin-like fold as illustrated in Figure 37A and B respectively, with each comprising of eight helices.

The two N-terminal helices of each apoprotein subunit extend away from the rest of the subunit and make substantial contacts with the other subunit to form a stable *αβ* monomer. Each monomer contains two PCB chromophores, the *α* and the *β* chromophores. Three of *αβ* monomers associate to form a disk-like $(\alpha\beta)^3$ trimeric structure in which *α*-subunits of one monomer interact with the *β*-subunit of neighbouring monomer (Figure 37C). Protein folding is a process in which a polypeptide folds into a specific, compact, stable, functional, three-dimensional structure known as the protein tertiary structure (Wathen and Jia 2009). Molecular modelling is helpful to know the assumed structure of molecules and used to investigate the dynamics and thermodynamics of inorganic, biological, and polymeric systems. Determining the structures of proteins is of fundamental importance for understanding the functions and behaviour of proteins at the molecular level.

Linkers polypeptides are involved in face-to-face aggregation C-PC trimers that are involved in the assembly of the PBS. The LPs are embedded in the central cavity of PBP discs by the combination of hydrophobic and multiple charged interactions. The process is facilitated by tail-to-tail joining of hexameric assemblies into cylinders of rods and core (Liu *et al*., 2005a). The L_R polypeptides with MW: 32 kDa (coded by cpcC) and 8 kDa (coded by cpcD) can be seen in Figure 38A and Figure 38B respectively. They are involved in the assembly of the peripheral rod sub-structure (link C-PC trimers to hexamers or C-PC hexamers to other C-PC hexamers (Chang *et al*., 2015). The L_{RC} polypeptides (MW: 28 kDa), encoded by cpcG, is

involved in attaching the peripheral rods to the AP cores and may function in the assembly of rod substructure is displayed Figure 38C. The core-membrane linker, L_{CM} polypeptides also known as ApcE (Table 30) or anchor polypeptide, acts in the organisation of the PBS core, involved in the PBSs attachment to the membrane and is also the major terminal energy acceptors (Chang *et al*., 2015). Figure 38D shows the LC (MW: 8 kDa), encoded by the apcC gene is associated with APC trimer disc at the periphery core, it is not required for assembly, however, essential for stability and energy transfer.

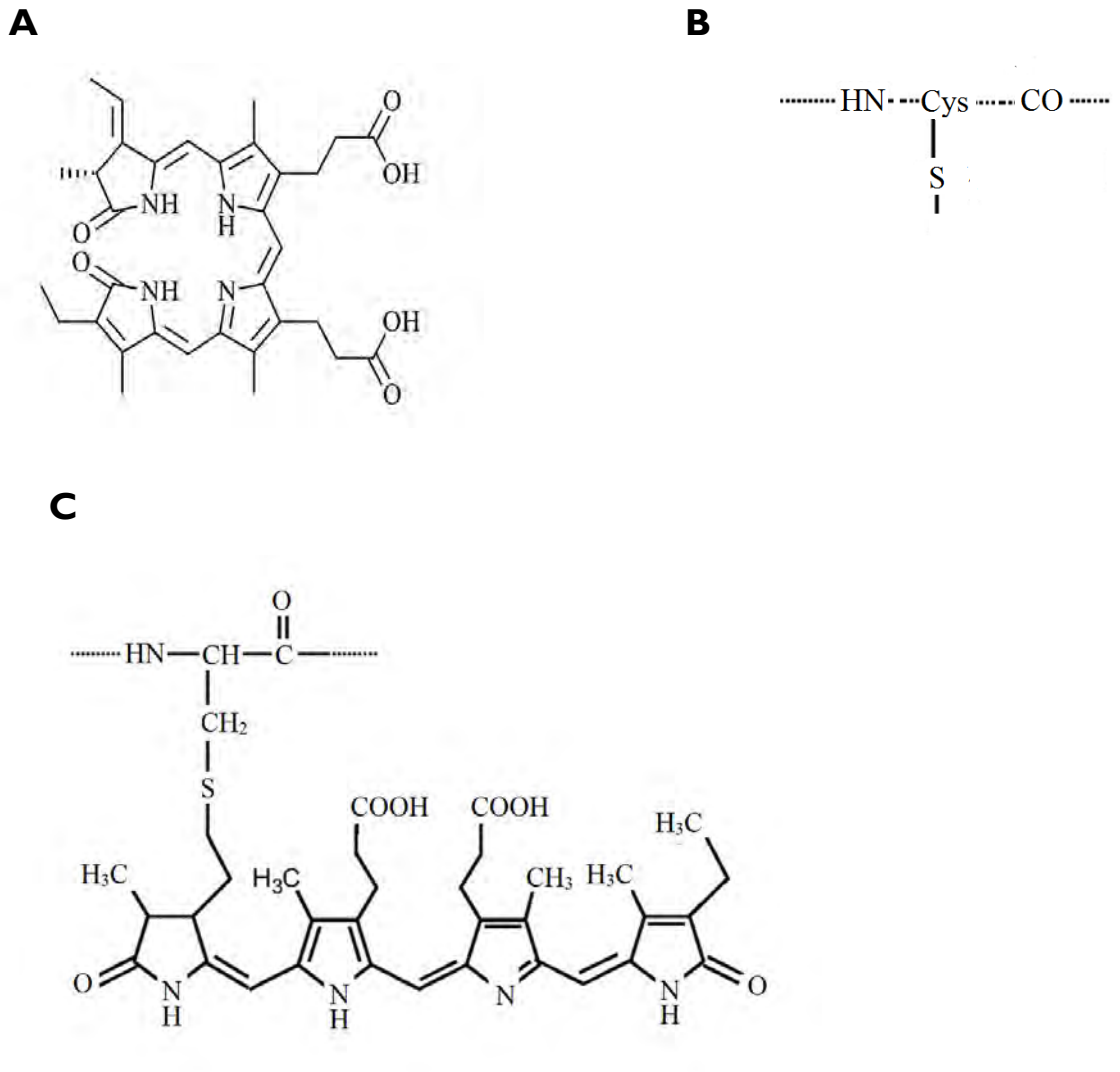

Figure 36: Chemical structure of (A) PCB chromophore showing the site of covalent binding to the protein(Cys), (B) apoprotein (D) C-PC (drawn using chemdoodle software.

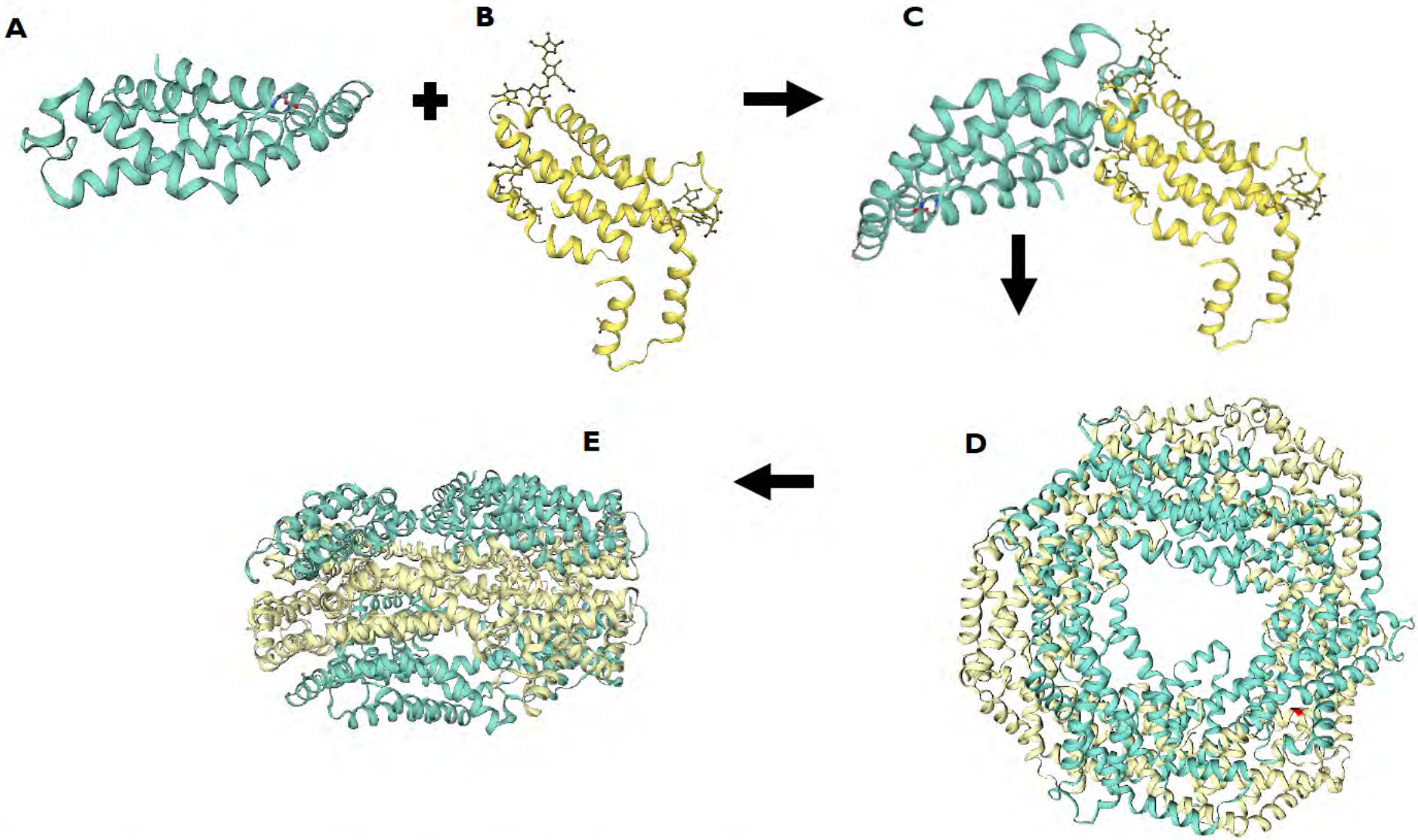

Figure 37: Homology model of *Euhalothece* sp C-PC showing (A) the α-subunit, with 50% a helix, 13.58% extended strand, 36.42% turn, (B)the β-subunit made up of 54.07% a helix, 9.03% extended strand, 36.63% turn (C) the C-PC ($\alpha\beta$)-heterodimer, (D) three heterodimers associated to form a disk-shaped $(\alpha\beta)^3$ subunit, (E) the 90° view of the $(\alpha\beta)_3$ subunit, two of $(\alpha\beta)^3$ subunits form an $(\alpha\beta)^6$ hexamer.

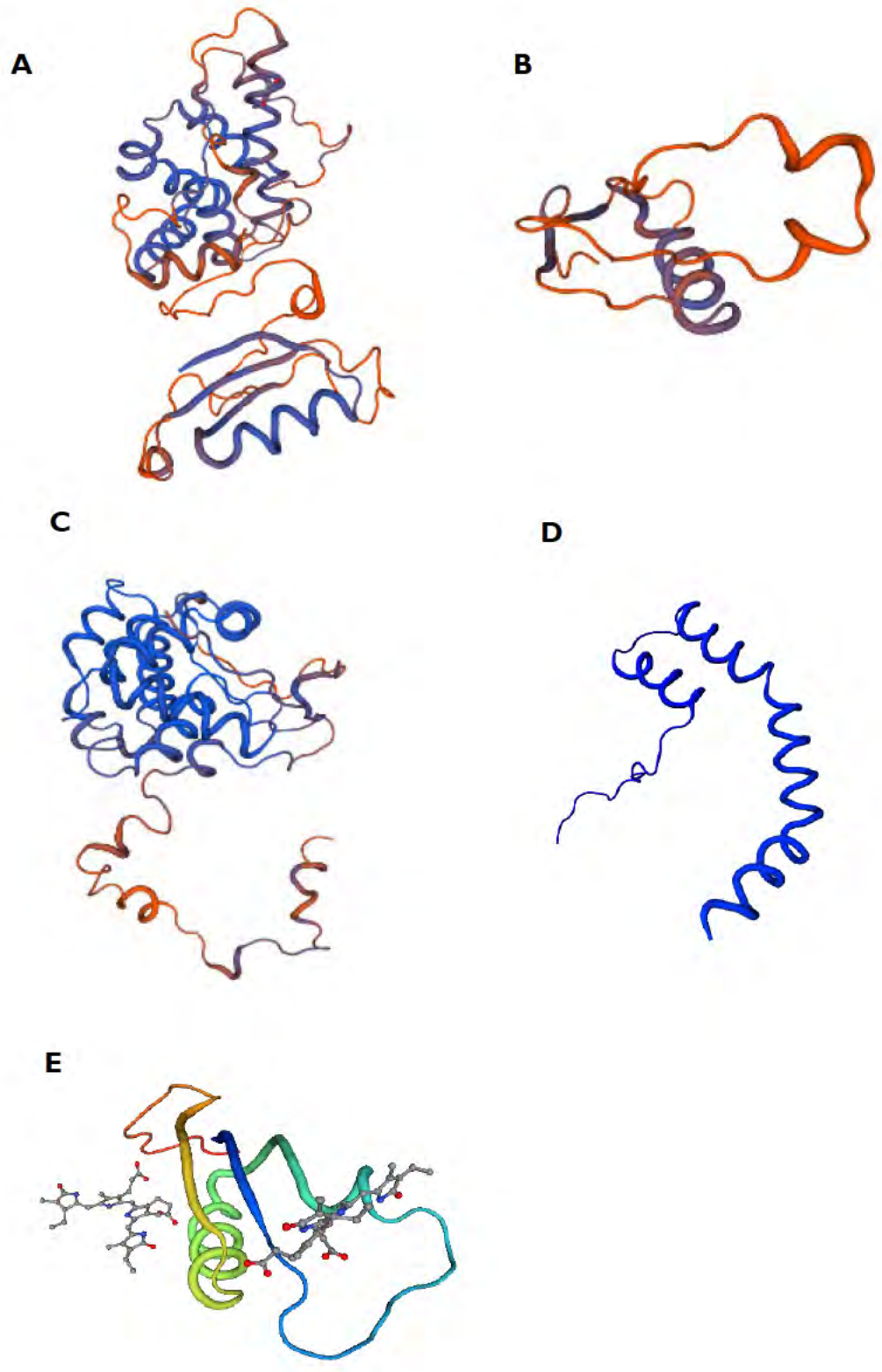

Figure 38: Tube representation of 3D structure of linker proteins (A) LRpc 32, (B) LRpc8.1, (C) LRC 28.5, (D) LCM and (E) L_C8.

6.3.4 Spectral Properties of C-phycocyanin

The characteristics of C-PC were determined by evaluating the absorption spectrum. As shown in Figure 39A the purified C-PC produced a single visible absorption peak at 620 nm. The fluorescence nature of purified C-PC was determined by a fluorescence emission spectrum, with fluorescence emission maximum at ~ 640 nm (Figure 39B). This means that the C-PC absorbs orange light and emits red light. The characteristic absorption spectrum of C-PC is a result of the presence of the prosthetics groups and their protein environment. As previously mentioned, the C-PC fluorescence property is due to the presence of covalently linked linear tetrapyrrole bilin chromophores (Moon *et al.*, 2014). The stability of these bilin chromophores can provide vital information regarding the structural stability of C-PC when exposed to various stress factors.

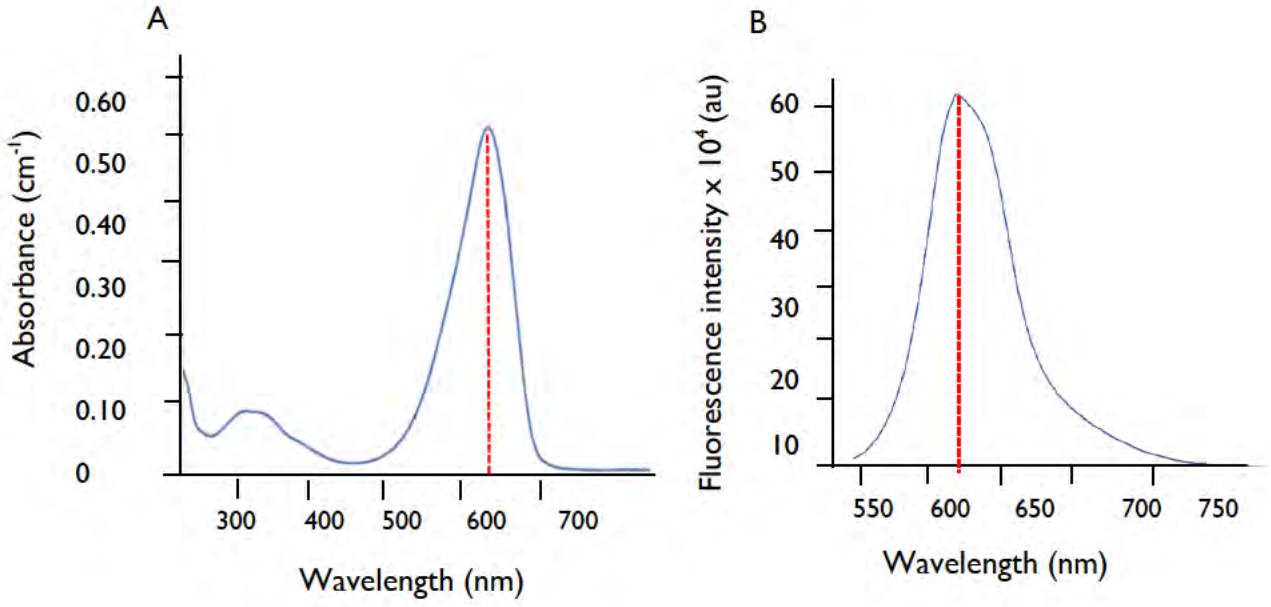

Figure 39: C-Phycocyanin characterisation showing (A) UV-vis absorption spectra and (B) emission spectra, with excitation at 580 nm.

6.3.5 C-phycocyanin *In vitro* Antioxidant Activity and Correlation with the Predicted Amino Acids

The antioxidant activities of C-PC were evaluated by the DPPH and reducing power methods. Antioxidants donate electron or hydrogen to reduce the stable radical DPPH to DPPH-H, non-radical form. The stable radical DPPH has been extensively used for the determination of antioxidant activities and abilities of compounds. The assay is based on the reduction of DPPH radicals in methanol which causes a decrease in absorbance at 517 nm (Kedare & Singh, 2011). This is visualised by a colour change from purple to yellow. The potency of a molecule to scavenge DPPH radicals results from the number of hydrogens available for donation by the hydroxyl groups. The decrease in DPPH absorbance is used to measure the DPPH free radical scavenging activity and thus, the antioxidant activity of C-PC. The C-PC extracted from *Euhalothece* sp. was able to reduce the stable radical DPPH to the yellow-coloured diphenylpicrylhydrazine (Bermejo *et al*., 2008; Sonani *et al*., 2017).

The DPPH radical scavenging activity of C-PC solution at different concentrations is shown in Figure 40A. A gradual increase in the scavenging activity of DPPH- radical was observed with an increase in C-PC concentration. The IC_{50} value was found to be 0.540 ± 0.02 mg/mL which is slightly higher than the positive control ascorbic acid. It clearly indicated the dose-dependent antioxidant activity of C-PC with a >90% DPPH-scavenging activity at 0.080 mg/mL. whereas the positive control ascorbic acid showing 88% scavenging at the same concentration. The results clearly indicated proton donating- and free radical scavenging activity of C-PC. Antioxidant capacity of standard compound (ascorbic acid) is shown in Figure 40B.

DPPH is a stable radical consisting of a nitrogen atom at the centre of the molecule. If the test substance can scavenge DPPH radical, it should effectively lower the concentration of –OH, alkane or peroxy radicals (Wang *et al.* 2016). The positive results in DPPH together with RP assays suggests that the C-PC's antioxidant activity is contributed by both reducing the oxidised metal ions as well as through scavenging the already produced ROS *via* a redox reaction (Zhan-Ping *et al*., 2005). Zhou *et al*. (2005) reported that under light conditions the ability of C-PC to eliminate hydroxyl radicals was much lower in the light. Since C-PC generates –OH radicals in the light rather than eliminating them.

Since C-PC can scavenge the free radicals like DPPH, this clearly indicates that the C-PC has the proton donating ability. C-phycocyanin has significantly higher donating ability ($p < 0.05$) (Figure 40) and a slightly lower reducing ability (Figure 41) than that of ascorbic acid. The DPPH radical scavenging activity of C-PC from *Geitlerinema* sp. TRV57 was found to be 78.75% at 0.2 mg/mL (Renugadevi *et al.*, 2018). Cys was reported to be most active antioxidant amino acid possibly due to the formation of strong disulfide bonds in the molecules (Zhang *et al.*, 2016a). The amino acids are a key factor in the peptide and proteins ability to scavenge radicals, thus play a crucial role in antioxidant activity of the proteins.

The antioxidant capacity of peptides are closely related to some their structural characteristics (molecular mass, amino acid compositions, sequences, and hydrophobicities) (Zou *et al.*, 2016). Garrett *et al.* (2014) reported that the presence of beneficial antioxidant chemical groups resulted in increased antioxidant activity of the molecule. Zou et al. reported that a high proportion of hydrophobic amino acids are found peptides with high antioxidant activity, compared to other hydrophilic amino acids, which is considered as the key factor in the ability to scavenge radicals.

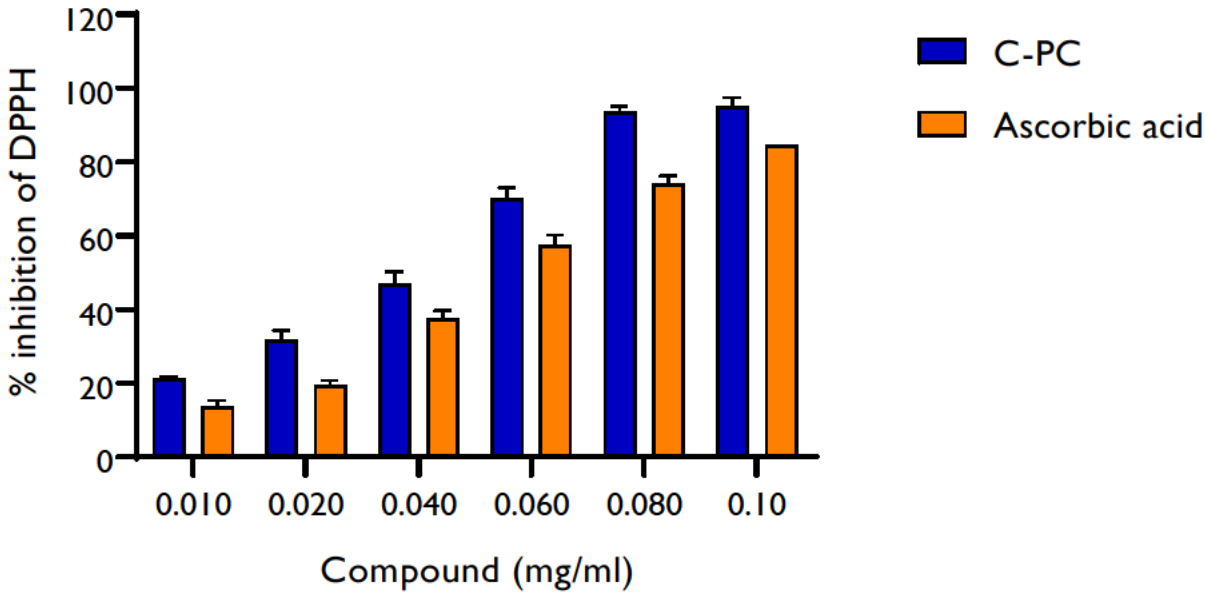

Figure 40: The DPPH-radical scavenging activity of varying concentrations of (A) C-PC, (B) positive control ascorbic acid. Data were expressed as mean of percentage inhibition ± difference of the mean.

Furthermore, the reducing ability significantly contributes to an antioxidant potential of any compound; hence the reducing ability of C-PC was analysed using the RP assay. In this assay, the ability of C-PC to reduce Fe^{3+} to Fe^{2+} was determined by measuring the formation of Perl's Prussian blue (Fe^{2+}-complex) at 700 nm (Sonani *et al.*, 2014). The increase in absorbance at 700 nm (Figure 41) indicated that the concentration of C-PC played a role in reducing ability. The RP assay signified the possible presence of high amount of amino acids that have reducing ability. These results demonstrated the efficient correlation between reducing power and antioxidant activity of C-PC. From the study, C-PC isolated from *Euhalothece* sp. does have radical scavenging and antioxidant potential and it is suggested that possible application of C-PC as immune-enhancer that can be of great importance to develop novel health products.

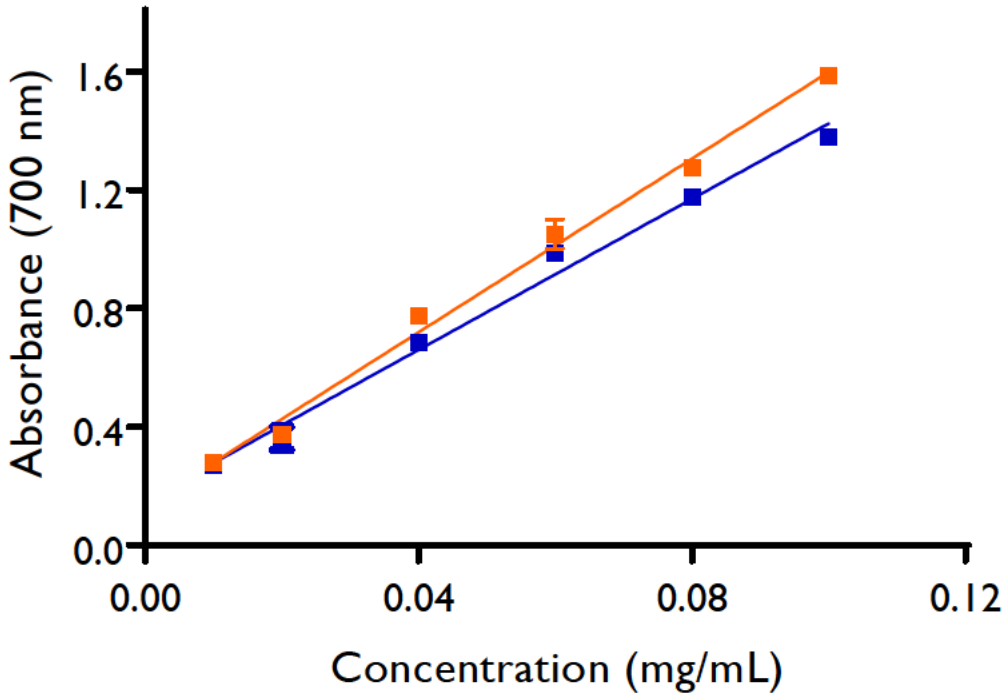

Figure 41: The RP activity of varying concentrations of C-PC (blue line) and positive control ascorbic acid (orange line). Reducing power of PC corresponded to their doses at 700 nm. Data were expressed as mean of percentage inhibition ± difference of the mean. Assays were done in triplicate (*n*=3).

The C-PC consists of > 70 % of non-polar amino acids, of which Ala, Arg, Gly, Leu, Pro and Ser account for 45% of the protein structure as seen in Figure 30. It is further reported that the antioxidant capacity could be enhanced notably by the presence of three aromatic amino acids *i.e.* Trp, Tyr and Pro. C-PC is found 7.65% of Pro and 4.93% Tyr, however a low Trp

(0.80%). Furthermore, the pyrrolidine ring and indole in Pro and Trp, respectively, has been reported to act as hydrogen donors *via* their hydroxyl groups, therefore serving as hydroxyl radical scavengers (Eckert *et al*., 2018). The linker protein, LRpc8.10 is made up of 40 Pro amino acids which accounts for 50% of the structure. Moreover, the antioxidant activities of PBPs are attributed to metal ion chelation or proton donation which depends largely on the amino acid composition. Acidic, basic and aromatic amino acids are known to facilitate the removal of metal ions (Kim et al., 2018).

The metal chelating ability of the PBP involves the formation of metal ion complexes through their binding ability with metal ions through two or more binding sites. Thus, the presence of certain functional groups such as carboxyl (COOH), sulphate (SO_2^{-4}), hydroxyl (OH), sulfhydryl (SH) and amide groups ($CONH_2$) could possibly facilitate complex formation and metal binding capacity. Moreover, the quantity of functional groups in the protein plays a crucial role to express effective chelation and scavenging activities. The C-PC subunits and linker sequences had a high content in Ala. Likewise, proteins with a high amount of hydrophobic amino acids compared to other hydrophilic amino acids have been reported to possess a high antioxidant activity (Masek *et al*., 2014; Zhang *et al*., 2016) Moreover, (COOH), sulphate (SO_2^{-4}) group can increase the chelating ability by increasing the acidic level resulting in the removal of free radicals. The presence of OH, –COOH, CO and -O- are responsible for its scavenging property through stronger activation of hydrogen atoms and higher water solubility.

The negatively charged amino acids *i.e.* Glu and Asp of the subunits of C-PC chelate the metal ions. Moreover, the hydrophobic amino acids are good proton donors as well as chelators of metal ions. The ring structure of histidine and carboxyl, as well as the amino groups in the side chains of acidic and basic amino acids, are thought to a play an important role in metal ion sequestration (Sonani *et al.* 2014). Additionally, C-PC has three PCB which contain long conjugated double bond system enabling them to be good electron exchanger. Therefore, the PCB chromophores attached to C-PC are proposed as a second possible source of C-PC's antioxidant activity.

6.3.6 Effect of pH and Temperature on C-PC Stability and Antioxidant Activity

Numerous factors contribute to a protein's structure and function (Alberts *et al*., 2002). The stability of these bilin chromophores can provide vital information regarding the structural stability of C-PC when exposed to various stress factors (Patel *et al*., 2018). Furthermore, the properties determine the application of the C-PC. Thus, in order to evaluate the potential application of C-PC for industrial or commercial purposes, the stability and behaviour of purified C-PC when exposed to change in pH, temperature and oxidation were assessed (Pan-utai & Iamtham, 2019; Wu *et al*., 2016b).

The stability of C-PC solutions at six different pH values was evaluated, the changes in C-PC spectra in response to pH are displayed in Figure 42A. The C-PC remained fairly stable in pH 5.0- 7.0 solutions. However, reductions in the absorption (A_{620nm}) of C-PC were observed as the buffer pH decreases in n very acidic (pH 4.0) and alkaline (>pH 8.0) environment respectively (Figure 42B). At pH 4.0, C-PC was less stable, and a decrease in absorbance was observed after 1 h incubation. In acidic solutions the C-PC structure is unfolded, resulting in protein precipitation (Wu *et al*., 2016b). This clarifies why the C-PC solutions at pH 4.0 exhibited lower intensities at 620 nm. Similar results of stability towards pH have been reported for other C-PCs. (Wu *et al.* 2016) and (Patil *et al*., 2008) reported that in acidic solutions (pH ≤ 4.5), the C-PC structure is unfolded, resulting in protein precipitation. Additionally, the spectral properties of C-PC are highly pH-dependent (Cai *et al*., 2014). (Liu *et al*., 2009) reported that in the pH range 3.5–10.0, the aggregation state of PBPs were maintained and at lower pH levels the PBPs dissociated into individual subunits and partial unfolding of subunits occurred. It was observed when C-PC was incubated at pH 9.0, the pigment lost its bright blue colour within the first hour. The loss of colour of the C-PC is due to the degradation of the protein fraction and absence of intact proteins, which helps makes the PBS stable (Seo *et al*., 2013).

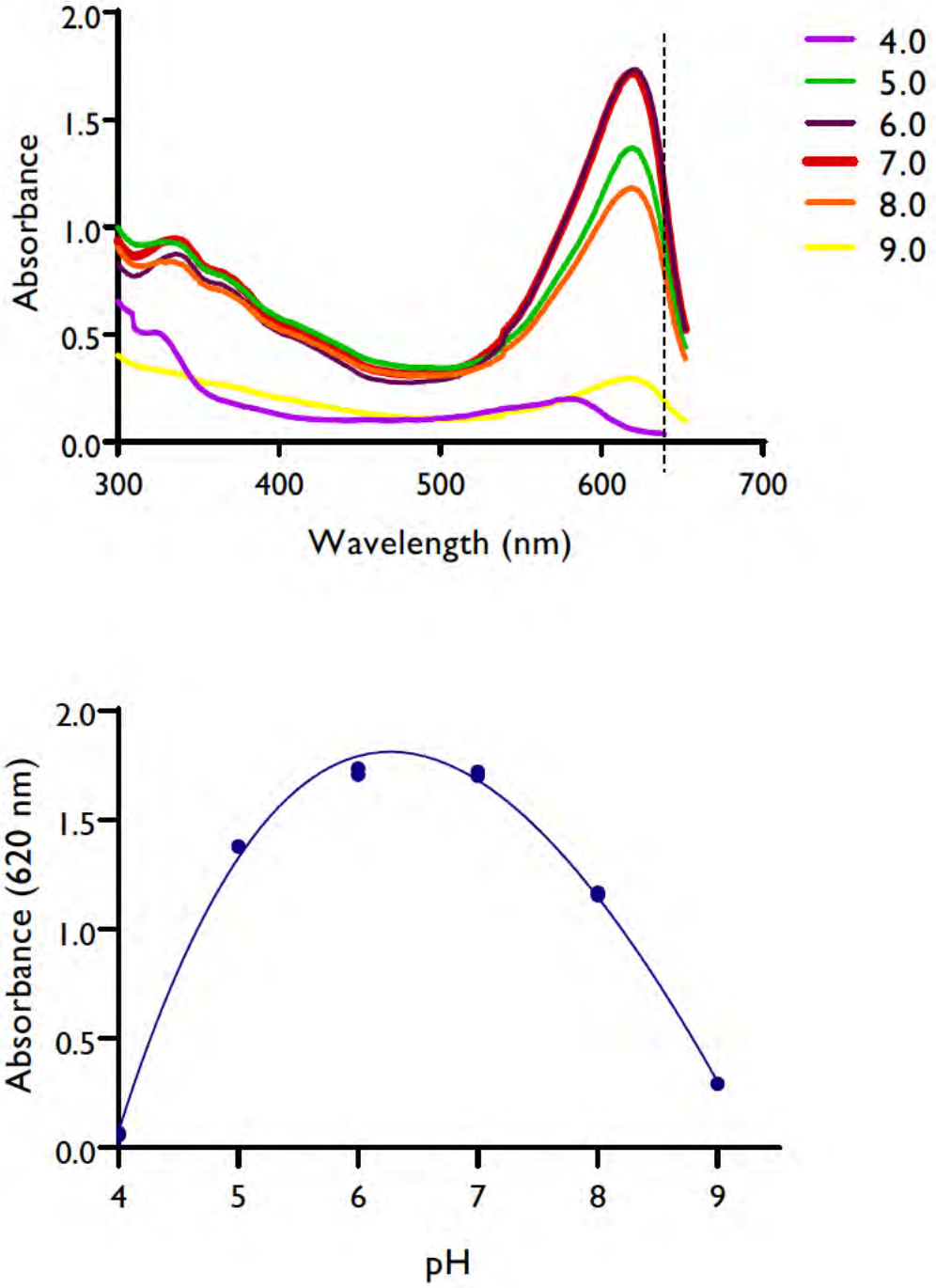

Figure 42: (A) Absorbance spectra from 300-650 nm of C-PC, (B) Absorbance of C-PC at 620 nm when exposed to varying pH.

At pH 4.0 and 9.0 the concentration of the C-PC decreased by ~30 and 50% respectively from the initial concentration after incubating for 2 h (Figure 43). After 24 h of incubation in the different pH, the C_R value of the C-PC solution at pH 9.0 significantly decreased ($p <$

0.05). Similar results were observed for pH 4. 0. The purified C-PC has stronger functional stability in the pH range of 5.0–8.0. There were no significant differences between the C-PC A_{620nm} results at pH 6 and 7.0 ($p > 0.05$).

C-Phycocyanin has been reported to be highly stable near-neutral pH (Chaiklahan *et al*., 2011). As the pH increases from the pI, the C-PC becomes more soluble due to the increase in electrostatic repulsion that decreases the aggregation and subsequent precipitation of the compounds (Orta-Ramirez *et al*., 2000). The pI is an important property since the protein is least soluble at the pH near this point and thus unstable. The net charge on a protein is zero at the pI, positive at pHs below the pI, and negative at pHs above the pI (Shaw *et al*., 2001). It should be noted that both below and above the pI the protein will be soluble. As previously reported in Chapter 3, the pI of a protein also assists when purifying the protein. The pI of c-pcA and c-pcB was 6.0 and 5.0 respectively, which is a high value. Linker peptides are positively charged with an pIs are >pH 9.0 (Table 34). In contrast, the C-PC are extremely water-soluble and are negatively charged at physiological pH. Between pH 5.0 and 8.0 at room temperature, the purified C-PC fraction was stable; more than 85% of the protein stayed in solution for 24 h. Furthermore, adaptation to an alkaline environment is due the increased number of Arg and neutral hydrophilic residues such as His, Asp and Glu, in turn a decrease of negatively charged amino acids and lysine residues as seen in Table 30 (Suplatov *et al*., 2014).

The pH value is one of the main factors controlling C-PC aggregation and dissociation to form monomers, trimers, hexamers and other oligomers in solution (Chaiklahan *et al*., 2012). C-Phycocyanin predominantly exists as a hexamer at pH 5, and it is believed that the hexametric form gives some protection against denaturation (Rahman *et al*., 2017). At pH >7.0, it is predominantly in a monomeric or trimeric form, resulting in lower thermo-stability (Edwards *et al*., 1997). Extreme changes in pH results in the disruption of electrostatic properties and hydrogen bonds involved in protein assembly, which induces changes in chromophore structure (Munier *et al*., 2014; Sua *et al*., 2014). The structural properties of the proteins suggested an increase in protein stability as its mode of adaptation to the environmental stress of high temperature.

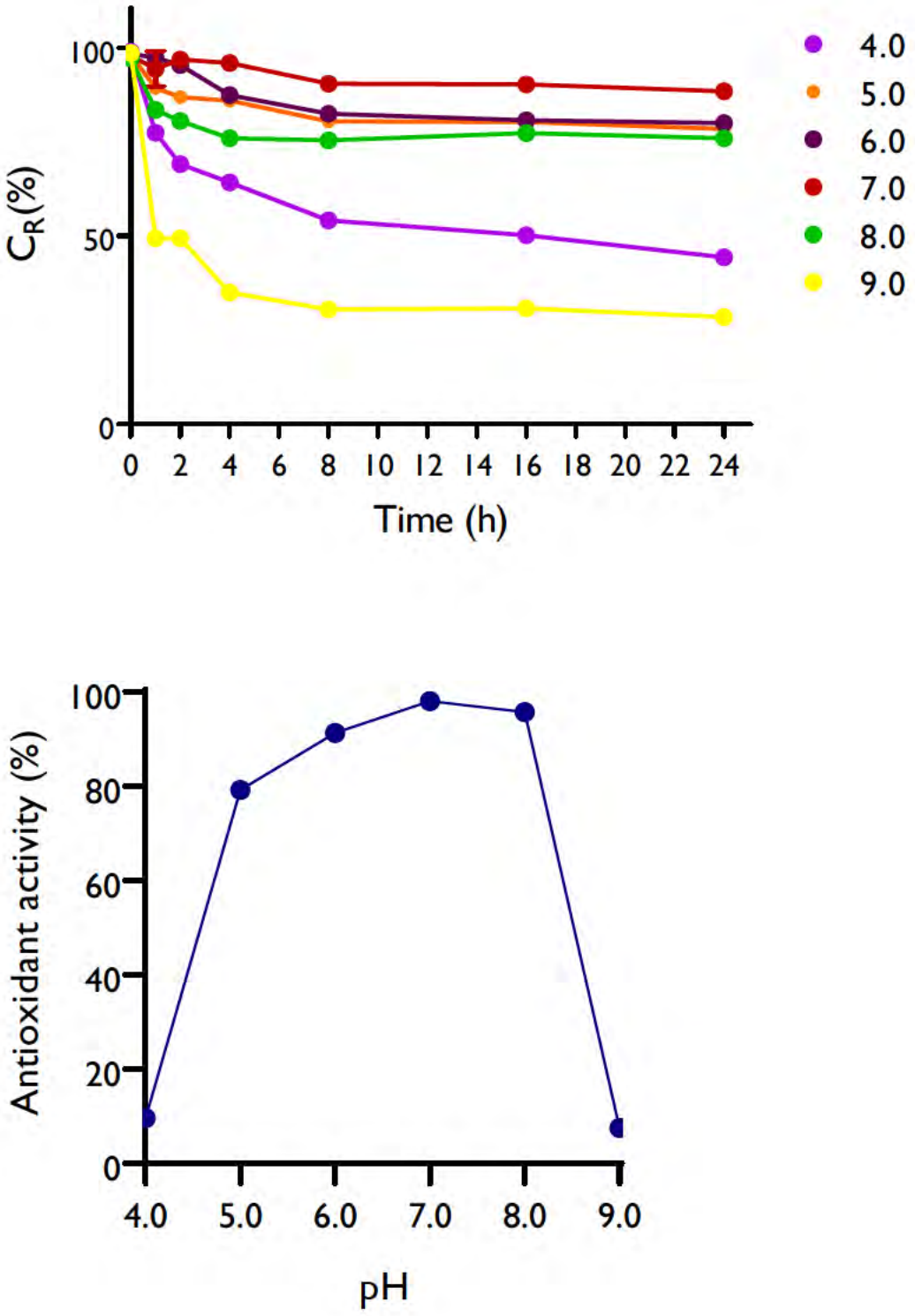

Figure 43 : (A) Effect of increasing pH on the solubility (C_R %) of C-PC over 24 h incubation period at 25°C, (B) Antioxidant activity of C-PC at varying pH.

It is well known that temperature also plays an important role in the stability of C-PC and greatly affects the structure of the protein (Leu *et al*., 2013). Since *Euhalothece* sp. can grow at relatively high temperatures up to 45°C (Mogany *et al*., 2018a), it is to be expected that the C-PC is relatively thermostable.

Thermostability of proteins results from a combination of several factors acting synergistically. The Ai values determined ranged from 48.69 to 81.70, this indicates the flexibility at a wide range of temperatures. Protein molecular adaptations to temperature are partially known to be based on specific substitutions of amino acids, with Gly, Ser, Lys and Asp in mesophiles, commonly replaced by Ala, Thr, Arg and Glu in thermophiles respectively (Pittera *et al*., 2017). As shown in Table 35 the amino acid content of each polypeptide revealed that C-PC subunit and linker sequences had a significantly higher content in Ala (Figure 30). It has been reported that the Ala accumulation in proteins increases hydrophobicity and thus decrease molecular flexibility, especially since this amino acid is an excellent helix former.

The thermal stability of the C-PC from *Euhalothece* sp. was examined by measuring the C-PC absorbance (peak at 620 nm) and C_R at temperatures ranging from 25 to 65°C (Figure 44) and compared with its DPPH scavenging activity (Figure 45). The C-PC was stable at 25°C, and up to 45°C also showed good stability. However, with a further increase in temperature degradation of C-PC was observed. C- There was a shift in the absorption spectrums at high temperatures and a slight loss in absorption (Figure 44). C-Phycocyanin lost its colour and the spectra after treatment at 50°C showed the decrease of an absorption peak at 620 nm.

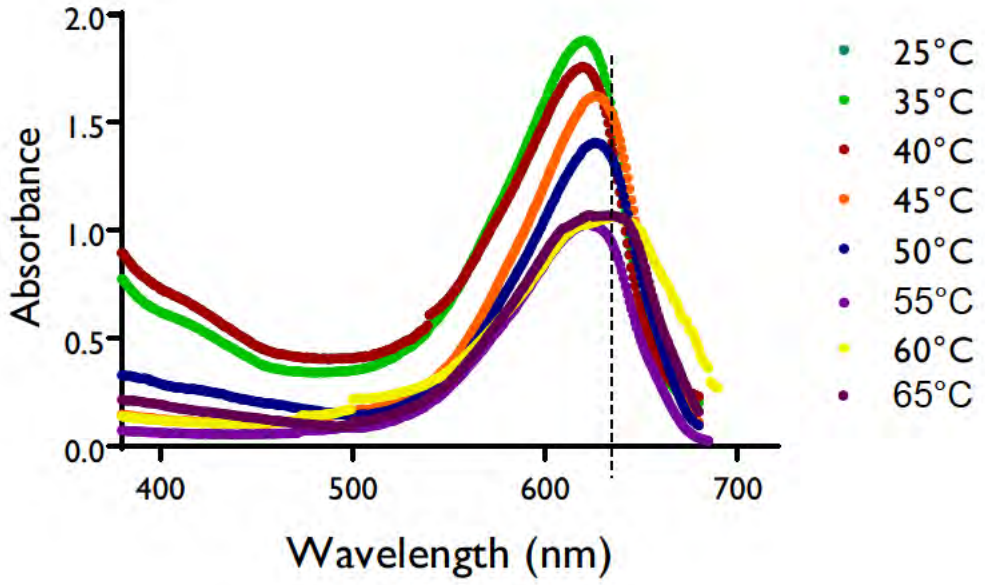

Figure 44: Absorbance spectra of C-PC when exposed to varying temperatures at pH 7.0.

After 2h incubation at 45°C, 80% of C-PC remained in solution. At pH 7.0 further increase up to 50°C, the C-PC solubility slowly decreased, and a loss of the blue colour was observed. At higher temperatures up to 60°C, a significantly decreased of the C-PC concentration in pH 7.0 solution was observed ($p < 0.005$). It was revealed that C-PC thermal stability was found to be correlated with its DPPH scavenging activity. Both C-PC and its antioxidant activity (±80%) was relatively stable at 45°C for 2 h. The AP results (%) when the C-PC was exposed to the varying temperatures are displayed in Figure 45. There was a statistically significant decrease ($p < 0.05$) in the AP obtained with an increase in temperatures.

The assembly level of oligomeric C-PC can be stabilised in thermophiles by additional ionic interactions at critical positions on the association interface of PBPs structures *via* amino acid residue substitutions (Adir *et al.*, 2001; Pumas *et al.*, 2011). The thermostability of proteins results from a combination of several factors acting synergistically. Protein molecular adaptations to temperature are partially known to be based on specific substitutions of amino acids, with Gly, Ser, Lys andAsp in mesophiles, commonly replaced by Ala, Thr, Arg and Glu in thermophiles respectively (Pittera *et al.*, 2017). Moreover, Cys residues (α-Cys84 and β-Cys82, β-Cys 109 and β-Cys 154) are essential for establishing the thermostability of proteins. The disulfide bonds that connect these Cys residues are important in the protein folding and

stability, which are generated between the thiol groups of Cys residues by the oxidative folding process (Fass, 2011).

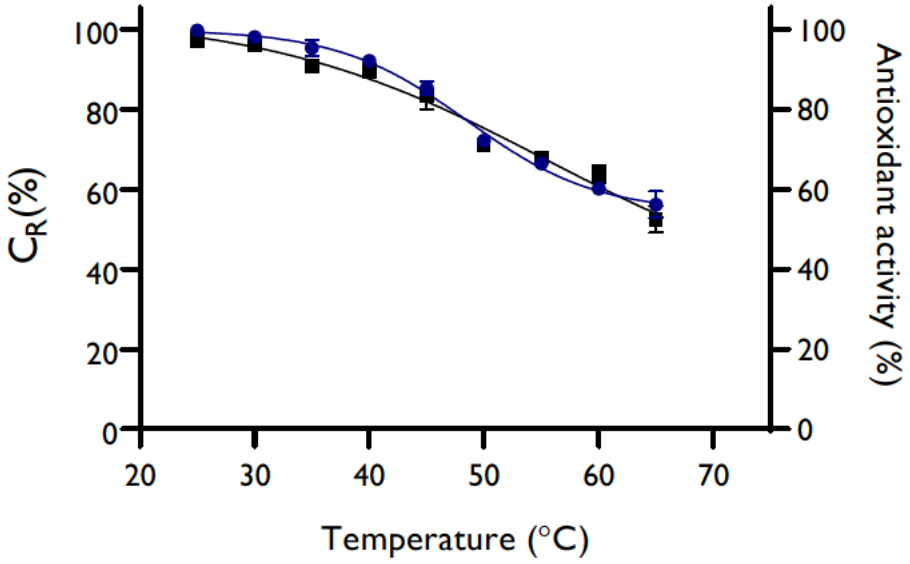

Figure 45: Solubility and antioxidant potential (%) of C-PC stored with exposure to temperatures ranging from 25 to 65°C (n = 3 ± standard deviation).

Aliphatic index (Ai), is defined as a relative volume of the protein occupied by aliphatic side chains *i.e.* Ala, Val, Ileu, and Leu. This is considered as a positive factor for the increase of the thermal stability of spherical proteins (Patel *et al.*, 2018). Studies conducted by Arun *et al.* (2012); Fujiwara *et al.* (2012) and Idicula-Thomas & Balaji (2007) show that there is a positive correlation between the structural stability and aliphatic amino acid content of proteins thermostable proteins have a high content of Ala, Val, Ileu, or Leu, furthermore, the hydrophobicity of aliphatic amino acids is potentially used to measure the stability of proteins at high temperatures as well as against denaturants such as urea (Ikai, 1980). As seen in Table 33, the subunits and linker proteins consist of a high content of these aliphatic residues. Aliphatic index values of α- and β-subunits are 75.56 and 81.22 respectively, which indicates proteins stability for a wide temperature range. This was proven by the experiment of

temperature effect of protein. These values give the instability value of 27.25 and 38.83 for these proteins, respectively. It has been reported that the Ala accumulation in proteins increases hydrophobicity and thus decrease molecular flexibility, especially since this amino acid is an excellent helix former.

Munier *et al.* (2014) reported that when the temperature rises, the amount of α helix decreases, resulting in the loss of stability of C-PC. The stability of the protein is predicted using the instability whereby an instability index <40 indicates that the proteins have an in vivo half-life of >16 h, whereas >40 means that proteins that have an in *vivo* half-life of <5 h. Therefore, a protein whose instability index is larger than 40 may be unstable. The values give the instability value of cpcA and cpcB are 27.25, respectively. Thus, this indicates that these proteins are stable. The linker proteins LRpc32 and LRC28.5 are moderately stable with an instability index of 36.28 and 40.65, respectively. However, the LR 8.1 was unstable (85.76). there is a relatively low frequency of unstable amino acids Met, Gln, Pro, Glu and Ser in the α- and β-subunits and LRpc32(Table 30). However, LR8.1 has a high number of Glu. Results showed that the antioxidant activities were stable up to 45°C. This suggests that the decrease of antioxidant activity is due to the denaturation of the C-PC structure.

The combined effects of both factors (temperature and pH) on purified C-PC was also analysed. Results indicate that C-PC from *Euhalothece* sp. is stable between 25– 45°C (Figure 45) in all pH solutions. At 45°C, the C_R values of the C-PC solutions at pH 5.0, 6.0, 70 and 8.0 were ~ 83, 90, 86 and 75% of the initial values, respectively, whereas at 60°C the CR values decreased to 50-60% (Figure 45). Similarly, Chaiklahan *et al.* (2011) observed a slow rate of C-PC degradation at 26-43°C, however, turbidity was evident due to microbial growth in natural pigments. The C-PC solution was highly stable at higher temperatures 45-55°C in pH 6.0. At higher pH values the C-PC hexameric structure dissociates to trimers. It has been previously reported that at pH 6.0, the hexameric, form of C-PC made up 77% of the protein with the remainder being trimeric, whereas, at pH 7.0, 82% of C-PC was trimeric (Wu *et al.*, 2016b). In this study, the hexameric form possibly dominated in the C-PC solution at pH 6.0, resulting in the higher stability observed.

The degradation followed first-order kinetics. At 55°C, C-PC was found to be more stable at pH 6.0, between 60-65°C, C-PC was stable in pH 5.0. With the temperature increase C-PC becoming decreasingly stable at pH 7. Similar results were reported by (Antelo *et al.*, 2008) who indicated with a temperature increase, C-PC was increasingly unstable at pH 7, However,

between 50-55°C C-PC was more stable at pH 6 and between 57-65°C at pH 5. Furthermore, our results were also consistent with the findings of Wu *et al.* (2016), who found that at 65°C, pH 5.0 and pH 5.5 and 6.0 at 55°C, C-PC was more stable.

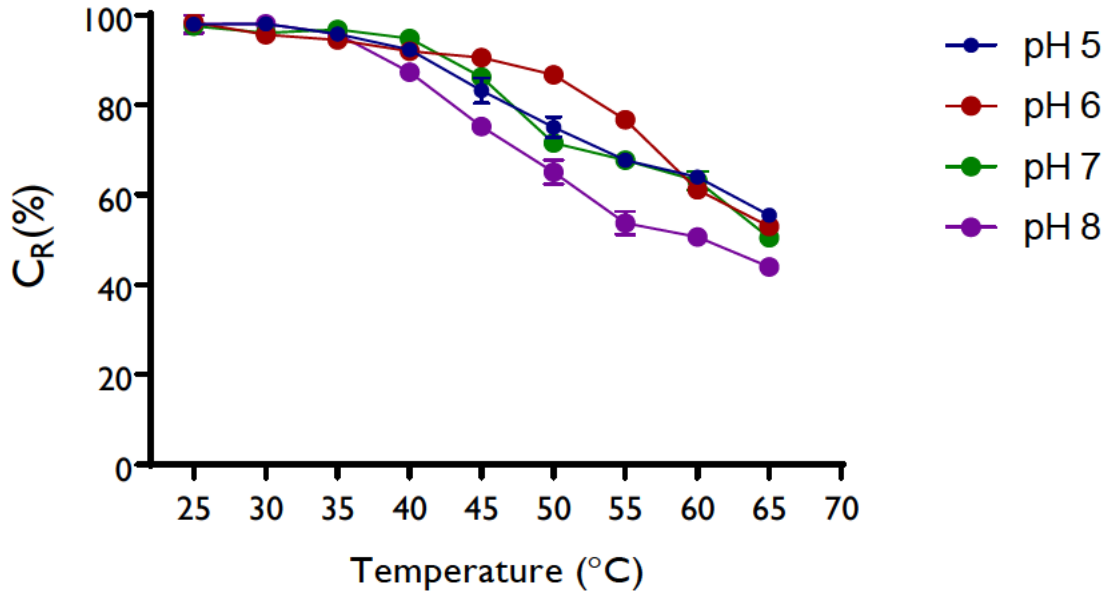

Figure 46: The solubility C-PC stability in pH 5.0-8.0. exposed to varying temperatures.

6.3.6.1 Effect of storage temperature of C-phycocyanin

At lower temperature, C-PC was stable for longer periods than at room temperature. The stability of C-PC during storage at 4 and 25°C in darkness was studied in order to determine how long C-PC can be stored before pigment degradation occurs. Storage at 4°C is the conventional method recommended to preserve pure C-PC (Chaiklahan *et al.*, 2012). As seen in Figure 46, C-PC showed good stability at 4°C, with a minimal loss (20%) of C-PC when the solutions were refrigerator for 42 days. However, at 25°C after 21 days of incubation the C_R of C-PC significantly declined ($p < 0.05$). A 50% decrease in the yield was observed when the C-PC was stored at 25°C for to 52 days. Similarly, Kannaujiya & Sinha (2016) reported that C-PC extracted from *Nostoc* sp. HKAR-2 remained stable up to 30 days when kept at 4°C, whereas C-PC was only stable for 7 days when kept at 25°C. Thus, a lower temperature (4°C) helped maintain the stability of the C-PC for longer periods.

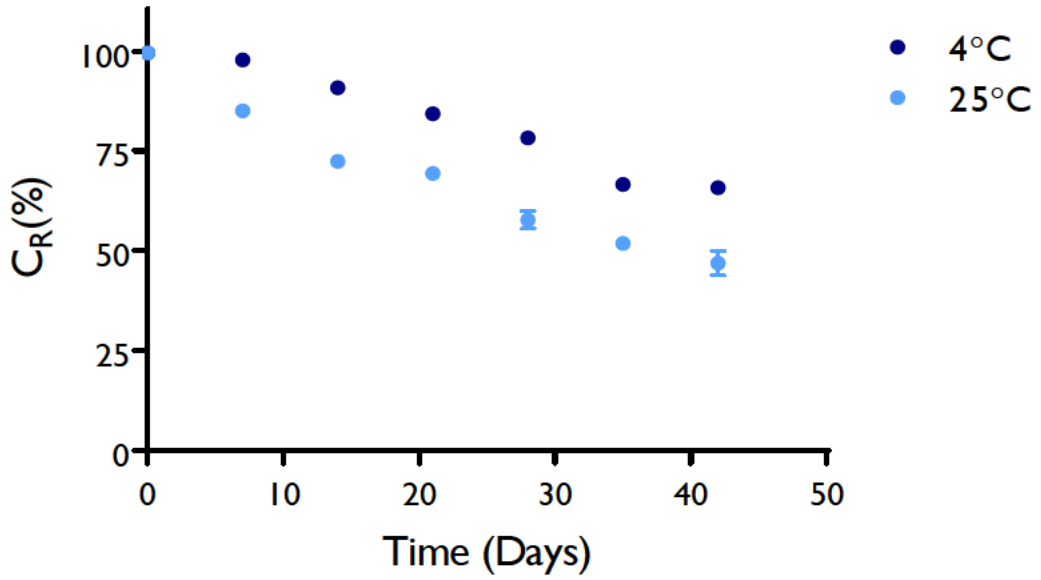

Figure 47: The solubility of C-PC at 4°C (black circles) and 25°C (white squares) for 42 days.

Table 33: Antioxidant activity of C-PC after 42 days of incubation at two storage temperatures

Time (Days)	Antioxidant potential (%)	
	4°C	25°C
0	93.2 ± 0.17	93.2 ± 0.17
7	91.1 ± 0.04	83.0 ± 0.04
14	90.5 ± 0.31	79.6 ± 0.02
21	89.9 ± 0.23	61.9 ± 0.90
28	85.0 ± 0.04	57.0 ± 0.05
35	78.4 ± 0.23	48 82 ± 0.08
42	75.9 ± 0.90	37.7 ± 0.19

6.3.7 Effect of an Oxidising Agent on C-phycocyanin

Hydrogen peroxide is a strong oxidising agent, it is not reactive, but it can be toxic to cell molecules due to the formation of hydroxyl radical in the cell. The C-PC was exposed to different concentration of hydrogen peroxide (H_2O_2), a well-known oxidative stress inducer. The C-PC yield decreased with increasing concentration from 0.2 to 1.0% H_2O_2. C_R % of C-PC was decreased by 25% at 0.4% and a 40% decrease at 1.0% H_2O_2. The addition of H_2O_2 can create oxidative stress through increased production of reactive oxygen species

(ROS). Sonani *et al.* (2017) indicated that oxidative stress does not significantly affect the apoproteins (*αβ* subunits) or PCB, however, some of apoprotein residues undergo oxidation that causes small changes in the protein folding. C-PC has potential as an antioxidant agent due to its stability under oxidative stress. The C-PC yield significantly decreased when exposed to > 0.6% H_2O_2 (Figure 48), accompanied by the change in blue colour, however, the antioxidant activity was consistent (Table 35). C-Phycocyanin exhibits radical scavenging activity in dark environments, though it generates hydroxyl radicals in light environments. Zhou *et al.* (2005) reported that the denaturation of C-PC proteins can completely diminish –OH radical production while radical scavenging activity continues. Thus, it is possible that PCB, itself, functions as an antioxidant while apoproteins functions as a pro-oxidant (Wada *et al.*, 2013).

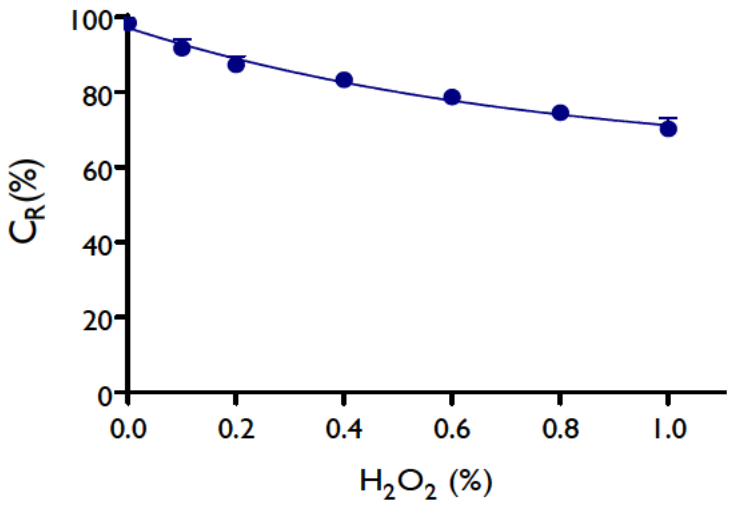

Figure 48: Effect of varying H_2O_2 concentration on the C-PC yield. Mean values S.D., n = 3. Significant differences from the control values were indicated with a $p < 0.05$.

Table 34: Antioxidant potential of C-PC after 2h exposure to varying H_2O_2 concentration

H_2O_2 concentration (%)	Antioxidant potential (%)
0	96.3 ± 0.29
0.1	94.9 ± 0.52
0.2	89.56 ± 0.43
0.4	86.34 ± 0.30
0.6	81.12 ± 0.85
0.8	78. 82 ± 0.88
1.0	77.67 ± 0.26

6.3.8 Effect of Preservatives on C-phycocyanin

To help prevent C-PC denaturation owing to chemical changes, stabilising agents are often used as preservatives to protect the structure of the protein chains. Antimicrobial agent NaN_3 and the protein reducing agent DTT are commonly used as preservatives in PC for analytical purposes (Chaiklahan *et al*., 2012; Wu *et al.,* 2016). Similarly, food-grade preservatives such as glucose sodium chloride, ascorbic acid and sodium citrate have also been used (Mishra, Shrivastav and Mishra 2008). To enhance the storage stability and maintain the quality of C-PC four preservatives were used in this study (Table 36). The results have shown NaN_3 +EDTA > sodium citrate > sodium chloride respectively and these were suitable for C-PC stability. Sodium azide acts as an antimicrobial agent inhibiting bacterial growth and EDTA a chelating agent; thus, it is being used to preserve. Sodium citrate also acts as a chelator and lowers the pH preventing the degradation of C-PC (Mishra *et al.* 2010).

The loss of C-PC with and without the preservatives at 4°C is less than 25°C. With preservatives a 15-18% loss in C-PC was found at 4°C, is very less, while at 25°C the C-PC content loss is 18–28% after 42 days as shown in Table 36. Mishra *et al.* (2008) found that $CaCl_2$ and sucrose were also found to be effective in maintaining the stability of C-PC at 4°C, whereas citric acid was the best preservatives for C-PC at 25°C. Similar results were observed in this study, whereby at 25°C the loss of C-PC was the least when sodium citrate was used. The addition of citric acid is reported to decrease the pH of the C-PC from 7.0 to 5.7, at higher temperatures a lower pH value *i.e.* pH 5.0 is known for maintaining the stability C-PC (Chaiklahan, Chirasuwan and Bunnag 2012). The loss of C-PC in aqueous solution with preservatives at 4°C is significantly less than at 25°C ($p < 0.05$). Loss of C-PC content observed after addition of NaN_3 at 4°C is < 5% while at 25°C the C-PC content loss is ±28% after 42 days. C-Phycocyanin in the aqueous phase was found to be more stable with sodium citrate as a preservative at 25°C.

Table 35: C_R values of C-phycocyanin with and without preservatives incubated at 4 °C and 25°C for 42 days

Temperature (°C)	Sample	Time (Days) 0	7	14	21	28	35	42
4	Control	100.00	98.52 ± 0.64	98.02 ± 0.69	95.34 ± 1.45	89.73 ± 0.76	85.86 ± 0.78	80.38 ± 1.61
	Sodium azide	100.00	99.91 ± 0.37	99.13 ± 0.95	97.92 ± 0.89	97.94 ± 1.34	96.34 ± 0.98	95.37 ± 2.34
	Sodium chloride	100.00	98.21 ± 0.47	98.13 ± 0.67	96.98 ± 1.76	90.96 ± 1.98	88.35 ± 1.12	87.37 ± 1.07
	Sodium citrate	100.00	98.78 ± 0.67	98.78 ± 0.56	97.78 ± 0.98	96.98 ± 0.45	94.34 ± 0.87	95.34 ± 0.92
25	Control	100.00	81.18 ± 0.51	77.63 ± 0.95	73.63 ± 0.43	67.93 ± 1.23	60.65 ± 2.26	55.14 ± 1.01
	Sodium azide	100.00	88.76 ± 0.23	82.90 ± 0.93	80.35 ± 0.53	72.60 ± 1.37	72.16 ± 1.42	72.08 ± 0.68
	Sodium chloride	100.00	88.15 ± 0.91	79.83 ± 1 .65	78.84 ± 1.45	62.93 ± 0.98	60.80 ± 2.01	62.98 ± 2.56
	Sodium citrate	100.00	85.74 ± 0.98	82.95 ± 1.23	80.35 ± 0.56	78.70 ± 0.91	78.87 ± 1.87	78.38 ± 1.03

6.4 CONCLUSIONS

The maximum fluorescence emission of purified C-PC is observed at 640 nm which confirmed the integration of protein-chromophore interaction. Computational analysis of the genes highlights its molecular features including its primary and secondary structural features as well as physicochemical features and major structural elements. The 3D structures assists in understanding chromophore-protein interactions. Amino acid sequences analysis of *Euhalothece* sp. C-PC displayed several important amino acid substitutions that potentially could play a significant role in protein stability. *In silico* analysis and physicochemical properties of the C-PC amino acids were correlated to the thermostability and antioxidant activity of the protein. The purified C-PC is relatively thermostable at a pH range from 5.0-8.0 with high antioxidant activity. The high content of non-polar, hydrophobic and aromatic amino acids positively contributed to the high antioxidant activity (IC_{50} value for DPPH assay was 0.540 ± 0.02 mg/mL). The purified C-PC is relatively thermostable at a pH range from 5-8 with high antioxidant activity (> 90% DPPH scavenging activity) and comparable acid-reducing power to that of ascorbic acid. At higher temperatures of 50 and 55°C, C-PC is found to be stable at pH 6.0 and 5.0 respectively, this indicates an inversely proportional relationship between the temperature and the pH. In addition, preservatives such as NaN_3 + EDTA and citric acid enhances the thermal stability of C-PC. Due to its protein nature, inherent brilliant blue colour, and antioxidant characteristic the C-PC extracted from novel *Euhalothece* sp. has the potential to be used in analytical applications, including pharmaceutical and biomedical research.

CHAPTER 7 : CONCLUSIONS AND RECOMMENDATIONS

7.1 CONCLUSIONS

C-Phycocyanin is a light-harvesting, water soluble pigment bound protein with several biotechnological applications. This study focused on i) characterisation and full genome analysis of a unique indigenous cyanobacteria with high C-PC content and ii) to develop a cost-effective method for the extraction of high purity C-PC from cyanobacteria. The strain was considered as a potential candidate for C-PC production because of their rapid growth rate, relatively high C-PC yield, and grow in a wide range of environmental conditions (temperatures up to 45°C, salinity >120 g/L, pH range between 6.0-9.0). The study contributes to our understanding of molecular, cellular and biochemical mechanisms of the C-PC biosynthesis as well as newly identified metabolites in cyanobacteria. The study also demonstrates an efficient and extraction method for analytical grade C-PC from cyanobacterial strains for industrial applications. The major conclusions drawn from the study are:

- According to morphological traits *i.e.* blue-green, unicellular, ovoid to rod-shapedd cells ~14–18 μm in size, the isolate is classified to belong to Subsection I (order Chroococcales).
- Based on 16S rRNA gene sequence similarities, the strain is related to members of the form-genera '*Euhalothece*' subcluster (99%). The annotated genes from the whole-genome sequence show sequence similarity (90%) to the gas-vacuolate, spindle-shaped *Dactylococcopsis salina* PCC 8305. The size of the genome is 5,113,178 bp with 4332 protein-coding genes and 69 RNA genes with a G + C content of 46.7%. Based on the information obtained from the 16S rDNA analyses, whole-genome sequencing, and the morphological analyse (light microscopy, TEM and SEM), the isolate is likely a novel species within the genus *Euhalothece*.
- A total of 348 genes encoding proteins is assigned to cofactors, vitamins, prosthetic groups, and pigments COG category. The genome contains >100 genes to be dedicated to the synthesis and regulation of the photosynthetic apparatus with

complete sets of genes encoding for PSI (psaA,-B,-C,-D,-E,-F,-J,-K,-L,-I, Ycf3,-4, -37, BtpA and IsiA), PS11 (psbA,-B,-C,-D,-L,-J,-O,-P-K,-U,-V,-N,-I,-X,-Z,-27,-28), cytochrome genes (psbEF), assembly factors (ycf39 and ycf48).

- According to genomic results, the isolate is possibly capable of adjusting their cellular machinery and able to synthesise, store, degrade, and use and metabolic storage products which could have provided the added advantage for survival in hypersaline environment. The adaptation of *Euhalothece* sp. to the hypersaline environment is reflected at the genomic level. *Euhalothece* sp. genome contains 33 phage-related genes (phage integrases—enzymes), as well as 36 genes composed of mobile elements, transposons, and Group II intron-associated genes not found in the other hypersaline/marine cyanobacteria.
- The genome analysis shows that it contains the whole set of genes necessary synthesise C-PC and partial set of APC genes. A gene cluster that encodes the components of the central oscillator for circadian clock genes function *i.e.* kaiABC is present. The complete set of genes (12 genes; some with additional homologs) required for the Calvin cycle, as well as nitrogen fixation (Nif) gene cluster, consists of the 21 genes, similar to other nitrogen-fixing species. *Euhalothece* sp. and *Halothece* PCC 7408 both had similar nitrogen-fixing genes however, PCC8305 does not contain any nitrogen-fixing genes.
- A two-component regulatory system comprising a sensor kinase and a response regulator is an essential way for the isolate to sense and respond to the changes in environmental conditions, *Euhalothece* sp. has twenty-two genes for the histidine kinases (Hiks), two genes for serine-threonine protein kinases (Spks), 35 response regulator genes (Rres) and 4 genes for RNA polymerase sigma factors.
- One of the key stress adaptations of the isolate is the ability to maintain protein conformational homeostasis by molecular chaperones. Multiple genes are found for heat-shock proteins belonging to family of Hsp100, Hsp90, Hsp70, Hsp40 and Hsp20 which included dnaK, dnaJ, GroEL/S htpG and ClpB is present.
- More than three hundred transporter-related genes are found in the genome. Among these transporters, ABC transporters accounted for the majority involved in Na^+/H^+, Fe, P, urea specific to halophiles. Other transporter related-genes included amino acid, oligopeptides and CO_2 transport. *Euhalothece* sp. also has a larger number of efflux

transporters (multidrug efflux systems) in the ABC family as well as genes coding an antitoxin system.

- Molecular mechanisms of *Euhalothece sp.* for salt adaptation were identified. The genome has genes are involved in osmoregulation, transport and synthesis of compatible solutes, which includes choline-sulfatase (3 betC genes) and high affinity choline protein uptake proteins (9 genes), thus have the ability actively take up glycine betaine (GB) from the environment as well as synthesised GB.
- *Euhalothece* sp. genome has 11 gas vesicle proteins which included, gvpA, gvpC, gvp J and gvpM, which provide buoyancy to move between illuminated surface waters and nutrient-rich bottom of the water
- The genes associated with UV-absorbing secondary metabolites particularly mycosporine-like amino acid (mysB, mysC, mysT, mysD and NRPSm) and protective and photoreceptor pigments are identified. Thus, the isolate also has the potential to produce products of biotechnological interest such the suncreens, mycosporines, as well as isoprenoids.
- The C-PC extraction was carried out using six different buffers with varying concentrations (10 mM – 1 M) and pH values (5.0-9.0). Sodium phosphate buffer (SPB, 50 mM, pH 7.0) gave the highest C-PC yields (~38mg/g) with a purity ratio of 1.7. A combination of three freezing temperatures (-196, -80 and -20°C) and two thawing temperatures (4 and 25°C) were also investigated. Freezing at -20 and thawing 4°C proved to be the most effective temperatures for lysing the cyanobacterial cells and releasing maximum C-PC. Extraction with SPB (50mM, pH 7) was tested further by adding lysozyme to the sample, which resulted in an increase in C-PC yield and purity, however, the concentration of lysozyme did not have a significant effect on C-PC yield ($p > 0.05$). Higher biomass concentration resulted in higher C-PC yield and purity ratio; however, biomass: buffer ratio > 0.0300 g/mL affected the interaction between buffer and biomass.
- Using response surface methodology *via* central composite design the optimised protocol for the extraction resulted in 78 mg/g C-PC (purity 2.5).
- Purification was performed using stepwise precipitation using 30-60% $(NH_4)_2SO_4$, adsorption using 6% w/v active charcoal and ultrafiltration. A 60% recovery (472 mg/mL) of analytical grade (purity ratio 5) C-PC is achieved. Therefore, this extraction

and purification procedure is found to be suitable for small scale and an alternative for industrial scale from *Euhalothec*e sp.

- The purified C-PC showed an absorption peak at 620 nm and emission at 640 nm. From the SDS-PAGE, the C-PC shows two bands corresponding to the *α*- and *β*-subunits in the range of 18-20 kDa, based on the amino acid analysis calculated molecular weight of *α*- and *β*-subunits are 17.7 kDa and 18.4 kDa, respectively.
- The primary, secondary and tertiary structures of C-PC proteins including the *α*- and *β*-subunits were further evaluated based on genome sequences. Knowing the structure and physicochemical properties of proteins is of great importance for understanding the molecular mechanisms of these proteins improving stability and extraction of C-PC. The number of amino acid sequences (*i.e.*162 and 172 amino acid residues) of *α*- and *β*-subunits of C-PC from *Euhalothece* sp. were similar to other hypersaline cyanobacteria (PCC 8305 and PCC 7418), however a difference in the in *α*- and *β*-subunits composition was found. Amino acid sequences analysis of *Euhalothece* sp. C-PC displayed several important amino acid substitutions that potentially could play a significant role in protein stability.
- The 2D and 3D structures were also analysed in order to understand the chromophore-protein interactions. The secondary structure prediction of the *α*- and *β*-subunits consisted of > 50% of AA residues in α-helices, with 9-13% of AA residues in the extended strand. High-quality C-PC homology models were built based on crystal structures of known C-PCs from thermophilic *Synechococcus elongatus* (1jbo.1.A) with a high level of sequence similarity of 78.44% and GMQE 0.91.
- *In silico* analysis and physicochemical properties of the C-PC amino acids were correlated to the thermostability and antioxidant activity of the protein.
- The antioxidant activity of C-PC was investigated by using two different *in vitro* antioxidant assay such as DPPH radical scavenging system and reducing power.The DPPH radical-scavenging activities of C-PC increased in a concentration-dependent manner. Highest radical scavenging activity of 90% of C-PC at the dose at 0.08 mg/mL was achieved. Whereas, DPPH-scavenging activity of ascorbic acid was 85% at 0.1 mg/mL. Reducing power efficiency of C-PC was 85.15 ± 0.012% as compared to ascorbic acid at 150 *μ*g/mL. The results clearly indicate proton donating- and free radical scavenging- the activity of C-PC.

- Amino acids play a crucial role in the antioxidant activity of C-PC. For DPPH assay amino acid such as Asp, Asn, Thr, Val, Ile are positive contributors, is found to in abundance in the subunits and linker proteins.
- The stability and antioxidant activity of C-PC under different stress conditions such as temperature, pH and varying concentration of the oxidising agent, H_2O_2. The purified C-PC is highly stable at 4°C (ideal storage temperature), with an increase in temperature up from 25 to 40°C, C-PC also shows good stability.
- The purified C-PC (C_R=85%) is stable in solutions of pH 5.0 and 8.0 after 24 h incubation, however, pH 4.0 and 9.0 the concentration of the C-PC decreased by ~30 and 50% respectively after 2h of incubation. Aliphatic index for α- and β-subunits were 75.56 and 81.22, respectively, which indicates the subunits are stable for a wide temperature range. This was proven by the experimental results whereby, the purified C-PC was stable at 45°C in pH7.0, 50°C at pH 6.0 and 55°C at pH 5.0. These results also demonstrates that relationship between the temperature and the pH is inversely proportional.
- The incubation of the purified C-PC with the oxidising agent H_2O_2 led to a successive decrease in C_R with an increase in H_2O_2 concentration, and antioxidant activity of > 70% at the 1.0% H_2O_2. In addition, preservatives such as NaN_3 + EDTA and citric acid enhanced the thermal stability of C-PC.

7.2 RECOMMENDATIONS

- The large-scale purification of phycocyanin is still difficult and remains to be explored. The cyanobacteria, *Euhalothece* sp. appear to be particularly interesting for the production of such high-value pigments as it is capable of growth in high salinity media reducing the risk of contamination thereby curtailing the production cost. Feasibility of outdoor growth of the cyanobacteria for high-level production of these commercially important C-PC needs to be further investigated. Research and development of C-PC may also focus on expanding the application of C-PC from functional foods to higher commodity products such as drugs and medical diagnostic reagents for its deeper development based on the research results of C-PC

bioactivities.

- Since large-scale cultivation can be costly it would not be economically feasible to use complex medium for industrial-scale growth of *Euhalothece* sp. Replacing the synthetic components of the media with highly saline waste stream could contribute to a reduction of the cultivation costs. For future work it could be beneficial to investigate different modes of cultivation including comparisons between fed-batch and continues cultivation since this is an area where it might be possible to increase the biomass productivity and feasibility.
- The economic, energy consumption and environmental aspects of the extraction method also need to also be investigated for large scale implementation in the future.
- Due to its protein structure, inherent brilliant blue colour, and antioxidant characteristic the C-PC extracted from this novel *Euhalothece* sp. has the potential to be used in analytical applications, including pharmaceutical and biomedical research. More research is needed to be undertaken to assess the conformational behaviour under other stress factors.
- A potential method for improving C-PC stability with high yields still needs to be developed. A method to improve the C-PC stability is by removing the protein part of C-PC as the protein part of the C-PC will precipitate and contribute to bleaching of the C-PC due to denaturation by heat. The protein part of phycocyanin can be cleaved of using methods such as acid cleavage, enzymatic treatment, or alcoholysis. Another option is to investigate microencapsulation of C-PC using different substances as coating materials with spray drying method.
- Detailed studies of the structure of C-PC will aid in understanding (i) autocatalytic self-assembly of C-PC, (ii) antioxidant and other pharmaceutical properties and (iii) the relationship between the environment and the spectroscopic properties. More in-depth studies using three-dimensional transmission electron microscopy (3DTEM), X-ray crystallography and nuclear magnetic resonance (NMR), circular dichroism spectroscopy, transient spectroscopy techniques for structure determination and energy transfer of PBPs will enable the potential applications.
- Additional research into genetically recombinant PBPs through the construction of genetically engineered bacteria such as *E.Coli* may potentially enhance the fluorescent abilities of the proteins and broaden the scope of their applications.

- *Euhalothece* sp. has gained a number of genes (some of them are still uncharacterised), including plasmids and phage related sequences. Identification of the number of genes with unidentified functions provides an opportunity to investigate the unique traits that are still not annotated and could provide information that could be further exploited.
- A complete understanding of the isolate requires the analysis of the full complement of proteins and the way they are regulated by analysing transcription and translation under conditions. Further investigations such transcriptomics is required to validate the proposed mechanism of salinity adaptation.

REFERENCES

Abed, R.M.M., Dobretsov, S., Sudesh, K. 2009. Applications of cyanobacteria in biotechnology. *Journal of Applied Microbiology*, 106(1), 1-12.

Adir N, D.M., Klartag M, McGregor A, Melamed-Frank M. 2006. Assembly and Disassembly of Phycobilisomes in: *Complex Intracellular Structures in Prokaryotes*, (Ed.) S. JM, Springer Berlin Heidelberg;, pp. 47–77.

Adir, N., Dobrovetsky, Y., Lerner, N. 2001. Structure of C-phycocyanin from the thermophilic cyanobacterium Synechococcus vulcanus at 2.5 A: structural implications for thermal stability in phycobilisome assembly. *Journal of Molecular Biology*, 313(1), 71-81.

Aftari, R.V., Rezaei, K., Bandani, A., Mortazavi, A. 2017. Antioxidant activity optimisation of Spirulina platensis C-phycocyanin obtained by freeze-thaw, microwave-assisted and ultrasound-assisted extraction methods. *Quality Assurance and Safety of Crops & Foods*, 9(1), 1-9.

Agrawal, C., Sen, S., Chatterjee, A., Rai, S., Yadav, S., Singh, S., Rai, L. 2015. Signal Perception and Mechanism of Salt Toxicity/Tolerance in Photosynthetic Organisms: Cyanobacteria to Plants, pp. 79-113.

Al-Haj, L., Lui, Y.T., Abed, R.M.M., Gomaa, M.A., Purton, S. 2016. Cyanobacteria as Chassis for Industrial Biotechnology: Progress and Prospects. *Life* (*Basel, Switzerland*), 6(4), 42.

Alberts, B., Johnson, A., Lewis, J., Raff, M., Roberts, K., Walt, P. 2002. The Shape and Structure of Proteins. 4th ed. in: *Molecular Biology of the Cell*, Garland Science. New York.

Aleksandra, V.D.-Č., Dulic, T., Stojanović, D., Zorica B, S. 2007. The importance of extremophile cyanobacteria in the production of biologically active compounds. *Proceedings of the National Academy of Sciences of the United States of America.*

Ali, A., Soares, S., Barbosa, E., Santos, A., Barh, D., Bakhtiar, S.m., Hassan, S., Ussery, D., Silva, A., A, M., Azevedo, V. 2013. Microbial Comparative Genomics: An Overview of Tools and Insights Into The Genus Corynebacterium. *Journal of Bacteriology & Parasitology*, 4.

Allakhverdiev, S.I., Murata, N. 2008. Salt stress inhibits photosystems II and I in cyanobacteria. *Photosynthesis Research,* 98, 529-539.

Alvarenga, D.O., Fiore, M.F., Varani, A.M. 2017. A Metagenomic Approach to Cyanobacterial Genomics. *Frontiers in Microbiology*, 8, 809. doi: 10.3389/fmicb.2017.00809

Anagnostidis, K., Komárek, J. 1990. Modern approach to the classification system of cyanophytes. 5 -Stigonematales. *Algological Studies*, 59, 1-73.

Anagnostidis, K., Komárek, J. 1985. Modern approach to the classification system of the Cyanophytes 1: Introduction. *Algological Studies, Archiv für Hydrobiologie*, 38, 291-302.

Anagnostidis, K., Komárek, J. 1988. Modern approach to the classification system of the cyanophytes. 3 -Oscillatoriales. *Algological Studies*, 50-53, 327-472. .

Antelo, F.S., Costa, J.A.V., Kalil, S.J. 2008. Thermal degradation kinetics of the phycocyanin from *Spirulina platensis*. *Biochemical Engineering Journal*, 41(1), 43-47.

Arun, P.V.P.S., Bakku, R.K., Subhashini, M., Singh, P., Prabhu, N.P., Suzuki, I., Prakash, J.S.S. 2012. CyanoPhyChe: a database for physico-chemical properties, structure and biochemical pathway information of cyanobacterial proteins. *PloS one*, 7(11), e49425-e49425.

Asada, K. 2006. Production and scavenging of reactive oxygen species in chloroplasts and their functions. *Plant Physiology and Biochemistry*, 141, 391-396.

Asadulghani., Nitta. K, Kaneko. Y, Kojima. K, Fukuzawa. H, Kosaka. H, H, N. 2004. Comparative analysis of the hspA mutant and wild-type *Synechocystis* sp. strain PCC

6803 under salt stress: evaluation of the role of hspA in salt-stress management. *Archives of Microbiology,* 182, 487-497.

Ashby, M.K., Houmard, J. 2006. Cyanobacterial two-component proteins: Structure, diversity, distribution, and evolution. *Microbiology and Molecular Biology Reviews*, 70(2), 472-509.

Auch, A.F., Klenk, H.-P., Göker, M. 2010. Standard operating procedure for calculating genome-to-genome distances based on high-scoring segment pairs. *Standards in Genomic Sciences*, 2(1), 142-148.

Babele, P.K., Kumar, J., Chaturvedi, V. 2019. Proteomic de-regulation in cyanobacteria in response to abiotic stresses. *Frontiers in Microbiology*, 10(1315).

Baier, K., Lehmann, H., Paul Stephan, D., Lockau, W. 2004. NblA is essential for phycobilisome degradation in Anabaena sp. strain PCC 7120 but not for development of functional heterocysts. *Microbiology (Reading, England)*, 150, 2739-49.

Bailey, T.L., Elkan, C. 1994. Fitting a mixture model by expectation maximisation to discover motifs in biopolymers. in: *Proceedings of the Second International Conference on Intelligent Systems for Molecular Biology,* AAAI Press. Menlo Park, California, pp. 28-36,.

Ballot, A., Dadheech, P.K., Haande, S., Krienitz, L. 2008. Morphological and phylogenetic analysis of *Anabaenopsis abijatae* and *Anabaenopsis elenkinii* (nostocales, cyanobacteria) from tropical inland water bodies. *Microbial Ecology,* 55(4), 608-18.

Bandyopadhyay, A., Elvitigala, T., Liberton, M., Pakrasi, H.B. 2013. Variations in the rhythms of respiration and nitrogen fixation in members of the unicellular diazotrophic cyanobacterial genus *Cyanothece*. *Plant Physiology*, 161(3), 1334-46.

Bandyopadhyay, A., Elvitigala, T., Welsh, E., Stockel, J., Liberton, M., Min, H., Sherman, L.A., Pakrasi, H.B. 2011. Novel metabolic attributes of the genus cyanothece, comprising a group of unicellular nitrogen-fixing *Cyanothece*. *MBio*, 2(5), e00214-00211

Bashan, Y., Perez-Garcia, O. 2015. Microalgal heterotrophic and mixotrophic culturing for bio-refining: From metabolic routes to techno-economics, Vol. 2, pp. 61-131.

Basheva, D., Moten, D., Stoyanov, P., Belkinova, D., Mladenov, R., Teneva, I. 2018. Content of phycoerythrin, phycocyanin, alophycocyanin and phycoerythrocyanin in some cyanobacterial strains: Applications. *Engineering in Life Sciences*, 18(11), 861-866.

Beale, S.I. 1993. Biosynthesis of phycobilins. *Chemical reviews*, 93(2), 785-802.

Beale, S.I., Cornejo, J. 1991. Biosynthesis of phycobilins. 3(Z)-phycoerythrobilin and 3(Z)-phycocyanobilin are intermediates in the formation of 3(E)-phycocyanobilin from biliverdin IX alpha. *Journal of Biological Chemistry*, 266(33), 22333-40.

Beck, C., Knoop, H., Axmann, I.M., Steuer, R. 2012. The diversity of cyanobacterial metabolism: genome analysis of multiple phototrophic microorganisms. *BMC Genomics*, 13(1), 56.

Benavente-Valdés, J.R., Aguilar, C., Contreras-Esquivel, J.C., Méndez-Zavala, A., Montañez, J. 2016. Strategies to enhance the production of photosynthetic pigments and lipids in chlorophycae species. *Biotechnology reports (Amsterdam, Netherlands)*, 10, 117-125.

Benedetti, S., Rinalducci, S., Benvenuti, F., Francogli, S., Pagliarani, S., Giorgi, L., Micheloni, M., D'Amici, G.M., Zolla, L., Canestrari, F. 2006. Purification and characterisation of phycocyanin from the blue-green alga Aphanizomenon flos-aquae. *Journal of Chromatography B: Analytical Technologies in the Biomedical and Life Sciences*, 833(1), 12-8.

Benkert, P., Biasini, M., Schwede, T. 2010. Toward the estimation of the absolute quality of individual protein structure models. *Bioinformatics*, 27(3), 343-350.

Berker, K.I., Güçlü, K., Tor, İ., Apak, R. 2007. Comparative evaluation of Fe(III) reducing power-based antioxidant capacity assays in the presence of phenanthroline, batho-

phenanthroline, tripyridyltriazine (FRAP), and ferricyanide reagents. *Talanta*, 72(3), 1157-1165.

Bermejo, P., Pinero, E., Villar, A. 2008. Iron-chelating ability and antioxidant properties of phycocyanin isolated from a protean extract of Spirulina platensis. *Food Chemistry*, 110(2), 436-445.

Bermejo, R., Gabriel Acién, F., Ibáñez, M.J., Fernández, J.M., Molina, E., Alvarez-Pez, J.M. 2003. Preparative purification of B-phycoerythrin from the microalga Porphyridium cruentum by expanded-bed adsorption chromatography. *Journal of Chromatography B*, 790(1-2), 317-325.

Bermejo, R., Ruiz, E., Acien, F.G. 2007. Recovery of B-phycoerythrin using expanded bed adsorption chromatography: Scale-up of the process. *Enzyme and Microbial Technology*, 40(4), 927-933.

Bertoni, M., Kiefer, F., Biasini, M., Bordoli, L., Schwede, T. 2017. Modeling protein quaternary structure of homo- and hetero-oligomers beyond binary interactions by homology. *Scientific Reports*, 7(1), 10480. doi: 10.1038/s41598-017-09654-8.

Billini, M., Stamatakis, K., Sophianopoulou, V. 2008. Two members of a network of putative Na+/H+ antiporters are involved in salt and pH tolerance of the freshwater cyanobacterium *Synechococcus elongatus*. *Journal of bacteriology*, 190(19), 6318-6329.

Birben, E., Sahiner, U.M., Sackesen, C., Erzurum, S., Kalayci, O. 2012. Oxidative stress and antioxidant defense. *The World Allergy Organisation journal*, 5(1), 9-19.

Biswas, A., Vasquez, Y.M., Dragomani, T.M., Kronfel, M.L., Williams, S.R., Alvey, R.M., Bryant, D.A., Schluchter, W.M. 2010. Biosynthesis of cyanobacterial phycobiliproteins in *Escherichia co*li: chromophorylation efficiency and specificity of all bilin lyases from *Synechococcus* sp. strain PCC 7002. *Applied Environmental Microbiology*, 76(9), 2729-39.

Biswas, S. 2001. In-vitro antimalarial activity of azithromycin against chloroquine sensitive and chloroquine resistant *Plasmodium falciparum*. *Journal of postgraduate medicine*, **47**, 240-3.

Böcker, L., Ortmann, S., Surber, J., Leeb, E., Reineke, K., Mathys, A. 2019. Biphasic short time heat degradation of the blue microalgae protein phycocyanin from Arthrospira platensis. *Innovative Food Science & Emerging Technologies*, 52, 116-121.

Boone D.R., Garrity G.M., Castenholz R.W., Brenner D.J., Krieg N.R.,. Staley J.T. 2001. *Bergey's Manual of Systematic Bacteriology: The Archaea and the Deeply Branching and Phototrophic Bacteria*, (2nd Ed) Vol. 1, Springer, New York pp. 499-504.

Borowitzka, M.A. 2013. High-value products from microalgae—their development and commercialisation. *Journal of Applied Phycology*, 25(3), 743-756.

Boyer, S.L., Flechtner, V.R., Johansen, J.R. 2001. Is the 16S-23S rRNA internal transcribed spacer region a good tool for use in molecular systematics and population genetics? A case study in cyanobacteria. *Molecular Biology and Evolution,*18(6), 1057-1069.

Bravakos, P., Kotoulas, G., Skaraki, K., Pantazidou, A., Economou-Amilli, A. 2016. A polyphasic taxonomic approach in isolated strains of Cyanobacteria from thermal springs of Greece. *Molecular Phylogenetics and Evolution*, 98, 147-160.

Broady, P., Merican, F. 2012. Phylum Cyanobacteria: blue-green bacteria, blue-green algae. *New Zealand inventory of biodiversity*, 3, 50-69.

Brookes, J.D., Ganf, G.G. 2001. Variations in the buoyancy response of Microcystis aeruginosa to nitrogen, phosphorus and light. *Journal of Plankton Research*, 23(12), 1399-1411.

Brown, S.B., Houghton, J.D., Vernon, D.I. 1990. Biosynthesis of phycobilins. Formation of the chromophore of phytochrome, phycocyanin and phycoerythrin. *Journal of Photochemistry and Photobiology B:Biology*, 5(1), 3-23.

Bryant, D.A., Hixson, C.S., Glazer, A. 1978. Structural studies on phycobiliproteins III. Comparison of bilin-containing peptides from the beta subunits of C-phycocyanin, R-phycocyanin, and phycoerythrocyanin. *Journal of Biological Chemistry*, 253(1), 220-225.

Burke, C.M. 1995. Benthic microbial production of oxygen supersaturates the bottom water of a stratified hypersaline lake. *Microbial Ecology*, 29(2), 163-171.

Cai, C., Wang, Y., Li, C., Guo, Z., Jia, R., Wu, W., Hu, Y., He, P. 2014. Purification and photodynamic bioactivity of phycoerythrin and phycocyanin from Porphyra yezoensis Ueda. *Journal of Ocean University of China*, 13(3), 479-484.

Cameron, J.C., Pakrasi, H.B. 2010. Essential Role of Glutathione in Acclimation to Environmental and Redox Perturbations in the Cyanobacterium Synechocystis sp. PCC 6803. *Plant Physiology*, 154(4), 1672-1685.

Campbell, D., Eriksson, M.J., Oquist, G., Gustafsson, P., Clarke, A.K. 1998. The cyanobacterium *Synechococcus* resists UV-B by exchanging photosystem II reaction-center D1 proteins. *Proceedings of the National Academy of Sciences of the United States of America*, 95(1), 364-369.

Carmichael, W.W., Li, R. 2006. Cyanobacteria toxins in the Salton Sea. *Saline Systems*, 2, 5-5.

Carrasco, N.K., Perissinotto, R. 2012. Development of a halotolerant community in the St. Lucia Estuary (South Africa) during a hypersaline phase. *PLOS ONE*, 7(1), e29927.

Case, R.J., Boucher, Y., Dahllöf, I., Holmström, C., Doolittle, W.F., Kjelleberg, S. 2007. Use of 16S rRNA and rpoB Genes as Molecular Markers for Microbial Ecology Studies. *Applied and Environmental Microbiology*, 73(1), 278-288.

Cassier-Chauvat, C., Chauvat, F. 2015. Responses to Oxidative and Heavy Metal Stresses in Cyanobacteria: Recent Advances. *International Journal of Molecular Sciences*, 16(1).

Castenholz, R.W. 2001a. Phylum BX. Cyanobacteria, Oxygenic Photosythetic Bacteria in: *Bergey´s Manual of Systematic Bacteriology* Volume (Eds.) B. D.R., C. R.W, Springer-Verlag,. ew York-Berlin-Heidelberg, pp. 721.

Cepák, V., Komárek, J. 2010. Cytomorphology of six halotolerant coccoid cyanobacteria using DAPI fluorescent and transmission electron microscopy, compared with molecular data. *Fottea*, 10, 229-234.

Cerveny, J., Sinetova, M.A., Valledor, L., Sherman, L.A., Nedbal, L. 2013. Ultradian metabolic rhythm in the diazotrophic cyanobacterium *Cyanothece* sp. ATCC 51142. *Proceedings of the National Academy of Sciences of the United States of America*, 110(32), 13210-5.

Chaiklahan, R., Chirasuwan, N., Bunnag, B. 2012. Stability of phycocyanin extracted from *Spirulina* sp.: Influence of temperature, pH and preservatives. *Process Biochemistry*, 47(4), 659-664.

Chaiklahan, R., Chirasuwan, N., Loha, V., Tia, S., Bunnag, B. 2011. Separation and purification of phycocyanin from *Spirulina* sp. using a membrane process. *Bioresource Technology*, 102(14), 7159-64.

Chakdar, H., Pabbi, S. 2015. Cyanobaceria phycobilins:production,purification and regulation. in: *Frontier Discoveries and Innovations in Interdisciplinary Microbiology*, (Ed.) P. Shukla, Springer. New Delhi, pp. 219.

Chakdar, H., Pabbi, S. 2012. Extraction and purification of Phycoerythrin from Anabaena variabil (CCC421). *Phykos*, 42, 25-31.

Chang, L., Liu, X., Li, Y., Liu, C.C., Yang, F., Zhao, J., Sui, S.F. 2015. Structural organization of an intact phycobilisome and its association with photosystem II. *Cell Research*, 25(6), 726-37.

Chatchawan, T., Peerapornpisal, Y., Komarek, J. 2011. Diversity of cyanobacteria in man-made solar saltern, Petchaburi Province, Thailand - a pilot study. *Fottea*, 11(1), 203-214.

Chen, C.-Y., Kao, P.-C., Tan, C.H., Show, P.L., Cheah, W.Y., Lee, W.-L., Ling, T.C., Chang, J.-S. 2016. Using an innovative pH-stat CO_2 feeding strategy to enhance cell growth and C-phycocyanin production from Spirulina platensis. *Biochemical Engineering Journal*, 112, 78-85.

Chen, F., Zhang, Y., Guo, S. 1996. Growth and phycocyanin formation of Spirulina platensis in photoheterotrophic culture. *Biotechnology Letters*, 18(5), 603-608.

Chen, H.-Y.S., Bandyopadhyay, A., Pakrasi, H.B. 2018. Function, regulation and distribution of IsiA, a membrane-bound chlorophyll a-antenna protein in cyanobacteria. *Photosynthetica*, 56(1), 322-333.

Chen, X., Wu, M., Yang, Q., Wang, S. 2017. Preparation, characterisation of food grade phycobiliproteins from *Porphyra haitanensis* and the application in liposome-meat system. *LWT - Food Science and Technology*, 77, 468-474.

Chen, Z., Zhan, J., Chen, Y., Yang, M., He, C., Ge, F., Wang, Q. 2015. effects of phosphorylation of beta subunits of phycocyanins on state transition in the model Cyanobacterium *Synechocystis* sp. PCC 6803. *Plant Cell Physiology*, 56(10), 1997-2013.

Chentir, I., Hamdi, M., Li, S., Doumandji, A., Markou, G., Nasri, M. 2018. Stability, bio-functionality and bio-activity of crude phycocyanin from a two-phase cultured Saharian *Arthrospira* sp. strain. *Algal Research*, 35, 395-406.

Cherdkiatikul, T., Suwanwong, Y. 2014. Production of the alpha and beta subunits of *Spirulina* allophycocyanin and C-phycocyanin in *Escherichia coli* : A comparative study of their antioxidant activities. *Journal of Biomolecular Screening*, 19(6), 959-65.

Cherng, S.C., Cheng, S.N., ATarn, Chou, T.C. 2007. Anti-inflammatory activity of C-phycocyanin in lipopolysaccharide-stimulated RAW264.7 macrophages.*Life Science*, 81, 1431-1435.

Cho, J.C., Tiedje, J.M. 2001. Bacterial species determination from DNA-DNA hybridization by using genome fragments and DNA microarrays. *Applied Environmental Microbiology*, 67(8), 3677-82.

Choi, W.Y., Lee, H.Y. 2018. Effect of Ultrasonic Extraction on Production and Structural Changes of C-Phycocyanin from Marine *Spirulina maxima*. *International Journal of Molecular Sciences*, 19(1), 220. doi: 10.3390/ijms19010220.

Choi, D.H., Noh, J.H., Lee, C.M., Rho, S. 2008. *Rubidibacter lacunae* gen. nov., sp. nov., a unicellular, phycoerythrin-containing cyanobacterium isolated from seawater of Chuuk 58(12), 2807-11.

Chrismas, N.A., Anesio, A.M., Sanchez-Baracaldo, P. 2015. Multiple adaptations to polar and alpine environments within cyanobacteria: a phylogenomic and Bayesian approach. *Frontiers in Microbiology*, 6, 1070-1080.

Chukhutsina, V., Bersanini, L., Aro, E.-M., van Amerongen, H. 2015. Cyanobacterial light-harvesting phycobilisomes uncouple from photosystem I during dark-to-light transitions. *Scientific Reports*, 5, 14193. doi.org/10.1038/srep14193.

Cohen, S.E., Golden, S.S. 2015. Circadian rhythms in cyanobacteria. *Microbiology and Molecular Biology Reviews,* 79(4), 373-85.

Cohen, Y., Aizenshtat, Z., Stoler, A., Jørgensen, B.B. 1980. The microbial geochemistry of solar lake, Sinai. in: *Biogeochemistry of Ancient and Modern Environments: Proceedings of*

the Fourth International Symposium on Environmental Biogeochemistry (ISEB) and, Conference on Biogeochemistry in Relation to the Mining Industry and Environmental Pollution (Leaching Conference), held in Canberra, Australia, 26 August – 4 September 1979, (Eds.) P.A. Trudinger, M.R. Walter, B.J. Ralph, Springer Berlin Heidelberg. Berlin, Heidelberg, pp. 167-172.

Cole, J.R., Wang, Q., Fish, J.A., Chai, B., McGarrell, D.M., Sun, Y., Brown, C.T., Porras-Alfaro, A., Kuske, C.R., Tiedje, J.M. 2014. Ribosomal Database Project: data and tools for high throughput rRNA analysis. *Nucleic acids research*, 42(Database issue), D633-D642.

Collins, A.M., Liberton, M., Jones, H.D.T., Garcia, O.F., Pakrasi, H.B., Timlin, J.A. 2012. Photosynthetic pigment localisation and thylakoid membrane morphology are altered in Synechocystis 6803 phycobilisome mutants. *Plant physiology*, 158(4), 1600-1609.

Cooper, Charlotte R., Daugherty, Amanda J., Tachdjian, S., Blum, Paul H., Kelly, Robert M. 2009. Role of vapBC toxin–antitoxin loci in the thermal stress response of *Sulfolobus solfataricus*. *Biochemical Society Transactions*, 37(1), 123-126.

Cosner, J.C. 1978. Phycobilisomes in spheroplasts of *Anacystis nidulans*. *Journal of Bacteriology*(135), 1137–1140.

Cuellar-Bermudez, S.P., Aguilar-Hernandez, I., Cardenas-Chavez, D.L., Ornelas-Soto, N., Romero-Ogawa, M.A., Parra-Saldivar, R. 2015. Extraction and purification of high-value metabolites from microalgae: essential lipids, astaxanthin and phycobiliproteins. *Microbial Biotechnology*, 8(2), 190-209.

Dagnino-Leone, J., Figueroa, M., Mella, C., Vorphal, M.A., Kerff, F., Vasquez, A.J., Bunster, M., Martinez-Oyanedel, J. 2017. Structural models of the different trimers present in the core of phycobilisomes from *Gracilaria chilensis* based on crystal structures and sequences. *PLoS One*, 12(5), e0177540.

Dall'agnol, L.T., Ghilardi-Junior, R., McCulloch, J.A., Schneider, H., Schneider, M.P.C., Silva, A., 2012. Phylogenetic and gene trees of *Synechococcus*: choice of the right marker to evaluate the population diversity in the Tucuruí Hydroelectric Power Station Reservoir in Brazilian Amazonia. *Journal of Plankton Research*. 34 (3), 245–257.

Daoud, H.M., Soliman, E.M. 2015. Evaluation of *Spirulina platensis* extract as natural antivirus against foot and mouth disease virus strains (A, O, SAT2). *Veterinary world*, 8(10), 1260-1265.

David, L., Prado, M., Arteni, A.A., Elmlund, D.A., Blankenship, R.E., Adir, N. 2014. Structural studies show energy transfer within stabilised phycobilisomes independent of the mode of rod–core assembly. *Biochimica et Biophysica Acta (BBA) - Bioenergetics*, 1837(3), 385-395. Dias, E., Oliveira, M., Jones-Dias, D., Vasconcelos, V., Ferreira, E., Manageiro, V., Caniça, M. 2015. Assessing the antibiotic susceptibility of freshwater Cyanobacteria spp. *Frontiers Microbiology*, 6, 799.

De Philippis, R., Vincenzini, M. 1998. Exocellular polysaccharides from cyanobacteria and their possible applications. *FEMS Microbiology Reviews*, 22(3), 151-175.

Demirel, Z., Sukatar, A. 2019. Purification of phycocyanin from isolated and identified hot spring cyanobacteria.

Derikvand, P., Llewellyn, C.A., Purton, S. 2017. Cyanobacterial metabolites as a source of sunscreens and moisturisers: a comparison with current synthetic compounds. *European Journal of Phycology*, 52(1), 43-56.

Deshmukh, D.V., Puranik, P.R. 2012. Statistical evaluation of nutritional components impacting phycocyanin production Synechocystis SP. *Brazilian journal of microbiology : publication of the Brazilian Society for Microbiology*, 43(1), 348-355.

Ding, W., Baumdicker, F., Neher, R.A. 2018. panX: pan-genome analysis and exploration. *Nucleic Acids Research*, 46(1), e5.

Donkor, E., Dayie, N., Adiku, T. 2014. Bioinformatics with basic local alignment search tool (BLAST) and fast alignment (FASTA). *Journal of Bioinformatics and Sequence Analysis*, 6, 1-6.

dos Santos, R.R., Corrêa, P.S., Dantas, F.M.L., Teixeira, C.M.L.L. 2019. Evaluation of the co-production of total carotenoids, C-phycocyanin and polyhydroxyalkanoates by Arthrospira platensis. *Bioresource Technology Reports*, 7.

Dragana Stanic-Vucinic, S.M., Milan R. Nikolic and Tanja Cirkovic Velickovic 2018. Spirulina Phycobiliproteins as Food Components and Complements. in: *Microalgal Biotechnology*,, (Ed.) L.Q.Z.a.M.I.Q. Eduardo Jacob-Lopes, IntechOpen.

Ducat, D., Way, J., Silver, P. 2011. Engineering cyanobacteria to generate high-value products. *Trends in Biotechnology*, 29, 95-103.

Duccio, V., Hervé, R. 2015. Ten years of pan-genome analyses. *Current opinion in microbiology*.

Ducret, A., Sidler, W., Wehrli, E., Frank, G., Zuber, H. 1996. Isolation, characterization and electron microscopy analysis of a hemidiscoidal phycobilisome type from the cyanobacterium Anabaena sp. PCC 7120. *European Journal of Biochemistry*, 236(3), 1010-1024.

Dyble, J., Paerl, H.W., Neilan, B.A. 2002. Genetic characterisation of Cylindrospermopsis raciborskii (cyanobacteria) isolates from diverse geographic origins based on nifH and cpcBA-IGS nucleotide sequence analysis. *Applied and Environmental Microbiology*, 68(5), 2567-2571.

Eckert, E., Zambrowicz, A., Bobak, Ł., Zabłocka, A., Chrzanowska, J., Trziszka, T. 2018. Production and Identification of Biologically Active Peptides Derived from By-product of Hen Egg-Yolk Phospholipid Extraction. *International Journal of Peptide Research and Therapeutics*, 25(2), 669-680.

Edwards, M.R., Hauer, C., Stack, R.F., Eisele, L.E., MacColl, R. 1997. Thermophilic C-phycocyanin: effect of temperature, monomer stability, and structure. *Biochimica et Biophysica Acta (BBA) - Bioenergetics*, 1321(2), 157-164.

Elanskaya, I.V., Zlenko, D.V., Lukashev, E.P., Suzina, N.E., Kononova, I.A., Stadnichuk, I.N. 2018. Phycobilisomes from the mutant cyanobacterium Synechocystis sp. PCC 6803 missing chromophore domain of ApcE. *Biochimica et Biophysica Acta (BBA) - Bioenergetics*, 1859(4), 280-291.

Eriksen, N.T. 2008. Production of phycocyanin—a pigment with applications in biology, biotechnology, foods and medicine. *Applied Microbiology Biotechnology* 80, 1-14.

Fan, J., Liu, Q., Hao, Q., Teng, M., Niu, L. 2007. Crystal structure of uroporphyrinogen decarboxylase from Bacillus subtilis. *Journal of Bacteriology*, 189(9), 3573-3580.

Fang, H., Kang, J., Zhang, D. 2017. Microbial production of vitamin B12: a review and future perspectives. *Microbial Cell Factories*, 16(1), 15. doi: 10.1186/s12934-017-0631-y.

Farias, M.E., Rasuk, M.C., Gallagher, K.L., Contreras, M., Kurth, D., Fernandez, A.B., Poiré, D., Novoa, F., Visscher, P.T. 2017. Prokaryotic diversity and biogeochemical characteristics of benthic microbial ecosystems at La Brava, a hypersaline lake at Salar de Atacama, Chile. *PLOS ONE*, 12(11), e0186867.

Fass, D. 2011. Disulfide Bonding in Protein Biophysics. *Annual review of biophysics*, **41**, 63-79.

FDA. 2017. Summary of Color Additives for Use in the United States in Foods, Drugs, Cosmetics, and Medical Devices.

Feist, P., Hummon, A.B. 2015. Proteomic challenges: sample preparation techniques for microgram-quantity protein analysis from biological samples. *International journal of Molecular Sciences*, 16(2), 3537-3563.

Fekrat, F., Nami, B., Ghanavati, H., Ghaffari, A., Shahbazi, M. 2019. Optimisation of chitosan/activated charcoal-based purification of *Arthrospira platensis* phycocyanin using response surface methodology. *Journal of Applied Phycology*, 31(2), 1095-1105.

Fernandes e Silva, E., Figueira, F.d.S., Lettnin, A.P., Carrett-Dias, M., Filgueira, D.d.M.V.B., Kalil, S., Trindade, G.S., Votto, A.P.d.S. 2018. C-Phycocyanin: Cellular targets, mechanisms of action and multi drug resistance in cancer. *Pharmacological Reports*, 70(1), 75-80.

Fernández-Juárez, V., Bennasar-Figueras, A., Tovar-Sanchez, A., Agawin, N.S.R. 2019. The Role of Iron in the P-Acquisition Mechanisms of the Unicellular N_2-Fixing Cyanobacteria Halothece sp., Found in Association With the Mediterranean Seagrass Posidonia oceanica. *Frontiers in Microbiology*, 10(1903).

Fernández-Rojas, B., Hernández-Juárez, J., Pedraza-Chaverri, J. 2014. Nutraceutical properties of phycocyanin. *Journal of Functional Foods*, 11, 375-392.

Figueira, F., Moraes, C., Kalil, S. 2018. C-phycocyanin purification: Multiple processes for different applications. *Brazilian Journal of Chemical Engineering*, 35, 1117-1128.

Fourcans, A., de Oteyza, T.G., Wieland, A., Sole, A., Diestra, E., van Bleijswijk, J., Grimalt, J.O., Kuhl, M., Esteve, I., Muyzer, G., Caumette, P., Duran, R. 2004. Characterization of functional bacterial groups in a hypersaline microbial mat community (Salins-de-Giraud, Camargue, France). *FEMS Microbiol Ecologyl*, 51(1), 55-70.

Foyer, C.H. 2018. Reactive oxygen species, oxidative signaling and the regulation of photosynthesis. *Environmental and Experimental Botany*, 154, 134-142.

Francoise, J., Robert, J., Martin, H. 1996. Dynamics of the response of cyanobacteria to salt stress: Deciphering the molecular events. *Physiologia Plantarum*, 96(4), 738-744.

Frankenberg, N., Lagarias, J.C. 2003. Phycocyanobilin:ferredoxin oxidoreductase of Anabaena sp. PCC 7120. Biochemical and spectroscopic. *Journal of Biological Chemistry*, 278(11), 9219-9226.

Fujita, Y., Tsujimoto, R., Aoki, R. 2015. Evolutionary aspects and regulation of tetrapyrrole biosynthesis in cyanobacteria under aerobic and anaerobic environments. *Life (Basel, Switzerland)*, 5(2), 1172-1203.

Fujiwara, K., Toda, H., Ikeguchi, M. 2012. Dependence of *α*-helical and *β*-sheet amino acid propensities on the overall protein fold type. *BMC Structural Biology*, 12(1), 18.

Fukuchi, S., Yoshimune, K., Wakayama, M., Moriguchi, M., Nishikawa, K. 2003. Unique amino acid composition of proteins in halophilic bacteria. *J Mol Biol*, **327**(2), 347-57.

Furmaniak, M.A., Misztak, A.E., Franczuk, M.D., Wilmotte, A., Waleron, M., Waleron, K.F. 2017. Edible Cyanobacterial Genus Arthrospira: Actual State of the Art in Cultivation Methods, Genetics, and Application in Medicine. *Frontiers in Microbiology*, 8(2541).

Furuki, T., Maeda, S., Imajo, S., Hiroi, T., Amaya, T., Hirokawa, T., Ito, K., Nozawa, H. 2003. Rapid and selective extraction of phycocyanin from *Spirulina platensis* with ultrasonic cell disruption. *Journal of Applied Phycology*, 15(4), 319-324.

Gaget, V., Gribaldo, S., Tandeau de Marsac, N. 2011. An rpoB signature sequence provides unique resolution for the molecular typing of cyanobacteria. *International Journal of Systematic and Evolutionary Microbiology*, 61(Pt 1), 170-83.

Galperin, M.Y., Koonin, E.V. 2010. From complete genome sequence to 'complete' understanding? *Trends in Biotechnology*, 28(8), 398-406.

Gammoudi, S., Athmouni, K., Nasri, A., Diwani, N., Grati, I., Belhaj, D., Bouaziz-Ketata, H., Fki, L., El Feki, A., Ayadi, H. 2019. Optimisation, isolation, characterisation and hepatoprotective effect of a novel pigment-protein complex (phycocyanin) producing microalga: Phormidium versicolorNCC-466 using response surface methodology. *International Journal of Biological Macromolecules,* 137, 647-656.

Gantar, M., Simović, D., Djilas, S., Gonzalez, W.W., Miksovska, J. 2012. Isolation, characterisation and antioxidative activity of C-phycocyanin from *Limnothrix* sp. strain 37-2-1. *Journal of Biotechnology*, 159(1), 21-26.

Gantt, E. 1975. Phycobilisomes: Light-harvesting pigment complexes. *Bioscience*, 25(12), 781-788.

Gantt, E. 1980. Structure and Function of Phycobilisomes: Light Harvesting Pigment Complexes in Red and Blue-Green Algae. in: *International Review of Cytology*, (Eds.) G.H. Bourne, J.F. Danielli, K.W. Jeon, Vol. 66, Academic Press, pp. 45-80.

Gantt, E., Conti, S. 1966a. Phycobiliprotein localisation in algae. *Brookhaven symposia in biology*. pp. 393-405.

Gantt, E., Conti, S.F. 1966b. Granules associated with the chloroplast lamellae *of Porphyridium cruentum*. *Journal of Cell Biology*, 29(3), 423-434.

Gao, Q., Garcia-Pichel, F. 2011. Microbial ultraviolet sunscreens. *Nature Reviews Microbiology,* 9(11), 791-802.

Garcia-Pichel, F., Castenholz, R. 2004. Characterisation and biological implications of scytonemin, a cyanobacterial sheath pigment. *Journal of Phycology*, 27, 395-409.

Garcia-Pichel, F., Nübel, U., Muyzer, G. 1998. The phylogeny of unicellular, extremely halotolerant cyanobacteria. *Archives of Microbiology*, 169(6), 469-482.

Garcia-Pino, A., Sterckx, Y., Vandenbussche, G., Loris, R. 2010. Purification and crystallisation of Phd, the antitoxin of the phd/doc operon. *Acta Crystallographica Section F*, 66(2), 167-171.

Garrett, A.R., Weagel, E.G., Martinez, A.D., Heaton, M., Robison, R.A., O'Neill, K.L. 2014. A novel method for predicting antioxidant activity based on amino acid structure. *Food Chem*, **158**, 490-6.

Garlick, S., Oren, A., Padan, E. 1977. Occurrence of facultative anoxygenic photosynthesis among filamentous and unicellular cyanobacteria. *Journal of Bacteriology*, 129(2), 623-9.

Gdara, N.B., Belgacem, A., Khemiri, I., Mannai, S., Bitri, L. 2018. Protective effects of phycocyanin on ischemia/reperfusion liver injuries. *Biomedicine & Pharmacotherapy*, 102, 196-202.

Gevers, D., Cohan, F.M., Lawrence, J.G., Spratt, B.G., Coenye, T., Feil, E.J., Stackebrandt, E., de Peer, Y.V., Vandamme, P., Thompson, F.L., Swings, J. 2005. Re-evaluating prokaryotic species. *Nature Reviews Microbiology*, 3, 733.

Glaeser, S.P., Kampfer, P. 2015. Multilocus sequence analysis (MLSA) in prokaryotic taxonomy. *Systematic and Applied Microbiology,* 38(4), 237-245.

Glauser, M., Bryant, D.A., Frank, G., Wehrli, E., Rusconi, S.S., Sidler, W., Zuber, H. 1992. Phycobilisome structure in the cyanobacteria Mastigocladus laminosus and Anabaena sp. PCC 7120. *European Journal of Biochemistry*, 205(3), 907-15.

Glazer, A.N., Clark, J.H. 1986. Phycobilisomes: macromolecular structure and energy flow dynamics. *Biophysical Journal,* 49(1), 115-6.

Glazer, A.N., Cohen-Bazire, G. 1971. Subunit Structure of the Phycobiliproteins of Blue-Green Algae. *Proceedings of the National Academy of Sciences*, 68(7), 1398.

Glazer, A.N., Fang, S. 1973. Chromophore content of blue-green algal phycobiliproteins. *Journal of Biological Chemistry*, 248(2), 659-662.

Glazer A.N, Stryer L. 1984. Phycofluor probes. *Trends Biochem*istry. Sci. 9: 423–427.

Global One-Stop Reports Center. 2016. Global phycocyanin industry 2015 *Market Research Report.*

Golden, S. 2004. Timekeeping in bacteria: The cyanobacterial circadian clock. *Current Opinion in Microbiology*, 6, 535-40.

González, A., Fillat, M.F., Bes, M.-T., Peleato, M.-L., Sevilla, E. 2018 The Challenge of Iron Stress in Cyanobacteria, . in: *Cyanobacteria*, IntechOpen. Archana Tiwari.

Goris, J., Konstantinidis, K.T., Klappenbach, J.A., Coenye, T., Vandamme, P., Tiedje, J.M. 2007. DNA–DNA hybridisation values and their relationship to whole-genome sequence similarities. *International Journal Of Systematic And Evolutionary Microbiology*, 57(1), 81-91.

Grant, J.R., Stothard, P. 2008. The CGView Server: a comparative genomics tool for circular genomes. *Nucleic Acids Research*, 36(Web Server issue), W181-W184.

Gray, B.H., Lipschultz, C.A., Gantt, E. 1973. Phycobilisomes from a blue-green alga *Nostoc* species. *Journal of Bacteriology*, 116(1), 471-8.

Gronlund, H., Gerdes, K. 1999. Toxin-antitoxin systems homologous with relBE of Escherichia coli plasmid P307 are ubiquitous in prokaryotes. *Journal of Molecular Biology,* 285(4), 1401-15.

Guan, X., Qin, S., Zhao, F., Zhang, X., Tang, X. 2007. Phycobilisomes linker family in cyanobacterial genomes: divergence and evolution. *International Journal of Biological Sciences*, 3(7), 434-445.

Guihéneuf, F., Khan, A., Tran, L.-S.P. 2016. Genetic Engineering: A Promising tool to engender physiological, biochemical, and molecular stress resilience in green microalgae. *Frontiers in Plant Science*, 7(400).

Guimarães, L.C., Florczak-Wyspianska, J., de Jesus, L.B., Viana, M.V.C., Silva, A., Ramos, R.T.J., Soares, S.d.C., Soares, S.d.C. 2015. Inside the Pan-genome - Methods and Software Overview. *Current Genomics*, 16(4), 245-252.

Gupta, A., Bedre, R., Thapa, S.S., Sabrin, A., Wang, G., Dassanayake, M., Grove, A. 2017. Global Awakening of Cryptic Biosynthetic Gene Clusters in *Burkholderia thailandensis*. *ACS Chemical Biology,*12(12), 3012-3021.

Gupta, A., Sainis, J.K. 2009. Isolation of C-phycocyanin from *Synechococcus* sp., (*Anacystis nidulans* BD1). *Journal of Applied Phycology*, 22(3), 231-233.

Gutiérrez, G.A., Cruz de Jesús, V., Hernández-Ortega, M., Valadez-Carmona, L., Mojica-Villegas, M., Gutiérrez-Salmeán, G., Chamorro, G. 2016. Methods for Extraction, Isolation and Purification of C-phycocyanin: 50 years of Research in Review. *International Journal of Food and Nutritional Science,* 3(3)1-10.

Haft, D.H. 2015. Using comparative genomics to drive new discoveries in microbiology. *Current Opinion in Microbiology*, 23, 189-196.

Hagemann, M. 2011. Molecular biology of cyanobacterial salt acclimation. *FEMS Microbiology Reviews*, 35(1), 87-123.

Hagen, J.B. 2000. The origins of bioinformatics. *Nature Reviews Genetics,* 1(3), 231-6.

Hakkila, K., Antal, T., Rehman, A.U., Kurkela, J., Wada, H., Vass, I., Tyystjärvi, E., Tyystjärvi, T. 2014. Oxidative stress and photoinhibition can be separated in the cyanobacterium *Synechocystis* sp. PCC 6803. *Biochimica et Biophysica Acta (BBA) - Bioenergetics*, 1837(2), 217-225.

Hall, B.G. 2013. Building Phylogenetic Trees from Molecular Data with MEGA. *Molecular Biology and Evolution*, 30(5), 1229-1235.
Hamilton, T.L., Bryant, D.A., Macalady, J.L. 2016. The role of biology in planetary evolution: cyanobacterial primary production in low-oxygen Proterozoic oceans. Environmental Microbiology, 18(2), 325-40.
Hayashi, N.R., Terazono, K., Hasegawa, N., Kodama, T., Igarashi, Y. 1997. Identification and characterisation of phycobiliprotein from a thermophilic cyanobacterium, *Chroococcidiopsis* sp. strain TS-821. *Journal of Fermentation and Bioengineering*, 84(5), 475-477.
Hao, S., Yan, Y., Huang, W., Gai, F., Wang, J., Liu, L., Wang, C. 2018. C-phycocyanin reduces inflammation by inhibiting NF-κB activity through downregulating PDCD5 in lipopolysaccharide-induced RAW 264.7 macrophages. *Journal of Functional Foods*, 42, 21-29.
Hausler, S., Weber, M., de Beer, D., Ionescu, D. 2014. Spatial distribution of diatom and cyanobacterial mats in the Dead Sea is determined by response to rapid salinity fluctuations. *Extremophiles*, 18(6), 1085-94.
Hayes, F., Van Melderen, L. 2011. Toxins-antitoxins: diversity, evolution and function. *Critical Reviews in Biochemistry and Molecular Biology*, 46(5), 386-408.
He, F. 2011. Laemmli-SDS-PAGE. *Bio-protocol*, 1(11), e80.
Heather, J.M., Chain, B. 2016. The sequence of sequencers: The history of sequencing DNA. *Genomics*, 107(1), 1-8.
Helliwell, Katherine E., Lawrence, Andrew D., Holzer, A., Kudahl, Ulrich J., Sasso, S., Kräutler, B., Scanlan, David J., Warren, Martin J., Smith, Alison G. 2016. Cyanobacteria and Eukaryotic algae use different chemical variants of vitamin B12. *Current Biology*, 26(8), 999-1008.
Hemlata, P.G., Bano, F., Fatma, T. 2011. Studies on *Anabaena* sp. NCCU-9 with special reference to phycocyanin. *Journal of Algal Biomass Ultilisation*, 2, 30-51.
Henson, B.J., Hesselbrock, S.M., Watson, L.E., Barnum, S.R. 2004. Molecular phylogeny of the heterocystous cyanobacteria (subsections IV and V) based on nifD. *International Journal of Systematic and Evolutionary Microbiology*, 54(2), 493-497.
Henz, S.R., Huson, D.H., Auch, A.F., Nieselt-Struwe, K., Schuster, S.C. 2005. Whole-genome prokaryotic phylogeny. *Bioinformatics*, 21(10), 2329-2335.
Hermanson, G.T. 2013. Chapter 10 - Fluorescent Probes. in: *Bioconjugate Techniques (Third Edition)*, (Ed.) G.T. Hermanson, Academic Press. Boston, pp. 395-463.
Hernández-Corona, A., Meckes, M., Chamorro, G., Barron, B. 2003. Antiviral activity of Spirulina maxima against Herpes simplex virus type 2. *Antiviral research*, 56, 279-85.
Hernandez-Prieto, M.A., Semeniuk, T.A., Futschik, M.E. 2014. Toward a systems-level understanding of gene regulatory, protein interaction, and metabolic networks in cyanobacteria. *Frontiers Genetics*, 5, 191.
Herrero, M., Simó, C., Ibáñez, E., Cifuentes, A. 2005. Capillary electrophoresis-mass spectrometry of *Spirulina platensis* proteins obtained by pressurized liquid extraction. *Electrophoresis*, 26(21), 4215-24.
Hershkovitz, N., Oren, A., Post, A., Cohen, Y. 1991. Induction of water-stress proteins in cyanobacteria exposed to matric- or osmotic-water stress. *FEMS Microbiology Letters*, 83(2), 169-172.
Hoffmann, L. 1988. Criteria for the classification of blue-green algae (cyanobacteria) at the genus and at the species level. *Algological Studies*, 50-53, 131-139.

Hoffmann, L., Komárek, J., í, Ka, tovský, J. 2005. System of cyanoprokaryotes (cyanobacteria); state in 2004. *Algological Studies*, 117(1), 95-115.
Hoiczyk, E., Baumeister, W. 1995. Envelope structure of four gliding filamentous cyanobacteria. *Journal of Bacteriology*, 177(9), 2387-2395.
Hoiczyk, E., Hansel, A. 2000. Cyanobacterial cell walls: news from an unusual prokaryotic envelope. *Journal of Bacteriology*, 182.
Holmes, K.L., Lantz, L.M. 2001. Protein labeling with fluorescent probes. *Methods Cell Biology*, 63, 185-204.
Horváth, H., Kovács, A.W., Riddick, C., Présing, M. 2013. Extraction methods for phycocyanin determination in freshwater filamentous cyanobacteria and their application in a shallow lake. *European Journal of Phycology*, 48(3), 278-286.
Hossain, M.F., Ratnayake, R.R., Meerajini, K., Wasantha Kumara, K.L. 2016. Antioxidant properties in some selected cyanobacteria isolated from fresh water bodies of Sri Lanka. *Food Science & Nutrition*, 4(5), 753-758.
Hsieh-Lo, M., Castillo, G., Ochoa-Becerra, M.A., Mojica, L. 2019. Phycocyanin and phycoerythrin: Strategies to improve production yield and chemical stability. *Algal Research*, 42.
Hsieh, P., Pedersen, J. 2014. Reactive oxygen species in cyanobacteria, pp. 1-41.
Hu, Q., Marquardt, J., Iwasaki, I., Miyashita, H., Kurano, N., Mörschel, E., Miyachi, S. 1999. Molecular structure, localisation and function of biliproteins in the chlorophyll a/d containing oxygenic photosynthetic prokaryote *Acaryochloris marina*. *Biochimica et Biophysica Acta (BBA) - Bioenergetics*, 1412(3), 250-261.
Huang, Z., Guo, B.J., Wong, R.N.S., Jiang, Y. 2007. Characterisation and antioxidant activity of selenium-containing phycocyanin isolated from Spirulina platensis. *Food Chemistry*, 100(3), 1137-1143.
Hunter, W.N. 2007. The non-mevalonate pathway of isoprenoid precursor biosynthesis. *Journal of Biological Chemistry*, 282(30), 21573-7.
Idicula-Thomas, S., Balaji, P.V. 2007. Correlation between the structural stability and aggregation propensity of proteins. *In Silico Biol*, 7(2), 225-37.
Ikai, A. 1980. Thermostability and Aliphatic Index of Globular Proteins. *The Journal of Biochemistry*, 88(6), 1895-1898.
İlter, I., Akyıl, S., Demirel, Z., Koç, M., Conk-Dalay, M., Kaymak-Ertekin, F. 2018. Optimisation of phycocyanin extraction from *Spirulina platensis* using different techniques. *Journal of Food Composition and Analysis*, 70, 78-88.
Imamura, S., Asayama, M. 2009. Sigma factors for cyanobacterial transcription. *Gene Regulation and Systems Biology*, 3, 65-87.
Inoguchi, T., Sonoda, N., Maeda, Y. 2016. Bilirubin as an important physiological modulator of oxidative stress and chronic inflammation in metabolic syndrome and diabetes: a new aspect on old molecule. *Diabetology International*, 7(4), 338-341.
Intorne, A.C., de Oliveira, M.V., de, M.P.L., de Souza Filho, G.A. 2012. Essential role of the czc determinant for cadmium, cobalt and zinc resistance in Gluconacetobacter diazotrophicus PAl 5. *International Microbiology*, 15(2), 69-78.
Iteman, I., Rippka, R., Tandeau De Marsac, N., Herdman, M. 2000. Comparison of conserved structural and regulatory domains within divergent 16S rRNA-23S rRNA spacer sequences of cyanobacteria. *Microbiology*, 146 (6), 1275-86.
Ismail, D., Indraputri, C., Taurina, Z. 2018. Optimization of phycocyanin extraction from microalgae *Spirulina platensis* by sonication as antioxidant. AIP Conference Proceeding. 10.1063/1.5023960.

Izumitsu, K., Yoshimi, A., Tanaka, C. 2007. Two-Component Response Regulators Ssk1p and Skn7p Additively Regulate High-Osmolarity Adaptation and Fungicide Sensitivity in Cochliobolus heterostrophus. *Eukaryotic Cell*, 6(2), 171-181.

Jacob, J.H., Hussein, E.I., Shakhatreh, M.A.K., Cornelison, C.T. 2017. Microbial community analysis of the hypersaline water of the Dead Sea using high-throughput amplicon sequencing. *MicrobiologyOpen*, 6(5), e00500.

Jaeschke, D.P., Mercali, G.D., Marczak, L.D.F., Muller, G., Frey, W., Gusbeth, C. 2019. Extraction of valuable compounds from *Arthrospira platensis* using pulsed electric field treatment. *Bioresource Technology*, 283, 207-212.

Janda, J.M., Abbott, S.L. 2007. 16S rRNA Gene Sequencing for Bacterial Identification in the Diagnostic Laboratory: Pluses, Perils, and Pitfalls. *Journal of Clinical Microbiology*, 45(9), 2761-2764.

Jensen, G.S., Attridge, V.L., Beaman, J.L., Guthrie, J., Ehmann, A., Benson, K.F. 2015. Antioxidant and anti-inflammatory properties of an aqueous cyanophyta extract derived from Arthrospira platensis: contribution to bioactivities by the non-phycocyanin aqueous fraction. *Journal of Medicinal Food*, 18(5), 535-541.

Jespersen, L., Strømdahl, L.D., Olsen, K., Skibsted, L.H. 2005. Heat and light stability of three natural blue colorants for use in confectionery and beverages. *European Food Research and Technology*, 220(3), 261-266.

Jiang, L., Wang, Y., Yin, Q., Liu, G., Liu, H., Huang, Y., Li, B. 2017. Phycocyanin: A Potential Drug for Cancer Treatment. *Journal of Cancer*, 8(17), 3416-3429.

Jiang, T., Zhang, J.-p., Chang, W.-r., Liang, D.-c. 2001. Crystal Structure of R-Phycocyanin and Possible Energy Transfer Pathways in the Phycobilisome. *Biophysical Journal*, 81(2), 1171-1179.

Johnson, E.M., Kumar, K., Das, D. 2014a. Physicochemical parameters optimisation, and purification of phycobiliproteins from the isolated *Nostoc* sp. *Bioresource Technology*, 166, 541-7.

Johnson, E.P., Strom, A.R., Helinski, D.R. 1996. Plasmid RK2 toxin protein ParE: purification and interaction with the ParD antitoxin protein. *Journal of Bacteriology*, 178(5), 1420-9.

Johnson, M.P., Vasilev, C., Olsen, J.D., Hunter, C.N. 2014b. Nanodomains of cytochrome b6f and photosystem II complexes in spinach grana thylakoid membranes. *The Plant cell*, 26(7), 3051-3061.

Jones, A.C., Gu, L., Sorrels, C.M., Sherman, D.H., Gerwick, W.H. 2009. New tricks from ancient algae: natural products biosynthesis in marine cyanobacteria. *Current Opinion in Chemical Biology*, 13(2), 216-223.

Jones, A.L. 2012. Chapter Two - The Future of Taxonomy. in: *Advances in Applied Microbiology*, (Eds.) S. Sariaslani, G.M. Gadd, Vol. 80, Academic Press, pp. 23-35.

Joshua, S., and Mullineaux, C. 2004. Phycobilisome Diffusion Is Required for Light-State Transitions in Cyanobacteria. *Plant physiology*, 135, 2112-9.

Juin, C., Chérouvrier, J.R., Thiéry, V., Gagez, A.L., Bérard, J.B., Joguet, N., Kaas, R., Cadoret, J.P., Picot, L. 2015. Microwave-assisted extraction of phycobiliproteins from *Porphyridium purpureum*. *Applied Biochemistry and Biotechnology*, 175(1), 1-15.

Kageyama, H., Tripathi, K., Rai, A.K., Cha-Um, S., Waditee-Sirisattha, R., Takabe, T. 2011. An alkaline phosphatase/phosphodiesterase, PhoD, induced by salt stress and secreted out of the cells of *Aphanothece halophytica,* a halotolerant cyanobacterium. *Applied Environmental Microbiology*, 77(15), 5178-83.

Kahlon, S., Beeri, K., Ohkawa, H., Hihara, Y., Murik, O., Suzuki, I., Ogawa, T., Kaplan, A. 2006. A putative sensor kinase, Hik31, is involved in the response of *Synechocystis* sp. strain PCC 6803 to the presence of glucose. *Microbiology*, 152, 647-55.

Kalia, D., Merey, G., Nakayama, S., Zheng, Y., Zhou, J., Luo, Y., Guo, M., Roembke, B.T., Sintim, H.O. 2013. Nucleotide, c-di-GMP, c-di-AMP, cGMP, cAMP, (p)ppGpp signaling in bacteria and implications in pathogenesis. *Chemical Society Reviews*, 42(1), 305-341.

Kalaitzis, J.A., Lauro, F.M., Neilan, B.A., 2009. Mining cyanobacterial genomes for genes encoding complex biosynthetic pathways. *Natural Product Reports*. 26 (11), 1447–1465.

Kamble, S.P., Gaikar, R.B., Padalia, R.B. 2012. Extraction and purification of C-phycocyanin from dry Spirulina and evaluating its antioxidant, anticoagulation and prevention of DNA damage activity. *Asian Pacific Journal of Tropical Biomedicine* 1, 1-4.

Kamble, S.P., Ganesh, P.V., Datta, R.C. 2018. Extraction and purification of phycoerythrin-a natural colouring agent from *Spirulina platensis*. *Journal of Pharmaceutical, Chemical and Biological Sciences*, 6(2), 78-84.

Kampinga, H.H. 2006. Chaperones in preventing protein denaturation in living cells and protecting against cellular stress. *Handbook Experimental Pharmacology* (172), 1-42.

Kanekar, P.P., Kaneka, r.S.P., Kelkar, A.S., Dhakephalkar, P.K. 2012. Halophiles – Taxonomy, Diversity, Physiology and Applications in: *Microorganisms in Environmental Management*, (Eds.) T. Satyanarayana, B. Johri, P. Anil, Springer. Dordrecht.

Kaneko, T., Sato, S., Kotani, H., Tanaka, A., Asamizu, E., Nakamura, Y., Miyajima, N., Hirosawa, M., Sugiura, M., Sasamoto, S., Kimura, T., Hosouchi, T., Matsuno, A., Muraki, A., Nakazaki, N., Naruo, K., Okumura, S., Shimpo, S., Takeuchi, C., Wada, T., Watanabe, A., Yamada, M., Yasuda, M., Tabata, S. 1996. Sequence analysis of the genome of the unicellular cyanobacterium *Synechocystis* sp. strain PCC6803. II. Sequence determination of the entire genome and assignment of potential protein-coding regions. *DNA Research*, 3(3), 109-136.

Kanesaki, Y., Yamamoto, H., Paithoonrangsarid, K., Shoumskaya, M., Suzuki, I., Hayashi, H., Murata, N. 2007. Histidine kinases play important roles in the perception and signal transduction of hydrogen peroxide in the cyanobacterium, *Synechocystis* sp. PCC 6803. *Plant Journal*, 49(2), 313-24.

Kannaujiya, V.K., Rastogi, R.P., Sinha, R.P. 2014. GC constituents and relative codon expressed amino acid composition in cyanobacterial phycobiliproteins. *Gene*, 546(2), 162-71.

Kannaujiya, V.K., Sinha, R.P. 2016. Thermokinetic stability of phycocyanin and phycoerythrin in food-grade preservatives. *Journal of Applied Phycology*, 28(2), 1063-1070.

Kannaujiya, V.K., Sundaram, S., Sinha, R.P. 2017. Gene Manipulation and Biosynthesis of Phycobiliproteins. in: *Phycobiliproteins: Recent Developments and Future Applications*, Springer Singapore. Singapore, pp. 45-69.

Kapoore, R.V., Butler, T.O., Pandhal, J., Vaidyanathan, S. 2018. Microwave-Assisted Extraction for Microalgae: From Biofuels to Biorefinery. *Biology (Basel)*, 7(1).

Karkos, P.D., Leong, S.C., Karkos, C.D., Sivaji, N., Assimakopoulos, D.A. 2011. Spirulina in clinical practice: evidence-based human applications. Evidence-based complementary and alternative medicine : Evidence Based Complementary Alternate Medicines, 2011, 531053-531053.

Karp, P., Ouzounis, C., Moore-Kochlacs, C., Goldovsky, L., Kaipa, P., Ahren, D., Tsoka, S., Darzentas, N., Kunin, V., Lopez-Bigas, N. 2005. Expansion of the biocyc collection of pathway/genome databases to 160 genomes. *Nucleic Acids Research*, 33(19), 6083 - 6089.

Kedare, S.B., Singh, R.P. 2011. Genesis and development of DPPH method of antioxidant assay. *Journal of Food Science and Technology*, 48(4), 412-422.

Kehr, J.-C., Gatte Picchi, D., Dittmann, E. 2011. Natural product biosyntheses in cyanobacteria: A treasure trove of unique enzymes. *Beilstein Journal of Organic Chemistry*, 7, 1622-1635.

Kenekar, A.A., Deodhar, M.A. 2013. Content of Indigenous Isolate *Geitlerinema sulphureum*. *Biotechnology*, 12(3), 146-154.

Khan, M.I., Shin, J.H., Kim, J.D. 2018a. The promising future of microalgae: current status, challenges, and optimisation of a sustainable and renewable industry for biofuels, feed, and other products. *Microbial Cell Factories*, 17(1), 36.

Khan, Z., Wan Maznah, W.O., Faradina Merican, M.S.M., Convey, P., Najimudin, N., Alias, S.A. 2018b. A comparative study of phycobilliprotein production in two strains of Pseudanabaena isolated from Arctic and tropical regions in relation to different light wavelengths and photoperiods. *Polar Science*.

Khatoon, H., Kok Leong, L., Abdu Rahman, N., Mian, S., Begum, H., Banerjee, S., Endut, A. 2018. Effects of different light source and media on growth and production of phycobiliprotein from freshwater cyanobacteria. *Bioresource Technology*, 249, 652-658.

Khattar, J.I.S., Kaur, S., Kaushal, S., Singh, Y., Singh, D.P., Rana, S., Gulati, A. 2015. Hyperproduction of phycobiliproteins by the cyanobacterium *Anabaena fertilissima* PUPCCC 410.5 under optimised culture conditions. *Algal Research*, 12, 463-469.

Kikuchi, H., Wako, H., Yura, K., Go, M., Mimuro, M. 2000. Significance of a Two-Domain Structure in Subunits of Phycobiliproteins Revealed by the Normal Mode Analysis. *Biophysical Journal*, 79(3), 1587-1600.

Kim, E.Y., Choi, Y.H., Nam, T.J. 2018. Identification and antioxidant activity of synthetic peptides from phycobiliproteins of Pyropia yezoensis. *International Journal of Molecular Medicine* 42(2), 789-798.

Kim, K.M., Park, J.H., Bhattacharya, D., Yoon, H.S. 2014a. Applications of next-generation sequencing to unravelling the evolutionary history of algae. *International Journal of Systematic and Evolutionary Microbiology,* 64(2), 333-45.

Kim, M., Oh, H.-S., Park, S.-C., Chun, J. 2014b. Towards a taxonomic coherence between average nucleotide identity and 16S rRNA gene sequence similarity for species demarcation of prokaryotes. *International Journal of Systematic and Evolutionary Microbiology*, 64.

Kim, Y.-R., Do, J.-M., Kim, K.H., Stoica, A.R., Jo, S.-W., Kim, U.-K., Yoon, H.-S. 2019. C-phycocyanin from Limnothrix Species KNUA002 Alleviates Cisplatin-induced ototoxicity by blocking the mitochondrial apoptotic pathway in auditory cells. *Marine Drugs*, 17(4), 235.

King, J.W. 2002. Supercritical fluid extraction: Present status and prospects. *Grasas y Aceites*, 53, 10.3989/gya.2002.v53.i1.286

Kirk Harris, J., Gregory Caporaso, J., Walker, J.J., Spear, J.R., Gold, N.J., Robertson, C.E., Hugenholtz, P., Goodrich, J., McDonald, D., Knights, D., Marshall, P., Tufo, H., Knight, R., Pace, N.R. 2012. Phylogenetic stratigraphy in the Guerrero Negro hypersaline microbial mat. *The Isme Journal*, 7, 50.

Kiss, É., Kós, P.B., Chen, M., Vass, I. 2012. A unique regulation of the expression of the psbA, psbD, and psbE genes, encoding the D1, D2 and cytochrome b559 subunits of the Photosystem II complex in the chlorophyll d containing cyanobacterium *Acaryochloris marina*. *Biochimica et Biophysica Acta (BBA) - Bioenergetics*, 1817(7), 1083-1094.

Klahn, S., Steglich, C., Hess, W.R., Hagemann, M. 2010. Glucosylglycerate: a secondary compatible solute common to marine cyanobacteria from nitrogen-poor environments. *Environmental Microbiology*, 12(1), 83-94.

Klein, B., Buchholz, R. 2013. 20 - Microalgae as sources of food ingredients and nutraceuticals. in: *Microbial Production of Food Ingredients, Enzymes and Nutraceuticals*, Woodhead Publishing, pp. 559-570.

Kolman, M.A., Nishi, C.N., Perez-Cenci, M., Salerno, G.L. 2015. Sucrose in cyanobacteria: from a salt-response molecule to play a key role in nitrogen fixation. *Life (Basel, Switzerland)*, 5(1), 102-126.

Komárek, J. 2006. Cyanobacterial Taxonomy: Current problems and prospects for the integration of traditional and molecular approaches. *Algae*, 21(4), 349-375.

Komárek, J. 2014. A polyphasic approach for the taxonomy of cyanobacteria: principles and applications. *European Journal of Phycology*, 51(3), 346-353.

Komárek, J. 1976. Taxonomic review of the genera *Synechocystis* Sauv.1892, *Synechococcus* Näg. 1849, and *Cyanothece* gen. nov. (Cyanophyceae). *Archiv für Protistenkunde*, 118, 119 -179.

Komárek, J., Cepák, V. 1998. Cytomorphological characters supporting the taxonomic validity ofCyanothece (Cyanoprokaryota). *Plant Systematics and Evolution*, 210(1-2), 25-39.

Komárek, J., Kaštovský, J., Jezberová, J. 2011. Phylogenetic and taxonomic delimitation of the cyanobacterial genus *Aphanothece* and description of *Anathece* gen. nov. *European Journal of Phycology*, 46(3), 315-326.

Konstantinidis, K.T., Tiedje, J.M. 2005. Genomic insights that advance the species definition for prokaryotes. *Proceedings of the National Academy of Sciences of the United States of America*, 102(7), 2567-2572.

Kopfmann, S., Roesch, S., Hess, W. 2016. Type II Toxin–Antitoxin Systems in the Unicellular Cyanobacterium Synechocystis sp. PCC 6803. *Toxins*, 8(7), 228.

Kuddus, M., Singh, P., Thomas, G., Al-Hazimi , A. 2013. Recent developments in production and biotechnological applications of C-phycocyanin. *Biomed Res Int*, 2013, 742859.

Kultschar, B., Llewellyn, C. 2018. Secondary metabolites in cyanobacteria. in: *Secondary Metabolites - Sources and Applications*.

Kumar, D., Dhar, D.W., Pabbi, S., Kumar, N., Walia, S. 2014. Extraction and purification of C-phycocyanin from *Spirulina platensis* (CCC540). *Indian Journal of Plant Physiology*, 19(2), 184-188.

Kumar, S., Nei, M., Dudley, J., Tamura, K. 2008. MEGA: a biologist-centric software for evolutionary analysis of DNA and protein sequences. *Brief Bioinformatics*, 9(4), 299-306.

Kupka, M., Scheer, H. 2008. Unfolding of C-phycocyanin followed by loss of non-covalent chromophore–protein interactions: 1. Equilibrium experiments. *Biochimica et Biophysica Acta (BBA) - Bioenergetics*, 1777(1), 94-103.

Kurtz, S., Phillippy, A., Delcher, A.L., Smoot, M., Shumway, M., Antonescu, C., Salzberg, S.L. 2004. Versatile and open software for comparing large genomes. *Genome Biology*, 5(2), R12.

Kuroiwa, Y., Al-Maamari, R.S., Tasaki, M. 2014. *Spirulina subsalsa* var. salina var. nov. : Thermo-Halotolerant Cyanobacteria Accumulating Two Kinds of Compatible Solute, Originated from the Sultanate of Oman. *Journal of environmental biotechnology*, 14(1), 43-56.

Laemmli, U.K. 1970. Cleavage of structural proteins during the assembly of the head of bacteriophage T4. *Nature*, 227(5259), 680-685.
Lambowitz, A.M., Zimmerly, S. 2011. Group II introns: mobile ribozymes that invade DNA. *Cold Spring Harbor perspectives in biology*, 3(8), a003616-a003616.
Land, M., Hauser, L., Jun, S.-R., Nookaew, I., Leuze, M.R., Ahn, T.-H., Karpinets, T., Lund, O., Kora, G., Wassenaar, T., Poudel, S., Ussery, D.W. 2015. Insights from 20 years of bacterial genome sequencing. *Functional & Integrative Genomics*, 15(2), 141-161.
Lange, B.M., Rujan, T., Martin, W., Croteau, R. 2000. Isoprenoid biosynthesis: The evolution of two ancient and distinct pathways across genomes. *Proceedings of the National Academy of Sciences*, 97(24), 13172-13177.
Larsson, J., Nylander, J.A., Bergman, B. 2011. Genome fluctuations in cyanobacteria reflect evolutionary, developmental and adaptive traits. *BMC Evolutionary Biology*, 11, 187.
Latifi, A., Ruiz, M., Zhang, C.-C. 2009. Oxidative stress in cyanobacteria. *FEMS Microbiology Reviews*, 33(2), 258-278.
Lau, N.S., Matsui, M., Abdullah, A.A. 2015. Cyanobacteria: Photoautotrophic microbial factories for the sustainable synthesis of industrial products. *BioMed Research International*, 2015, 754934.
Lawrenz, E., Fedewa, E.J., Richardson, T.L. 2010. Extraction protocols for the quantification of phycobilins in aqueous phytoplankton extracts. *Journal of Applied Phycology*, 23(5), 865-871.
Laybourn-Parry, J., Pearce, D.A. 2007. The biodiversity and ecology of Antarctic lakes: models for evolution. *Philosophical transactions of the Royal Society of London. Series B, Biological sciences*, 362(1488), 2273-2289.
Leão, P.N., Ramos, V., Gonçalves, P.B., Viana, F., Lage, O.M., Gerwick, W.H., Vasconcelos, V.M. 2013. Chemoecological screening reveals high bioactivity in diverse culturable portuguese marine cyanobacteria. *Marine Drugs*, 11(4), 1316-1335.
Lenton, S., Walsh, D., Rhys, N., Soper, A., Dougan, L. 2016. Structural evidence for solvent-stabilisation by aspartic acid as a mechanism for halophilic protein stability in high salt concentrations. *Physical Chemistry Chemical Physics,*18, 18054-18062
Lee, H., Ryu, G., Choi, W., Yang, W., Lee, H., Ma, C. 2018. Protective effect of water extracted *Spirulina maxima* on glutamate-induced neuronal cell death in mouse hippocampal HT22 cell. *Pharmacognosy Magazine*, 14(54), 242-247.
Leu, J.-Y., Lin, T.-H., Selvamani, M.J.P., Chen, H.-C., Liang, J.-Z., Pan, K.-M. 2013. Characterisation of a novel thermophilic cyanobacterial strain from Taian hot springs in Taiwan for high CO_2 mitigation and C-phycocyanin extraction. *Process Biochemistry*, 48, 41-48.
Levy, S.E., Myers, R.M. 2016. Advancements in Next-Generation Sequencing. *Annual Review of Genomics and Human Genetics*, 17(1), 95-115.
Ley, R.E., Harris, J.K., Wilcox, J., Spear, J.R., Miller, S.R., Bebout, B.M., Maresca, J.A., Bryant, D.A., Sogin, M.L., Pace, N.R. 2006. Unexpected diversity and complexity of the guerrero negro hypersaline microbial mat. *Applied and Environmental Microbiology*, 72(5), 3685-3695.
Li, B., Gao, M.-H., Chu, X.-M., Teng, L., Lv, C.-Y., Yang, P., Yin, Q.-F. 2015. The synergistic antitumor effects of all-trans retinoic acid and C-phycocyanin on the lung cancer A549 cells in vitro and in vivo. *European Journal of Pharmacology*, 749, 107-114.
Li, W., Su, H.-N., Pu, Y., Chen, J., Liu, L.-N., Liu, Q., Qin, S. 2019. Phycobiliproteins: Molecular structure, production, applications, and prospects. *Biotechnology Advances*, 37(2), 340-353.

Liang, Y., Kaczmarek, M.B., Kasprzak, A.K., Tang, J., Shah, M.M.R., Jin, P., Klepacz-Smółka, A., Cheng, J.J., Ledakowicz, S., Daroch, M. 2018. *Thermosynechococcaceae* as a source of thermostable C-phycocyanins: properties and molecular insights. *Algal Research*, 35, 223-235.

Liao, G., Gao, B., Gao, Y., Yang, X., Cheng, X., Ou, Y. 2016. Phycocyanin inhibits tumorigenic potential of pancreatic cancer cells: role of apoptosis and autophagy. *Scientific Reports*, 6, 34564.

Liao, X., Zhang, B., Wang, X., Yan, H., Zhang, X. 2011. Purification of C-Phycocyanin from *Spirulina platensis* by single-step ion-exchange chromatography. *Chromatographia*, 73(3-4), 291-296.

Liu, L.-N. 2016. Distribution and dynamics of electron transport complexes in cyanobacterial thylakoid membranes. *Biochimica et Biophysica Acta (BBA) - Bioenergetics*, 1857(3), 256-265.

Liu, L.-N., Chen, X.-L., Zhang, Y.-Z., Zhou, B.-C. 2005a. Characterisation, structure and function of linker polypeptides in phycobilisomes of cyanobacteria and red algae: An overview. *Biochimica et Biophysica Acta (BBA) - Bioenergetics*, 1708(2), 133-142.

Liu, Q., Huang, Y., Zhang, R., Cai, T., Cai, Y. 2016. Medical Application of Spirulina platensis Derived C-Phycocyanin. *Evidence-Based Complementary and Alternative Medicine*, 2016, 14.

Liu, L., Li, Y., Li, S., Hu, N., He, Y., Pong, R., Lin, D., Lu, L., Law, M. 2012. Comparison of Next-Generation Sequencing Systems. *Journal of Biomedicine and Biotechnology*, e2012:251364. doi:10.1155/2012/251364.

Liu, L.N., Chen, X.L., Zhang, Y.Z., Zhou, B.C. 2005. Characterisation, structure and function of linker polypeptides in phycobilisomes of cyanobacteria and red algae: an overview. *Biochimica et Biophysica Acta*, 1708(2), 133-42.

Liu, L.N., Su, H.N., Yan, S.G., Shao, S.M., Xie, B.B., Chen, X.L., Zhang, X.Y., Zhou, B.C., Zhang, Y.Z. 2009. Probing the pH sensitivity of R-phycoerythrin: investigations of active conformational and functional variation. *Biochimica et Biophysica Acta*, 1787(7), 939-46.

Liu, Q., Huang, Y., Zhang, R., Cai, T., Cai, Y. 2016. Medical application of *Spirulina platensis* derived C-phycocyanin. *Evidence-Based Complementary and Alternative Medicine*, e2016:7803846. doi: 10.1155/2016/7803846.

Liu, Z., Fu, X., Huang, W., Li, C., Wang, X., Huang, B. 2018. Photodynamic effect and mechanism study of selenium-enriched phycocyanin from *Spirulina platensis* against liver tumours. *Journal of Photochemistry and Photobiology B: Biology*, 180, 89-97.

Loman, N.J., Constantinidou, C., Chan, J.Z., Halachev, M., Sergeant, M., Penn, C.W., Robinson, E.R., Pallen, M.J. 2012. High-throughput bacterial genome sequencing: an embarrassment of choice, a world of opportunity. *Nature Reviews in Microbiology*, 10(9), 599-606.

Los, D.A., Zorina, A., Sinetova, M., Kryazhov, S., Mironov, K., Zinchenko, V.V. 2010a. Stress sensors and signal transducers in cyanobacteria. *Sensors (Basel, Switzerland)*, 10(3), 2386-2415.

Loza, V., Perona, E., Carmona, J., Mateo, P. 2013. Phenotypic and genotypic characteristics of Phormidium-like cyanobacteria inhabiting microbial mats are correlated with the trophic status of running waters. *European Journal of Phycology*, 48(2), 235-252.

Lu, W., Evans, E.H., McColl, S.M., Saunders, V.A. 1997. Identification of cyanobacteria by polymorphisms of PCR-amplified ribosomal DNA spacer region. *FEMS Microbiology Letters*, 153(1), 141-149.

Ludwig, W., Klenk, H.-P., pp. 2001. Overview: A phylogenetic backbone and taxonomic framework for procaryotic systematics. 2 ed. in: *In Bergey's manual of systematic bacteriology.*, (Eds.) B. D.R, C.R. W., Springer-Verlag,. New York, USA, pp. 49-65.

Madern, D., Ebel, C., Zaccai, G. 2000. Halophilic adaptation of enzymes. *Extremophiles*, **4**(2), 91-98.

Madamwar, D., Patel, D.K., Desai, S.N., Upadhyay, K.K., Devkar, R.V. 2015. Apoptotic potential of C-phycoerythrin from *Phormidium* sp. A27DM and *Halomicronema* sp. A32DM on human lung carcinoma cells. *Experimental and Clinical Sciences, International Online Journal for Advances in Sciences*, 14, 527-39.

Manirafasha, E., Murwanashyaka, T., Ndikubwimana, T., Rashid Ahmed, N., Liu, J., Lu, Y., Zeng, X., Ling, X., Jing, K. 2018. Enhancement of cell growth and phycocyanin production in *Arthrospira* (*Spirulina*) *platensis* by metabolic stress and nitrate fed-batch. *Bioresource Technology*, 255, 293-301.

Manirafasha, E., Murwanashyaka, T., Ndikubwimana, T., Yue, Q., Zeng, X., Lu, Y., Jing, K. 2017. Ammonium chloride: a novel effective and inexpensive salt solution for phycocyanin extraction from *Arthrospira* (*Spirulina*) *platensis*. *Journal of Applied Phycology*, 29(3), 1261-1270.

Manirafasha, E., Ndikubwimana, T., Zeng, X., Lu, Y., Jing, K. 2016. Phycobiliprotein: Potential microalgae derived pharmaceutical and biological reagent. *Biochemical Engineering Journal*, 109, 282-296.

Mardis, E.R. 2013. Next-Generation Sequencing Platforms. *Annual Review of Analytical Chemistry*, 6(1), 287-303.

Margheri, M.C., Bosco, M., Giovannetti, L., Ventura, S. 1999. Assessment of the genetic diversity of halotolerant coccoid cyanobacteria using amplified 16S rDNA restriction analysis. *FEMS Microbiology Letters*, 173(1), 9-16.

Marin, K., Kanesaki, Y., Los, D.A., Murata, N., Suzuki, I., Hagemann, M. 2004. Gene expression profiling reflects physiological processes in salt acclimation of *Synechocystis* sp. strain PCC 6803. *Plant physiology*, 136(2), 3290-3300.

Marquez, F.J., Sasaki, K., Kakizono, T., Nishio, N., Nagai, S. 1993. Growth characteristics of *Spirulina platensis* in mixotrophic and heterotrophic conditions. *Journal of Fermentation and Bioengineering*, 76(5), 408-410.

Martelli, G., Folli, C., Visai, L., Daglia, M., Ferrari, D. 2014. Thermal stability improvement of blue colorant C-Phycocyanin from *Spirulina platensis* for food industry applications. *Process Biochemistry*, 49(1), 154-159.

Martens, M., Dawyndt, P., Coopman, R., Gillis, M., De Vos, P., Willems, A. 2008. Advantages of multilocus sequence analysis for taxonomic studies: a case study using 10 housekeeping genes in the genus Ensifer (including former Sinorhizobium). *International Journal of Systematic and Evolutionary Microbiology*, 58(Pt 1), 200-14.

Martínez-Maqueda, D., Hernández-Ledesma, B., Amigo, L., Miralles, B., Gómez-Ruiz, j.a. 2013. Extraction/Fractionation Techniques for proteins and Peptides and Protein Digestion. in: *Proteomics in Foods: Principles and Applications*, (Eds.) Toldrá.F, L.M.L. Nollet, springer.

Martínez, J.M., Delso, C., Álvarez, I., Raso, J. 2019. Pulsed electric field permeabilisation and extraction of phycoerythrin from Porphyridium cruentum. *Algal Research*, 37, 51-56.

Martínez, J.M., Luengo, E., Saldaña, G., Álvarez, I., Raso, J. 2017. C-phycocyanin extraction assisted by pulsed electric field from *Artrosphira platensis*. *Food Research International*, 99, 1042-1047.

Marx, A., Adir, N. 2014. Structural characteristics that stabilise or destabilise different assembly levels of phycocyanin by urea. *Photosynthetic Research*, 121(1), 87-93.

Masek, A., Chrzescijanska, E., Zaborski, M. 2014. Estimation of the antioxidative properties of amino acids - an electrochemical approach. *International Journal of Electrochemical Science*, 9, 7904-7915.

Masojidek, J., Koblizek, M., Torzillo, G. 2013. *Photosynthesis in Microalgae*.

McCarty, M.F. 2017. Supplementation with phycocyanobilin, citrulline, taurine, and supranutritional doses of folic acid and biotin—potential for preventing or slowing the progression of diabetic complications. *Healthcare*, 5(1), 15.

McKay, C.P., Rask, J.C., Detweiler, A.M., Bebout, B.M., Everroad, R.C., Lee, J.Z., Chanton, J.P., Mayer, M.H., Caraballo, A.A., Kapil, B., Al-Awar, M., Al-Farraj, A., 2016. An unusual inverted saline microbial mat community in an interdune sabkha in the rub' al khali (the empty quarter), United Arab Emirates. *PLoS One* 11 (3), e0150342.

Medema, M.H., Blin, K., Cimermancic, P., de Jager, V., Zakrzewski, P., Fischbach, M.A., Weber, T., Takano, E., Breitling, R. 2011. antiSMASH: rapid identification, annotation and analysis of secondary metabolite biosynthesis gene clusters in bacterial and fungal genome sequences. Nucleic acids research, 39(2), W339-W346.

Meier-Kolthoff, J.P., Goker, M., Sproer, C., Klenk, H.P. 2013. When should a DDH experiment be mandatory in microbial taxonomy? *Archives of Microbiology*, 195(6), 413-8.

Mesbah, N.M., Abou-El-Ela, S.H., Wiegel, J. 2007. Novel and unexpected prokaryotic diversity in water and sediments of the alkaline, hypersaline lakes of the Wadi An Natrun, Egypt. *Microbiology Ecology*, 54(4), 598-617.

Micallef, M.L., D'Agostino, P.M., Sharma, D., Viswanathan, R., Moffitt, M.C. 2015. Genome mining for natural product biosynthetic gene clusters in the Subsection V cyanobacteria. *BMC Genomics*, 16(1), 669.

Mikhodyuk, O.S., Gerasimenko, L.M., Akimov, V.N., Ivanovsky, R.N., Zavarzin, G.A. 2008. Ecophysiology and polymorphism of the unicellular extremely natronophilic cyanobacterium *Euhalothece* sp. Z-M001 from Lake Magadi. *Microbiology*, 77(6), 717-725.

Minkova, K., Tchorbadjieva, M., Tchernov, A., Stojanova, M., Gigova, L., Busheva, M. 2007. Improved procedure for separation and purification of *Arthronema africanum* phycobiliproteins. *Biotechnology Letters*, 29(4), 647-651.

Minkova, K.M., Tchernov, A.A., Tchorbadjieva, M.I., Fournadjieva, S.T., Antova, R.E., Busheva, M.C. 2003. Purification of C-phycocyanin from *Spirulina* (*Arthrospira*) *fusiformis*. *Journal of Biotechnology*, 102(1), 55-59.

Mironov, K.S., Sinetova, M.A., Shumskaya, M., Los, D.A. 2019. Universal molecular triggers of stress responses in cyanobacterium *Synechocystis. Life (Basel)*, 9(3), 67-85.

Mishra, S.K., Shrivastav, A., Mishra, S. 2008. Effect of preservatives for food grade C-PC from Spirulina platensis. *Process Biochemistry*, 43(4), 339-345.

Mishra, S.K., Shrivastav, A., Pancha, I., Jain, D., Mishra, S. 2010. Effect of preservatives for food grade C-Phycoerythrin, isolated from marine cyanobacteria *Pseudanabaena* sp. *International Journal of Biological Macromolecules*, 47(5), 597-602.

Miskiewicz, E., Ivanov, A.G., Huner, N.P.A. 2002. Stoichiometry of the photosynthetic apparatus and phycobilisome structure of the cyanobacterium Plectonema boryanum UTEX 485 are regulated by both light and temperature. *Plant physiology*, 130(3), 1414-1425.

Mitrophanov, A.Y., Groisman, E.A. 2008. Signal integration in bacterial two-component regulatory systems. *Genes Development*, 22(19), 2601-11.

Mittal, R., Tavanandi, H., A. Mantri, V., Raghavarao, K. 2017. Ultrasound assisted methods for enhanced extraction of phycobiliproteins from marine macro-algae, *Gelidium pusillum* (Rhodophyta). *Ultrasonics Sonochemistry,* 38, 92-103

Mlouka, A., Comte, K., Castets, A.M., Bouchier, C., Tandeau de Marsac, N. 2004. The gas vesicle gene cluster from *Microcystis aeruginosa* and DNA rearrangements that lead to loss of cell buoyancy. *Journal of Bacteriology*, 186(8), 2355-65.

Mogany, T. 2013. Optimisation of culture conditions and extraction method for maximum phycocyanin production from a hypersaline cyanobacterium. in: *Biotechnology and Food Technology*, Master of Technology, Durban University of Technology. Durban.

Mogany, T., Kumari, S., Swalaha, F.M., Bux, F. 2019. Extraction and characterisation of analytical grade C-phycocyanin from *Euhalothece* sp. *Journal of Applied Phycology*, 31(3), 1661-1674.

Mogany, T., Swalaha, F.M., Allam, M., Mtshali, P.S., Ismail, A., Kumari, S., Bux, F. 2018a. Phenotypic and genotypic characterisation of an unique indigenous hypersaline unicellular cyanobacterium, Euhalothece sp.nov. *Microbiology Research*, 211, 47-56.

Mogany, T., Swalaha, F.M., Kumari, S., Bux, F. 2018b. Elucidating the role of nutrients in C-phycocyanin production by the halophilic cyanobacterium *Euhalothece* sp. *Journal of Applied Phycology*.

Mohammadi-Gouraji, E., Soleimanian-Zad, S., Ghiaci, M. 2019. Phycocyanin-enriched yogurt and its antibacterial and physicochemical properties during 21 days of storage. *Lebensmittel-Wissenschaft & Technologie*, 102, 230-236.

Mohanta, T.K., Pudake, R.N., Bae, H. 2017. Genome-wide identification of major protein families of cyanobacteria and genomic insight into the circadian rhythm. *European Journal of Phycology*, 52(2), 149-165.

Montgomery, B.L. 2014. The regulation of light sensing and light-harvesting impacts the use of cyanobacteria as biotechnology platforms. *Frontiers in Bioengineering and Biotechnology*, 2 (22), doi.org/10.3389/fbioe.2014.00022

Moon, M., Mishra, S.K., Kim, C.W., Suh, W.I., Park, M.S., Yang, J.-W. 2014. Isolation and characterisation of thermostable phycocyanin from *Galdieria sulphuraria*. *Korean Journal of Chemical Engineering*, 31(3), 490-495.

Moon, Y.-J., Kim, S., Chung, Y.-H. 2012. Sensing and responding to UV-A in Cyanobacteria. *International Journal of Molecular Sciences*, 13(12), 16303.

Moraes, C.C., Kalil, S.J. 2009. Strategy for a protein purification design using C-phycocyanin extract. *Bioresource Technology*, 100(21), 5312-5317.

Moraes, C.C., Sala, L., Cerveira, G.P., Kalil, S.J. 2011. C-phycocyanin extraction from Spirulina platensis wet biomass. *Brazilian Journal of Chemical Engineering*, 28, 45-49.

Mota, R., Guimarães, R., Büttel, Z., Rossi, F., Colica, G., Silva, C.J., Santos, C., Gales, L., Zille, A., De Philippis, R., Pereira, S.B., Tamagnini, P. 2013. Production and characterisation of extracellular carbohydrate polymer from *Cyanothece* sp. CCY 0110. *Carbohydrate Polymers*, 92(2), 1408-1415.

Muir, D.G., Perissinotto, R. 2011. Persistent phytoplankton bloom in Lake St. Lucia (iSimangaliso Wetland Park, South Africa) caused by a cyanobacterium closely associated with the genus *Cyanothece* (Synechococcaceae, Chroococcales). *Applied and Environmental Microbiology*, 77(17), 5888-5896.

Mukherjee, C., Ray, K. 2015. An improved DAPI staining procedure for visualisation of polyphosphate granules in cyanobacterial and microlagal cells.

Mullineaux, C.W. 1992. Excitation energy transfer from phycobilisomes to Photosystem I in a cyanobacterium. *Biochimica et Biophysica Acta (BBA) - Bioenergetics*, 1100, 285-292.

Muthulakshmi, M., Sudha, M., Gopal, S. 2012. Extraction, partial purification and antibacterial activity of phycocyanin from *Spirulina* isolated from fresh water body against various human pathogens. *Journal of Algal Biomass Utilisation*. 3(3), 7– 11

Munier, M., Jubeau, S., Wijaya, A., Morancais, M., Dumay, J., Marchal, L., Jaouen, P., Fleurence, J. 2014. Physicochemical factors affecting the stability of two pigments: R-phycoerythrin of Grateloupia turuturu and B-phycoerythrin of Porphyridium cruentum. *Food Chemistry*, 150, 400-407.

Muruga, B.N., Wagacha, J.M., Kabaru, J.M., Amugune, N., Duboise, S.M. 2014. Effect of physicochemical conditions on growth rates of cyanobacteria species isolated from Lake Magadi, a soda lake in Kenya. *Journal of Scientific Research*, 2, 41-50.

Myers, R.H., Montgomery, D.C. 1995. *Response Surface Methodology: Process and Product in Optimisation Using Designed Experiments*. John Wiley & Sons Inc. , New York, NY, USA.

Nag Dasgupta, C. 2015. Algae as a source of phycocyanin and other industrially important pigments, pp. 253-276.

Nagasathya, A., Thajuddin, N. 2008a. Cyanobacterial Diversity in the Hypersaline Environment of the Saltpans of Southeastern Coast of India. *Asian Journal of Plant Sciences*, 7, 473-478.

Najdenski, H.M., Gigova, L.G., Iliev, I.I., Pilarski, P.S., Lukavský, J., Tsvetkova, I.V., Ninova, M.S., Kussovski, V.K. 2013. Antibacterial and antifungal activities of selected microalgae and cyanobacteria. International *Journal of Food Science & Technology*, 48(7), 1533-1540.

Nesbitt, N.M., Arora, D.P., Johnson, R.A., Boon, E.M. 2015. Modification of a bi-functional diguanylate cyclase-phosphodiesterase to efficiently produce cyclic diguanylate monophosphate. *Biotechnology Reports*, 7, 30-37.

Nies, D.H. 1992. Resistance to cadmium, cobalt, zinc, and nickel in microbes. *Plasmid*, 27(1), 17-28.

Niu, J.F., Wang, G.C., Lin, X.Z., Zhou, B.C. 2007. Large-scale recovery of C-phycocyanin from Spirulina platensis using expanded bed adsorption chromatography. *J Chromatogr B Analyt Technol Biomed Life Sci*, 850(2), 267-76.

Nowruzi, B., Khavari-Nejad, R.-A., Sivonen, K., Kazemi, B., Najafi, F., Nejadsattari, T. 2012. Phylogenetic and morphological evaluation of two species of Nostoc (Nostocales, Cyanobacteria) in certain physiological conditions. *African Journal of Agricultural Research* 7(27), 3887-3897.

Nübel, U., Garcia-Pichel, F., Muyzer, G. 1997. PCR primers to amplify 16S rRNA genes from cyanobacteria. *Applied and Environmental Microbiology*, 63(8), 3327-3332.

Offner, G.D., Brown-Mason, A.S., Ehrhardt, M.M., Troxler, R.F. 1981. Primary structure of phycocyanin from the unicellular rhodophyte *Cyanidium caldarium*. I. Complete amino acid sequence of the alpha subunit. *Journal of Biological Chemistry*, 256(23), 12167-75.

Okada, K. 2009. HO1 and PcyA proteins involved in phycobilin biosynthesis form a 1:2 complex with ferredoxin-1 required for photosynthesis. *FEBS Letters*, 583(8), 1251-1256.

Orta-Ramirez, A., MerrillJ, E., Smith, D.M. 2000. pH Affects the Thermal Inactivation Parameters of R-Phycoerythrin from *Porphyra yezoensis*. *Journal of Food Science*, **65**(6), 1046-1050.

Oren, A. 2012. Salts and Brines. 401-426.

Oren, A., Baxter, B.K., Weimer, B.C. 2009. Microbial Communities in Salt Lakes: Phylogenetic Diversity, Metabolic Diversity, and In Situ Activities in: *ISSLR 10th International Conference & FRIENDS of Great Salt Lake 2008 Forum*, Vol. 15.

Oren, A., Tindall, B.J. 2005. Nomenclature of the cyanophyta/cyanobacteria/cyanoprokaryotes under the International Code of Nomenclature of Prokaryotes. *Algological Studies*, 117(1), 39-52.

Oren, A., Ventura, S. 2017. The current status of cyanobacterial nomenclature under the "prokaryotic" and the "botanical" code. Antonie van Leeuwenhoek.110 (1257), 1257–1269.

Orta-Ramirez, A., Merrill, J.E., Smith, D.M. 2000. pH affects the thermal inactivation parameters of R-Phycoerythrin from *Porphyra yezoensis*. *Journal of Food Science*, 65(6), 1046-1050.

Pade, N., Hagemann, M. 2015. Salt acclimation of cyanobacteria and their application in biotechnology. *Life*, 5(1), 25.

Pagels, F., Guedes, A.C., Amaro, H.M., Kijjoa, A., Vasconcelos, V. 2019. Phycobiliproteins from cyanobacteria: Chemistry and biotechnological applications. *Biotechnology Advances*, 37(3), 422-443.

Palinska, K.A., Surosz, W. 2014. Taxonomy of cyanobacteria: a contribution to consensus approach. *Hydrobiologia*, 740(1), 1-11.

Palinska, K.A., Thomasius, C.F., Marquardt, J., Golubic, S. 2006. Phylogenetic evaluation of cyanobacteria preserved as historic herbarium exsiccata. *International Journal of Systematic and Evolutionary Microbiology*, 56 (10), 2253-63.

Pan-utai, W., Iamtham, S. 2019. Extraction, purification and antioxidant activity of phycobiliprotein from Arthrospira platensis. *Process Biochemistry*.

Pan-utai, W., Kahapana, W., Iamtham, S. 2018. Extraction of C-phycocyanin from Arthrospira (Spirulina) and its thermal stability with citric acid. *Journal of Applied Phycology*, 30(1), 231-242.

Pan, R., Lu, R., Zhang, Y., Zhu, M., Zhu, W., Yang, R., Zhang, E., Ying, J., Xu, T., Yi, H. 2015. Spirulina phycocyanin induces differential protein expression and apoptosis in SKOV-3 cells. *International Journal of Biological Macromolecules*, 81, 951-959.

Pandey, M., Tiwari, D.N. 2003. Characteristics of alkaline phosphatase in cyanobacterial strains and in an APasedef mutant of Nostoc muscorum. *World Journal of Microbiology and Biotechnology*, 19(3), 279-284.

Pandhal, J., Wright, P.C., Biggs, C.A. 2008. Proteomics with a pinch of salt: a cyanobacterial perspective. *Saline Systems*, 4, doi: 10.1186/1746-1448-4-1.

Parmar, A., Singh, N.K., Kaushal, A., Sonawala, S., Madamwar, D. 2011. Purification, characterisation and comparison of phycoerythrins from three different marine cyanobacterial cultures. *Bioresource Technology*, 102(2), 1795-802.

Patel,V., Berthold, D.E., Dhandayuthapani,S.,Rathinavelu, A., Gantar. M. 2016. Optimisation of C-phycocyanin production by *Limnothrix* sp. 37-2-1. *Journal of Algal Biomass Utlilisation*, 7, 104-111.

Patel, A., Mishra, S., Pawar, R., Ghosh, P.K. 2005. Purification and characterisation of C-Phycocyanin from cyanobacterial species of marine and freshwater habitat. *Protein Expression and Purification*, 40(2), 248-55.

Patel, H.M., Rastogi, R.P., Trivedi, U., Madamwar, D. 2018. Structural characterisation and antioxidant potential of phycocyanin from the cyanobacterium *Geitlerinema* sp. H8DM. *Algal Research*, 32, 372-383.

Patil, G., Chethana, S., Madhusudhan, M.C., Raghavarao, K.S. 2008. Fractionation and purification of the phycobiliproteins from *Spirulina platensis*. *Bioresource Technology*, 99(15), 7393-6.

Patil, G., Chethana, S., Sridevi, A.S., Raghavarao, K.S. 2006. Method to obtain C-phycocyanin of high purity. *Journal of Chromatography A*, 1127(1-2), 76-81.
Patil, G., Raghavarao, K.S.M.S. 2007. Aqueous two phase extraction for purification of C-phycocyanin. *Biochemical Engineering Journal*, 34(2), 156-164.
Patwardhan, A., Ray, S., Roy, A. 2014. Molecular Markers in Phylogenetic Studies-A Review. *Journal of Phylogenetics & Evolutionary Biology*, 2(2), 1-9.
Paul, V.G., Mormile, M.R. 2017. A case for the protection of saline and hypersaline environments: a microbiological perspective. *FEMS Microbiology Ecology*, 93(8).
Peant, B., LaPointe, G., Gilbert, C., Atlan, D., Ward, P., Roy, D. 2005. Comparative analysis of the exopolysaccharide biosynthesis gene clusters from four strains of Lactobacillus rhamnosus. *Microbiology*, 151(Pt 6), 1839-51.
Pearson, W. 2013. An introduction to sequence similarity ("homology") searching. *Current Protocol Bioinformatics*, doi:10.1002/0471250953.bi0301s42.
Pernthaler, A., Pernthaler, J. 2005. Simultaneous fluorescence in situ hybridisation of mRNA and rRNA for the detection of gene expression in environmental microbes. *Methods in enzymology*, 397, 352-371.
Peter, A.P., Lakshmanan, K., Mohandass, S., Varadharaj, S., Thilagar, S., Abdul Kareem, K.A., Dharmar, P., Gopalakrishnan, S., Lakshmanan, U. 2015. Cyanobacterial KnowledgeBase (CKB), a Compendium of Cyanobacterial Genomes and Proteomes. *PLoS one*, 10(8), e0136262.
Pikuta, E.V., Hoover, R.B., Tang, J. 2007. Microbial Extremophiles at the Limits of Life. *Critical Reviews in Microbiology*, 33(3), 183-209.
Pinevich, A.V. 2015. Proposal to consistently apply the International Code of Nomenclature of Prokaryotes (ICNP) to names of the oxygenic photosynthetic bacteria (cyanobacteria), including those validly published under the International Code of Botanical Nomenclature (ICBN)/International Code of Nomenclature for algae, fungi and plants (ICN), and proposal to change Principle 2 of the ICNP. *International Journal of Systematic and Evolutionary Microbiology*, 65(3), 1070-4.
Pittera, J., Partensky, F., Six, C. 2017. Adaptive thermostability of light-harvesting complexes in marine picocyanobacteria. *Multidisciplinary Journal of Microbial Ecology*, 11(1), 112-124.
Pizarro, S.A., Sauer, K. 2001. Spectroscopic Study of the Light-harvesting Protein C-Phycocyanin Associated with Colorless Linker Peptides. *Photochemistry and Photobiology*, 73(5), 556-563.
Plemenitas, A., Lenassi, M., Konte, T., Kejzar, A., Zajc, J., Gostinčar, C., Gunde-cimerman, N. 2014. Adaptation to high salt concentrations in halotolerant/halophilic fungi: A molecular perspective. *Frontiers in Microbiology*, 5, 199. doi.org/10.3389/fmicb.2014.00199
Pleonsil, P., Soogarun, S., Suwanwong, Y. 2013. Anti-oxidant activity of holo- and apo-c-phycocyanin and their protective effects on human erythrocytes. *International Journal of Biological Macromolecules*, 60, 393-398.
Pogoryelov, D., R Sudhir, P., Kovács, L., Gombos, Z., Brown, I., Garab, G. 2003. Sodium dependency of the photosynthetic electron transport in the alkaliphilic cyanobacterium *Arthrospira platensis*. *Journal of Bioenergetics and Biomembranes*. 35(5):427-37.
Porta, D., Rippka, R., Hernández-Mariné, M. 2000. Unusual ultrastructural features in three strains of Cyanothece (cyanobacteria). *Archives of Microbiology*, 173(2), 154-163.
Post, F.J. 1977. The microbial ecology of the Great Salt Lake. *Microbial Ecology*, 3(2), 143-165.

Prabha, R., Singh, D.P., Somvanshi, P., Rai, A. 2016. Functional profiling of Cyanobacterial genomes and its role in ecological adaptations. *Genomics Data*, 9, 89-94.

Prasanna, R., Sood, A., Jaiswal, P., Nayak, S., Gupta, V., Chaudhary, V., Joshi, M., Natarajan, C. 2010. Rediscovering Cyanobacteria as valuable sources of bioactive compounds (Review). *Applied Biochemistry and Microbiology*, 46(2), 119-134.

Pumas, C., Vacharapiyasophon, P., Peerapornpisal, Y., Leelapornpisid, P., Boonchum, W., Ishii, M., Khanongnuch, C. 2011. Thermostablility of phycobiliproteins and antioxidant activity from four thermotolerant cyanobacteria. *Phycological Research*, 59(3), 166-174.

Punjabi, M., Bharadvaja, N., Sachdev, A., Krishnan, V. 2018. Molecular characterisation, modeling, and docking analysis of late phytic acid biosynthesis pathway gene, inositol polyphosphate 6-/3-/5-kinase, a potential candidate for developing low phytate crops. *3 Biotechology*, 8(8), 344. doi: 10.1007/s13205-018-1343-7.

Rae, B.D., Long, B.M., Whitehead, L.F., Forster, B., Badger, M.R., Price, G.D. 2013. Cyanobacterial carboxysomes: microcompartments that facilitate CO_2 fixation. *Journal of Molecular Microbiology and Biotechnology,* 23(5), 300-307.

Rahman, D.Y., Sarian, F.D., van Wijk, A., Martinez-Garcia, M., van der Maarel, M.J.E.C. 2017. Thermostable phycocyanin from the red microalga *Cyanidioschyzon merolae*, a new natural blue food colorant. *Journal of Applied Phycology*, 29(3), 1233-1239.

Rai, S., Pandey, S., Srivastava, A., Singh, P., Agrawal, C., Rai, L. 2013. Understanding the mechanisms of abiotic stress management in cyanobacteria with special reference to proteomics, pp. 93-112.

Rajaniemi, P., Hrouzek, P., Kastovska, K., Willame, R., Rantala, A., Hoffmann, L., Komarek, J., Sivonen, K. 2005. Phylogenetic and morphological evaluation of the genera *Anabaena, Aphanizomenon*, *Trichormus* and *Nostoc* (Nostocales, Cyanobacteria). *International Journal of Systematic and Evolutionary Microbiology*, 55(Pt 1), 11-26.

Rajaram, H., Chaurasia, A.K., Apte, S.K. 2014. Cyanobacterial heat-shock response: role and regulation of molecular chaperones. *Microbiology (Reading, England)*, 160(4), 647-658.

Rajendhran, J., Gunasekaran, P. 2011. Microbial phylogeny and diversity: Small subunit ribosomal RNA sequence analysis and beyond. *Microbiological Research*, 166(2), 99-110.

Rajneesh, Singh, S.P., Pathak, J., Sinha, R.P. 2017. Cyanobacterial factories for the production of green energy and value-added products: An integrated approach for economic viability. *Renewable and Sustainable Energy Reviews*, 69, 578-595.

Ramos, A., Acién, F.G., Fernández-Sevilla, J.M., González, C.V., Bermejo, R. 2010. Large-scale isolation and purification of C-phycocyanin from the cyanobacteria Anabaena marina using expanded bed adsorption chromatography. *Journal of Chemical Technology & Biotechnology*, 85(6), 783-792.

Ramos, V., Morais, J., Vasconcelos, V.M. 2017. A curated database of cyanobacterial strains relevant for modern taxonomy and phylogenetic studies. *Scientific Data*, 4, 170054.

Rampel Rame, R., Nilawati, Silvy, D., Novarina, I., Agus, P., Ganang, R. 2018. Cell-wall disruption and characterization of phycocyanin from microalgae: *Spirulina platensis* using Catalytic ozonation. *E3S Web of Conferences*, 73, 08010.

otto, P.H. 2010. Resistance of Microorganisms to Extreme environmental conditions and its contribution to astrobiology. *Sustainability*, 2(6), 1602.

Rastogi, R., Sonani, R., Madamwar, D., Incharoensakdi, A. 2016. Characterisation and antioxidant functions of mycosporine-like amino acids in the cyanobacterium Nostoc sp. R76DM. *Algal Research,* 16, 110-118.

Rastogi, R.P., Sonani, R.R., Madamwar, D. 2015. Physico-chemical factors affecting the in vitro stability of phycobiliproteins from *Phormidium rubidum* A09DM. *Bioresource Technology*, 190, 219-226.

Ravi, R.K., Walton, K., Khosroheidari, M. 2018. MiSeq: A Next Generation Sequencing Platform for Genomic Analysis. *Methods Molecular Biology*, 1706, 223-232.

Reddy, C.M., Bhat, V.B., Kiranmai, G., Reddy, M.N., Reddanna, P., Madyastha, K.M. 2000. Selective Inhibition of Cyclooxygenase-2 by C-Phycocyanin, a Biliprotein from Spirulina platensis. *Biochemical and Biophysical Research Communications*, 277(3), 599-603.

Reddy, K.J., Haskell, J.B., Sherman, D.M., Sherman, L.A. 1993. Unicellular, aerobic nitrogen-fixing cyanobacteria of the genus Cyanothece. *Jourmal of Bacteriology*, 175(5), 1284-92.

Reed, C.J., Lewis, H., Trejo, E., Winston, V., Evilia, C. 2013. Protein adaptations in archaeal extremophiles. *Archaea (Vancouver, B.C.)*, 2013, 373275-373275.

Reinders, A., Hee, C.-S., Ozaki, S., Mazur, A., Boehm, A., Schirmer, T., Jenal, U. 2016. Expression and Genetic Activation of Cyclic Di-GMP-Specific Phosphodiesterases in Escherichia coli. *Journal of Bacteriology*, 198(3), 448-462.

Renugadevi, K., Valli Nachiyar, C., Sowmiya, P., Sunkar, S. 2018. Antioxidant activity of phycocyanin pigment extracted from marine filamentous cyanobacteria Geitlerinema sp TRV57. *Biocatalysis and Agricultural Biotechnology*, 16, 237-242.

Richaud, C., Zabulon, G., Joder, A., Thomas, J.C. 2001. Nitrogen or sulfur starvation differentially affects phycobilisome degradation and expression of the nblA gene in Synechocystis strain PCC 6803. *Journal of Bacteriology*, 183(10), 2989-2994.

Ricker, N., Qian, H., Fulthorpe, R.R. 2012. The limitations of draft assemblies for understanding prokaryotic adaptation and evolution. *Genomics*, 100(3), 167-175.

Rippka, R. 1988. [2] Recognition and identification of cyanobacteria. in: *Methods in Enzymology*, Vol. 167, Academic Press, pp. 28-67.

Rippka, R., Deruelles, J., Waterbury, J.B., Herdman, M., Stanier, R.Y. 1979. Generic Assignments, Strain Histories and Properties of Pure Cultures of Cyanobacteria. *Journal of General Microbiology*, 111.

Roberts, M.F. 2005. Organic compatible solutes of halotolerant and halophilic microorganisms. *Saline Systems*, 1, 5-5.

Robertson, B.R., Tezuka, N., Watanabe, M.M. 2001. Phylogenetic analyses of *Synechococcus* strains (cyanobacteria) using sequences of 16S rDNA and part of the phycocyanin operon reveal multiple evolutionary lines and reflect phycobilin content. *International Journal of Systematic and Evolutionary Microbiology,* 51(3), 861-71.

Roger, P. 1982. *An introduction to blue-green algae and their role in paddy fields*.

Romay, C., Gonzalez, R., Ledon, N., Remirez, D., Rimbau, V. 2003. C-phycocyanin: a biliprotein with antioxidant, anti-inflammatory and neuroprotective effects. *Current Protein & Peptide Science,* 4(3), 207-16.

Rosaria, L., Chini Zittelli, G., Maserti, B.E., Torzillo, G. 2018. Purification of phycocyanin from *Arthrospira platensis* by hydrophobic interaction membrane chromatography. *Algal Research*, 35, 333-340.

Rosselló-Mora, R., Amann, R. 2001. The species concept for prokaryotes. *FEMS Microbiology Reviews*, 25(1), 39-67.

Rossi, F., De Philippis, R. 2015. Role of cyanobacterial exopolysaccharides in phototrophic biofilms and in complex microbial mats. *Life (Basel)*, 5(2), 1218-38.

Ruiz-Domínguez, M.C., Jáuregui, M., Medina, E., Jaime, C., Cerezal, P. 2019. Rapid green extractions of C-phycocyanin from *Arthrospira maxima* for functional applications. *Applied Sciences*, 9(1987), 1-13.

Ruiz-Ruiz, F., Benavides, J., Rito-Palomares, M. 2013. Scaling-up of a B-phycoerythrin production and purification bioprocess involving aqueous two-phase systems: practical experiences. *Process Biochemistry*, 48, 738-745.

Rutledge, P.J., Challis, G.L. 2015. Discovery of microbial natural products by activation of silent biosynthetic gene clusters. *Nature Reviews Microbiology*, 13, 509.

Safaei, M., Maleki, H., Soleimanpour, H., Norouzy, A., Zahiri, H.S., Vali, H., Noghabil, K.A. 2019. Development of a novel method for the purification of C-phycocyanin pigment from a local cyanobacterial strain *Limnothrix* sp. NS01 and evaluation of its anticancer properties. *Scientific Reports*, 9, 16.

Safi, C., Ursu, A.V., Laroche, C., Zebib, B., Merah, O., Pontalier, P.-Y., Vaca-Garcia, C. 2014. Aqueous extraction of proteins from microalgae: Effect of different cell disruption methods. *Algal Research*, 3, 61-65.

Saibil, H. 2013. Chaperone machines for protein folding, unfolding and disaggregation. *Nature reviews. Molecular Cell Biology*, 14(10), 630-642.

Saitou, N., Nei, M. 1987. The neighbor-joining method: a new method for reconstructing phylogenetic trees. *Molecular Biology and Evolution*, 4(4), 406-25.

Sakiyama, T., Ueno, H., Homma, H., Numata, O., Kuwabara, T. 2006. Purification and characterisation of a hemolysin-like protein, sll1951, a nontoxic member of the rtx protein family from the Cyanobacterium *Synechocystis* sp. Strain PCC 6803. *Journal of Bacteriology*, 188(10), 3535-3542.

Salama, A., Ghany, A.A., Osman, A., Sitohy, M. 2015. Maximising phycocyanin extraction from a newly identified Egyptian cyanobacteria strain: *Anabaena oryzae* SOS13. *International Food Research Journal*, 22(2), 517.

Samydurai, S., Karthick Raja Namasivayam, S., Pandey, V.K. 2016. Influence of algal based protein nanoparticles loading on antibacterial activity, in vitro drug release and cytotoxicity of cephalosporine derivative. *Asian Journal of Pharmaceutics*, 10, S693-S699.

Samylina, O.S., Zaytseva, L.V. 2019. Characterisation of modern dolomite stromatolites from hypersaline Petukhovskoe Soda Lake, Russia. *Lethaia*, 52(1), 1-13.

Santiago-Santos, M.C., Ponce-Noyola, T., Olvera-Ramírez, R., Ortega-López, J., Cañizares-Villanueva, R.O. 2004. Extraction and purification of phycocyanin from *Calothrix* sp. *Process Biochemistry*, 39(12), 2047-2052.

Sarada, R., Pillai, M.G., Ravishankar, G.A. 1999a. Phycocyanin from *Spirulina* sp: influence of processing of biomass on phycocyanin yield, analysis of efficacy of extraction methods and stability studies on phycocyanin. *Process Biochemistry*, 34(8), 795-801.

Sarethy, I.P., Pan, S., Danquah, M.K. 2014. Modern Taxonomy for Microbial Diversity, Biodiversity. in: *The Dynamic Balance of the Planet*, (Ed.) O. Grillo, IntechOpen.

Schirrmeister, B.E., Dalquen, D.A., Anisimova, M., Bagheri, H.C. 2012. Gene copy number variation and its significance in cyanobacterial phylogeny. *BMC Microbiology*, 12(1), 177.

Schirrmeister, B.E., Gugger, M., Donoghue, P.C.J. 2015. Cyanobacteria and the Great Oxidation Event: evidence from genes and fossils. *Palaeontology*, 58(5), 769-785.

Schmidt, R.A., Wiebe, M.G., Eriksen, N.T. 2005. Heterotrophic high cell-density fed-batch cultures of the phycocyanin-producing red alga *Galdieria sulphuraria*. *Biotechnology and Bioengineering*, 90(1), 77-84.

Schneegurt, M.A. 2012. Media and Conditions for the Growth of Halophilic and Halotolerant Bacteria and Archaea. in: *Advances in Understanding the Biology of Halophilic Microorganisms,*, (Ed.) R.H. Vreeland, Vol. 35, Springer Science Business Media Dordrecht pp. 35-57.

Schubert, H., Fulda, S., Hagemann, M. 1993. Effects of adaptation to different salt concentrations on photosynthesis and pigmentation of the cyanobacterium *Synechocystis* sp. PCC 6803. *Journal of Plant Physiology*, 142(3), 291-295.

Schuergers, N., Wilde, A. 2015. Appendages of the cyanobacterial cell. *Life (Basel)*, 5(1), 700-15.

Sciuto, K., Moro, I. 2015. Cyanobacteria: the bright and dark sides of a charming group. *Biodiversity and Conservation*, 24(4), 711-738.

Sekar, S., Chandramohan, M. 2008. Phycobiliproteins as a commodity: trends in applied research, patents and commercialisation. *Journal of Applied Phycology* 20, 113-136.

Sentausa, E., Fournier, P.E. 2013. Advantages and limitations of genomics in prokaryotic taxonomy. *Clinical Microbiology and Infection*, 19(9), 790-5.

Seo, P.S., Yokota, A. 2003. The phylogenetic relationships of cyanobacteria inferred from 16S rRNA, gyrB, rpoC1 and rpoD1 gene sequences. *The Journal of General and Applied Microbiology*, 49(3), 191-203.

Seo, Y.C., Choi, W.S., Park, J.H., Park, J.O., Jung, K.H., Lee, H.Y. 2013. Stable isolation of phycocyanin from *Spirulina platensis* associated with high-pressure extraction process. *International Journal of Molecular Sciences*, 14(1), 1778-87.

Setyoningrum, Tutik M., Nur, M.M.A. 2015. Optimisation of C-phycocyanin production from S. platensis cultivated on mixotrophic condition by using response surface methodology. *Biocatalysis and Agricultural Biotechnology*, 4(4), 603-607.

Shah, V., Ray, A., Garg, N., Madamwar, D. 2000. Characterisation of the extracellular polysaccharide produced by a marine cyanobacterium, *Cyanothece* sp. ATCC 51142, and its exploitation toward metal removal from solutions. *Current Microbiology*, 40(4), 274-278.

Shalaby, E.A., Dubey, N.K. 2018. This widespread distribution reveals a large diversity of species, covering a broad spectrum of physiological properties and tolerance to environmental stress. *Indian Journal of Geo Sciences*, 47, 21-23.

Shaw, K.L., Grimsley, G.R., Yakovlev, G.I., Makarov, A.A., Pace, C.N. 2001. The effect of net charge on the solubility, activity, and stability of ribonuclease Sa. *Protein Science*, 10(6), 1206-1215.

Sherman, D., Sherman, L. 1983. Effect of iron deficiency and iron restoration on ultrastructure of Anacystis nidulans. *Journal of Bacteriology*, 156, 393-401.

Shi, T., Falkowski, P.G. 2008. Genome evolution in cyanobacteria: the stable core and the variable shell. *Proceedings of the National Academy of Sciences of the United States of America*, 105.

Shi, T., Ilikchyan, I., Rabouille, S., Zehr, J.P. 2010. Genome-wide analysis of diel gene expression in the unicellular N_2-fixing cyanobacterium *Crocosphaera watsonii* WH 8501 *Multidisciplinary Journal of Microbial Ecology*, 4(5), 621-632.

Sidler, W. 2004. The Molecular Biology of Cyanobacteria. *Advances in Photosynthesis*, 1.

Siglioccolo, A., Paiardini, A., Piscitelli, M., Pascarella, S. 2011. Structural adaptation of extreme halophilic proteins through decrease of conserved hydrophobic contact surface. *BMC structural biology*, 11(50), doi.org/10.1186/1472-6807-11-50.

Silva, L.A., Kuhn, K.R., Moraes, C.C., Burkert, C.A.V., Kalil, S.J. 2009. Experimental design as a tool for optimisation of C-phycocyanin purification by precipitation from *Spirulina platensis*. *Journal of Brazilian Chemical Society* 20, 5-21.

Silveira, S.T., Burkert, J.F., Costa, J.A., Burkert, C.A., Kalil, S.J. 2007. Optimisation of phycocyanin extraction from *Spirulina platensis* using factorial design. *Bioresource Technology*, 98(8), 1629-1634.

Simbolo, M., Gottardi, M., Corbo, V., Fassan, M., Mafficini, A., Malpeli, G., Lawlor, R.T., Scarpa, A. 2013. DNA Qualification Workflow for Next Generation Sequencing of Histopathological Samples. *PLoS one*, 8(6), e62692.

Sinetova, M.A., Los, D.A. 2016. New insights in cyanobacterial cold stress responses: Genes, sensors, and molecular triggers. *Biochimica et Biophysica Acta (BBA) - General Subjects*, 1860(11, Part A), 2391-2403.

Singh, N., Sonani, R., Rastogi, R., Madamwar, D. 2015. The phycobilisomes: an early requisite for efficient photosynthesis in cyanobacteria. *Experimental and Clinical Sciences, International Online Journal for Advances in Sciences.*, 14, 268-289.

Singh, N.K., Parmar, A., Madamwar, D. 2009a. Optimisation of medium components for increased production of C-phycocyanin from *Phormidium ceylanicum* and its purification by single step process. *Bioresource Technology*, 100(4), 1663-9.

Singh, N.K., Parmar, A., Sonani, R.R., Madamwar, D. 2012. Isolation, identification and characterisation of novel thermotolerant *Oscillatoria* sp. N9DM: Change in pigmentation profile in response to temperature. *Process Biochemistry*, 47(12), 2472-2479.

Singh, P., Kuddus, M., Thomas, G. 2009b. An efficient method for extraction of C-phycocyanin from *Spirulina* sp. and its binding affinity to blood cells, nuclei and genomic. *DNA*. 1(5), 80-85.

Singh, P., Kuddus, M., Thomas, G. 2011. Isolation and binding affinity of C-phycocyanin to blood cells and genomic DNA as well as its diagnostic applications. *Journal of Biotechnology and Pharmaceutical Research*, 2, 001-008.

Singh, R., Parihar, P., Singh, M., Bajguz, A., Kumar, J., Singh, S., Singh, V.P., Prasad, S.M. 2017. Uncovering potential applications of cyanobacteria and algal metabolites in biology, agriculture and medicine: Current status and future prospects. *Frontiers in Microbiology*, 8(515), doi.org/10.3389/fmicb.2017.00515.

Skizim, N.J., Ananyev, G.M., Krishnan, A., Dismukes, G.C. 2012. Metabolic pathways for photobiological hydrogen production by nitrogenase- and hydrogenase-containing unicellular cyanobacteria *Cyanothece*. *Journal of Biology Chemistry*, 287(4), 2777-2786.

Sloth, J.K., Jensen, H.C., Pleissner, D., Eriksen, N.T. 2017. Growth and phycocyanin synthesis in the heterotrophic microalga *Galdieria sulphuraria* on substrates made of food waste from restaurants and bakeries. *Bioresource Technology*, 238, 296-305.

Sloth, J.K., Wiebe, M.G., Eriksen, N.T. 2006. Accumulation of phycocyanin in heterotrophic and mixotrophic cultures of the acidophilic red alga *Galdieria sulphuraria*. *Enzyme and Microbial Technology*, 38(1), 168-175.

Smit, S., Widmann, J., Knight, R. 2007. Evolutionary rates vary among rRNA structural elements. *Nucleic Acids Research*, 35(10), 3339-3354.

Snel, B., Bork, P., Huynen, M.A. 2002. Genomes in flux: the evolution of archaeal and proteobacterial gene content. *Genome Research*, 12(1), 17-25.

Sohm, J.A., Edwards, B.R., Wilson, B.G., Webb, E.A. 2011. Constitutive Extracellular Polysaccharide (EPS) Production by Specific Isolates of Crocosphaera watsonii. *Frontiers in microbiology*, 2, 229-229.

Sonani, R.R., Patel, S., Bhastana, B., Jakharia, K., Chaubey, M.G., Singh, N.K., Madamwar, D. 2017. Purification and antioxidant activity of phycocyanin from Synechococcus sp. R42DM isolated from industrially polluted site. *Bioresource Technology*, 245, 325-331.

Sonani, R.R., Rastogi, R.P., Patel, R., Madamwar, D. 2016. Recent advances in production, purification and applications of phycobiliproteins. *World Journal of Biological Chemistry*, 7(1), 100-109.

Sonani, R.R., Singh, N.K., Kumar, J., Thakar, D., Madamwar, D. 2014. Concurrent purification and antioxidant activity of phycobiliproteins from *Lyngbya* sp. A09DM: An antioxidant and anti-aging potential of phycoerythrin in *Caenorhabditis elegans*. *Process Biochemistry*, 49(10), 1757-1766.

Song, W., Zhao, C., Wang, S. 2013. A Large-Scale Preparation Method of High Purity C-Phycocyanin. *International Journal of Bioscience, Biochemistry and Bioinformatics*, 3(4).

Soni A, Dubey M, Verma M, Dhankhar R, Kaushal V, R, A., R, S. 2005. Revisiting the Role of Phycocyanin in Current Clinical Practice. *International Journal of Pharmaceutical Sciences And Research*, 6(11), 4588-4600.

Soni, B., Kalavadia, B., Trivedi, U., Madamwar, D. 2006. Extraction, purification and characterisation of phycocyanin from *Oscillatoria quadripunctulata*—Isolated from the rocky shores of Bet-Dwarka, Gujarat, India. *Process Biochemistry*, 41(9), 2017-2023.

Soni, B., Trivedi, U., Madamwar, D. 2008. A novel method of single step hydrophobic interaction chromatography for the purification of phycocyanin from *Phormidium fragile* and its characterisation for antioxidant property. *Bioresource Technology*, 99(1), 188-94.

Soucy, S.M., Huang, J., Gogarten, J.P. 2015. Horizontal gene transfer: building the web of life. *Nature Reviews Genetics*, 16(8), 472-782.

Spurr, A.R. 1969. A low viscosity epoxy resin embedding medium for electron microscopy. . *Journal of Ultrastructure Research,* 26, 31–34.

Stackebrandt, E., Goebel, B.M. 1994. Taxonomic note: A place for DNA-DNA reassociation and 16s rrna sequence analysis in the present species definition in bacteriology. *International Journal of Systematic and Evolutionary Microbiology*, 44(4), 846-849.

Stanier, R.Y., Kunisawa, R., Mandel, M., Cohen-Bazire, G. 1971. Purification and properties of unicellular blue-green algae (order Chroococcales). *Bacteriology Reviews*, 35(2), 171-205.

Stanier, R.Y., Sistrom, W.R., Hansen, T.A., Whitton, B.A., Castenholz, R.W., Pfennig, N., Gorlenko, V.N., Kondratieva, E.N., Eimhjellen, K.E., Whittenbury, R., Gherna, R.L., Trüper, H.G. 1978. Proposal to place the nomenclature of the cyanobacteria (Blue-Green Algae) under the rules of the international code of nomenclature of bacteria. *International Journal of Systematic and Evolutionary Microbiology*, 28(2), 335-336.

Stockel, J., Jacobs, J.M., Elvitigala, T.R., Liberton, M., Welsh, E.A., Polpitiya, A.D., Gritsenko, M.A., Nicora, C.D., Koppenaal, D.W., Smith, R.D., Pakrasi, H.B. 2011. Diurnal rhythms result in significant changes in the cellular protein complement in the cyanobacterium Cyanothece 51142. *PLoS One*, 6(2), e16680.

Stone, M.T., Kozlov, M. 2014. Separating Proteins with Activated Carbon. *Langmuir*, 30(27), 8046-8055.

Sua, C.H., Liu, C.S., Yanga, P.C., Syu, K.S., Chiuh, H.S. 2014. Solid-liquid extraction of phycocyanin from *Spirulina platensis*: Kinetic modeling of influential factors. *Separation and Purification Technology* 123, 64-68.

Suarez Ruiz, C.A., Emmery, D.P., Wijffels, R.H., Eppink, M.H., van den Berg, C. 2018. Selective and mild fractionation of microalgal proteins and pigments using aqueous two-phase systems. *Journal of Chemical Technology & Biotechnology*, 93(9), 2774-2783.

Sudhakar. M.P, Jagatheesan. A, Perumal K, Arunkumar. K. 2015. Methods of phycobiliprotein extraction from *Gracilaria crassa* and its applications in food colourants. *Algal Research*, 8, 115-120.

Sundh, J., Nylander, J., Bergman, B. 2011. Genome fluctuations in cyanobacteria reflect evolutionary, developmental and adaptive traits. *BMC evolutionary biology*, **11**, 187.

Sun, L., Wang, S., Chen, L., Gong, X. 2003. Promising fluorescent probes from phycobiliproteins. *IEEE Journal of Selected Topics in Quantum Electronics*, 9(2), 177-188.

Sun, L., Wang, S., Gong, X., Zhao, M., Fu, X., Wang, L. 2009. Isolation, purification and characteristics of R-phycoerythrin from a marine macroalga *Heterosiphonia japonica. Protein Expression and Purification*, 64(2), 146-54.

Suplatov, D., Panin, N., Kirilin, E., Shcherbakova, T., Kudryavtsev, P., Švedas, V. 2014. Computational design of a pH Stable Enzyme: Understanding molecular mechanism of penicillin acylase's adaptation to alkaline conditions. *PLoS One*, 9(6), e100643.

Suzery, M., Hadiyanto, Majid, D., Setyawan, D., Sutanto, H. 2017. Improvement of stability and antioxidant activities by using phycocyanin - chitosan encapsulation technique. *IOP Conference Series: Earth and Environmental Science*, 55, 012052.

Suzuki, I., Kanesaki, Y., Hayashi, H., Hall, J.J., Simon, W.J., Slabas, A.R., Murata, N. 2005. The histidine kinase Hik34 is involved in thermotolerance by regulating the expression of heat shock genes in *Synechocystis*. *Plant Physiology*, 138(3), 1409-21.

Takagi, D., Takumi, S., Hashiguchi, M., Sejima, T., Miyake, C. 2016. Superoxide and singlet oxygen produced within the thylakoid membranes both cause Photosystem I photoinhibition. *Plant physiology*, 171(3), 1626-1634.

Tal, O., Trabelcy, B., Gerchman, Y., Adir, N. 2014.Investigation of phycobilisome subunit interaction interfaces by coupled cross-linking and mass spectrometry. *The Journal of Biological Chemistry*, 289(48), 33084-33097.

Tamagnini, P., Leitão, E., Oliveira, P., Ferreira, D., Pinto, F., Harris, D.J., Heidorn, T., Lindblad, P., 2002. Cyanobacterial hydrogenases: diversity, regulation and applications. *FEMS Microbiology Reviews*. 31 (6), 692–720.

Tan, B.F., Te, S.H., Boo, C.Y., Gin, K.Y.-H., Thompson, J.R. 2016. Insights from the draft genome of the subsection V (Stigonematales) cyanobacterium Hapalosiphon sp. Strain MRB220 associated with 2-MIB production. *Standards in Genomic Sciences*, 11(1), 58.

Tandeau de Marsac, N. 2003a. Phycobiliproteins and phycobilisomes: the early observations. *Photosynthetic Research*, 76(1-3), 193-205.

Tandeau de Marsac, N. 2003b. *Phycobiliproteins and phycobilisomes: The early observations*.

Tang, J., Du, L.-M., Liang, Y.-M., Daroch, M. 2019. Complete genome sequence and comparative analysis of *Synechococcus* sp. CS-601 (SynAce01), a cold-adapted cyanobacterium from an oligotrophic antarctic habitat. *International Journal of Molecular Sciences*, 20(1), 152.

Tangtua, J. 2014. Evaluation and comparison of microbial cells disruption methods for extraction of pyruvate decarboxylase. *International Food Research Journal*, 21(4), 1331-1336.

Tanizawa, Y., Tohno, M., Kaminuma, E., Nakamura, Y., Arita, M. 2015. Complete genome sequence and analysis of *Lactobacillus hokkaidonensis* LOOC260T, a psychrotrophic lactic acid bacterium isolated from silage. *BMC Genomics*, 16(1), 240.

Tatusova, T., DiCuccio, M., Badretdin, A., Chetvernin, V., Nawrocki, E.P., Zaslavsky, L., Lomsadze, A., Pruitt, K.D., Borodovsky, M., Ostell, J. 2016. NCBI prokaryotic genome annotation pipeline. *Nucleic Acids Research*, 44(14), 6614-6624.

Taufiqurrahmi, N., Religia, P., Mulyani, G., Suryana, D., Ichsan, Tanjung, F.A., Arifin, Y. 2017. Phycocyanin extraction in Spirulina produced using agricultural waste. *IOP Conference Series: Materials Science and Engineering*, 206(1), 012097.

Tavanandi, H.A., Mittal, R., Chandrasekhar, J., Raghavarao, K.S.M.S. 2018. Simple and efficient method for extraction of C-Phycocyanin from dry biomass of Arthospira platensis. *Algal Research*, 31, 239-251.

Tettelin, H., Masignani, V., Cieslewicz, M.J., Donati, C., Medini, D., Ward, N.L., Angiuoli, S.V., Crabtree, J., Jones, A.L., Durkin, A.S., Deboy, R.T., Davidsen, T.M., Mora, M., Scarselli, M., Margarit, y., Ros, I., Peterson, J.D., Hauser, C.R., Sundaram, J.P., Nelson, W.C., Madupu, R., Brinkac, L.M., Dodson, R.J., Rosovitz, M.J., Sullivan, S.A., Daugherty, S.C., Haft, D.H., Selengut, J., Gwinn, M.L., Zhou, L., Zafar, N., Khouri, H., Radune, D., Dimitrov, G., Watkins, K., O'Connor, K.J., Smith, S., Utterback, T.R., White, O., Rubens, C.E., Grandi, G., Madoff, L.C., Kasper, D.L., Telford, J.L., Wessels, M.R., Rappuoli, R., Fraser, C.M. 2005. Genome analysis of multiple pathogenic isolates of Streptococcus agalactiae: implications for the microbial "pan-genome". *Proceedings of the National Academy of Sciences of the United States of America,* 102.

Thangam, R., Suresh, V., Asenath Princy, W., Rajkumar, M., Senthilkumar, N., Gunasekaran, P., Rengasamy, R., Anbazhagan, C., Kaveri, K., Kannan, S. 2013. C-Phycocyanin from Oscillatoria tenuis exhibited an antioxidant and in vitro antiproliferative activity through induction of apoptosis and G0/G1 cell cycle arrest. *Food Chemistry*, 140(1-2), 262-72.

Thiel, T. 2006. Genetic Analysis of Cyanobacteria, pp. 581-611.

Thompson, C.C., Chimetto, L., Edwards, R.A., Swings, J., Stackebrandt, E., Thompson, F.L. 2013. Microbial genomic taxonomy. *BMC Genomics*, 14(1), 913.

Tiwari, O.N., Bhunia, B., Chakraborty, S., Goswami, S., Devi, I. 2019. Strategies for improved production of phycobiliproteins (PBPs) by *Oscillatoria* sp. BTA170 and evaluation of its thermodynamic and kinetic stability. *Biochemical Engineering Journal*, 145, 153-161.

Tooley, A.J., Cai, Y.A., Glazer, A.N. 2001. Biosynthesis of a fluorescent cyanobacterial C-phycocyanin holo-alpha subunit in a heterologous host. *Proceedings of the National Academy of Sciences of the United States of America*, 98(19), 10560-5.

Tsunekawa, K., Shijuku, T., Hayashimoto, M., Kojima, Y., Onai, K., Morishita, M., Ishiura, M., Kuroda, T., Nakamura, T., Kobayashi, H., Sato, M., Toyooka, K., Matsuoka, K., Omata, T., Uozumi, N. 2009. Identification and characterisation of the Na+/H+ antiporter Nhas3 from the thylakoid membrane of *Synechocystis* sp. PCC 6803. *The Journal of Biological Chemistry*, 284(24), 16513-16521.

Tu, S.L., Gunn, A., Toney, M.D., Britt, R.D., Lagarias, J.C. 2004. Biliverdin reduction by cyanobacterial phycocyanobilin:ferredoxin oxidoreductase (PcyA) proceeds via linear tetrapyrrole radical intermediates. *Journal of the American Chemical Society*, 126(28), 8682-93.

Valerio, E., Chambel, L., Paulino, S., Faria, N., Pereira, P., Tenreiro, R. 2009. Molecular identification, typing and traceability of cyanobacteria from freshwater reservoirs. *Microbiology*, 155(Pt 2), 642-56.

Vandecraen, J., Chandler, M., Aertsen, A., Van Houdt, R. 2017. The impact of insertion sequences on bacterial genome plasticity and adaptability. *Critical Reviews in Microbiology*, 43(6), 709-730.

Ventosa, A. 2006. Unusual micro-organisms from unusual habitats: hypersaline environments. in: *Prokaryotic Diversity: Mechanisms and Significance*, (Eds.) H.M. Lappin-Scott, N.A. Logan, P.C.F. Oyston, Cambridge University Press. Cambridge, pp. 223-254.

Vera-Gargallo, B., Ventosa, A. 2018. Metagenomic Insights into the Phylogenetic and Metabolic Diversity of the Prokaryotic Community Dwelling in Hypersaline Soils from the Odiel Saltmarshes (SW Spain). *Genes*, 9(3), 152.

Vernès, L., Granvillain, P., Chemat, F., Vian, M. 2015. Phycocyanin from *Arthrospira Platensis.* Production*, Extraction and Analysis*.

Větrovský, T., Baldrian, P. 2013. The Variability of the 16S rRNA Gene in Bacterial Genomes and Its Consequences for Bacterial Community Analyses. *PLOS ONE*, 8(2), e57923.

Vickers, C.E., Bongers, M., Liu, Q., Delatte, T., Bouwmeester, H. 2014. Metabolic engineering of volatile isoprenoids in plants and microbes. *Plant, Cell & Environment*, 37(8), 1753-1775.

Viskari, P.J., Colyer, C.L. 2003. Rapid extraction of phycobiliproteins from cultured cyanobacteria samples. *Analytical Biochemistry*, 319(2), 263-271.

Viskari, P.J., Colyer, C.L. 2002. Separation and quantitation of phycobiliproteins using phytic acid in capillary electrophoresis with laser-induced fluorescence detection. *Journal of Chromatography A*, 972(2), 269-76.

Wada, N., Sakamoto, T., Matsugo, S. 2013. Multiple Roles of photosynthetic and sunscreen pigments in cyanobacteria focusing on the oxidative stress. *Metabolites*, 3(2), 463.

Walsby, A.E., Van Rijn, J., Cohen, Y. 1983. The biology of a new gas-vacuolate cyanobacterium, *Dactylococcopsis salina* sp. nov., in Solar Lake. *Proceedings of the Royal Society B: Biological Sciences*, 217, 417-447.

Walter, J.M., Coutinho, F.H., Dutilh, B.E., Swings, J., Thompson, F.L., Thompson, C.C. 2017. Ecogenomics and Taxonomy of Cyanobacteria Phylum. *Frontiers in Microbiology*, 8(2132).

Wan, D.-H., Zheng, B.-Y., Ke, M.-R., Duan, J.-Y., Zheng, Y.-Q., Yeh, C.-K., Huang, J.-D. 2017. C-Phycocyanin as a tumour-associated macrophage-targeted photosensitiser and a vehicle of phthalocyanine for enhanced photodynamic therapy. *Chemical Communications*, 53(29), 4112-4115.

Wang, H., Fewer, D.P., Sivonen, K. 2011. Genome mining demonstrates the widespread occurrence of gene clusters encoding bacteriocins in cyanobacteria. *PLoS One*, 6(7), e22384.

Wang, H., Liu, Y., Gao, X., Carter, C.L., Liu, Z.R. 2007. The recombinant beta subunit of C-phycocyanin inhibits cell proliferation and induces apoptosis. *Cancer Letters*, 247(1), 150-8.

Wang, L., Qu, Y., Fu, X., Zhao, M., Wang, S., Sun, L. 2014. Isolation, Purification and Properties of an R-Phycocyanin from the Phycobilisomes of a Marine Red Macroalga *Polysiphonia urceolata*. *PLoS One*, 9(2), e87833.

Wang, X., Li, L., Chang, W., Zhang, J., Gui, L., Guo, B., Liang, D. 2001. Structure of C-phycocyanin from Spirulina platensis at 2.2 Å resolution: A novel monoclinic crystal form for phycobiliproteins in phycobilisomes. *Acta crystallographica. Section D, Biological crystallography*, 57, 784-92.

Watanabe, M., Sato, M., Kondo, K., Narikawa, R., Ikeuchi, M. 2012. Phycobilisome model with novel skeleton-like structures in a glaucocystophyte Cyanophora paradoxa. *Biochimica et Biophysica Acta (BBA) - Bioenergetics*, 1817(8), 1428-1435.

Waterhouse, A., Bertoni, M., Bienert, S., Studer, G., Tauriello, G., Gumienny, R., Heer, F.T., de Beer, T.A P., Rempfer, C., Bordoli, L., Lepore, R., Schwede, T. 2018. SWISS-MODEL: homology modelling of protein structures and complexes. *Nucleic Acids Research*, 46(W1), W296-W303.

Welsh, E.A., Liberton, M., Stöckel, J., Loh, T., Elvitigala, T., Wang, C., Wollam, A., Fulton, R.S., Clifton, S.W., Jacobs, J.M., Aurora, R., Ghosh, B.K., Sherman, L.A., Smith, R.D., Wilson, R.K., Pakrasi, H.B. 2008. The genome of *Cyanothece* 51142, a unicellular diazotrophic cyanobacterium important in the marine nitrogen cycle. *Proceedings of the National Academy of Sciences*, 105(39), 15094-15099.

Whitton, B.A., Potts, M. 2000. Introduction to the Cyanobacteria in: *The Ecology of Cyanobacteria-Their Diversity In Time and Space*, (Ed.) P. M., Kluwer Academic Publishers. Dordrecht.

Wieland, A., Kühl, M. 2000. Short-term temperature effects on oxygen and sulfide cycling in a hypersaline cyanobacterial mat (Solar Lake, Egypt). *Marine Ecology Progress Series*, 196, 87-102.

Williams, D.L., Slayden, R.A., Amin, A., Martinez, A.N., Pittman, T.L., Mira, A., Mitra, A., Nagaraja, V., Morrison, N.E., Moraes, M., Gillis, T.P. 2009. Implications of high level pseudogene transcription in Mycobacterium leprae. *BMC Genomics*, 10(1), 397.

Wilmotte, A., Herdman, M. 2001. Phylogenetic Relationships Among the Cyanobacteria Based on 16S rRNA Sequences in: Bergey's Manual of Systematics of Archaea and Bacteria. (Ed.) W. B., Whitman *et al*., John Wiley & Sons.

Wingfield, P.T. 2001. Protein precipitation using ammonium sulphate. *Current Protocol Protein Science*.

Wong, H.L., Ahmed-Cox, A., Burns, B.P. 2016. Molecular Ecology of Hypersaline Microbial Mats: Current Insights and New Directions. *Microorganisms*, 4(1), 6.

Wu, F., Zang, X., Zhang, X., Zhang, R., Huang, X., Hou, L., Jiang, M., Liu, C., Pang, C. 2016a. Molecular cloning of CPCU and heterodimeric bilin lyase activity analysis of CPCU and CPCS for attachment of phycocyanobilin to Cys-82 on the *β*-subunit of phycocyanin in arthrospira platensis fachb314. *Molecules*, 21(3), 357.

Wu, H.-L., Wang, G.-H., Xiang, W.-Z., Li, T., He, H. 2016b. Stability and antioxidant activity of food-grade phycocyanin isolated from *Spirulina platensis*. *International Journal of Food Properties*, 19(10), 2349-2362.

Wu, X.J., Yang, H., Chen, Y.T., Li, P.P. 2018. Biosynthesis of Fluorescent beta subunits of c-phycocyanin from *Spirulina subsalsa* in *Escherichia coli*, and their antioxidant properties. *Molecules*, 23(6).

Xie, Y., Jin, Y., Zeng, X., Chen, J., Lu, Y., Jing, K. 2015. Fed-batch strategy for enhancing cell growth and C-phycocyanin production of *Arthrospira* (*Spirulina*) *platensis* under phototrophic cultivation. *Bioresource Technology*, 180, 281-287.

Yan, S.-G., Zhu, L.-P., Su, H.-N., Zhang, X.-Y., Chen, X.-L., Zhou, B.-C., Zhang, Y.-Z. 2011. Single-step chromatography for simultaneous purification of C-phycocyanin and allophycocyanin with high purity and recovery from *Spirulina* (*Arthrospira*) *platensis*. *Journal of Applied Phycology*, 23(1), 1-6.

Yoon, S.H., Ha, S.M., Lim, J., Kwon, S., Chun, J. 2017. A large-scale evaluation of algorithms to calculate average nucleotide identity. *Antonie Van Leeuwenhoek*, 110(10), 1281-1286.

Young, I.-C., Chuang, S.-T., Hsu, C.-H., Sun, Y.-J., Lin, F.-H. 2016. C-phycocyanin alleviates osteoarthritic injury in chondrocytes stimulated with H2O2 and compressive stress. *International Journal of Biological Macromolecules*, 93, 852-859.

Yu, P., Li, P., Chen, X., Chao, X. 2016. Combinatorial biosynthesis of *Synechocystis* PCC6803 phycocyanin holo-α-subunit (CpcA) in *Escherichia coli* and its activities. *Applied Microbiology and Biotechnology*, 100(12), 5375-5388.

Yu, P., Wu, Y., Wang, G., Jia, T., Zhang, Y. 2017. Purification and bioactivities of phycocyanin. *Critical Reviews in Food Science and Nutrition*, 57(18), 3840-3849.

Yu, Y., You, L., Liu, D., Hollinshead, W., Tang, Y.J., Zhang, F. 2013. Development of Synechocystis sp. PCC 6803 as a phototrophic cell factory. *Marine drugs*, 11(8), 2894-2916.

Zakhia, F., Jungblut, A.-D., Taton, A., Vincent, W.F., Wilmotte, A. 2008. Cyanobacteria in Cold Ecosystems. in: *Psychrophiles: from Biodiversity to Biotechnology*, (Eds.) R. Margesin, F.

Schinner, J.-C. Marx, C. Gerday, Springer Berlin Heidelberg. Berlin, Heidelberg, pp. 121-135.

Zhan-Ping, Z., Lu-Ning, L., Xiu-Lan, C., Jin-Xia, W., Min, C., Yu-Zhong, Z., Bai-Cheng, Z. 2005. Factors that effect antioxidant activity of c-phycocyanins from *Spirulina platensis*. *Journal of Food Biochemistry*, 29(3), 313-322.

Zhang, J. 2012. Protein-Protein Interactions in Salt Solutions. in: *Protein-Protein Interactions - Computational and Experimental Tools.* (Ed.) W. Cai, In Tech. Europe, pp. 359-376.

Zhang, L., Zhang, C., Gao, R., Yang, R., Song, Q. 2016a. Sequence Based Prediction of Antioxidant Proteins Using a Classifier Selection Strategy. *PLOS ONE*, 11(9), e0163274.

Zhang, R., Grimi, N., Marchal, L., Lebovka, N., Vorobiev, E. 2019. Effect of ultrasonication, high pressure homogenisation and their combination on efficiency of extraction of bio-molecules from microalgae Parachlorella kessleri. *Algal Research*, 40.

Zhang, X., Liu, X., He, Q., Dong, W., Zhang, X., Fan, F., Peng, D., Huang, W., Yin, H. 2016b. Gene Turnover Contributes to the Evolutionary Adaptation of Acidithiobacillus caldus: Insights from Comparative Genomics. *Frontiers in Microbiology*, 7(1960).

Zhang, X., Zhang, F., Luo, G., Yang, S., Wang, D. 2014. extraction and separation of phycocyanin from *Spirulina* using aqueous two-phase systems of ionic liquid and salt. *Journal of Food and Nutrition Research*, 3, 15-19.

Zhang, X., Zhang, Y., Chen, F. 1998. Kinetic models for phycocyanin production by high cell density mixotrophic culture of the microalga *Spirulina platensis*. *Journal of Industrial Microbiology and Biotechnology*, 21(6), 283-288.

Zhang, Y., Chi, Z., Lu, W. 2007. Exopolysaccharide production by four cyanobacterial isolates and preliminary identification of these isolates. *Journal of Ocean University of China*, 6(2), 147-152.

Zhao, C., Höppner, A., Xu, Q.-Z., Gärtner, W., Scheer, H., Zhou, M., Zhao, K.-H. 2017. Structures and enzymatic mechanisms of phycobiliprotein lyases CpcE/F and PecE/F. *Proceedings of the National Academy of Sciences*, 114(50), 13170-13175.

Zhao, F., Qin, S. 2006. Evolutionary analysis of phycobiliproteins: implications for their structural and functional relationships. *Journal of Molecular Evolution*, 63(3), 330-40.

Zhao, K.-H., Su, P., Tu, J.-M., Wang, X., Liu, H., Plöscher, M., Eichacker, L., Yang, B., Zhou, M., Scheer, H. 2007. Phycobilin:cystein-84 biliprotein lyase, a near-universal lyase for cysteine-84-binding sites in cyanobacterial phycobiliproteins. *Proceedings of the National Academy of Sciences*, 104(36), 14300-14305.

Zhao, K.H., Su, P., Li, J., Tu, J.M., Zhou, M., Bubenzer, C., Scheer, H. 2006. Chromophore attachment to phycobiliprotein beta-subunits: phycocyanobilin:cysteine-beta84 phycobiliprotein lyase activity of CpeS-like protein from *Anabaena* Sp. PCC7120. *Journal of Biological Chemistry*, 281(13), 8573-81.

Zhao, L., Peng, Y.-l., Gao, J.-m., Cai, W.-m. 2014. Bioprocess intensification: an aqueous two-phase process for the purification of C-phycocyanin from dry Spirulina platensis. *European Food Research and Technology*, 238(3), 451-457.

Zheng, J., Inoguchi, T., Sasaki, S., Maeda, Y., McCarty, M.F., Fujii, M., Ikeda, N., Kobayashi, K., Sonoda, N., Takayanagi, R. 2013. Phycocyanin and phycocyanobilin from Spirulina platensis protect against diabetic nephropathy by inhibiting oxidative stress. *American Journal of Physiology-Regulatory, Integrative and Comparative Physiology*, 304(2), R110-R120.

Zorina, A., S. Mironov, K., S. Stepanchenko, N., Sinetova, M., V. Koroban, N., Zinchenko, V., Kupriyanova, E., Allakhverdiev, S., Los, D. 2011. *Russian Journal of Plant Physiology* 58 (5) 749-767.

Zou, T.B., He, T.P., Li, H.B., Tang, H.W., Xia, E.Q. 2016. The structure-activity relationship of the antioxidant peptides from natural proteins. *Molecules*, 21(1), 72.

Żyszka-Haberecht, B., Niemczyk, E., Lipok, J. 2019. Metabolic relation of cyanobacteria to aromatic compounds. *Applied Microbiology and Biotechnology*, 103(3), 1167-1178.

Żyszka, B., Anioł, M., Lipok, J. 2017. Modulation of the growth and metabolic response of cyanobacteria by the multifaceted activity of naringenin. *PLOS ONE*, 12(5), e0177631.

APPENDICES

Appendix 1: List of Cyanobacteria Species with Complete Sequenced Genome

Table A1: Cyanobacteria genome sequenced and information related to genome size (Size, MB), GC %, and the number of genes

Organisms	Size MB	GC %	Genes
Chroococcales			
Candidatus *Atelocyanobacterium thalassa* UCYN-A1	1.44	31	1200
Candidatus *Atelocyanobacterium thalassa* UCYN-A2			
Cyanobacterium aponinum PCC 10605	4.72	60.50	4562
Cyanobacterium stanieri PCC 7202	4.66	62.00	4482
Cyanothece sp. ATCC 51142	7.06	38.80	6258
Cyanothece sp. PCC 7424	5.31	38.10	4797
Cyanothece sp. PCC 7425	7.11	41.40	5813
Cyanothece sp. PCC 7822	69.96	39.80	5841
Cyanothece sp. PCC 8801	7.02	42.20	6250
Cyanothece sp. PCC 8802	7.61	42.20	6738
Dactylococcopsis salina PCC 8305	5.49	38.30	5380
Gloeocapsa sp. PCC 7428	9.06	41.30	7164
Halothece sp. PCC 7418	6.33	40.40	5538
Microcystis aeruginosa NIES-843	7.21	41.20	6213
Microcystis aeruginosa NIES-2549	4.29	42.92	4329
Microcystis panniformis FACHB-1757	5.84	42.35	6363
Chroococcidiopsidales			
Chroococcidiopsis thermalis PCC 7203	6.72	41.50	5687
Gloeobacteriales			
Gloeobacter kilaueensis JS1	8.73	37.5	6946
Gloeobacter violaceus PCC 7421	8.36	47.00	8571
Nostocales			
Anabaena cylindrica PCC 7122	6.79	44.30	6676
Anabaena sp. 90	6.76	45.60	6426
Anabaena sp. wa102	5.78		4801
Anabaena variabilis ATCC 29413	5.62	40.20	5059
Calothrix sp. 336/3	6.42		5108
Calothrix sp. PCC 630	4.18	35.00	3614

Organisms	Size MB	GC %	Genes
Calothrix sp. PCC 7507	3.16	38.70	2941
Cylindrospermum stagnale PCC 7417	3.34	68.70	3437
Moorea producens	9.71	43.52	7571
Nostoc azollae 0708	5.46	38.00	5364
Nostoc punctiforme PCC 73102	6.55	38.50	5942
Nostoc sp. PCC 7107	5.79	50.70	5507
Nostoc sp. PCC 7120	7.84	39.90	7042
Nostoc sp. PCC 7524	4.79	39.80	4619
Rivularia sp. PCC 7116	4.8	39.80	4700
Oscillatoriales			
Arthrospira platensis (***A.*** *platensis)* NIES-39	3.78	42.40	3684
Crinalium epipsammum PCC 9333	4.68	58.50	3912
Geitlerinema sp. PCC 7407	5.88	43.40	5304
Microcoleus sp. PCC 7113	4.18	42.90	3920
Oscillatoria acuminata PCC 6304	5.13	43.90	4654
Oscillatoria nigro-viridis PCC 7112	7.97	46.20	6821
Trichodesmium erythraeum IMS101	5.84	42.30	6364
Pleurocapsales			
Pleurocapsa sp. PCC 7327	7.8	47.60	6100
Stanieria cyanosphaera PCC 7437	8.27	45.80	7006
Synechococcales			
Acaryochloris marina MBIC11017	4.89	46.20	4014
Chamaesiphon minutus PCC 6605	2.7	55.50	2581
Cyanobium gracile PCC 6307	2.74	55.50	2715
Synechococcus elongatus PCC 6301	2.61	52.40	2944
Synechococcus elongatus PCC 7942	2.51	59.20	2756
Synechococcus sp. CC9311	2.23	54.20	2357
Synechococcus sp. CC9605	3.05	58.50	2942
Synechococcus sp. CC9902	2.93	60.20	2897
Synechococcus sp. JA-2-3B'a (2–13)	3.72	48.50	3794
Synechococcus sp. JA-3-3Ab	3.41	49.20	3238
Synechococcus sp. KORDI-100	2.79	57.50	3105
Synechococcus sp. KORDI-49	2.59	61.37	2783
Synechococcus sp. KORDI-52	2.57	59.09	2875
Synechococcus sp. PCC 6312	3.58	40.60	3666

Organisms	Size MB	GC %	Genes
Synechococcus sp. PCC 7002	2.22	60.80	2581
Synechococcus sp. PCC 7502	2.37	60.20	2586
Synechococcus sp. RCC307	2.43	59.40	2581
Synechococcus sp. WH 7803	3.57	47.70	3219
Synechococcus sp. UTEX 2973	2.74	55.44	2696
Synechococcus sp. WH 8102	3.95	47.30	3625
Synechococcus sp. WH 7803	2.37	60.24	2586
Synechococcus sp. WH 8109	2,11	60.09	2697
Synechocystis sp. PCC 6714	3.74	47.55	3848
Synechocystis sp. PCC 6803	3.95	47.30	3610
Synechocystis sp. PCC 6803	3.57	47.70	3218
Synechocystis sp. PCC 6803 substr. GT-I	3.57	47.70	3217
Synechocystis sp. PCC 6803 substr. PCC-N	2.59	53.90	2525
Synechocystis sp. PCC 6803 substr. PCC-P	2.52	53.80	2400
Thermosynechococcus elongatus BP-1	7.75	34.10	5126
Thermosynechococcus sp. NK55	6.69	44.40	6033
Leptolyngbya sp. PCC 7376	4.99	45.20	4665
Pseudanabaena sp. PCC 7367	5.54	36.30	5041
Prochlorococcus marinus str. AS9601	1.67	31.30	1965
Prochlorococcus marinus str. MIT 9211	1.69	38.00	1900
Prochlorococcus marinus str. MIT 9215	1.74	31.10	2054
Prochlorococcus marinus str. MIT 9301	1.64	31.30	1962
Prochlorococcus marinus str. MIT 9303	2.68	50.00	3136
Prochlorococcus marinus str. MIT 9312	1.71	31.20	1856
Prochlorococcus marinus str. MIT 9313	2.41	50.70	2330
Prochlorococcus marinus str. MIT 9515	1.7	30.80	1964
Prochlorococcus marinus str. NATL1A	1.86	35.00	2250
Prochlorococcus marinus str. NATL2A	1.84	35.10	2228
Prochlorococcus marinus subsp. *marinus* CCMP1375	1.75	36.40	1930
Prochlorococcus marinus subsp. *pastoris* CCMP1986	1.66	30.80	1762
Prochlorococcus sp. MIT 0604	1.78	31.17	2102
Prochlorococcus sp. MIT 0801	1.93	34.91	2330

Appendix 2: Map Showing Lister Point, False bay Lake St Lucia

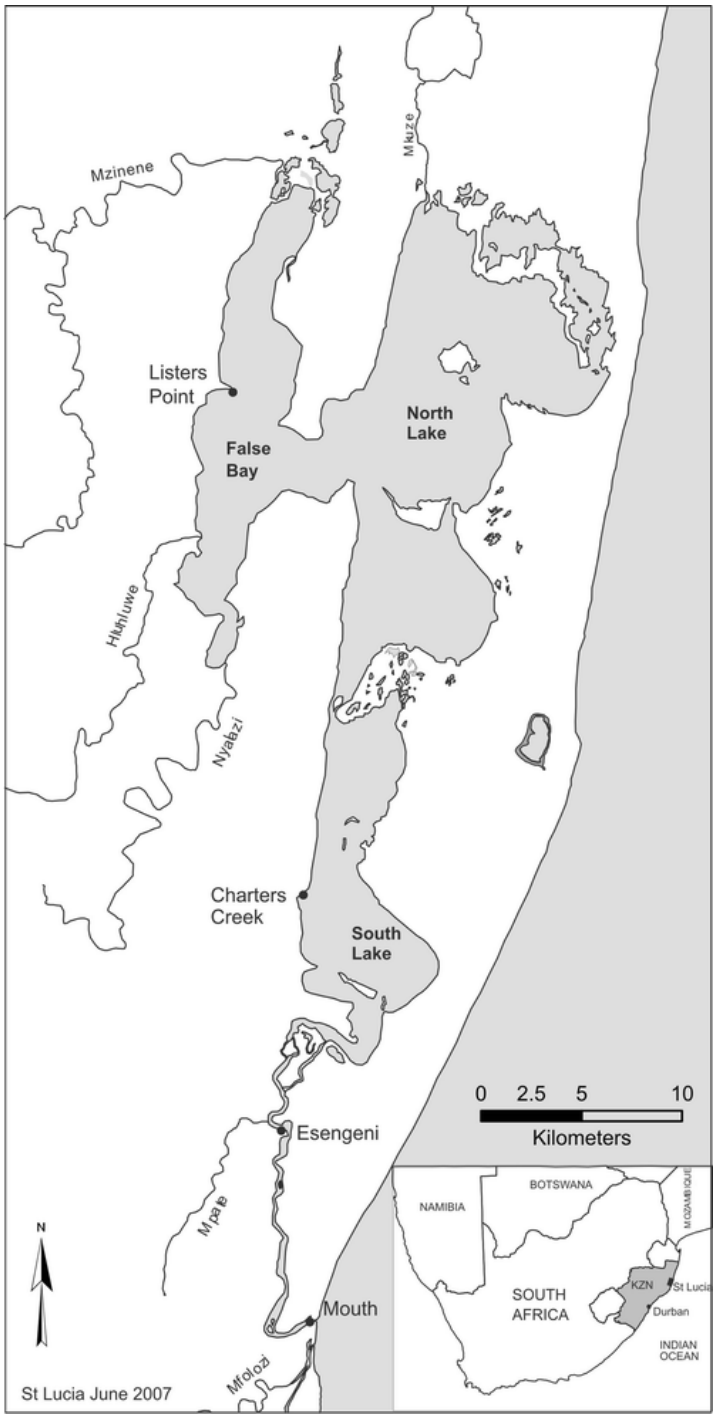

Sample size 500ml
Water temperature 29±2 ˚C
DO 8mg/ml
pH 8
Salinity 112 g/L

Figure A1: Map of sampling point and conditions of Lister Point, False bay Lake St Lucia

Appendix 3: Protocol for DNA Extraction using FastDNA® SPIN Kit

Components

Lysing Matrix A	2 mL tubes
1/4 Ceramic Spheres	100 spheres
Binding Matrix	66 mL
Concentrated SEWS-M	12 mL (add 100 mL of 100% ethanol)
DES	25 mL
CLS-VF	90 mL
PPS	25 mL
Cell Lysis Solution (CLS)	110 mL
SPIN Modules	
Catch Tubes	

Method

1. Samples ~ 200 mg wet biomass was added to Lysing Matrix A tube.

2. Cell Lysis Solution (CLS) -800 µl CLS-VF and 200 µl PPS was added

3. Samples were homogenised using in a bead beater for 40 seconds at a speed setting of 6.0.

4. Centrifuged at 14,000 x g for 5-10 min to pellet debris.

5. Supernatant (600 – 700 μL) was transferred to a 2.0 mL microcentrifuge tube and equal volume of Binding Matrix was added and inverted to mix.

6. Thereafter, incubated with gentle agitation for 5 min at room temperature on a shaker.

7. Centrifuged at 14,000 x g for 10 s to pellet Binding Matrix. Supernatant discarded

8. Following the addition of 500 μL of SEWS-M and gently resuspended the pellet using the

9. The resuspended Binding Matrix was then transferred to a SPIN™ Filter and centrifuged at 14,000 x g for 1 min, the contents of Catch Tube was discarded and replaced.

10. Centrifuged a second time at 14,000 x g for 1 min and replaced the Catch Tube with a new, clean tube.

11. DNA was eluted by gently resuspending Binding Matrix above the SPIN filter in 100 μL of DES. Incubated for 5 min at 55˚C in a water bath.

12. Centrifuged at 14,000 x g for 1 min to bring eluted DNA into the clean catch tube and the SPIN filter discarded.

13. DNA was stored at -20°C.

Appendix 4: Electrophoresis of Extracted DNA

The DNA was extracted in triplicate and the yield was 80-95 ng/μL. The purity of extracted nucleic acids was determined by the sample absorbance (A) ratios at A_{260nm}/A_{280nm} and A_{260nm}/A_{230nm}. The ideal ratios for pure DNA is an A260nm/A280nm of ~1.8 and an A260nm/A230nm of ~2.0. All three samples had purity ratios > 1.8 and >2.0. Agarose-gel electrophoresis was used to determine the integrity of the genomic DNA extracted. The isolated DNA was used for sequencing. Electrophoresis of extracted DNA in 0.8% (w/v) agarose gel. Lane 1: 100 bp DNA step ladder as a marker, Lane 2 and 3: ±80 ng of DNA.

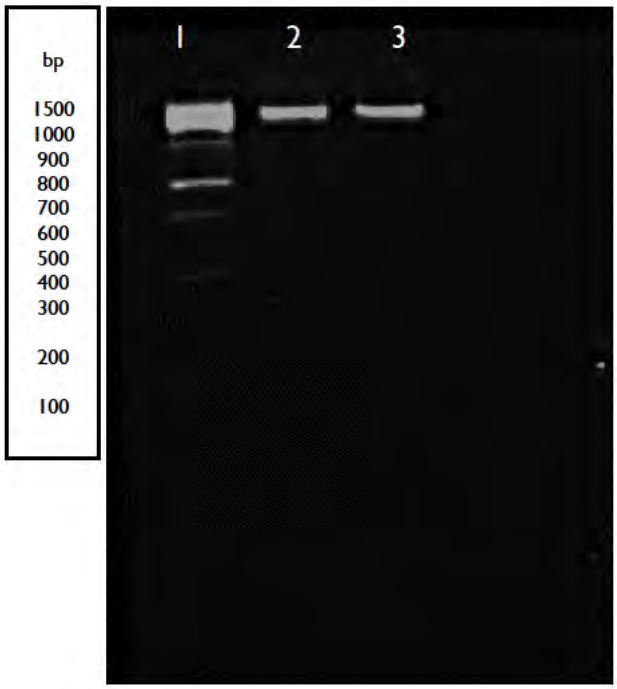

Figure A2: Electrophoresis of extracted DNA in 0.8% (w/v) agarose gel. Lane 1: 100 bp DNA step ladder as a marker, Lane 2 and 3: ±80 ng of DNA.

Appendix 5: Comparison between *Cyanothece* strains

Table A2: Morphology and description of Cyanothece starins

	Cluster1			Cluster2			Cluster 3		
								Sub cluster1 *Euhalothece*	Sub cluster 2 *Halothece*
	PCC 7424	PCC 7822	PCC 9224	PCC 7425	8801	8802	ATCC 51142	PCC 7418	*H.californica* MPI96P605
	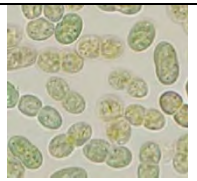	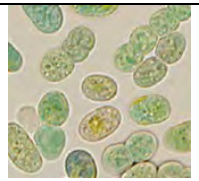	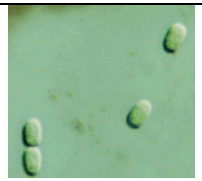	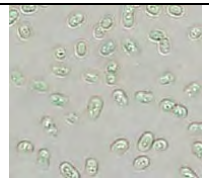	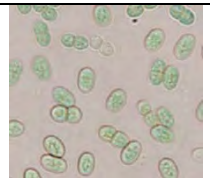	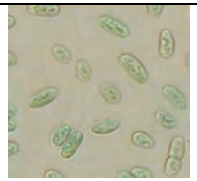	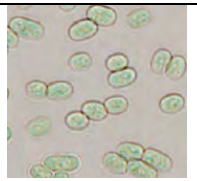	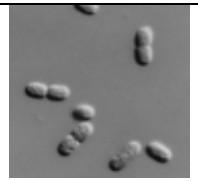	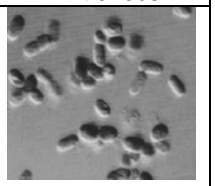
Location	Rice field Sengal	Rice field India	Water	Rice field Sengal	Rice field Taiwan	Rice field Taiwan	Benthic marine Port Aranas	Solar evaporation pond	Mat, Baja California, Mexico
	Freshwater						Marine		
Cell size μm	5-6	6-8	4-6	3-4	4	4-5	4-5	6-7	2.5-12.6
Genome size Mbp	6.55	7.84	6.35	5.79	4.79	4.80	4.46	3.1	
No. of coding sequences	5,710	6,642	6,234	5,327	4,367	4,444	5,304	3,313	
% GC Content	38,0	39,6	48,6	49,9	39	39	37,1	42,2	

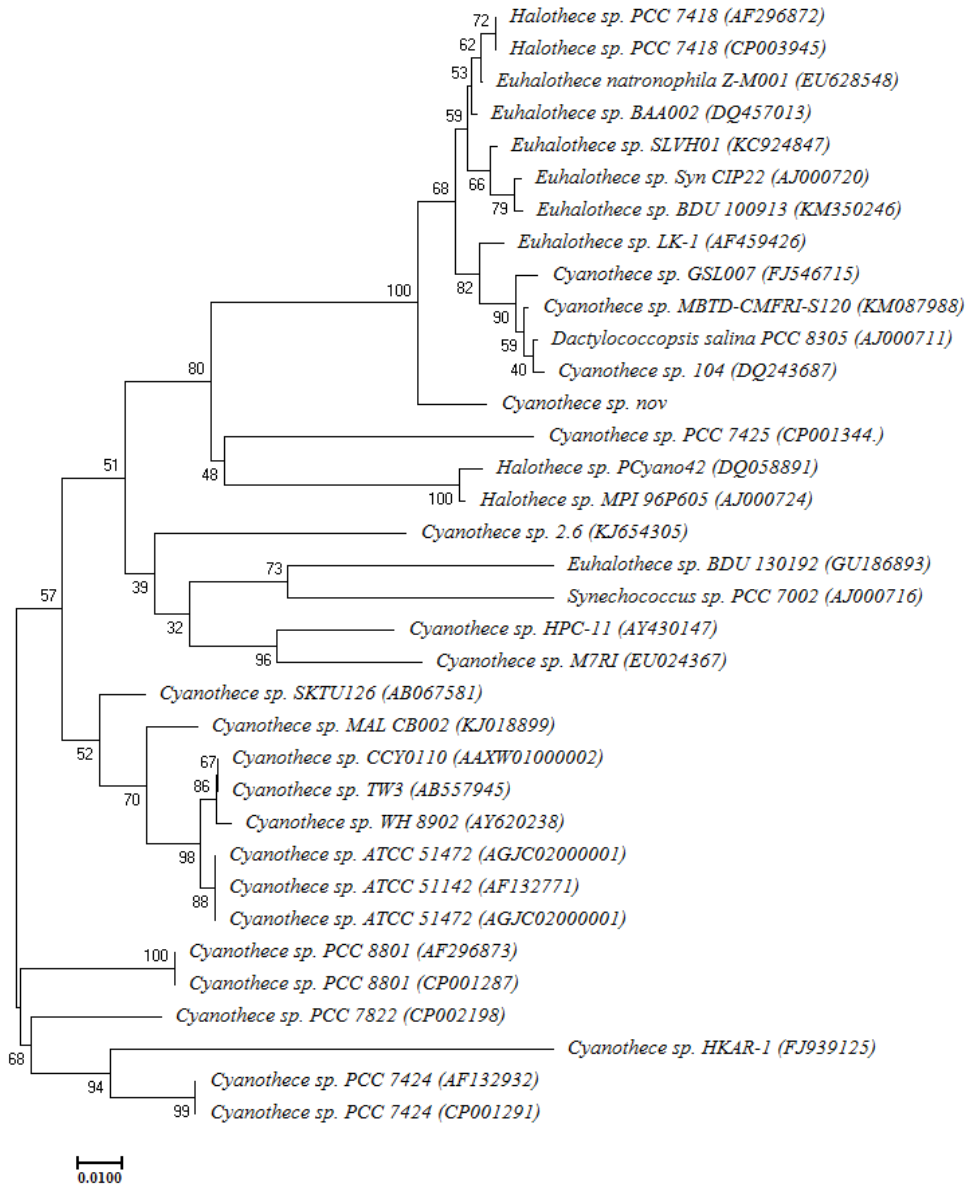

Figure A3: Phylogenetic tree of *Cyanothece* species. The tree was constructed using the neighbor-joining algorithm based on 18S RNA genes.

Appendix 6 : QC Report per Sequence Analysis

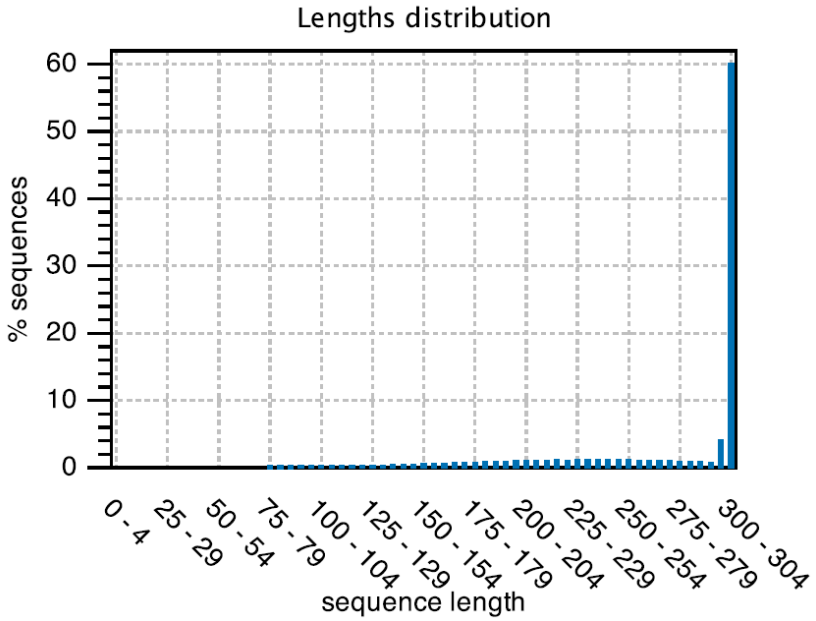

Figure A4.1: Distribution of sequence lengths. In cases of untrimmed Illumina or SOLiD reads it will ju st contain a single peak. x: sequence length in base-pairs. y: number of sequences featuring a particular length normalised to the total number of seq uences

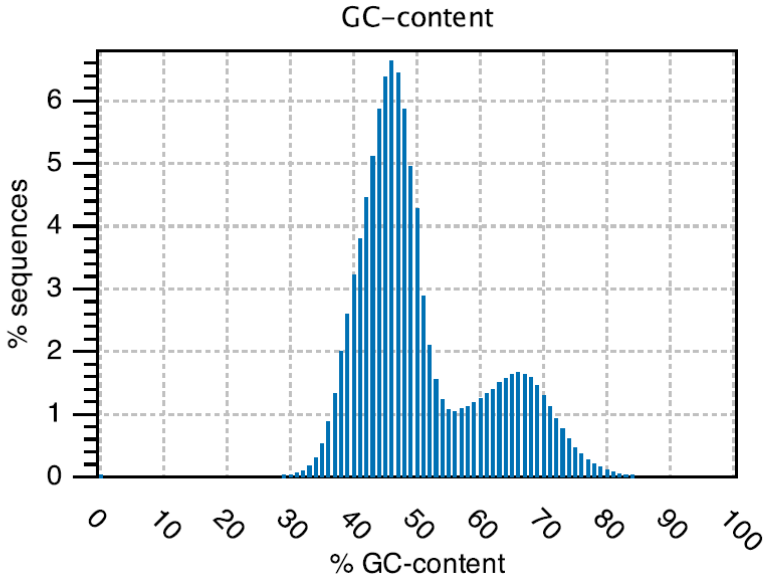

Figure A4.2: Distribution of GC-contents. The GC-content of a sequence is calculated as the number of G C-bases compared to all bases (including ambiguous bases). x: relative GC-content of a sequence in percent. y: number of sequences featuring particular GC-percentages normalised to the total number of sequences

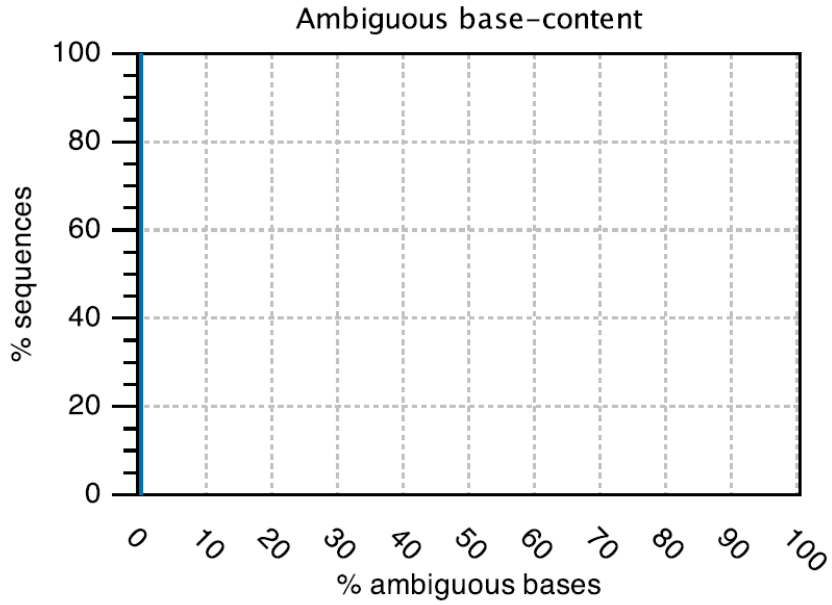

Figure A4.3: Distribution of N-contents. The N-content of a sequence is calculated as the number of amb iguous bases compared to all bases. x: relative N-content of a sequence in percent. y: number of

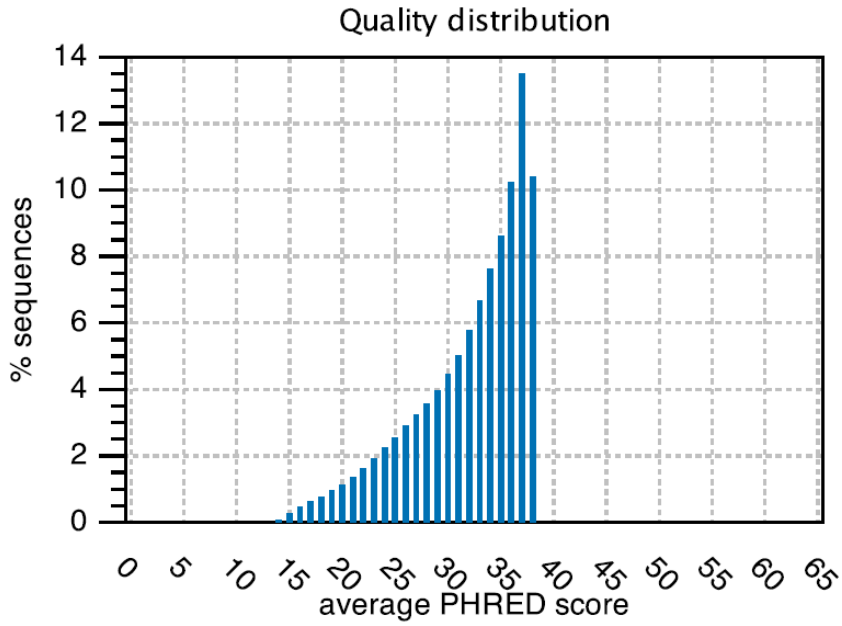

Figure A4.4: Distribution of average sequence qualitie scores. The quality of a sequence is calculated as the arithmetic mean of its base qualities. x: PHRED-score y: number of sequences observed at that qual. score normalised to the total number of sequ encessequences featuring particular N-percentages normalised to the total number o f sequences

Appendix 6 : QC Report per base analysis

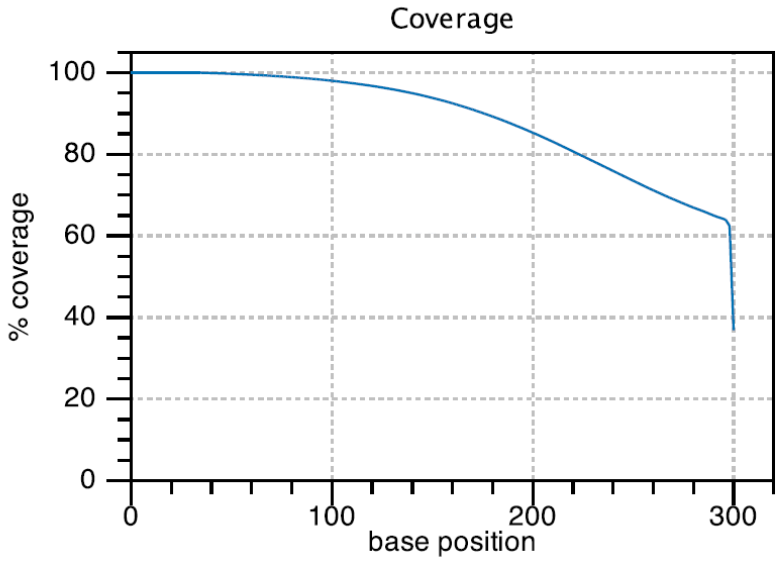

Figure A4.5: The number of sequences that support (cover) the individual base positions. In cases of un trimmed Illumina or SOLiD reads it will just contain a rectangle. x: base position y: number of sequences covering individual base positions normalised to the total number o f sequences

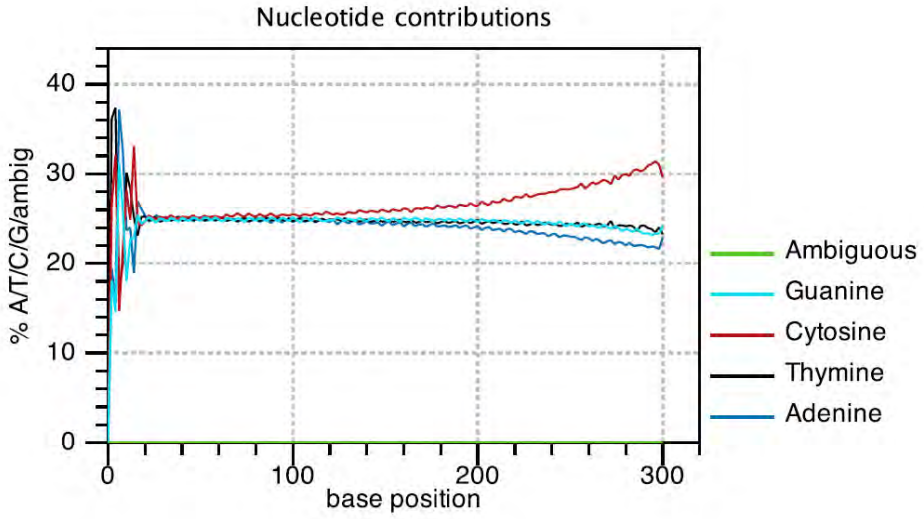

Figure A4.6: Coverages for the four DNA nucleotides and ambiguous bases. x: base position. y: number of nucleotides observed per type normalised to the total number of nucleotides o bserved at that position

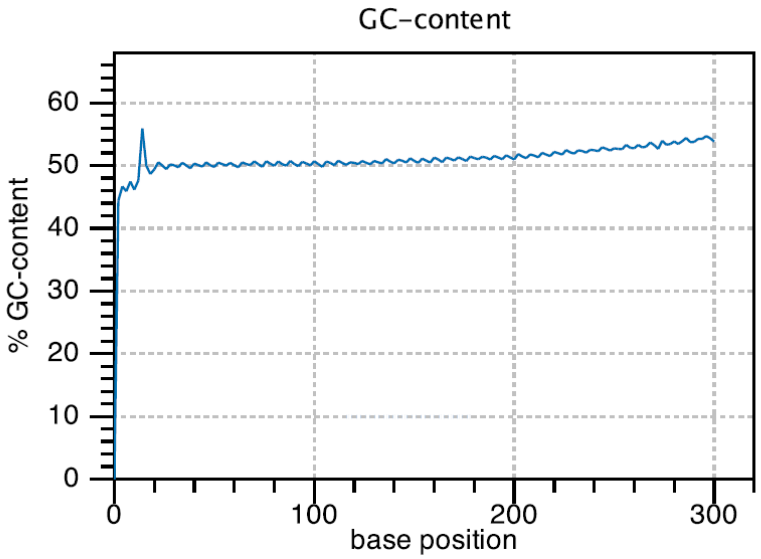

Figure A4.7: Combined coverage of G- and C-bases. x: base position y: number of G- and C-bases observed at current position normalised to the total number of bases observed at that position

Appendix 7: Multiple Cluster Alignment -16s rRNA genes

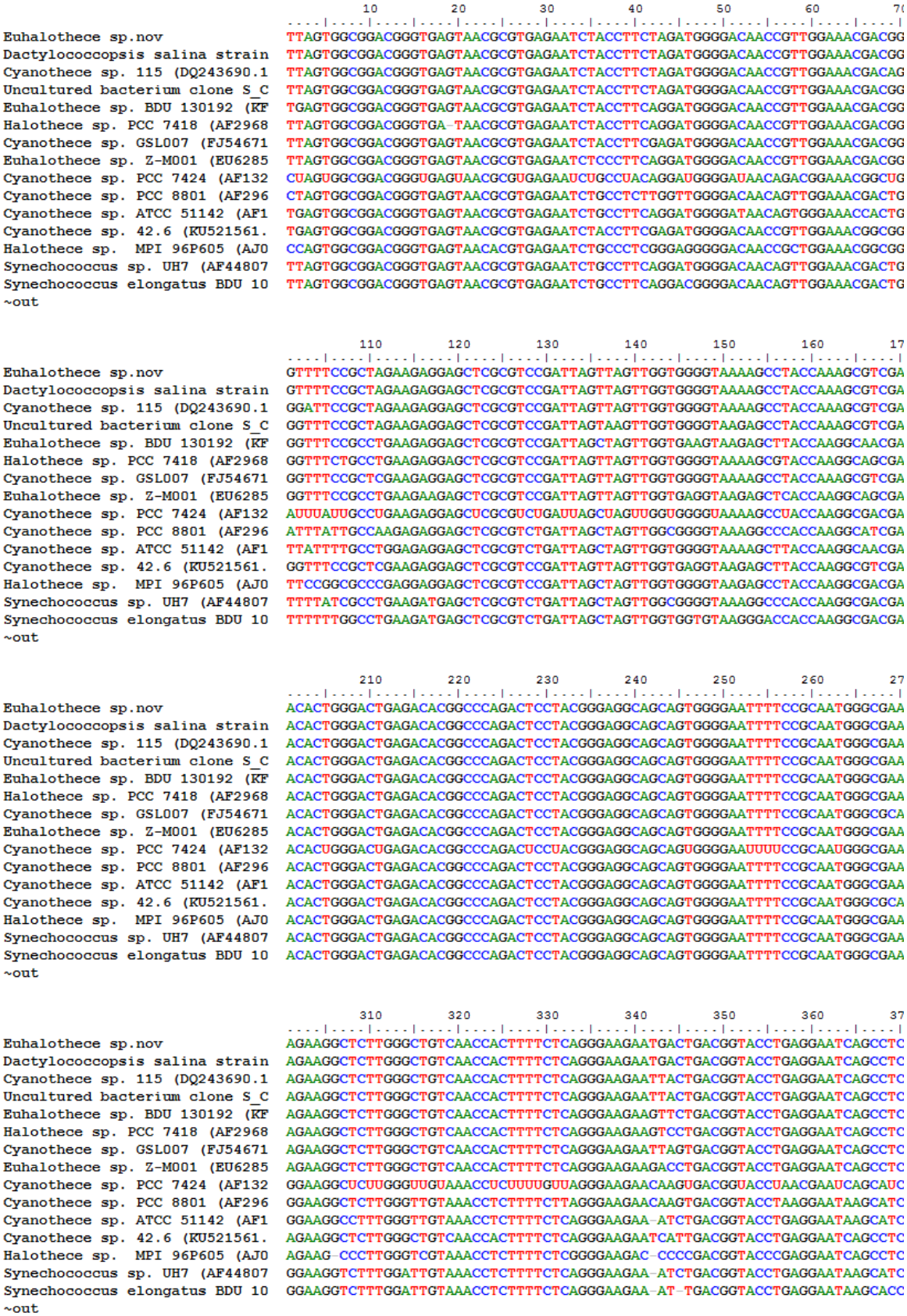

Figure A5: Multiple cluster alignment of the 16s rRNA genes of the 14 strains.

Appendix 8 : *Euhalothece* sp. Genome

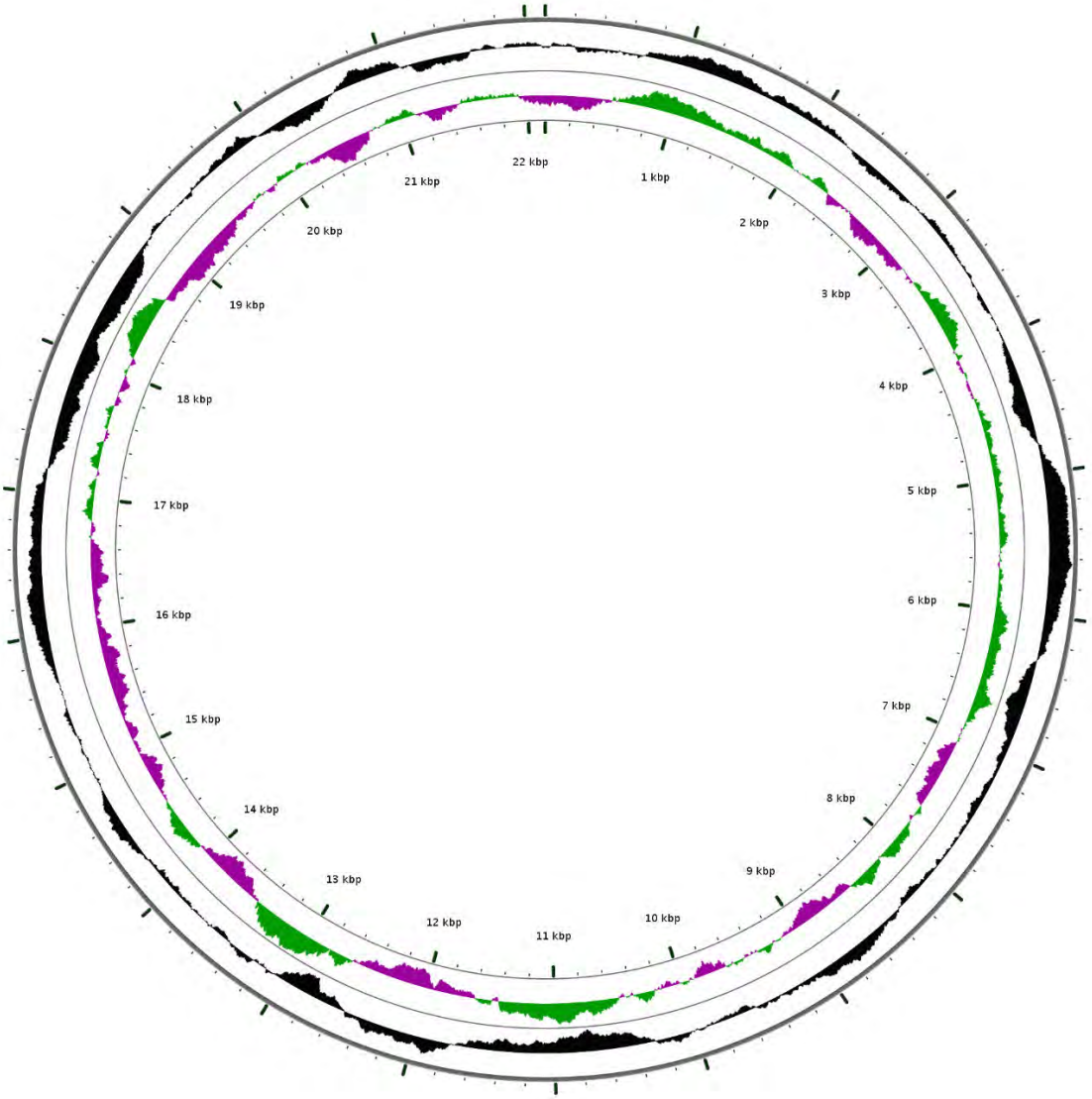

Figure A6.1: Circular map of *Euhalothece* sp. draft genome. Circles from outside in: (black) GC % plot; and GC skew plot.

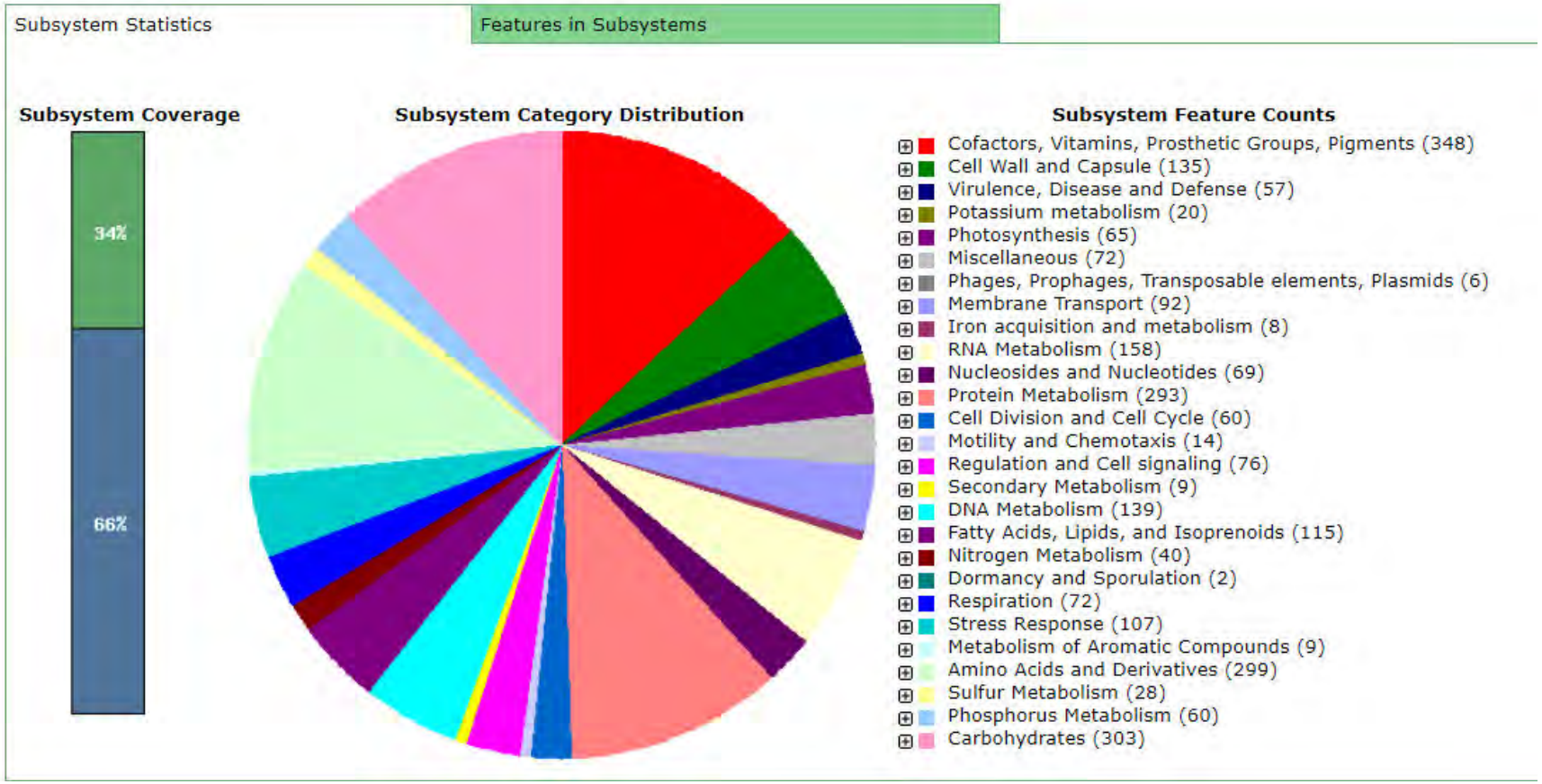

Figure A6.2: Major genes distrusted in the major subsystem

Appendix 9: Reagents and Gel Preparation for SDS-PAGE Slab Gel (Laemmli buffer system)

Reagents were purchased from Sigma-Alrich and Biorad. The catalogue number is in brackets

Reagents and materials:

- Acrylamide/bis 30% (Bio-Rad 30% Acrylamide/BIS solutions 37.5:1 mixture, catalog number 161-0158, 500 ml)
- Sodium dodecyl sulphate 10% (10 g SDS in 100 ml ddH2O)
- 0.5 M Tris-HCl, pH 6.8 (6 g Tris base in 100 ml ddH2O store at 4°C).
- Ammonium persulfate
- N,N,N′,N′-tetramethylelthylenediamine (TEMED)
- Dithiothreitol (DTT), 1 g (1610610)
- β-mercaptoethanol (1610710)
- Bromophenol blue
- 10X Tris glycine/SDS (1610732): 25 mM Tris, 192 mM glycine, 0.1% SDS, pH 8.3
- 2x Laemmli Sample Buffer (1610737)
- Oriole™ Fluorescent Gel Stain (161-0495)

Apparatus:

- Vertical gel electrophroesis unit including glass plates (15 cm X 10 cm)
- combs (10 wells)
- 1mm spacers
- Power pack
- plastic tapes
- Clips

A. Stacking gel (5%)

Combine and mix the chemicals in a beaker in the following order:

2 ml of 30% acrylamide mix,
3 ml of 0.5 M Tris-HCl (pH 6.8),
0.12 ml of 10% (w/v) SDS,
6.76 ml of H_2O,
0.12 ml of 10% ammonium persulfate,
0.006 ml of TEMED.

B. Resolving Gel (15%)

C.

3.3ml of Acrylamide/bis (30% 37.5:1; Bio-Rad),
1.25 mL of 4X Tris-Cl (pH 6.8),
3.05 ml of H_2O,
30 µl of 10% APS,
10 µl TEMED

AS and TEMED was added prior to pouring

D. Sample preparation

E. **Preparation and running of 15% SDS- poly acrylamide gel**:

- Glass plates and spacers were assembled in gel casting apparatus–according to BioRad instruction manual.
- The separating gel was poured between the plates up to 2 cm below from the top portion of the plates.
- The top portion of the gel was overlaid with a thin layer of propanol and left at room temperature for one hour.
- After 30-45 minutes, when the gel is polymerised completely, propanol was drained out and the top portion of the gel was washed several times with double distilled water. Remaining water was soaked out using a filter paper.
- The stacking gel was prepared as per the recipe given above following the same steps as for separating gel and immediately poured over the separating gel between the plates.
- The comb was then inserted between the plates and left at room temperature to let the gel polymerise.
- After one and half hours when the stacking gel was completely polymerised the clips, tapes, comb and spacer were removed from the assembled plates.

F. Loading the gel in chamber

- The lower buffer reservoir of the electrophoresis chamber was half-filled with 1X SDS gel running buffer and the gel plate was placed into the chamber. The lower buffer reservoir was filled up to the level of wells and upper buffer reservoir was also filled sufficiently with 1X SDS gel running buffer.
- 50 µL of sample protein was mixed with 10 µL of 2x Laemmli Sample Buffer and 40 µL of this was loaded on the gel.
- 15 µL of the prestained protein marker was also loaded in a separate well.

G. Running gel

- Place the lid on top of the lower buffer chamber to fully enclose the cell. The correct orientation was made by matching the colours of the plugs on the lid with the jacks on the inner cooling core.
- The electrophoresis chamber was connected to the power pack and the gel was run at 40V until the dye front (bromophenol blue) enters the separating gel.
- Afterwards, voltage was increased to 70 volts and continued until the dye front reached the bottom of the separating gel.
- The glass plates were then removed carefully and gel was taken out.

H. Staining and destaining

- Firstly, 400 ml methanol (AR grade) – 10 ml of Oriole fluorescent gel stain concentrate was added to the 1 L bottle holding 590 ml of diluent.
- Gel was placed in a tray containing staining solution and the tray was put on shaker for 90 mins.
- After 90 mins, the staining solution was drained out and replaced with water
- The gel was documented (photograph) using gel documentation unit (xxxxx) using standard (302 nm) UV lamp with Standard Filter (580 nm bandpass for ethidium bromide).

Appendix 10: Extraction Buffers

Phosphate Buffer (pH 5.8–8.0 at 25°C)

To create 100 mL of a 0.1M phosphate buffer, mix sodium phosphate, dibasic dihydrate and sodium phosphate monobasic monohydrate, as given below, and dilute to 100ml with water.

Solution A: 0.2M sodium phosphate, dibasic dihydrate ($Na_2HPO_4 \cdot 2H_2O$ FW = 178.05)
Solution B: 0.2M sodium phosphate, monobasic, monohydrate ($NaH_2PO_4 \cdot H_2O$ FW = 138.01)

pH	Solution A (mL)	Solution B (mL)
5.8	4	46
6	6.15	43.85
6.2	9.25	40.75
6.4	13.25	36.75
6.6	18.75	31.25
6.8	24.5	25.5
7	30.5	19.5
7.2	36	14
7.4	40.5	9.5
7.6	43.5	6.5
7.8	45.75	4.25
8	47.35	2.65

Phosphate-buffered saline (PBS)

• 8g NaCl, 0.2g KCl • 1.44g Na2HPO4 • 0.24g KH2PO4

Dissolve salts in 800ml of distilled water. Adjust to pH 7.4 with HCl. Add water to 1 liter. Dispense into aliquots. Sterilise by autoclaving.

Potassium phosphate buffer

K_2HPO_4 (mw: 174.2 g/mol)	12.814 g	0.0736 M
KH_2PO_4 (mw: 136.086 g/mol)	3.598 g	0.0264 M

1. Prepare 800 mL of dH_2O in a suitable container.
2. Add 12.814 g of K_2HPO_4 to the solution.
3. Add 3.598 g of KH_2PO_4 to the solution.
4. Add distilled water until volume is 1 L.

Appendix 11: Predicted Values for Maximum C-PC and Purity

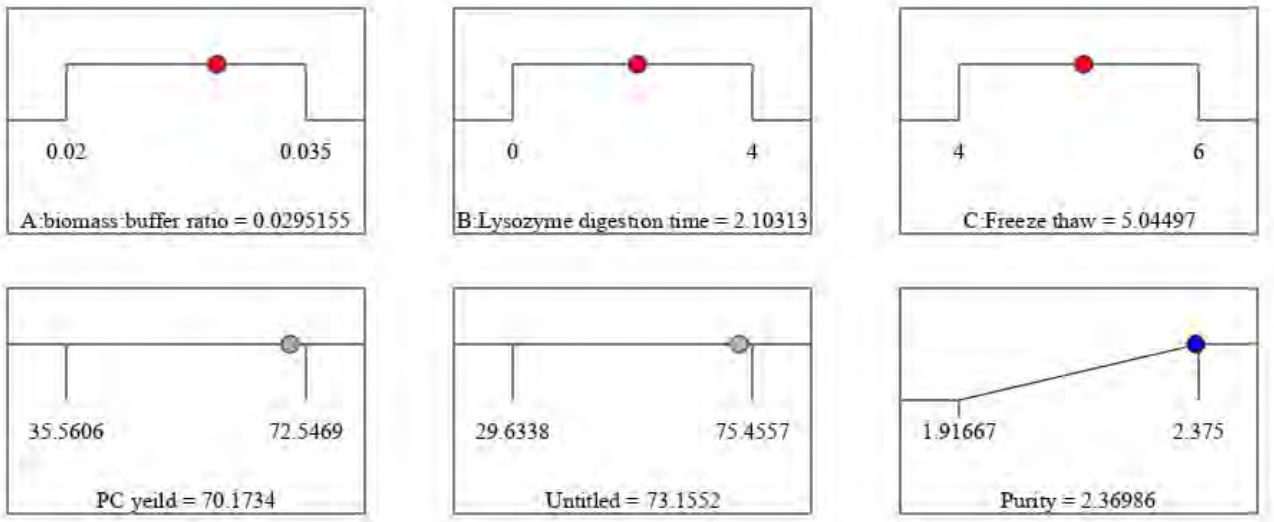

Desirability = 0.989
Solution 1 out of 1

Appendix 12: C-Phycocyanin Amino Acids Subunits Phylogentic Tree

A

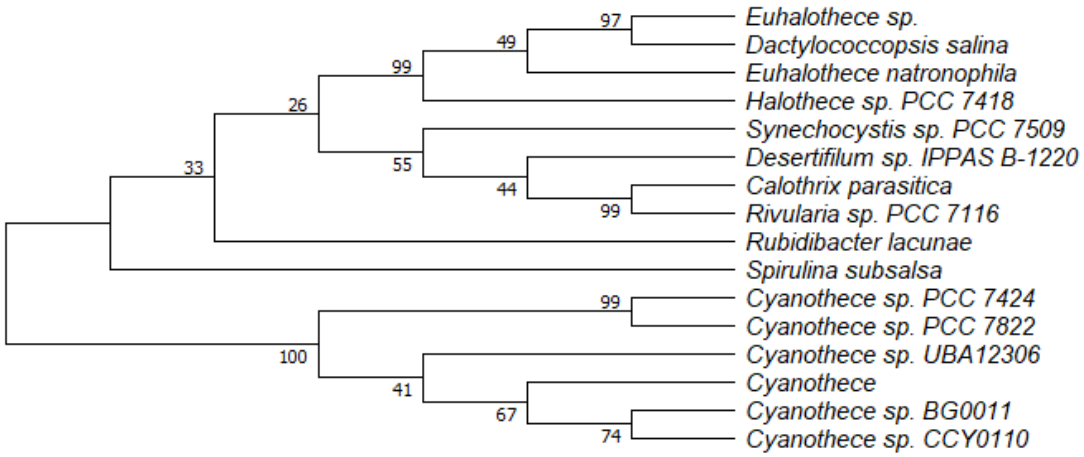

B

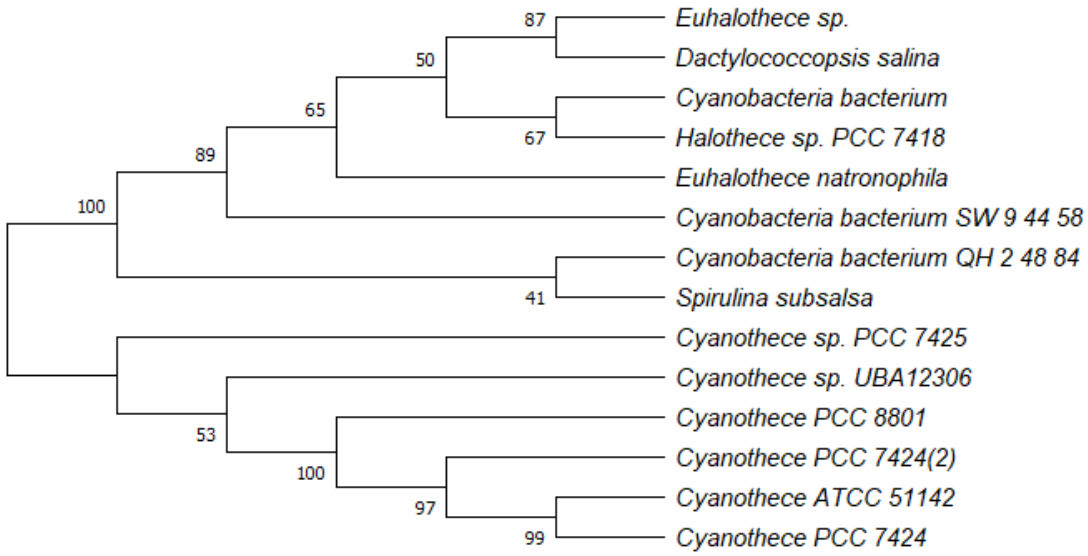

Fig. A7: Phylogenetic analysis of amino acid sequences for (A) C-PC *α*-subunit and (B) *β* subunits. There were a total of 162 and 172 positions in the *α*- and *β*-subunits. respectively in the final dataset. Evolutionary analyses were conducted in MEGA X.

Appendix 13: The α - and β - Amino Acid Composition

Table A.3 : Comparison of amino acid composition between thermotolerant and mesophilic cyanobacteria isolated from hypersaline, marine and freshwater

	Hypersaline thermotolerant		Marine thermotolerant		Marine mesophilic		Marine		Freshwater mesophilic	
	Dactylococcopsis salina		*Spirulina subsalsa*		*Cyanothece* ATCC 51142		*Cyanothece UBA12306*		*Synechococcus sp. PCC 6301*	
Amino Acids	***α***	***β***	***α***	***β***	***α***	***β***	***α***	***β***	***α***	***β***
Polar (Acidic)										
Asp (D)	8	12	7	13	10	13	10	11	9	13
Glu (E)	9	8	9	7	7	12	8	7	7	7
Polar (Basic)										
Arg (R)	8	13	8	12	7	14	7	11	6	13
His (H)	4	0	2	0	1	1	2	0	1	0
Lys (K)	7	4	6	4	8	5	9	4	8	5
Polar (Hydroxy acids)										
Ser (S)	7	13	17	12	13	11	12	12	14	11
Thr (T)	10	10	10	7	9	10	8	8	10	9
Non-polar (Aliphatic)										
Ala (A)	23	25	20	31	25	17	26	33	27	30
Gly (G)	14	12	12	12	12	10	14	15	13	13
Asn(N)	11	8	9	8	6	6	5	6	10	8
Ile (I)	10	4	9	6	9	10	12	11	7	11
Leu (L)	14	15	12	14	12	15	11	13	16	14
Cys (C)	2	3	2	3	2	1	2	3	1	3
Met(M)	5	7	5	6	4	6	4	6	1	4
Pro (P)	5	4	5	4	6	7	6	4	6	3
Gln (Q)	9	10	8	8	7	3	6	6	3	4
Val (V)	2	14	5	15	6	13	4	12	7	5
Trp(W)	1	0	1	0	1	0	1	0	1	0
Aromatic										
Phe (F)	4	5	4	5	5	5	5	5	6	6
Tyr (Y)	9	5	11	5	11	10	10	5	10	5
Total	**162**	**172**	**162**	**172**	**161**	**169**	**162**	**172**	**163**	**173**